

*TRANSPORTATION RESEARCH RECORD* 836

# Pavement Roughness and Skid Properties

*TRANSPORTATION RESEARCH BOARD*

*COMMISSION ON SOCIOTECHNICAL SYSTEMS  
NATIONAL RESEARCH COUNCIL*

*NATIONAL ACADEMY OF SCIENCES  
WASHINGTON, D.C. 1981*

**Transportation Research Record 836**

Price \$10.40

Edited for TRB by Susan Singer-Bart and Mary McLaughlin

**modes**

1 highway transportation

4 air transportation

**subject areas**

24 pavement design and performance

40 maintenance

**Library of Congress Cataloging in Publication Data**

National Research Council (U.S.). Transportation Research Board. Meeting (60th: 1981: Washington, D.C.)

Pavement roughness and skid properties.

(Transportation research record; 836)

Reports prepared for the 60th annual meeting of the Transportation Research Board.

1. Pavements—Testing—Addresses, essays, lectures.  
2. Roads—Riding qualities—Testing—Addresses, essays, lectures. 3. Pavements—Skid resistance—Testing—Addresses, essays, lectures.

I. Title. II. Series.

TE7.H5 no. 836 [TE250] 380.5s [625.8] 82-6364

ISBN 0-309-03313-6 ISSN 0361-1981 AACR2

**Sponsorship of the Papers in This Transportation Research Record**

**GROUP 2—DESIGN AND CONSTRUCTION OF TRANSPORTATION FACILITIES**

*R. V. LeClerc, Washington State Department of Transportation, chairman*

**Pavement Design Section**

*W. Ronald Hudson, University of Texas at Austin, chairman*

**Committee on Surface Properties-Vehicle Interaction**

*Don L. Ivey, Texas A&M University, chairman*

*Glenn G. Balmer, Frederick E. Behn, Robert R. Blackburn, John C. Burns, A. Y. Casanova III, John D. Eagleburger, Robert D. Ervin, Carlton M. Hayden, Rudolph R. Hegmon, Edward D. Howerter, Kenneth J. Law, David C. Mahone, W. E. Meyer, Thomas H. Morrow, Jr., W. Grigg Mullen, Bobby G. Page, A. Scott Parrish, Bayard E. Quinn, John J. Quinn, J. Reichert, Hollis B. Rushing, Elson B. Spangler, James C. Wambold, E. A. Whitehurst*

**Committee on Pavement Condition Evaluation**

*K. H. McGhee, Virginia Highway and Transportation Research Council, chairman*

*Doyt Y. Bolling, Michael I. Darter, Karl H. Dunn, Asif Faiz, Robert H. Gietz, Wouter Gulden, Lawrence E. Hart, William H. Highter, W. Ronald Hudson, Don H. Kobi, Scott A. Kutz, J. W. Lyon, Jr., Robert L. Novak, Richard D. Pavlovich, William A. Phang, Freddy L. Roberts, Albert F. Sanborn, Lawrence L. Smith, Herbert F. Southgate, Elson B. Spangler, Shiraz D. Tayabji, Loren M. Womack*

**Committee on Theory of Pavement Systems**

*Ralph C. G. Haas, University of Waterloo, chairman*

*G. H. Argue, Yu. T. Chou, Santiago Corro Caballero, Michael I. Darter, Paul J. Diethelm, David C. Esch, Fred N. Finn, Per E. Fossberg, W. Ronald Hudson, Lynne H. Irwin, Ali S. Kemahli, William J. Kenis, Ramesh Kher, Robert L. Lytton, Carl L. Monismith, Leon M. Noel, Robert G. Packard, Dale E. Peterson, James F. Shook, William T. Stapler, Ronald L. Terrel, Kornelis Wester*

Lawrence F. Spaine, Transportation Research Board staff

Sponsorship is indicated by a footnote at the end of each report. The organizational units, officers, and members are as of December 31, 1980.

# Contents

---

ROAD ROUGHNESS: ITS ELEMENTS AND MEASUREMENT W.R. Hudson .....	1
ROUGHNESS AND ROADWAY SAFETY John C. Burns .....	8
ROLE OF ROAD ROUGHNESS IN VEHICLE RIDE T.D. Gillespie and M. Sayers .....	15
STATE OF THE ART OF MEASUREMENT AND ANALYSIS OF ROAD ROUGHNESS J.C. Wambold, L.E. DeFrain, R.R. Hegmon, K. McGhee, J. Reichert, and E.B. Spangler .....	21
OVERVIEW OF ROAD METER OPERATION IN MEASURING PAVEMENT ROUGHNESS, WITH SUGGESTED IMPROVEMENTS (Abridgment) M. Sayers and T.D. Gillespie .....	29
BETTER METHOD FOR MEASURING PAVEMENT ROUGHNESS WITH ROAD METERS M. Sayers and T.D. Gillespie .....	35
ROAD ROUGHNESS: ITS EVALUATION AND EFFECT ON RIDING COMFORT AND PAVEMENT LIFE A.A.A. Molenaar and G.T. Sweere .....	41
REFLEX-PERCUSSIVE GROOVES FOR RUNWAYS: ALTERNATIVE TO SAW-CUTTING Satish K. Agrawal and Hector Daiutolo .....	49
EFFECTS OF GROOVE SPACING ON BRAKING PERFORMANCE OF AN AIRCRAFT TIRE Satish K. Agrawal and Hector Daiutolo .....	55
EFFECTS OF DIFFERENTIAL PAVEMENT FRICTION ON THE RESPONSE OF CARS IN SKIDDING MANEUVERS Gordon F. Hayhoe and John J. Henry .....	61
GROOVE-DEPTH REQUIREMENTS FOR TINE-TEXTURED PAVEMENTS John E. Grady and William P. Chamberlin .....	67
SHORT-TERM, WEATHER-RELATED SKID RESISTANCE VARIATIONS Barry J. Hill and John J. Henry .....	76
ECONOMIC FACTORS RELATED TO RAISING LEVELS OF SKID RESISTANCE AND TEXTURE Don L. Ivey and W. Frank McFarland .....	82

## Authors of the Papers in This Record

---

- Agrawal, Satish K., Technical Center, Federal Aviation Administration, Atlantic City Airport, NJ 08405  
Burns, John C., Testing Engineers—San Diego, 3467 Kurtz Street, P.O. Box 80985, San Diego, CA 92138  
Chamberlin, William P., Engineering Research and Development Bureau, New York State Department of Transportation, 1220 Washington Avenue, State Campus, Albany, NY 12232  
Daiutolo, Hector, Technical Center, Federal Aviation Administration, Atlantic City Airport, NJ 08405  
DeFrain, L.E., Michigan Department of Transportation, P.O. Box 30050, Lansing, MI 48909  
Gillespie, Thomas D., Highway Safety Research Institute, University of Michigan, Ann Arbor, MI 48109  
Grady, John E., Engineering Research and Development Bureau, New York State Department of Transportation, 1220 Washington Avenue, State Campus, Albany, NY 12232  
Hayhoe, Gordon F., Pennsylvania Transportation Institute, Pennsylvania State University, Research Building B, University Park, PA 16802  
Hegmon, R.R., Federal Highway Administration, U.S. Department of Transportation, 400 Seventh Street, S.W., Washington, DC 20590  
Henry, John J., Pennsylvania Transportation Institute, Pennsylvania State University, Research Building B, University Park, PA 16802  
Hill, Barry J., Pennsylvania Transportation Institute, Pennsylvania State University, Research Building B, University Park, PA 16802  
Hudson, W.R., College of Engineering, University of Texas at Austin, Austin, TX 78712  
Ivey, Don L., Texas Transportation Institute, Texas A&M University, College Station, TX 77843  
McFarland, W. Frank, Texas Transportation Institute, Texas A&M University, College Station, TX 77843  
McGhee, K.H., Virginia Highway and Transportation Research Council, Box 3817, University Station, Charlottesville, VA 22903  
Molenaar, A.A.A., Department of Civil Engineering, Laboratory for Road and Railroad Research, Delft University of Technology, 4 Stevinweg, Delft, the Netherlands  
Reichert, J., Centre de Recherches Routieres, Boulevard de la Woluvre 42, W1200 Brussels, Belgium  
Sayers, Michael, Highway Safety Research Institute, University of Michigan, Ann Arbor, MI 48109  
Spangler, Elson B., K.J. Law Engineers, Inc., 23660 Research Drive, Farmington Hills, MI 48024  
Sweere, G.T., Department of Civil Engineering, Laboratory for Road and Railroad Research, Delft University of Technology, 4 Stevinweg, Delft, the Netherlands  
Wambold, James C., Pennsylvania Transportation Institute, Pennsylvania State University, University Park, PA 16802



# Road Roughness: Its Elements and Measurement

W.R. HUDSON

The purpose of this paper is to summarize the importance of rational and compatible measurements of road roughness and to point out some of the problems of and possible methods for making such compatible measurements. Some ideas are also set forth for a general roughness index that could be used on a worldwide basis for comparing roughness of both paved and unpaved surfaces and for evaluating both road serviceability and vehicle operating costs. It is intended to provide an assessment of the current state of the art and a comparative evaluation of alternative surface (paved and unpaved) roughness measurement methodologies, with particular attention to evaluating and using the important relationships between vehicle operating costs and road surface condition. There is a need for a common scale for measuring roughness. First, we must be able to compare results of research on vehicle operating cost relationships from several research studies (for example, in Kenya, Brazil, and India) and to evaluate the magnitude and nature of errors associated with applying relationships developed in one country to other countries. Second, if we apply the vehicle operating costs and road deterioration relationships to other countries (which is already being done), then we obviously need to measure roughness on a common scale.

One of the primary operating characteristics of a road, whether paved or unpaved, is the level of service that it provides to its users. In turn, the variation of this level of service or serviceability with time provides one measure of the road's performance. This performance, and the cost and benefit implications thereof, are the primary outputs of a pavement management system. In 1960, Carey and Irick (1) showed that surface roughness was the primary variable needed to explain the driver's opinion of the quality of the serviceability provided by a pavement surface, (i.e., its desirability for use). More recently, research has shown that user costs are also related to roughness, particularly on rougher-paved and unpaved roads. The Kenya highway design standards study, conducted by the Transport and Road Research Laboratory (TRRL) and the World Bank from 1971 to 1975 demonstrated the relation of vehicle operating costs to road roughness (2). Preliminary results of a similar study in Brazil give the same general conclusions.

What is road roughness and how can it best be defined? Some people talk about smoothness; others, serviceability. The Canadians talk of riding comfort, and there are national committees in the United States to evaluate riding quality. Still others talk of surface profile. In the European committees of the Permanent International Association of Road Congresses (PIARC), the English term roughness translates as unevenness, because their literal translation of roughness has come to be associated with surface texture and skid resistance or hydroplaning. In this paper, road roughness and smoothness are defined as being opposite ends of the same scale. A general definition of roughness must describe those surface characteristics of a pavement that affect vehicle operating costs and the riding quality of that pavement as perceived by the highway user.

The measuring of roughness is important in terms of evaluating road surfaces and their performance. It is also very important in terms of evaluating vehicle operating costs, as outlined above. The accuracy in measurement required for these various purposes may vary, as it may also vary between very rough roads (such as gravel and earth roads) and relatively smooth, or paved, roads. In the face of these diverse needs, it is important that a compatible roughness scale be made available for worldwide use.

## NEED FOR COMPATIBILITY OR GENERALITY

Diverse measurements of roughness are used around the world. Comparison of equality among these measurements is not feasible because no roughness measuring system is capable of giving equal results for all conditions. Rather, it is essential to ensure that we have compatible measurements. Given proper consideration, compatibility among the various measuring systems can be provided. This compatibility involves two levels of concern:

1. External compatibility, which is related to whether the results of one agency's or country's work have a quantitative relationship or meaning with those of another agency or country, and
2. Internal compatibility, which is related to correlation of results and repeatability, within an agency or country.

This second aspect of compatibility is well illustrated by the Brazilian project. It is essential that all measurements made in Brazil be compatible with each other, even though it is not possible to make all the measurements with a single instrument.

As an illustration of the problem of external compatibility, results of studies in Kenya can be compared with the findings in Brazil only if the two sets of roughness data are compatible. It will be important to compare data from Kenya, Brazil, and India to examine transferability of data. This can best be accomplished by establishing a General Roughness Index (GRI) that can be used as a compatible base of comparison. This is preferable to selecting any particular measurement system, which itself may be changing and may not be available to a particular potential user agency.

If a GRI is used, then the matter resolves to the providing of a way to determine the GRI in a particular instance.

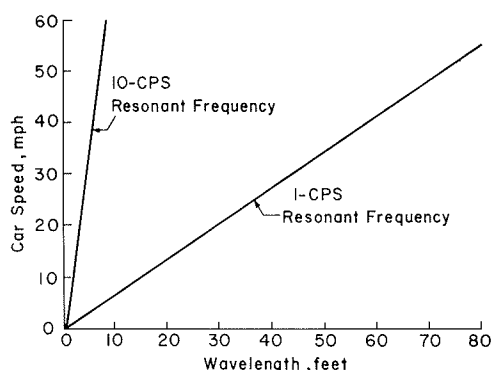
## ROAD ROUGHNESS

Road serviceability, or riding quality, is largely a function of road roughness. Studies made at the American Association of State Highway Officials (AASHO) road test (1) have shown that about 95 percent of the road user's perception of the serviceability of a road results from the roughness of its surface profile. That is to say, the correlation coefficients in the present serviceability index (PSI) equation studies improved only about 5 percent when other factors were added (1) to the index. Hveem discusses this problem in several papers (3). He states that "there is no doubt that mankind has long thought of road smoothness or roughness as being synonymous with pleasant or unpleasant." New economic engineering research has shown that the effect of roughness on transportation costs may be more important than the effect on riding comfort. This aspect is of overwhelming importance in low-income, developing countries. Roughness of the road surface is not easily described or defined, and the effects of a given degree of roughness vary considerably with the speed and characteristics of the vehicle that uses the road.

### Definition of Roughness

Road roughness is a phenomenon that results from the

Figure 1. Relation among resonant frequencies of cars, car speed, and pavement surface wavelength.



interaction of the road surface profile and any vehicle that travels over that surface. It is experienced by the vehicle, its operator, and any passengers or cargo. Roughness is a function of the road surface profile and certain parameters of the vehicle, including tires, suspension, body mounts, and seats as well as of the sensibilities of the passengers and driver to acceleration and speed.

Hudson and Haas (4) refer to "pavement roughness" as the "distortion of ride quality." This definition is intended to refer to the road surface, whether paved or unpaved. Safety considerations influence the acceptance of roughness, and the important economic aspects of roughness on vehicle operating costs should be recognized. For this paper, the following definition of road roughness is suggested: the distortion of the road surface that contributes to an undesirable, unsafe, uneconomical, or uncomfortable ride. A slightly different definition might be as follows: the distortion of the road surface that imparts undesirable vertical accelerations and forces to the vehicle or to its riders and thus contributes to an undesirable, uneconomical, unsafe, or uncomfortable ride.

A rider in a vehicle that passes over a road surface experiences a ride sensation. This ride sensation is a function of (a) the longitudinal road profile, (b) the vehicle parameters, and (c) the vehicle speed. A variation of any one of these three variables can make a rough road profile appear smooth or rough. Therefore, we might say that, from a passenger's viewpoint, roughness is an undesirable combination of road profile, vehicle parameters, and speed. Riding characteristics of airplanes are also affected by the properties of airfield surfaces and of the aircraft. Vertical accelerations of sufficient magnitude to critically affect safety of aircraft operations are sometimes obtained over poor surfaces.

Most drivers have experienced the sensation of improving a ride on a particular road by either slowing down or speeding up. This indicates that the road surface profile contains roughness waves or undulations of a length that, when driven over at a particular speed, produce an excitation in the vehicle at one of the vehicle's resonant frequencies. Since a normal vehicle is a simple mechanical vibrating system made up of the mass of the vehicle, the springs on which it rides, and the shock absorbers, at a particular frequency of vibration or bouncing of any vehicle, the vibrations tend to increase in amplitude. This is normally called the resonant frequency. The typical passenger car has resonant frequencies of between 1 and 10 cycles/s (Figure 1). This relationship indicates that, at

any particular speed of travel, there is a road profile wavelength that will excite the vehicle at one of its resonant frequencies and thus cause excessive vibration or bouncing. If the amplitude of that resonant wavelength is large, the vibration or vertical accelerations imparted to the vehicle may be quite noticeable. Since vertical accelerations impart significant vertical force, these wavelengths result in significant forces applied to the vehicle, which can result in damage to vehicle components and increased operating costs, as well as in an unsafe and uncomfortable ride.

In general, most vehicles in a particular class (e.g., passenger cars as one class and trucks as another class) possess similar characteristics and, for any particular road surface, most vehicles in the same class will be driven at about the same speed. With two of these variables held relatively fixed, the excitation of the vehicle, and thus the riding quality and vertical forces on the vehicle, becomes primarily a function of the wavelength content of the road profile surface.

### Evaluation

Roughness evaluation has received considerable attention from many highway and airport agencies in North America in the last three decades. Roughness is the primary component of pavement serviceability, and a large number of different roughness measures are in current use to evaluate such serviceability. Some of the more widely used methods for measuring roughness, correlating measurements, and applying the results are outlined elsewhere (5). Many of these measurements have involved roughness perception by the highway user as a very important factor, and thus roughness measurements have generally excluded surface texture and microtexture of surface aggregates because these are not perceived by the user to affect riding comfort.

The diameter of surface stone used in gravel and surface-treated roads that causes noise discernable to the user does have an effect on user perception and affects road roughness by this definition. It is not yet known whether these kinds of microvariations affect vehicle operating costs and safety.

### Road Profile

Many authors, such as Darlington (6) and Carey (7), think that pavement profile does the best job of characterizing roughness. In terms of pavement profile, roughness can be defined as the summation of variations in the surface profile of the pavement. Profiles in this sense do not include the overall geometry of the road but are limited to wavelengths in the surface of the pavement between approximately 0.031 and 152.4 m (0.1 and 500 ft) in length. In Darlington's terms, roughness is "the analysis of the pavement profile or of the random signal known as profile."

Carey (7) points out four fundamental uses of pavement surface profiles or roughness measurements:

1. To maintain construction quality control;
2. To locate abnormal changes in the highway, such as drainage, subsurface problems, or extreme construction deficiencies;
3. To establish a systemwide basis for allocation or road maintenance resources; and
4. To identify road serviceability-performance life histories for evaluation of alternative designs.

In summary, then, a road profile is a detailed recording of surface characteristics, and roughness or smoothness is a statistic that summarizes these

characteristics and provides a measure of riding quality of a road.

Once the surface characteristics of a road are summarized, it is essential to establish a scale for this statistic, or summary, value. This can be done in many ways, as pointed out by Darlington (6). Traditionally, the two basic ways of determining this statistic are

1. Mechanical integration and
2. Mathematical integration or analysis.

The first of these methods is the most common; that is, the use of some mechanical instrument or device such as the Bureau of Public Roads (BPR) Roughometer (Figure 2) or TRRL Bump Integrator to mechanically filter and summarize the data in a specified way. The second method involves recording the profile as faithfully as possible and then analyzing or integrating this profile mathematically with some standard mathematical procedure, such as that outlined by Walker and Hudson (8,9), Roberts and Hudson (10,11), Quinn (12), and Darlington (6). The most common methods in current use for mechanical measurement and summary include the BPR Roughometer (13,5), the very similar TRRL Bump Integrator (14), the Portland Cement Association (PCA) Roadmeter (15), the Mays Meter (9,16), the Carey Hucks, Leathers, and other Engineers (CHLOE) Profilometer (17), and the land plane, Profilograph, or rolling straightedge (Figure 3) (17). A number of studies have been made to compare these instruments, as outlined elsewhere (5,6).

A word of elaboration is needed on the term mechanically filtered, outlined above for the BPR Roughometer. Instruments such as the BPR Roughometer, the PCA Road Meter, and the Mays Meter use the vehicle itself as a mechanical filter for processing the profile and summarizing, in effect, the response of a particular vehicle (in its specific condition) to the road profile.

If the mechanical characteristics of the measuring vehicle could be set and maintained at a desired preselected level, then the resulting summary statistics could be directly related to the economics or safety of a specific vehicle class. Unfortunately, due to the many parameters and the great variability involved, the use of the Bump Integrator or BPR Roughometer results, rather than the profile itself, introduces great measurement and analytical complications.

Since so much has been written about the various instruments available, we will not attempt in this short paper to review all these measurement methods in detail. Summaries are included elsewhere (5,18).

#### COMPARISON OF MEASUREMENT AND SUMMARY TECHNIQUES

Regardless of the type of measurement and summary techniques used, it is essential that a good reference be established and maintained. It is equally important that accuracy in summation be maintained. Every different instrument has a different readout scale, and even seemingly identical instruments must be calibrated so that the observed readout is meaningful. This readout scaling and consistency are central to this paper.

Darlington (6) points out that three basic reference methods have been used historically:

1. A so-called rolling straightedge, or land plane, as illustrated in Figure 3;
2. An inertial mass, as used in the BPR Roughometer (Figure 2), the Mays Meter, and the PCA Road Meter (in the latter two cases, the automobile forms the inertial mass); and

3. An inertial reference profilometer, such as the Surface Dynamics or General Motors Profilometer, where an external reference is provided.

Figure 4 illustrates by means of a Bode plot the transfer function or response of several types of profilometers to the input of road roughness. The problem is that the straightedge, or land plane device, is so erratic in its response as to be relatively useless. The course shown in Figure 4 reflects that roughness wavelengths that are any multiple of the length of the straightedge result in zero output from the device.

Darlington simulated the response of the BPR Roughometer, vibrometer, or seismic reference device (whichever you prefer to call it) on an analog computer, by using measured physical characteristics of the instrument. His analysis shows that the roughometer-type device yields reasonable results for wavelengths in the range of 1.22-4.26 m (4-14 ft). Wavelengths in the range of 4.26-5.48 m (14-18 ft) are badly distorted, and wavelengths beyond 6.70 m (22 ft) rapidly attenuate to zero effect.

Figure 2. Schematic diagram of BPR roughometer.

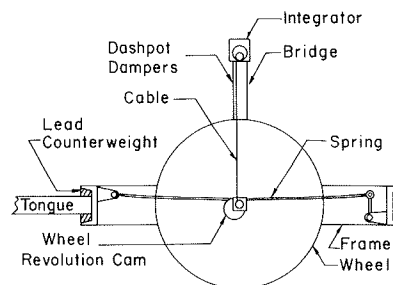


Figure 3. Land plane roughness device sometimes called profilograph or rolling straightedge.

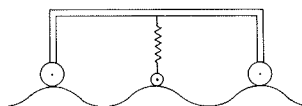


Figure 4. Theoretical differences between SD Profilometer, CHLOE, rolling straightedges, and seismic roughometer.

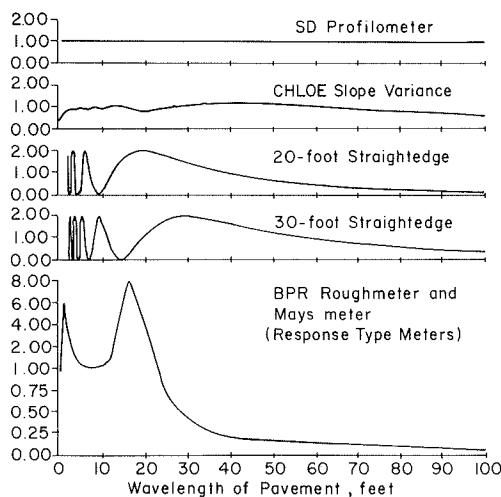
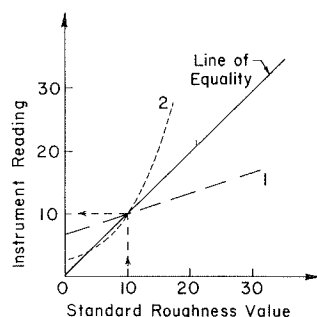


Figure 5. Single-Point BPR calibration problems.



#### ROUGHNESS CALIBRATION AND CORRELATION

The earliest roughness measurements were reported by Hogentogler as far back as 1923. Early development of the Roughometer was reported in 1926 (19). Even in these early developments, the need for calibration was readily recognized. From 1941, when the BPR Roughometer became standardized, BPR (now the Federal Highway Administration) maintained a standard calibration section for testing any new or modified BPR Roughometer. It was observed from the beginning that instruments manufactured as nearly alike as possible did not record the same roughness value for the same pavement. The fallacy of this calibration section is discussed by Hudson and Hain (13).

It is not possible to calibrate a dynamic instrument at a single point over its range and expect the calibration to be satisfactory for use of the instrument over a full range of roughness. This is illustrated in Figure 5, where a standard roughness section that has a value of 10 has been set up. We might assume that any other instrument that reads 10 would be calibrated to the standard value. In fact, this assumption is depicted by the solid line of equality in the figure. This line assumes that, if an instrument reads 10, it is calibrated and thus will read 20 when the standard instrument reads 20, and 30 when the standard instrument reads 30. Alternatively, line 1 illustrates a plausible case of a linear relationship, where instrument 1 is calibrated to the standard instrument on the section of value 10. Without additional test points we would not realize that the slope of the calibration line is really different from the assumed line of equality. Dashed line 2 illustrates a more complex case of nonlinear relationship that would, of course, also be missed with the single-point calibration.

#### Roughometer Calibration Course: AASHTO Road Test

As reported by Hudson and Hain (11), there was a need to use the Roughometer in the AASHTO road test. But, it became obvious very early, with the AASHTO Profilometer as a comparison, that the BPR Roughometer was a variable instrument difficult to keep in calibration. In work at the AASHTO road test we were not only involved in measuring the roughness of all pavement with the AASHTO Profilometer and in developing and operating the BPR Roughometer, but we also checked and calibrated at least six additional roughometers from states such as Michigan, North Dakota, Minnesota, and Wisconsin, which brought their instruments to the road test for calibration against the AASHTO Profilometer for determining serviceability.

Basically, the method involved the installation of aluminum bars on the surface of a smooth rigid

pavement to establish four separate test sections of different but known roughness. The roughometers could then be checked against the standard sections at any required time.

#### TRRL Pipe Calibration Course

Another artificial calibration technique has been proposed and used by TRRL in England. This concept appears to have promise for use as a calibrating device or standardization method around the world. Briefly, the method involves the selection of a smooth, standard pavement section approximately 300 m (985 ft) long. This smooth section becomes the smoothest section in a series of calibration sections. Subsequent rough sections are created by adding artificial bumps to the surface of the standard section by means of pipes that have an external diameter of 3.413 cm (1.344 in). A total of six levels of roughness are created. Thus, the problem of one-point calibration is alleviated and yet the calibrating agency need find only one smooth, relatively unchanging pavement section. The absolute profile of this basic smooth standard section can likewise be checked with precise rod and levels on a quarterly or semiannual basis, as necessary.

This method has great attraction and may be a practical all-around method, but it also has pitfalls that make it fall short for ultimate use. For example, all of the roughness introduced in this way is artificial roughness of a step-input nature, whereas much of the roughness in a normal road profile is composed of a combination of sinusoids. As pointed out by Darlington (6), these real profiles lend themselves to analysis by a variety of analytical methods. The step-input roughness of the TRRL calibration track does not yield to analysis so readily. Nevertheless it is a practical method and a prime candidate for consideration. The other major observation relates to use of the method. To date it has been used primarily as a calibration tool for the towed one-wheel trailer Bump Integrator or BPR Roughometer-type device, and apparently works well for this situation. The problems of using the method on an automobile-mounted device, such as the Mays Meter, where all four wheels of the vehicle and the resulting vehicle motions will become involved, are yet to be determined. Finally, as pointed out in the Bode plot or transfer function for the BPR Roughometer, that the instruments respond and stay calibrated in wavelengths from 1.22 to 4.28 m (4 to 14 ft) does not tell us how they will respond at other wavelengths. Note from the computer simulation of Darlington that the response of the instrument to step-inputs should be on the first peak (i.e., very short wavelengths). If some type of resonance is generated in the measurement system, say for roughness level six, then the multiplication amplitude could be even higher. Nevertheless, this method certainly bears further evaluation.

#### Use of a Standard Device for Calibration

Probably the most widely used method of calibration and correlation has involved some type of so-called standard device. Really, this approach should be divided into two parts. The first involves the selection of one replicate from a group of similar devices being used and using this copy of the device for calibration purposes, so that it presumably does not wear out. I liken this approach to gold plating a crowbar. If you have two dozen crowbars and select the one that appears to be more perfect in shape and weight than any of the others and plate it with gold as a reference, what do you have? Still a crowbar, albeit a shiny and expensive one.

The only validity of this approach is lack of wear in routine use. However, many of the errors we must deal with do not result from wear alone. There is little evidence that this type of standard device has been successful in use for calibration and correlation.

The second part involves the use of a master device, which is itself calibratable or has a standard of accuracy that is perhaps a magnitude greater than the other devices for which it is to be the master control. The AASHO Road Test Profilometer was such a device; it became a standard against which dozens of CHLOE Profilometers and BPR Roughometers were calibrated during and soon after the AASHO road test. This approach is discussed below as the Texas calibration course.

#### Use of Hydraulic Shaker Table

The General Motors (GM) profilometer was originally developed for obtaining road profile input that could be fed into a vehicle-ride simulator for testing vehicle suspensions at the GM proving ground (20, 21). Some authorities think that a similar approach can be used for inputting standard roughness to a machine in an analytically controlled manner to calibrate other devices. This method involves observing the responses in a laboratory of a wheeled measuring device that has a servo-controlled hydraulic ram resting under each wheel. Known excitation is applied through the hydraulic rams to the device to determine its response. More specifically, the wheels of the device are vibrated by the shaker table in a manner to simulate operation of the device on each of a set of standard test sections. Road profile data obtained with an instrument such as the GM Profilometer are used to drive the shaker table. The profile data tape could be used for any number of successive recalibrations over any period of time and, in that sense, would never change.

There is, of course, some question about the correspondence between readings obtained by using a shaker table and roughness measurements obtained in the field. The major source of discrepancy remains in the fact that the vehicle is normally moving and the wheels are rotating while measurements are being made in the field but not while it is on a shaker table. The dynamic versus static tire conditions are of particular concern. The National Cooperative Highway Research Program (NCHRP) has just completed a research project that has investigated the shaker table approach to calibration of roughness devices. In general, this method does not seem feasible for use worldwide because the shaker table is cumbersome and expensive.

#### Texas Calibration Course With Surface Dynamics Profilometer

The Center for Transportation Research and the Texas State Department of Highways and Public Transportation use the Surface Dynamics Profilometer (SDP) or GM Profilometer as a master calibration device for a series of Mays Meters that are used routinely throughout the state. This approach is reported by Walker, Hudson, and Williamson (9,16,22). To some degree, a similar approach has been taken by the Michigan Highway Department, as reported by Holbrook and Darlington (23). A similar approach is also being taken at the present time in the United Nations Development Program Brazil study (24). A SDP was purchased and is used for measuring a set of calibration sections. These sections are run regularly by four Mays Meters to ensure that their calibration remain stable. A control chart proce-

dures and regular check procedure similar to that outlined by Williamson are followed.

Basically, Texas maintains a group of 25 pavement sections that together exhibit a range of roughness. Every three months the profile of each of these sections is measured and analyzed with the SDP. In this way a set of pavements with known roughness is always available for use in checking and calibrating any other roughness instrument. Any instrument that appears to be giving erroneous readings is run regularly on several check sections and the values are plotted on a typical control chart. If a device is out-of-control on three or four sections, it is thoroughly checked mechanically and recalibrated.

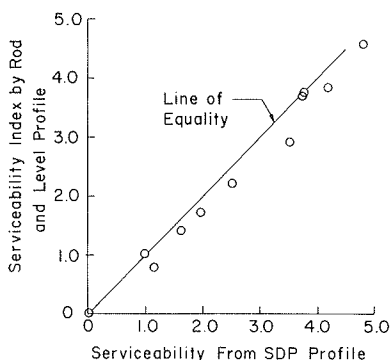
#### Rod and Level Surveys

Many people think that it is possible to establish vehicle roughness calibrations over standard pavement sections by running control rod and level surveys of the calibration sections to see if and how their profiles are changing. There are two basic problems associated with this methodology. First, the response of the vehicle and most roughness measuring instruments to a profile is an integration of everything the measuring instrument sees on the road surface. This is a continuous process and not one that involves discrete points such as are used in a rod and level survey. This problem is magnified because even the best manual leveling techniques make it expensive to make measurements of test sections 300 m (985 ft) long at spacings closer than about 0.5 m (1.6 ft). Even in this case, a total of 600 measuring points is required each time a calibration section is checked.

Perhaps more difficult than the accuracy and the detailed problem outlined above is the need to integrate and summarize and analyze the profile. To date, little has been done in this area. Recently, we have investigated the use of second derivatives of the profile to yield estimates of vertical accelerations present in the profile. A relationship has, in turn, been developed between vertical accelerations and serviceability index (SI).

Calculations are simple and do not require a large computer facility, as do existing profile analysis methods, such as power spectral density, Fourier transform, and digital filtering. Road profile root-mean-square vertical accelerations have a strong correlation with Mays Meter roughness readings, and they have been employed successfully as a Mays Meter calibration standard in Texas (25). Figure 6 illustrates a very good agreement in terms of SI from 10 road surface profiles obtained by rod and level method and the SDP. This plot also suggests that road profile data from rod and level and

Figure 6. Comparison of SIs derived from rod and level profile and SDP profile.



SDP are interchangeable and that rod and level can be used to provide commonality among road roughness scales currently in use.

Certainly these discrete rod and level surveys have some practical advantages, particularly in developing countries where labor-intensive methods are economical. It might be far more practical to obtain detailed, discrete profiles with rod and levels of, say, 10 or 12 pavement test sections on a regular basis than to maintain a high-technology, expensive electronic device for continuous profile measurements. Such a method will be practical if data analysis techniques can be developed and automated for easy use of the data.

#### Rating Panel Approach: Canadian Good Roads Association

Immediately following the AASHO road test, the Canadian Good Roads Association wanted to put the findings of the AASHO road test into practice. In order to do this, they thought it was essential to run a complete survey of the existing roughness of their pavement system. They did not agree totally with the serviceability concept outlined at the AASHO road test and they chose to develop a riding-comfort index scale from 1 to 10. This index is basically an evaluation of pavement riding quality or roughness (26).

After they carefully established their riding comfort index, a standard procedure was adopted by using a small panel of well-trained raters to go from location to location and evaluate the riding quality of these pavements and record this riding quality in a data management system. A great deal of work has been done on rating scales and other subjective evaluation (1,10,27-30). There are some shortcomings to this approach, but it has the benefits of being practical, relatively inexpensive, and reasonably stable, although its detailed accuracy may be questioned. This approach deserves further consideration.

#### Standard Rating Panel

Although it is not in current use, I believe that the concept of using a standard panel of pavement-riding-quality raters to establish a time-and-condition-stable standard roughness scale offers promise as a practical solution. Yoder and Milhous (18) show in their studies of rating panels and various instrumentation that rating panels of 15 persons or more are quite stable in predicting pavement serviceability. Since roughness is so highly correlated with serviceability, there is little doubt that the panel would be equally stable in predicting pavement roughness. Carey and Irick (1) report similar results when comparing panels at the AASHO road test, as do Roberts and Hudson (10,11).

One major problem exists: What about panels from different cultures? For example, a panel from the United States rides predominately on paved roads. Can it rate accurately on the same scale used by a panel from a developing country, who rides predominately on gravel roads? How could this dichotomy be solved? If as many as three common members could be made available to participate in panel ratings in each of the major areas of the world, then I believe adequate geographic and cultural stability could be obtained.

This method will never have the precision or detail of physical calibration; however, it could help ensure that different classes or road roughness are adequately separated with a good degree of confidence.

#### DISCUSSION OF RESULTS

Ultimately, the best practical approach that can be used to provide a GRI may involve some combination of the factors discussed above. For example, a GRI could be set up that has a scale based on second derivatives of a rod and level profile such that, for example, the number of vertical accelerations that exceed some specified value might be used as an indicator of the GRI or roughness number. In such cases, the pavement sections might be surveyed with a rod and level once or twice a year to provide objective support for this subjective rating.

Major problems with the roughness rating approach are the possibilities of cultural differences among countries, as discussed above. There is considerable concern that these cultural or historic differences, which are also, by the way, aggravated by traditional types and quality of vehicles used, would affect any relationship developed by a rating scheme and thus would completely invalidate the concept of relative ratings.

I feel, however, that, as suggested previously, reasonable roughness ratings could be established and that the problem of comparing one rating panel with another could be alleviated by ensuring that basic rating panels, at least among major research efforts, have at least three members in common in the initial stages of development. These common members could be employees or advisors of the World Bank or other research personnel who would be involved in one or more of the research projects and who could visit the other activities to provide the necessary commonality of ratings.

At the present time, no roughness measuring and evaluation technique exists that alone is constant enough to become the appropriate standard. The SDP might be considered, but work in adopting and using this instrument in Brazil and in comparing it with the Texas instrument manufactured 10 years ago shows considerable difference in hardware and data processing techniques. Many people feel we are on the threshold of developing a noncontact probe to replace the road-following wheel. Thus, the standard would change again. Many other examples could be cited, but for simplicity let it suffice to say that no real standard exists.

Similar problems exist with the TRRL laser profilometer, the Swedish device, the automatic road analyzer (ARAN) unit, and others. All have potential but none has generality and stability at the present time.

#### SUMMARY AND RECOMMENDATIONS

The purpose of this paper has been to set forth information on the elements of roadway roughness and its measurement. As pointed out, the major problem associated with such use is the problem of providing simple, direct, and relatively inexpensive roughness measurements that remain stable from day to day, year to year, and country to country around the world. A number of seemingly simple devices exist, but close examination of the devices in service, as pointed out here, shows many deficiencies in practice.

Efforts should continue in this important area, but a coordinated funded effort is needed to develop the high quality of measurement equipment and calibration techniques required for regular effective worldwide use. Support for this research effort is strongly solicited.

#### REFERENCES

1. W.N. Carey, Jr., and P.E. Irick. The Pavement

- Serviceability-Performance Concept. HRB, Bull. 250, 1960, pp. 40-58.
2. H. Hide, S.W. Abayanayaka, I. Sayer, and R.J. Wyatt. The Kenya Road Transport Cost Study: Research on Vehicle Operating Costs. Transport and Road Research Laboratory, Crowthorne, Berkshire, England, TRRL L. R672, 1975.
  3. F.N. Hveem. Devices for Recording and Evaluating Pavement Roughness. HRB, Bull. 264, 1960, pp. 1-26.
  4. R.G. Haas and W.R. Hudson. Pavement Management Systems. McGraw-Hill, New York, 1978.
  5. State of the Art of Pavement Condition Evaluation. In Rigid Pavement Design Research on Skid Resistance Pavement Condition Evaluation, HRB, Special Rept. 95, 1968, pp. 49-68.
  6. J.R. Darlington. Evaluation and Application Study of the General Motors Corporation Rapid Travel Profilometer. Michigan Department of State Highways, Lansing, Rept. R-731, April 1973.
  7. W.N. Carey, Jr. Uses of Surface Profile Measurements. In Pavement Evaluation Using Road Meters, HRB, Special Rept. 133, 1973, pp. 5-7.
  8. R.S. Walker and W.R. Hudson. Practical Uses of Spectral Analysis with Surface Dynamics Road Profilometer. HRB, Highway Research Record 362, 1971, pp. 104-119.
  9. R.S. Walker and W.R. Hudson. A Correlation Study of the Mays Road Meter with the Surface Dynamics Profilometer. Research Rept. 156-1, Center for Highway Research, University of Texas at Austin, Aug. 1972.
  10. R.L. Roberts and W.R. Hudson. Pavement Serviceability Equations Using the Surface Dynamics Profilometer. Research Rept. 73-3, Center for Highway Research, University of Texas at Austin, April 1970.
  11. F.L. Roberts and W.R. Hudson. Pavement Serviceability Equations Using the Surface Dynamics Profilometer. In Improving Pavement and Bridge Deck Performance, HRB, Special Rept. 116, 1971, pp. 68-79.
  12. B.E. Quinn and J.L. Zable. Evaluating Highway Elevation Power Spectra from Vehicle Performance. HRB, Highway Research Record 121, 1966, pp. 15-26.
  13. W.R. Hudson and R.C. Hain. Calibration and Use of the BPR Roughometer at the AASHO Road Test. In AASHO Road Test Technical Staff Papers, HRB, Special Rept. 66, 1961, pp. 19-38.
  14. W.G. Keir. Bump-Integrator Measurements in Routine Assessment of Highway Maintenance Needs. Transport and Road Research Laboratory, Crowthorne, Berkshire, England, TRRL Supplementary Rept. 26UC, 1974.
  15. M.P. Brokaw. Development of the PCA Road Meter: A Rapid Method for Measuring Slope Variance. HRB, Highway Research Record 189, 1967, pp. 137-149.
  16. R.S. Walker and W.R. Hudson. Method for Measuring Serviceability Index with the Mays Road Meter. In Pavement Evaluation Using Road Meters, Special Rept. 133, 1973, pp. 68-72.
  17. W.N. Carey, Jr., H.C. Huckins, and R.C. Leathers. Slope Variance as a Measure of Roughness and the CHLOE Profilometer. In The AASHO Road Test: Proceedings of a Conference Held May 16-18, 1962, St. Louis, MO., HRB, Special Rept. 73, 1962, pp. 126-137.
  18. E.J. Yoder and R.T. Milhous. Comparisons of Different Methods of Measuring Pavement Condition--Interim Report. NCHRP, Rept. 7, 1964, 29 pp.
  19. An Instrument for the Measurement of Relative Road Roughness. Public Roads, Vol. 7, No. 7, Sept. 1926, p. 144.
  20. E.B. Spangler and W.J. Kelly. Servo-Seismic Method of Measuring Road Profile. HRB, Bull. 328, 1962, pp. 33-51.
  21. E.B. Spangler and W.J. Kelly. GMR Road Profilometer--A Method for Measuring Road Profile. HRB, Highway Research Record 121, 1966, pp. 27-54.
  22. H.J. Williamson, W.R. Hudson, and C.D. Zinn. A Study of the Relationships Between Various Classes of Road-Surface Roughness and Human Ratings of Riding Quality. Center for Transportation Research, University of Texas at Austin, Research Rept. 156-5F, Aug. 1975.
  23. L.F. Holbrook and J.R. Darlington. Analytical Problems Encountered in the Correlation of Subjective Response and Pavement Power Spectral Density Functions. HRB, Highway Research Record 471, 1973, pp. 83-90.
  24. Republica Federativa Do Brasil and United Nations Development Program. Inception Report, Research Concepts and Procedures. Rept. 1 of Research on the Interrelationships Between Costs of Highway Construction, Maintenance, and Utilization, Republic of Brazil, April 1976.
  25. D. McKenzie and M. Srinarawat. Root Mean Square Vertical Acceleration (RMSA) as a Basis for Mays Meter Calibration. University of Texas at Austin, Brazil Project Tech. Memo BR-23, Feb. 1978.
  26. Field Performance Studies of Flexible Pavements in Canada. Proc., Second International Conference on Structural Design of Asphalt Pavements, Univ. of Michigan, Ann Arbor, 1967.
  27. B.G. Hutchinson. Principles of Subjective Rating Scale Construction. HRB, Highway Research Record 46, 1964, pp. 60-70.
  28. V.F. Nakamura and H.L. Michael. Serviceability Ratings of Highway Pavements. HRB, Highway Research Record 40, 1963, pp. 21-36.
  29. R.J. Weaver and R.O. Clark, Jr. Psychophysical Scaling of Pavement Serviceability. Soil Mechanics Bureau, New York State Department of Transportation, Albany, Manual SEM-9, May 1977.
  30. R.J. Weaver. Quantifying Pavement Serviceability as Judged by the Highway Users. New York State Department of Transportation, Albany, (unpublished).

*Publication of this paper sponsored by Committee on Pavement Condition Evaluation.*

# Roughness and Roadway Safety

JOHN C. BURNS

Roughness can play a significant role in roadway accidents and should be considered when evaluating pavement safety as well as when planning and designing safety improvements. Roadway roughness can cause problems with steering, braking, maneuvering, and response that can lead to loss of vehicle control and can result in an accident. In addition, rough pavements can sometimes shake or bounce a vehicle so severely that it will lose part or all of the load it is carrying, which then leads to lost-load accidents. This paper discusses the magnitude of the various problems associated with vehicle performance on rough roads and the types of accidents and safety problems that result. The various individual parameters that cause roughness are examined and their overall effect on safety are prioritized. Examples of corrective actions and their benefits are discussed. In the future additional consideration should be given to this problem and to using safety funds to make rehabilitations that decrease roughness and improve the ride quality and safety of a highway.

For many years the driving public has been keenly aware of the effects of pavement roughness. The driver usually can gage the relative comfort and safety of the road. Comfort factors, however, are more easily identified by engineers and the driving public than are safety factors. Most people recognize the potential for hazardous vehicle-driver-pavement reactions on unusually rough roads, but quantification of the problem and all its variables has not been accomplished and it is difficult to pinpoint why this hazardous condition exists.

For example, Why is the smooth road safer than the rough road and to what degree? In some cases, the level of comfort does not have to be at a very low level to cause safety problems. It may never be possible to quantify all variables that affect this relation, but it is important that the highway official be aware of the underlying key factors and relations that exist in order to deal effectively with these problems. In order to do this, the individual variables that affect the safety of a vehicle driving on the surface of a roadway need to be identified. Numerous variables can be considered; however, this paper will deal with those related primarily to the smoothness or roughness of the roadway surface.

## KEY FACTORS

The condition of a roadway can range from excellent to very poor, depending on the various distress manifestations of the surface. The roughness of a roadway will vary with time and usually follows a trend of decreasing performance with age. Roughness can be caused by many variables, all of which lead to surface irregularities. These irregularities can be created during the original construction or can occur afterward because of cracking, wear, subsidence, or surface degradation. The increase in roughness with time will vary for each roadway depending on its structural qualities, exposure to traffic, and environment. When a roadway becomes extremely distressed and vehicles can no longer travel at reasonable speeds because of extreme roughness, it becomes obvious that a safety problem will occur. Unfortunately, there is a gray zone where roughness levels may be in a fair-to-poor range but may still present a safety problem to the user.

Ivey and Griffin (1) wrote a report several years ago that analyzed and ordered various roadway attributes by level of significance in relation to accidents. This work was based in part on North Carolina's analysis of 15 968 accidents that oc-

curred in the state in 1974 and also by use of the Delphi technique of using a panel of highway and highway safety engineers to evaluate various characteristics. The list below shows the results of this investigation and lists the importance of various road conditions in relation to safety.

1. Pavement edge-shoulder drop-off,
2. Curbs and raised medians,
3. Hydrodynamic drag (standing water),
4. Poor shoulder maintenance (includes soft shoulders),
5. Washboard surfaces,
6. Corrugations due to weak subgrade,
7. Blow-ups of continuously reinforced concrete pavements,
8. Corrugations due to braking at intersections,
9. Expansive clay and shale waves,
10. Frost heave boils,
11. Grade crossings at railroads,
12. Superelevation--too much or too little,
13. Drainage dips on low volume roads,
14. Intersections that cross drainage channels along intersection roads,
15. Patches or absence of patches,
16. Rutting,
17. Joint faulting,
18. Potholes,
19. Depressions or elevations at drainage structures, and
20. Bridge approach slabs.

Note that the washboard and corrugated surfaces were the first two items in the list that actually dealt with the pavement riding surface. In addition, these two items were numbers 5 and 6 on the list as compared with potholes, which were number 18. Thus, washboard or wavy surfaces may have a potentially greater impact on safety than do potholed or patched surfaces. This may be due in part to the possible localized problems of potholes and their usual rapid repair by maintenance crews, as compared to the washboard surface that may be of a lower maintenance priority. In any case, all of the items listed are of concern and should be considered in any pavement safety evaluation.

The following general groups and their effects are presented in order to help analyze the relations that exist.

## Major Distress

Major distress, such as large and numerous potholes or depressions in the pavement, can present a safety problem by physically causing a tire to blow, be totally deformed, or cause large differential forces to be applied to the vehicle that the driver may not be able to correct.

## Loss of Tire-Pavement Friction

This problem can be a major contributor to accidents and is not as easily identified as the problems associated with vehicle damage. The problem with loss of friction or pavement traction is twofold. The first part deals with side force, or cornering frictional components that affect steering. The second part deals with braking or stopping power.



Figure 1. Tire slip angle.

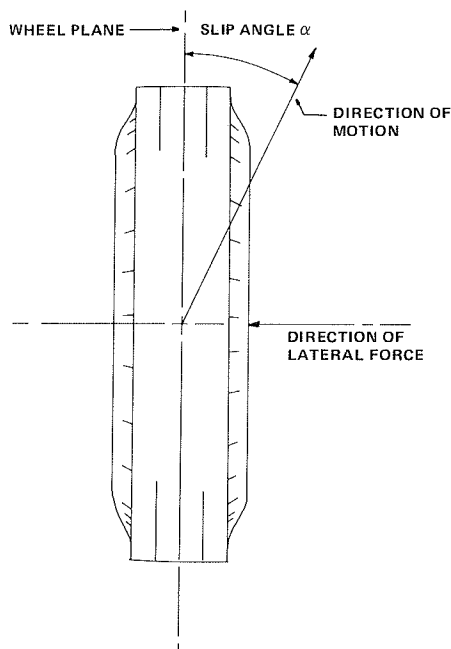
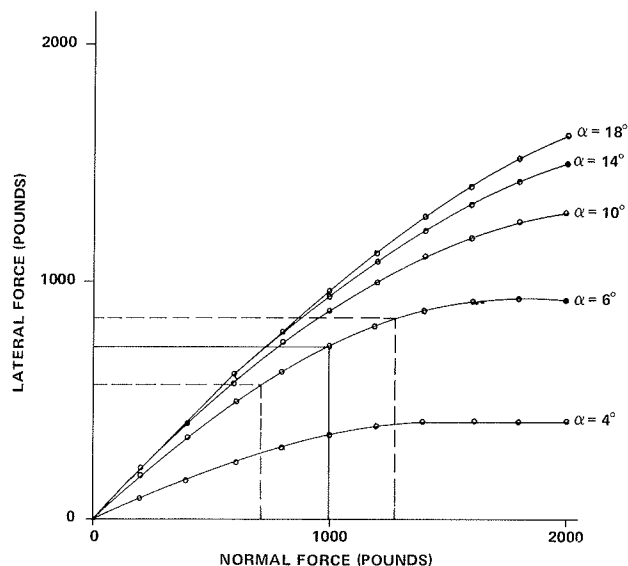


Figure 2. Tire force characteristics.



### Effects on Steering

The roughness of a pavement influences the steering capabilities of a vehicle by changing the normal forces that act at the tire-pavement interface and by affecting the lateral forces needed to control a vehicle. Some of the many factors that will affect steering are vehicle characteristics, cornering, stiffness of tires, vehicle loading, and surface friction. The roughness attributes we will discuss are those that deal with the roadway surface alone.

A driver guides the vehicle down the road by a series of understeer and oversteer inputs. This allows the driver to maintain the vehicle in the desired position on the roadway and to make the necessary turns, lane changes, and other maneuvers necessary to traverse the roadway safely. In order

to make these steering corrections, lateral forces must be generated between the tire and pavement. These are forces that act parallel to the road and at right angles to the axis of the wheel plane. As a result of this side force, the direction of motion is at an angle to the plane, which is called the slip angle. The magnitude of the force that acts at the tire-road interface is dependent on the normal force exerted by the tire and the slip angle. This is usually not a linear relation, and thus changes in loading can have different effects on the steering input necessary for a particular maneuver. Figure 1 shows a typical tire and the side forces acting on it. Figure 2 shows the typical relation among slip angle, normal force, and lateral forces. This example is for a reasonable level of friction, and the effect of a very slippery pavement would be to greatly reduce the values of the lateral force generated. However, in this paper the effect of actual pavement slipperiness is not shown. Figure 2 shows that the relation is nonlinear. For a normal force of 1000 lb and a slip angle of  $6^\circ$ , the lateral force generated is 760 lb.

If the normal force is increased by 300 lb, however, the lateral force will only be increased by 160 lb. This is extremely important to note in evaluating the safety aspects of roughness because if pavement roughness causes the normal force to fluctuate as the tire rises and falls, the resulting average of the lateral force for an average of say 1000 lb normal force will not be 760 lb, but will be less. On relatively smooth pavements, the variation in normal force is very small; however, on rough pavements, these variations can be very large and reduce significantly the lateral force available to control the vehicle. In situations where high lateral forces are necessary or where a vehicle requires a particular lateral friction level to make a maneuver, this loss of force could lead to loss of control of the vehicle.

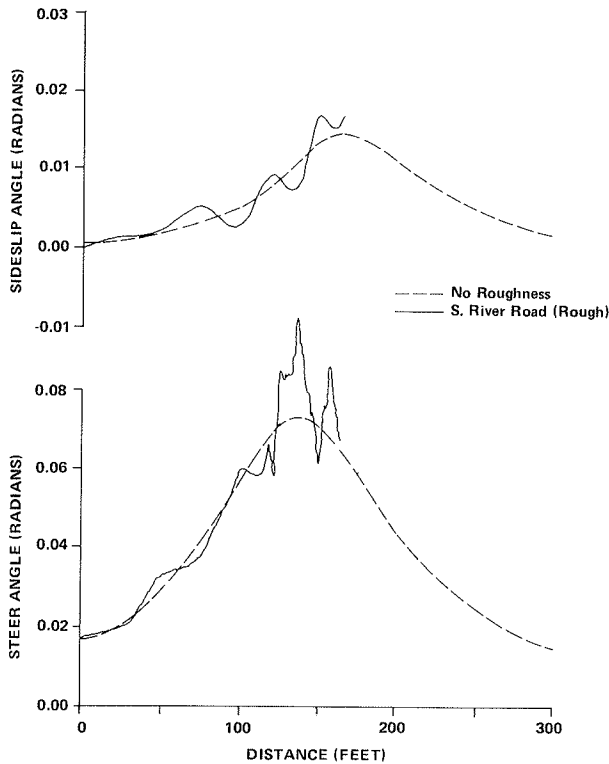
A lot of research has been done in this area. Quinn and Hildebrand (2) reported on the various factors that affect lateral force, and Figure 3 is an example of their findings. It shows the side slip and steer angle necessary to make a  $90^\circ$  turn on smooth and rough pavements. It can be seen that this maneuver is possible on the smooth surface without excessive values or loss of control. On the rough surface, however, this is not true, and there is considerable variation and more steering required. For the rough road, the steer angle and side slip angle curves are terminated at a point where there exists no steer angle that will produce the required forces to hold the vehicle on the desired path. For this study, at that point the vehicle was out of control.

This problem is magnified during turning operations because, as the driver compensates for this loss of lateral force, he or she inputs a greater steer angle. Unfortunately, in many circumstances the road is not uniformly rough. As the driver progresses down the highway and hits a smoother section of pavement, he or she will be oversteering and so must correct back again. If this happens too frequently, the driver cannot respond rapidly enough and will lose control of the vehicle.

### Effects on Vehicle Braking

In addition to the reduction of lateral force on a cornering tire, roughness can also cause significant loss of braking force or slip resistance on a vehicle. Wambold and others (3) conducted research in this area several years ago to determine the effects of roughness on braking force. They studied a range of five roughness amplitudes from 0.041 to 0.707 in,

Figure 3. 90° turn on rough road at 30 mph.

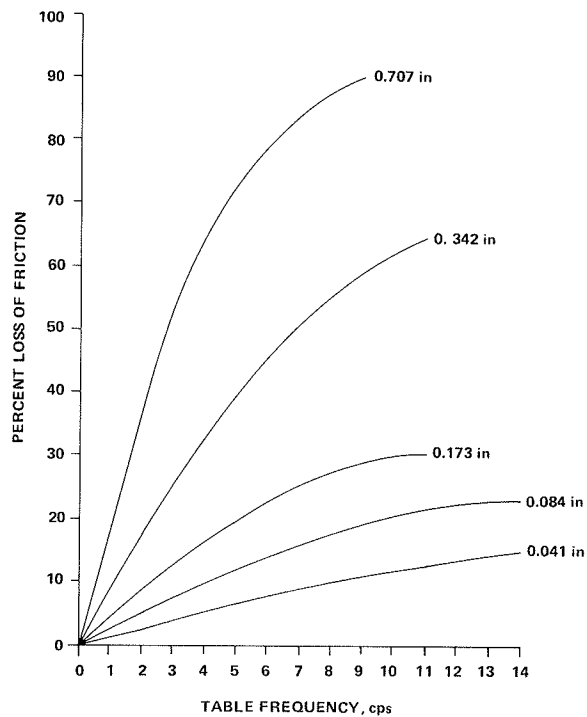


a range of roughness frequencies from 0 to 14 Hz, and three speeds that ranged from 0.18 to 0.46 mph. They found that, as roughness and amplitude increased, the coefficient of friction generated between the tire and pavement in a braking mode decreased. At a small amplitude that produced barely observable gross movements of the tire tread, roughness increased to 14 Hz and caused a 30 percent loss of friction value. When they used low frequency values around 3 Hz and increased roughness amplitude to 0.707 in, they found it caused a friction loss of 60-80 percent, depending on the amplitude.

This reduction in friction is caused by a reduction of actual sliding speed of the tread elements caused by tread windup and also by an overall lowering of the adhesion and hysteresis components of friction. Figure 4 shows an example of the results they developed. Although the sliding speeds tested in the laboratory were low, they depict the relation of how tire-pavement friction is related to roughness without the effects of vehicle suspension interfering.

Under highway braking conditions, the normal force on a tire will change on a rough or undulating roadway. If the roughness is great enough, the tire may lose partial or complete contact. In such cases, the sliding friction component can be reduced almost to zero. When the tire makes full contact with the pavement surface, the additional normal forces will be increased to compensate for the loss of contact; however, the frictional forces generated on renewed contact may not make up for the loss of contact time. This inability to obtain as high a level of friction as might be expected with renewed contact can occur because of the frictional limitations of the pavement surface or because of destructive actions that occur at the tire-pavement interface at high-load, high-friction contacts. In such cases, the tire or pavement is physically damaged

Figure 4. Average loss of friction versus table frequency at nominal load of 400 lb.



and causes the dissipation of energies that would have otherwise been used to stop the vehicle.

In addition to these problems with stopping, other problems can arise because roadway roughness can (and usually does) vary in each of the wheel-tracks of a lane. When a vehicle brakes, these differences in roughness in each wheel path can cause differences in the braking and sliding forces that act on the vehicle. The final result is that the vehicle is exposed to different levels of friction on each side, which can cause a significant safety problem. The effect of differential friction has been studied (4), and the results show that the situation can have a significant effect on a braking vehicle and can cause a potential hazard to the driving public.

#### Driver Response

A rough pavement can reduce friction, cause uneven lateral and vertical forces, and do physical damage to a vehicle. In any and all of these, the driver may or may not be able to maintain control of the vehicle and proceed safely. In considering the severity of the problem, one must break the problem into two parts to evaluate a driver's response. These two parameters are magnitude and frequency. Magnitude would represent the size of the bump or pothole, and frequency would represent the number of bumps or potholes per second or distance. When a driver experiences a rough pavement, he or she must correct for any effect it has on the vehicle. The time it takes will be a function of the magnitude and frequency. Variation of roughness in a transverse and longitudinal direction adds to this problem. When a roadway requires steering inputs that reach or exceed driver response time, then either the driver must slow down, the roadway must be improved, or safety will be reduced.

### Vehicle Suspension

Vehicle suspension also plays a role in the effects of roughness on safety. Considerable research has been done in this area, and several computer programs have been written to analyze their relation and determine how a vehicle with given suspension will react to various roadway geometrics and vertical and horizontal deviations. Besides conventional considerations, frequency can have a major effect on automobiles and trucks that can cause severe safety problems. When roughness occurs at a repeated amplitude and frequency, it can have two effects. First, if the frequency is in phase with the vehicle, a rough road can seem to be smooth. Second, if the roughness is out of phase with the natural frequency, the roughness can be magnified. This phenomenon causes a problem when repeated upward forces continually reinforce already existing, upward forces of the vehicle. When this occurs, the vehicle starts to move up and down with the roadway in ever-increasing movements until the car or truck tires actually leave the roadway and become airborne. This crow-hopping can cause numerous problems associated with cornering, braking, and loss of material from the bed of the vehicle. Long-bed trucks that are lightly loaded are usually more affected by this problem; however, passenger cars can also find similar problems with roughness.

### Roughness Related to Accidents

In general, loss of control, running off the road, and hitting fixed or moving objects are the typical types of accidents associated with rough roads and do not need much further discussion. Another type of accident, however, is less recognized but is significant and can be attributed to rough roadways. This is the lost-load accident that occurs when vehicles are bounced so much in driving over a rough road that they actually lose part of their load, which falls on the roadway. After this occurs, the material lying in the road becomes a serious hazard that can cause massive chain reaction accidents on congested roadways. Besides loads being lost, parts of vehicles can be lost, such as chains, repair equipment, boxes, tires, and other such material. There have also been repeated occurrences of accidents where a tire has been jarred loose and bounced down a roadway until it ran or bounced over a median wall into the path of an oncoming vehicle, resulting in severe damage or loss of life. Roughness can cause problems not only with the vehicle in question but also with other vehicles on the roadway. Therefore, other accident statistics may have to be examined for an accurate safety analysis.

The problem of the lost-load accident has been around for many years; it was probably first recognized by public safety personnel rather than engineers. One department of public safety's district commander wrote in 1971 to the superintendent of the state and suggested ways of improving the urban freeway system in the capital city. He wrote

...Our suggestion would, we admit, be quite costly, but in the interest of safety we feel it is necessary. This suggestion is for the planning of the concrete surface of the present urban freeway....At the present time, as is well known by anyone that uses this system, the surface is so rough it literally shakes vehicles apart. Heavy equipment, such as gravel trucks, when unloaded bounce down the freeway rather than roll....I am told that the City Police Supervisors have instructed their "motors" to stay off

the freeway, unless absolutely necessary, because of the hazard of riding at high speed on the rough surface.

Although not an engineer, the commander seemed to identify the appropriate points and made a fair assessment of the problem and its solution. How many other roadways in the United States have similar problems that are familiar to the public safety community but not to the engineering community?

### CASE HISTORY

The Arizona Department of Transportation has always been safety conscious. This is especially true for a section of Interstate located within the City of Phoenix that is a six-lane concrete freeway with the greatest traffic levels in the state.

In the 1970s, an increase began to occur in wet-pavement and lost-load accidents due to a polishing of the portland cement concrete pavement (PCCP) and an increase of pavement roughness due to warping of the roadway from expansion of the concrete. An example of the increase in lost-load accidents is shown in Figure 5. This figure shows a disproportionate increase of lost-load accidents with increase in traffic. It was later shown that this increase in lost-load accidents was primarily attributed to increased roughness. Figure 6 further shows that the heaviest periods of lost loads were not at the peak traffic hours but at moderate average daily traffic (ADT) periods when traffic was able to move at greater speeds. In fact, the peak periods for lost loads were at 11 a.m. and 9 p.m. Due to this increase in lost loads, a section of highway in this area was experimentally ground to

Figure 5. Traffic volume and lost-load accidents on I-17, milepost 195.0-210.0.

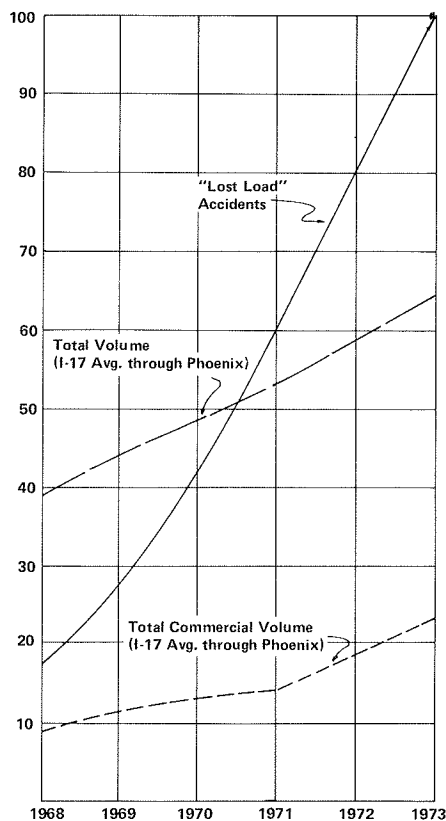
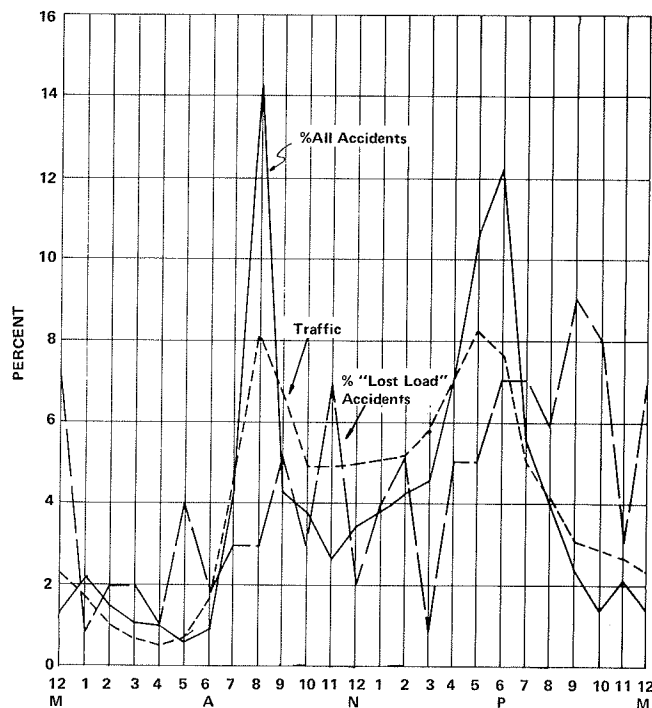


Figure 6. Hourly distribution of accidents.



determine the effects of grinding on future reduction in accidents. This was done in hopes of reducing the lost-load-accident rate by smoothing the roadway and by decreasing wet-pavement accidents by improving the skid resistance of the pavement.

The section selected for grinding was on Interstate 17 north-and-south-bound in all three lanes from milepost 200.9 to 201.9. To compare the effects of grinding, an unground control section of comparable roughness, accident history, and ADT was selected on I-17 from milepost 195.0 to 196.0. In addition, the overall accident history for I-17 from milepost 198.8 to 208.23 was also compared.

Table 1 shows total dry and wet pavement accidents for a two-year period before and after the pavement grinding was completed. In all cases there was a significant increase in all types of accidents. All of these increases were of a higher percentage increase than the actual increase in vehicular travel. Especially significant was the increase in wet pavement accidents. By using the methodology developed elsewhere (5), it was found that, during the before period, the pavement was wet only 1.82 percent of the time. During the after period, the pavement was wet 2.65 percent of the time for a 45.6 percent increase in the hours of wet pavement. Wet pavement accidents in both the control section and the entire freeway section were significantly higher, but the ground section only experienced approximately the same increase as the hours of wet pavement. A better analysis can be seen in Table 1, which shows the accident rates based on miles of vehicular traffic.

When wet-pavement accident rates were used as a measure of the ground sections' effectiveness, the ground section showed a 15.1 percent decrease in wet-pavement accident rate, however, the control and the Black Canyon Freeway sections experienced from 34.7 to 81.8 percent increases in wet-pavement accident rates. If the ground section had not been improved, a conservative estimate of 34.7 percent increase in wet-pavement accident rate or 26.12 wet-pavement accidents/100 million vehicle miles of

Table 1. Before and after analysis of I-17 pavement grinding.

Item	Control Section <sup>a</sup>		Grinding Section <sup>b</sup>		Black Canyon Freeway <sup>c</sup>	
	No.	Rate	No.	Rate	No.	Rate
Total accidents						
Before	84	1.80 <sup>d</sup>	170	3.16 <sup>d</sup>	876	1.74 <sup>d</sup>
After	278	4.83 <sup>d</sup>	296	4.61 <sup>d</sup>	1846	3.15 <sup>d</sup>
Change (%)	+231.0	+168.3	+74.1	+45.9	+110.7	+81.0
Total injuries						
Before	32	0.69 <sup>d</sup>	84	1.56 <sup>d</sup>	430	0.85 <sup>d</sup>
After	104	1.81 <sup>d</sup>	152	2.37 <sup>d</sup>	704	1.20 <sup>d</sup>
Change (%)	+225.0	+162.3	+81.0	+51.9	+63.7	+41.2
Total fatalities						
Before	1	2.15 <sup>e</sup>	0	0 <sup>e</sup>	2	3.97 <sup>e</sup>
After	0	0 <sup>e</sup>	0	0 <sup>e</sup>	5	8.54 <sup>e</sup>
Change (%)	-100	-100.0	-	-	+150	+115.1
Dry pavement accidents						
Before	76	1.65 <sup>d</sup>	151	2.86 <sup>d</sup>	811	1.64 <sup>d</sup>
After	252	4.50 <sup>d</sup>	268	4.29 <sup>d</sup>	1698	2.98 <sup>d</sup>
Change (%)	+231.6	+172.7	+77.5	+50.0	+109.4	+81.7
Wet pavement accidents						
Before	8	9.41 <sup>d</sup>	19	19.39 <sup>d</sup>	65	7.08 <sup>d</sup>
After	26	17.11 <sup>d</sup>	28	16.47 <sup>d</sup>	148	9.54 <sup>d</sup>
Change (%)	+225.0	+81.8	+47.4	-15.1	+127.7	+34.7
Total travel						
Before	46.85 <sup>d</sup>		53.79 <sup>d</sup>		504.36 <sup>d</sup>	
After	57.50 <sup>d</sup>		64.17 <sup>d</sup>		585.31 <sup>d</sup>	
Change (%)	+22.7		+19.3		+16.0	
Wet pavement travel						
Before		0.85		0.98		9.18
After		1.52		1.70		15.51
Change (%)		+78.8		+73.5		+69.0

<sup>a</sup>I-17, mileposts 195.0-196.0.

<sup>b</sup>I-17, mileposts 200.9-201.9.

<sup>c</sup>Mileposts 198.8-208.23.

<sup>d</sup>Rate or number per million vehicle miles.

<sup>e</sup>Rate per 100 million vehicle miles.

wet-pavement travel would have been expected. This rate translates into a total number of expected wet-pavement accidents of 45, or 60.7 percent more than was reported.

The table below reflects the change in anticipated accidents based on adjacent section accidents:

Accident Type	Actual After	Anticipated After	Significant Difference	Change (%)
Wet	28	47	19	-40
Dry	268	317	49	-15
Total	296	364	68	-19

The number of anticipated after accidents assumes that the same percentage change in accidents would have occurred on the treated section as occurred on the adjacent control section [27 (after) - 11 (before)]/11 = 145.5 percent increase on adjacent section]. The reduction in wet and total accidents by calculating anticipated after accidents was 40 percent and 19 percent, respectively. Thus, 68 percent more wet-pavement accidents and 23 percent more total accidents would have potentially occurred if the pavement had not been ground.

The ride quality of this section of highway was poor and the results on ride quality before and after grinding are shown in Table 2. Arizona uses the Mays ride meter and converts inches of roughness into a ride index, which in Arizona is similar to present serviceability index (PSI) but is based solely on roughness and then correlated back to a panel rating. A ride index of 2.5 or less is considered a terminal level for design, and the panel rating indicated that a rating of 2.0 or less could produce an unsafe driving condition. The test results showed that there was a major decrease in roughness and major improvements in ride quality after grinding with diamond saws. The ride index changed from poor to good after grinding on all

Table 2. Grinding section.

Direction	Lane	Milepost-Milepost	Before 1/19/76		After 9/30/76		After 12/22/76		After 4/12/77		After 12/1/78	
			Inches of Roughness/Mile	Ride Index	Inches of Roughness/Mile	Ride Index	Inches of Roughness/Mile	Ride Index	Inches of Roughness/Mile	Ride Index	Inches of Roughness/Mile	Ride Index
Northbound	Center lane	200.00-200.87, unground	310.68	2.14	346.21	1.91	116.16	3.53	350.40	1.89	304.53	2.18
		200.87-201.91, ground	267.47	2.43	166.21	3.10			164.94	3.11	139.48	3.31
	Right lane	200.00-200.87, unground	321.51	2.07	337.04	1.97	99.61	3.70	336.53	1.98	302.93	2.19
Southbound	Center lane	200.87-201.91, ground	314.49	2.12	144.36	3.27			145.43	3.26	144.85	3.27
		200.00-200.87, unground	283.20	2.32	317.29	2.10	228.51	2.68	332.67	2.07	279.50	2.35
	Right lane	200.87-201.91, ground	276.34	2.37	135.08	3.35	76.86	3.95	126.71	3.43	108.72	3.60
		200.00-200.87, unground	293.72	2.25	298.31	2.22	101.43	3.68	309.58	2.15	282.18	2.33
		200.87-201.91, ground	299.41	2.22	143.27	3.24			136.62	3.34	139.93	3.31

Table 3. Before and after analysis of lost-load accidents.

Location	Traffic			Lost-Load Accidents			Lost-Load Accident Rate		
	Before	After	Change (%)	Before	After	Change (%)	Before	After	Change (%)
Control section A-I-17, milepost 195.0-196.0	46.85	57.50	+22.7	4	72	+1700	0.09	1.25	+1289
Grinding section-I-17, milepost 200.9-201.9	53.79	64.17	+19.3	4	35	+775	0.07	0.55	+686
Black Canyon Freeway	504.36	585.31	+16.0	32	381	+1091	0.06	0.65	+983

sections and the friction level increased from a Mu meter reading of 30 to 78.

Tests two years after grinding showed that the ground section had an average ride index of 3.4 as compared with 2.19 for the unground control section. This is a significant increase and, with proper maintenance, there should be only a gradual decrease in ride quality in the future. Note that the roughness on all sections changed in a cyclic fashion with time. This was because the major cause of roughness on this freeway was due to buckling or warping of the concrete slabs with heating. During the summer periods the pavement was much rougher than during the winter period on any given section. This is an important factor to note in planning any type of grinding or overlaying operation. The reason for this is that the time of year can determine how effective grinding or smoothing may be. If the grinding is conducted during cold periods when the pavement is smooth, it may not eliminate much of the roughness that will occur later when hot temperatures are reached. In addition, it is advisable to beware of excessively harsh grinding to remove high spots that, at a later date, may subside and become low spots. In addition to the planning operation, consideration should be given to such items as improving joints to avoid future buckling or structural problems. Thus, the cause as well as the result, must be addressed.

Table 3 compares lost-load accidents that have been reported on the previously described three sections of Interstate freeway. All sections reported significantly higher numbers and rates of lost-load accidents from the before to the after periods. This significantly higher amount of lost-load accidents is explained partly by the increase in traffic, the increase in reportability of lost-load accidents due to the increased cost to the motorist of these accidents, and the need to substantiate those losses to insurance companies.

Although the data are limited, the control section reported lower numbers of lost-load accidents and lower rates of lost-load accidents per million vehicle miles of travel--51 percent lower than the adjacent comparative section of I-17.

Based on a comparison of the 1-mile grinding

section of I-17 on Phoenix Black Canyon Freeway with other sections of the Black Canyon Freeway, Arizona conservatively estimated that grinding of the concrete pavement had the following net effects:

1. Reduction in wet-pavement accident rate by 60.7 percent,
2. Reduction in the rate of lost-load accidents per million miles of vehicular travel by 51 percent, and
3. Reduction in total wet-pavement accidents expected by 40 percent (i.e., 68 percent more accidents would have occurred if the pavement had not been ground).

The information developed in this study was used in developing a project to grind for safety a 6.3-mile section of the northbound, PCCP lanes on the same highway in 1979. Better beneficial results were found with this project than were anticipated from the test section studies. In the test section, the ride index improved from 2.12 to 3.15 after grinding; however, on the large 6.3-mile project section, it was found that the ride index was improved on a reported average from 2.14 to 3.55. It is interesting to note that on the 6.3-mile section, additional federal safety funds were made available for the grinding operation. This was reportedly the first time such an operation had ever been eligible for safety funding. This is because of the Federal Highway Administration's open attitude to implementing better techniques and systems and improving safety practices via experience gained from observing the performance on new methods, and also due to Arizona's efforts to document the effects and benefits of this technique. Due to Arizona's study, it was shown that grinding of the 6-mile section of silicious, polish-resistant PCCP would produce greater friction and a smoother ride, and thus a safer surface. It is hoped that similar programs that smooth pavements or increase their frictional properties will also be eligible for safety funding.

#### PLANNING SAFETY IMPROVEMENTS

As we have seen, roughness plays a role in the

safety of a highway and should be considered when planning safety improvements and rehabilitation strategies. In order to make the most use of this information, the level and cause of roughness and deterioration must be identified correctly. In addition, the benefit to be derived from rehabilitating the roadway must be evaluated. Evaluation of the benefit means determination of how smooth the new roadway will be after the corrective action, the number of years the roadway will maintain its new acceptable ride, the cost of the improvement, and the additional safety areas that will be improved in addition to smoothing the roadway. For the last item, certain operations can also increase friction, improve geometrics, and improve drainage. With regard to life expectancy, engineers can better predict this variable if a thorough pavement evaluation is made beforehand to identify the true cause of roughness. The first factor of knowing the present condition can be done by use of various pavement evaluation techniques or ride analysis. There exists today several devices that can accurately monitor and profile the pavement by using accelerometers and peripheral computer equipment. These devices can give an almost-true profile of the pavement surface. Recently, additional computer programs have been developed not only to analyze the profile of pavements but also to determine the amount of material needed to be added or removed to give the desired new profile. The programs are so sophisticated they can also determine quantities and costs if given the type of equipment and screed or sensor lengths. This information is now available on a project-by-project basis; however, these types of devices and analyses are usually costly and are not often used on a system approach or for preliminary engineering where oftentimes the actual priority decisions are made. In an effort to allow such information to be used in priority programming, the Arizona Department of Transportation recently developed (6) an equation that is used in their pavement management system to predict what the new ride quality will be after a pavement is overlaid with a given thickness of asphaltic concrete. The equation in use is as follows:

$$R_N = 65.29 - 0.78(R_B) - 7.76(TH) \quad R^2 = 0.938 \quad (1)$$

where

$R_N$  = change in roughness one year following an overlay by using Mays ride meter (in/mile),  
 $TH$  = thickness of overlay (in), and  
 $R_B$  = roughness before overlay (in/mile).

Note, if calculated  $R_N$  is less than 50, roughness is equal to 50. In Arizona's work, it also related the Mays ride meter number in inches per mile to slope variance (SV) by the equation

$$SV = 3.819 \times 10^3 (MAYS)^{1.56} \quad R^2 = 0.97 \quad (2)$$

Thus, if a pavement had a Mays ride meter reading of 384 in/mile (ride index of 1.68, poor ride) and a 1-in overlay was applied, then the calculation would be as follows:

$$R_N = 65.29 - 0.78(384) - 7.76(1) \text{ or } R_N = -242.$$

The Mays ride meter reading would then decrease 242 in from the original 384 in; thus, one year after, the Mays ride meter reading would be 142 in/mile (ride index of 3.3, good ride).

This work was based on overlay data that ranged from 0.75 in and up on a great number of overlays throughout Arizona. This equation is currently used in the Arizona Department of Transportation's pavement management system, which also predicts change in roughness with time for any section of its entire highway system. By using such a program, effective priorities can be established. Other states, such as California, are now adding such decision-making information to their pavement evaluation and management systems.

#### CONCLUSION

The information in this paper has shown that roughness affects safety in many ways and needs to be considered in any evaluation of pavement safety. Roughness can reduce the steering and braking forces and significantly affect the controllability of a vehicle. Washboard surfaces and repeated cyclic undulations of the surface can cause significant control problems and can shake a vehicle and cause it to lose part of the load it is carrying. Thus, in addition to creating problems for the driver, it may affect the safety of others in surrounding lanes.

In establishing the priority of corrective actions, the effects of road roughness on safety must be considered. Besides evaluating present conditions, the future condition and performance of the pavement need to be analyzed. In evaluating benefits of certain measures, the value of other improvements derived from certain leveling operations needs to be addressed.

Further consideration should be given to allow federal safety funds to be made available for improving road roughness, as this problem has a significant impact on highway safety.

#### REFERENCES

1. D.L. Ivey and L. Griffen III. Driver/Vehicle Reaction to Road Surface Discontinuities and Failures--The Hidden Trigger to Accidents. 16th International Congress of International Federation of SAE, Tokyo, May 1976.
2. B.E. Quinn and S.D. Hildebrand. Effect of Road Roughness on Vehicle Steering. HRB, Highway Research Record 471, 1973, pp. 62-75.
3. J.C. Wambold, A.D. Brickman, W.H. Park, and J. Ingram. Effect of Road Roughness on Vehicle Braking. HRB, Highway Research Record 471, 1973, pp. 76-82.
4. J.C. Burns. Differential Friction: A Potential Skid Hazard. TRB, Transportation Research Record 602, 1976, pp. 46-53.
5. J.C. Burns. Frictional Properties of Highway Surfaces. Arizona Department of Transportation, Phoenix, HPR-1-12(146), Aug. 1975, 123 pp.
6. G.B. Way and J. Eisenberg. Pavement Management System for Arizona Phase II--Verification of Performance Prediction Models and Development of Data Base. Aug. 1980, 136 pp.

*Publication of this paper sponsored by Committee on Pavement Condition Evaluation.*

# Role of Road Roughness in Vehicle Ride

T.D. GILLESPIE AND M. SAYERS

This paper describes the gross mechanics of motor vehicle ride vibrations to acquaint the highway engineer with the role played by road roughness. The acceleration spectrum observed on a typical passenger car is compared against available measures of human vibration tolerance to illustrate the frequency range of general interest. The characteristics of road roughness are presented in terms of both the elevation spectral density and the equivalent acceleration excitation to the vehicle. The mechanisms of ride isolation achieved through the suspension systems of motor vehicles are illustrated by attenuation of the response gain at high frequency. Examples are given to show effects of mass, suspension, and tire properties. Additional attenuation effects derive from wheelbase filtering and tire envelopment. In the case of commercial trucks, the compromises that occur in the ride isolation as a result of suspension friction and low frequency structural resonances are illustrated.

To the highway engineer, roughness is an important measure of roadway performance because of its known influence on user acceptability (1) and its potential link with highway safety. Anyone who rides in a highway vehicle is aware of road roughness as the major source of the ride vibrations experienced. Concurrently, the roughness may degrade the handling qualities of the vehicle (2,3) and contribute to wear and tear on the vehicle.

This paper examines the relation between road roughness and vehicle ride to illustrate the mechanisms involved and to reveal those aspects of road roughness that play the major role in determining the public judgment of road quality. In order to appreciate the significance of the ride motions observed, it is helpful to first begin with a brief introduction to the subject of human sensitivity to vibration as it relates to the perception of vehicle ride.

## HUMAN PERCEPTION OF VIBRATION

Vehicle motion due to pavement roughness fits the general category of broad-band random vibrations. That is, the vibrations are not characterized by discrete frequencies but instead extend over a broad band of frequencies. Because they are random, the vibrations cannot be described exactly as a function of time but instead must be described statistically in terms of average properties.

The most basic statistical measures of random motion are the mean (average) value and the mean-square value. In the context of vehicle ride motions, mean values are zero and thus not useful numerics. However, the mean-square values, which are also the variances, are reasonable measures. In the automotive and trucking industry, the basic measure of ride has traditionally been the root-mean-square (RMS) accelerations measured at various points in the passenger compartment.

In other fields of transportation, particularly those of military aircraft and ground vehicles, the vibrations of the passenger compartment can be more severe than in ordinary passenger cars--to the point that the occupants can be impaired in their normal tasks and even risk injury in some cases. In early research to evaluate human tolerance to vibration in these environments, tests would frequently involve subjects seated or standing while exposed to sine-wave vibrations from laboratory shaker facilities. Such tests have shown that people are sensitive not only to the amplitude of the excitation but also to the frequency and the direction. The maximum sensitivity is usually found to be between 1 and 10 Hz, in which range various internal organs vibrate in

resonance with the excitation. Because these tests involve sine waves and vehicle vibrations are broad band, the research has logically expanded to examine the influence of multiple components of sine waves (4) and the actual broad-band environments of transport vehicles (5,6).

In order to quantify the frequency content of the acceleration, the statistical power spectral density (PSD) function is employed. PSD is the partial derivative of the mean-square value of acceleration with respect to frequency and has units  $g^2/Hz$ . (The name power spectral density is based on its earliest applications in the electronics and communications field, when it was used to characterize voltage signals and had the units  $volts^2/Hz$ . Although  $volts^2$  is proportional to power, a PSD is, in general, not a measure of power; clearly, an acceleration PSD, which has units of  $g^2/Hz$ , is not physically a measure of power.) Figure 1 shows the PSD of a measured vertical acceleration in a passenger car, plotted on linear axes, in which case the area under the entire curve is equal to the mean-square value. The area encompassed by any frequency band is the portion of the overall mean-square acceleration due only to that band.

A variety of ride quality standards have been proposed that, in one way or another, weight the acceleration PSD based on test results from the sine wave laboratory tests (7). But these various ride quality standards are largely incompatible with each other, probably because (a) they reflect different ideas about the subjective judgment of a good ride and (b) they are based on tests that are not always well documented and were designed and conducted for different applications. In order to provide a common measure for human vibration levels, the International Standards Organization (ISO) developed vibration standards that define an interaction among frequency, amplitude, direction (vertical or lateral and fore-aft vibrations), time of exposure, and human response level (i.e., noticeable reduced comfort, impaired efficiency, dangerous) (8). The standard provides boundaries of amplitude versus frequency that apply for a given direction, time of exposure, and response level. Figure 2 shows some of the boundaries. To apply the standard, the RMS value of the measured acceleration must be determined in third octave bands (either by using band pass filters or by taking the areas under the PSD in third octave frequency bands), and the resulting values are compared with the boundary in each band. The vertical bars in Figure 2 are taken from the PSD

Figure 1. Typical vertical acceleration PSD of a point on floor of passenger car.

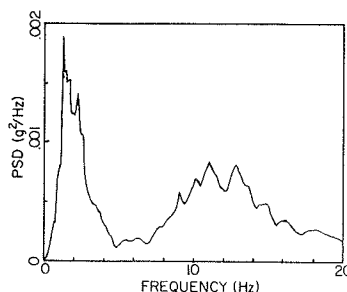
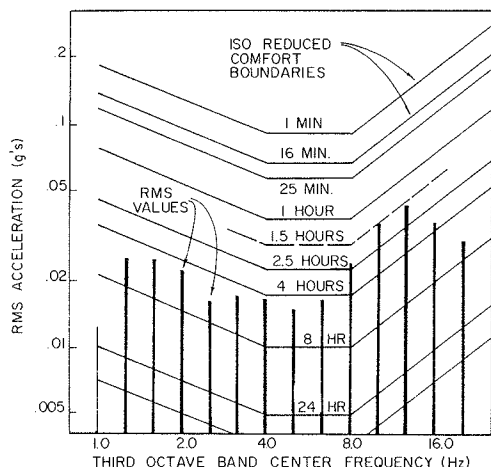


Figure 2. Example use of ISO vibration standard for PSD shown in Figure 1.



shown in Figure 1 and, when compared with the reduced comfort criterion, show that the ISO reduced comfort criterion is satisfied for exposure times less than 1.5 h. But for longer exposure times, the boundary is violated for the third octave band centered at 10 Hz. The ISO standard can also be applied by multiplying the acceleration PSD by a weighting function and then using the resulting weighted RMS acceleration level.

The ISO criteria, along with a few other ride quality weighting functions [notably the absorbed power criterion (9) and the urban tracked air-cushion vehicle (UTACV) specification (10)] have been used at times by the research and automotive communities to objectively compare rides of different vehicles under different operating conditions. But ultimately, none of these criteria have been validated for highway applications by comparisons with subjective ratings of ride, and recent efforts to do so for passenger cars (11) have found that the simple total RMS acceleration in the passenger compartment correlates as well with the subjective ratings as does any one of the ride quality numerics.

Whether ride is quantified by RMS acceleration or by a more complex, frequency-weighted numeric, the PSD of the acceleration serves to characterize the vibrations of a vehicle as induced by road roughness.

#### NATURE OF ROAD ROUGHNESS

Road roughness encompasses everything from the tooth-jarring potholes that result from localized pavement failures to the ever-present random deviations that reflect the practical limits of precision to which a road surface can be constructed and maintained. Although potholes are the more spectacular examples in the public eye, random roughness is the more pervasive problem for the highway engineer, whose objective is to maintain the best possible highway network with the limited funds available.

Road roughness may be described by the elevation profile obtained along the wheel tracks over which vehicles pass. Such profiles fit the general category of broad-band random signals, and hence are well suited for the statistical description offered by the PSD function. Figure 3 shows such a PSD, with units elevation<sup>2</sup>/wave number (wave number is 1/wavelength), for a section of road 1 mile long.

The PSD of any particular road section is unique. However, when a number of PSDs of different sections are compared, a general similarity in their shape is evident. This leads to the notion of an average road, defined by a model PSD. A number of PSDs

Figure 3. Typical road elevation PSD.

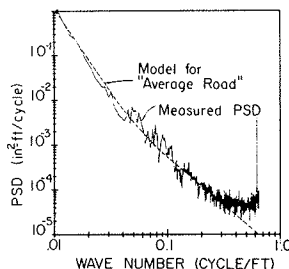
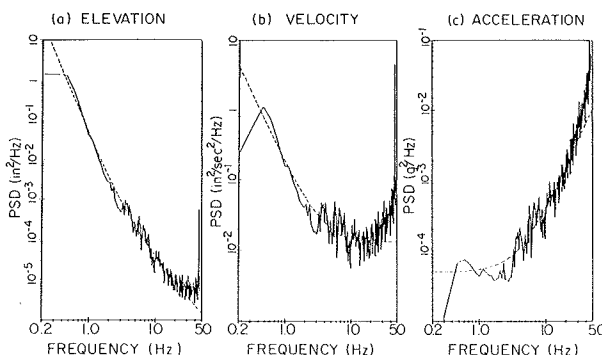


Figure 4. Elevation, velocity, and acceleration PSDs of road roughness input to vehicle traveling at 50 mph on real and model roads from Figure 3.



measured for European roads (12) led to the formulation of the average road model (13) shown in Figure 3, along with the measured PSD. Various types of road models have been in use for years (14) as a means to represent roads, in general, for analyzing vehicle ride behavior. In contrast to actual road profiles, such models eliminate effects of features that might be present in a single road but are not generally representative.

When traversed by a vehicle, the profile is perceived as an elevation that changes with time, where time and longitudinal distance are related by the speed of the vehicle. The time-varying elevation can also be characterized by a PSD that has units elevation<sup>2</sup>/frequency, where frequency and wave number are also related by speed. Figure 4a shows the PSD for the same section of road as used in Figure 3, when traversed at 50 mph.

As the elevation is perceived to be changing with time, it also has a velocity (proportional to slope) and acceleration (proportional to the derivative of slope), which also have PSDs as shown in Figures 4b and 4c for the same road section. Since velocity is the derivative of position, the velocity PSD is related to the elevation PSD by the scale factor  $(2\pi f)^2$ , where  $f$  is frequency in hertz. And, likewise, the acceleration PSD is related to the velocity PSD by the same scale factor. Although the elevation PSD is seen to be largest at low frequencies (long wavelengths) and to fall off drastically at higher frequencies, the scaling between elevation and velocity PSDs means that the velocity PSD is more uniform across the frequency range shown, and the acceleration PSD increases tremendously with frequency. The concept of the road as an acceleration input to the vehicle is important to understand because its ultimate effect--vehicle ride vibrations--are invariably quantified as accelerations.

The speed at which a vehicle travels affects the pavement acceleration PSD in two ways. First,



Figure 5. Effect of speed on perceived road input and vertical acceleration of car floor output.

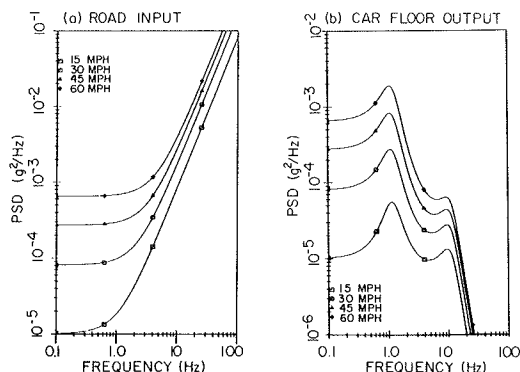


Figure 6. Simple suspended mass system.

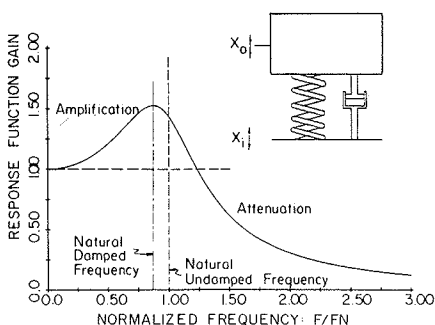
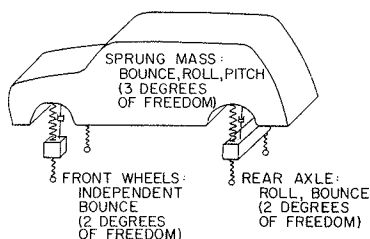


Figure 7. Ride model of passenger car with 7 df.

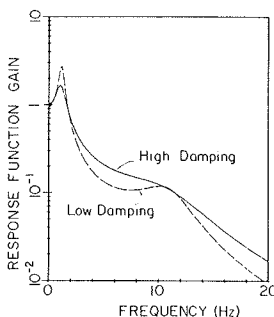


physical features occur at different wavelengths. A 44-ft wavelength is seen as a 2-Hz frequency at 60 mph and as a 1-Hz frequency at 30 mph. Second, the elevation changes faster at higher speeds. A slope of 1:88 is seen as a vertical velocity of 1 ft/s at 60 mph, but at 30 mph it is seen as a vertical velocity of 0.5 ft/s. Figure 5a illustrates the effect of speed on the acceleration PSD of the average road model, and Figure 5b shows the resulting effect on the vertical acceleration PSD in the passenger compartment. The RMS acceleration increases with speed, and more of the overall acceleration derives from the lower frequencies at higher speeds.

#### VEHICLE RESPONSE TO ROAD ROUGHNESS

The motor vehicle can be thought of as a multi-degree-of-freedom dynamic system, one function of which is to isolate the rider from the roughness imperfections of the roadway. The isolation is obtained by supporting the passenger compartment on a soft suspension system. Conceptually, at the most

Figure 8. Automobile response function between road and floor movement.



basic level, isolation of the vehicle ride capitalizes on the transmissibility benefits of the simple suspended mass system shown in Figure 6. For such a system, the ratio of the amplitude of the motion of the mass ( $x_o$ ) to the motion of the input ( $x_i$ ) varies with frequency. At very low frequency the mass will move with the input and provide no isolation. At a certain frequency (termed the natural frequency) the mass resonates and, in fact, amplifies the input motion. Then, at higher frequencies, the mass does not respond to the input and attenuation (or isolation) is obtained. When ride is important to the automotive designer, the objective is to achieve a low natural frequency so that most of the objectionable input occurs on the attenuating portion of the transmissibility curve.

The main application of a frequency response plot to vehicle ride is the way it relates the input PSD of the road to the output PSD of the body acceleration. The relation is a simple one:

$$PSD_{out} = PSD_{in} \times Gain^2 \quad (1)$$

Thus, the frequency response function acts to weight the input PSD.

#### Passenger Cars

The basic ride model of a passenger car (shown in Figure 7) has suspension points at each of the four wheels, and the wheels or axles also have mass. For simultaneous vertical inputs at all wheels, this model has the vertical transmissibility characteristics to the sprung mass center of gravity shown in Figure 8. The vehicle designer attempts to keep the body bounce resonant frequency as low as possible; however, 1 Hz is about the lowest that can be achieved because of constraints on the softness of the suspension imposed by the available range of suspension travel. Sport cars usually have higher natural frequencies and more damping due to considerations about their performance in handling. Figure 8 shows that reduction in the suspension damping improves isolation near 5 Hz and at higher frequencies but at the expense of a greater amplitude at body resonance.

Although Figure 8 would suggest that good ride isolation is obtained near the axle resonance at 10 Hz, the much greater road acceleration input at this frequency (see Figure 4c) can cause the transmissibility characteristics in this range to be critical. As seen in Figure 2, the vibrations at the axle resonance may often be as objectionable (or more so) than the vibrations at the body resonance. The vehicle designer attempts to minimize the transmissibility at axle resonance by holding down the mass of the unsprung components (e.g., driveline and brakes) and by using tires that have a low radial

Figure 9. Effect of tire radial stiffness on automobile response function.

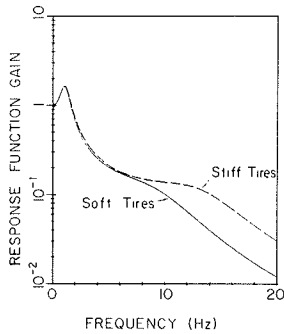
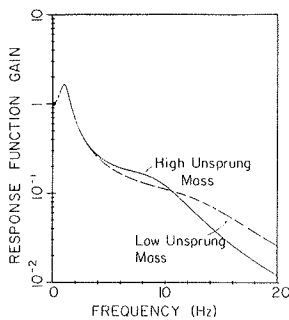


Figure 10. Effect of unsprung mass (axle weight) on automobile response function.



stiffness. Figures 9 and 10 illustrate the effects of these parameters.

Above axle resonance, the transmissibility attenuates even further because the axle can no longer follow the road inputs; roughness features are simply absorbed by deflection of the tire.

In actuality, the vehicle, as it travels down a road, does not experience equivalent inputs at all wheels simultaneously, as shown above. Instead, the rear wheels of the vehicle are excited by the same inputs as that of the front wheels, but delayed in time by an amount determined by the wheelbase and speed.

This type of excitation introduces a filtering effect to the frequency response function of the vehicle. The phenomenon can be easily visualized for a car that has uncoupled bounce and pitch modes. Vehicle bouncing is clearly excited when two axles move up and down together, and vehicle pitching is excited when the axles move completely out of phase. Figure 11 shows that a wavelength that is equal to the wheelbase can only excite the bounce motions, but a wavelength that is twice the wheelbase can only excite pitch motions. The effective wave number response function for bounce, which is the ratio of the average of the pavement elevation at the two axles to the elevation at the front axle, is shown in Figure 12.

When the frequency response function of a vehicle is found for a profile input, the wheelbase filtering effect is included, as shown in Figure 13. Although the vehicle response (discussed earlier) derives from dynamic (i.e., time-based) resonances and is purely a function of temporal frequency (Hz), the wheelbase filtering is purely a geometric property—characterized as a function of spatial frequency (wave number). Hence, the overall vehicle response function, as shown in the figure, would change with speed.

Figure 11. Relation of wheelbase and wavelength to bounce and pitch.

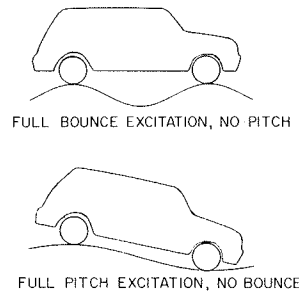


Figure 12. Effective wheelbase filtering for bounce excitation.

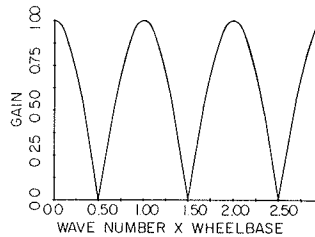


Figure 13. Automobile response function with wheelbase filtering.

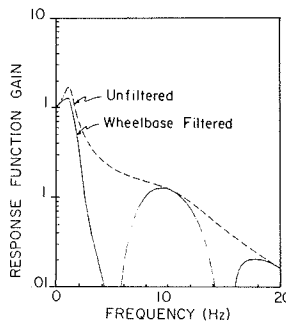
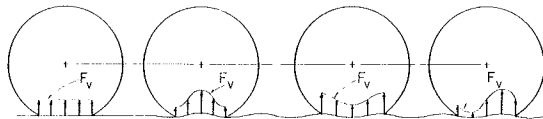


Figure 14. Illustration of tire envelopment phenomena at certain wavelengths.



A second source of geometric filtering is introduced into the vehicle response because the tires contact the pavement over an area rather than at a single point. At certain wavelengths, the increased vertical forces produced at one section of the contact patch between tire and road are completely cancelled by decreased forces from another section, with the net result that no variation in force occurs as the tire rolls over the profile. Figure 14 illustrates this phenomenon. For other wavelengths, there is imperfect cancellation and the tire experiences some force change, but not as much as would be expected from the linear spring representation shown in Figure 7. This behavior, called tire enveloping, results in the filtering effect shown in Figure 15 for a typical passenger-car tire (13). Again, the tire-enveloping effect will depend

on the vehicle speed. Since the effect is only significant for short wavelengths, its effect on ride is only important at lower speeds.

In addition to these mechanisms that determine vertical response, similar analyses are necessary to determine motion in the pitch and roll degrees of freedom. Response characteristics similar to those shown in Figure 8 would be observed, although the resonances may be at different frequencies.

The potential for ride motions in all three of these directions exists with modern passenger cars. Although large luxury cars are easily designed to minimize pitch motions, this problem becomes more acute with smaller cars, which have shorter wheel-

bases. Likewise, the excitation of roll (or lateral) motions depends on the vehicle and type of road. Most vehicle ride studies represent the proprietary work of the vehicle manufacturers. In the limited published studies (11) that relate subjective ride ratings to vehicle accelerations, both vertical and lateral accelerations have been found to correlate with the ratings. Since the vertical and lateral accelerations are also highly correlated, it is not possible to identify which is the most significant, although it was noted that the higher correlation was usually found with the acceleration that had the higher amplitude at the location of the accelerometers.

#### Commercial Vehicles

Figure 15. Typical tire enveloping function.

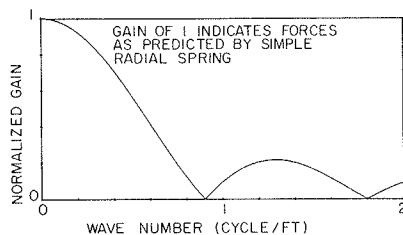


Figure 16. Ride model of tractor-trailer combination.

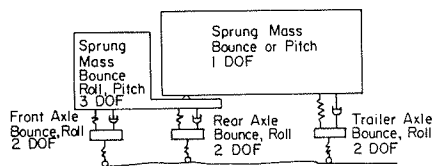


Figure 17. Typical impedance characteristics of commercial trucks.

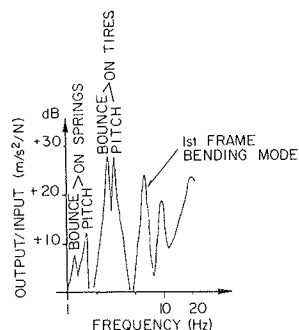
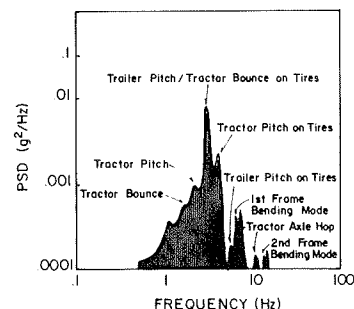


Figure 18. Typical PSD of vertical cab acceleration for tractor-trailer.



Heavy trucks and tractor-trailers rely basically on the same physical concept for ride isolation as the passenger car, although different results are achieved. The differences arise from factors related to the suspension system, structural differences, and rider location. Furthermore, the articulation of a tractor-trailer gives it additional degrees of freedom, as illustrated in the model of Figure 16. Instead of just bounce, pitch, and roll motions, the trailer is also free to move independently, which adds other resonances to the system.

The suspensions commonly used on trucks are proportionately much stiffer than on passenger cars. In part, this is necessary to limit height changes with loading. In addition, multiple leaf springs that have a high level of coulomb friction are commonly used. These deflect readily on large bumps, which yields a natural frequency near 1 Hz, as shown in Figure 17 for a straight truck that has a tank-type vocational body (15). But they may be effectively rigid on smaller bumps with the result that the tires may act as the primary suspension on smooth roads. Hence, pronounced vehicle resonances may also be observed in the figure in the vicinity of 3 Hz.

The longer wheelbases of trucks and trailers and the absence of a rigid body structure extending over the length of the vehicle allows chassis bending resonances to occur at low frequencies. First-order bending modes typically occur at 5-10 Hz on trucks and tractors. To allow for the load transport function, the riders must also be located at the vehicle extremities, far from the center of mass, where ride vibrations due to pitching and frame bending are more severe.

These factors, all combined, result in commercial vehicle ride motions that are more severe in all directions and richer in resonances in the mid-frequency range.

The additional modes of a tractor-trailer are indicated on the on-road acceleration spectrum of Figure 18 measured on a tractor-trailer (16). Here again, the characteristic resonant modes on the tires occur in the vicinity of 3 Hz and structural bending modes near 6-7 Hz.

As with passenger cars, roll or lateral modes may also exist, and the same wheelbase filtering and tire enveloping effects influence the final result. The preponderance of research on truck ride behavior in the United States focuses on the vertical and pitch modes with very little attention to the roll-lateral behavior. Hence, one may consider the behavior represented in Figures 17 and 18 indicative of the major response modes of commercial vehicles to road roughness. Although they, in general, cover the same frequency range as is important to the passenger car, road roughness has a more serious influence on rider comfort in commercial vehicles because of their greater responsiveness and the

concentration of vibration energy in the 3-8 Hz frequency range.

#### SUMMARY AND CONCLUSIONS

The perceived ride of highway vehicles depends not only on the road characteristics and vehicle response but also on the rider's sensitivity to vibration. Viewed as an acceleration input to the moving vehicle, road roughness, on the average, tends to present a uniform excitation at lower frequencies and an increasing amplitude at higher frequencies. Highway vehicles, both cars and trucks, are designed to isolate the rider from road inputs above the body resonant frequency by the vibration attenuation properties of the suspension system. Vehicle designers attempt to keep the body resonant frequency as low as possible to maximize the attenuation. On passenger cars, body resonance as low as 1 Hz is often achieved, but the high-friction, leaf-spring suspensions common on commercial vehicles often result in a 3-Hz resonance.

Although the suspension serves to attenuate inputs at higher frequency, much of the benefit is offset by the growth in road roughness acceleration amplitude at higher frequencies. Secondary resonances of the axles or chassis compromise the attenuation achieved so that significant vibrations on the vehicle body may be evident out to 20 Hz.

The highway engineer, who is responsible for maintenance of road condition, has a direct influence on what is normally the major source of excitation for vehicle vibrations that involve body resonance through the axle resonance. Vehicle ride in the frequency range of approximately 0.5-20 Hz is dominated by the physics of these resonances with current vehicle designs. Vehicle manufacturers can alter, but not eliminate, their effects. Hence, the interest of the highway engineer should focus on roughness in that frequency range that then corresponds to a wave number range appropriate for the prevailing traffic speed.

#### REFERENCES

1. W.N. Carey, Jr., and P.E. Irick. The Pavement Serviceability-Performance Concept. HRB, Bull. 250, 1960, pp. 40-58.
2. P.S. Fancher and others. Limit Handling Performance as Influenced by Degradation of Steering and Suspension Systems. Highway Safety Research Institute, Univ. of Michigan, Ann Arbor, Rept. UM-HSRI-PF-72-3, Nov. 1972.
3. A.D. Brickman, W.H. Park, and J.C. Wambold. Road Roughness Effects on Vehicle Performance. Pennsylvania Transportation and Traffic Safety Center, Pennsylvania State Univ., University Park, Rept. No. TTSC-7207, 1972.
4. H.H. Cohen, D.E. Wasserman, and R.W. Hornung. Human Performance and Transmissibility under Sinusoidal and Mixed Vertical Vibration. Ergonomics, Vol. 20, No. 3, 1977, pp. 207-216.
5. L.G. Richards, I.D. Jacobson, R.W. Barber, and R.C. Pepler. Ride Quality Evaluation in Ground Vehicles: Passenger Comfort Models for Buses and Trains. Ergonomics, Vol. 21, No. 6, 1978, pp. 463-472.
6. J.D. Leatherwood, T.K. Dempsey, and T.K. Clevenson. A Design Tool for Estimating Passenger Ride Discomfort Within Complex Ride Environments. Human Factors, Vol. 22, No. 3, 1980, pp. 291-312.
7. R.M. Hanes; Applied Physics Laboratory. Human Sensitivity to Whole-Body Vibration in Urban Transportation Systems: A Literature Review. U.S. Department of Transportation, Rept. APL/JHU TPR 004, May 1970.
8. Guide for the Evaluation of Human Exposure to Whole-Body Vibration. International Organization for Standardization, Geneva, ISO 2631, 1974.
9. R.A. Lee and F. Pradko. Analytical Analysis of Human Vibration. SAE, Warrendale, PA, Paper No. 680 091, Jan. 1968.
10. Performance Specifications and Engineering Design Requirements for the UTACV. U.S. Department of Transportation, Specification, 1972.
11. C.C. Smith and others. The Prediction of Passenger Riding Comfort from Acceleration Data. Council for Advanced Transportation Studies, Univ. of Texas at Austin, Res. Rept. 16, March 1976, 107 pp.
12. R.P. LaBarre and others. The Measurement and Analysis of Road Surface Roughness. The Motor Industry Research Assoc., Nuneaton, England, Report 1970/5, Dec. 1969, 31 pp.
13. T.D. Gillespie, M. Sayers, and L. Segel; Highway Safety Research Institute, University of Michigan. Calibration and Correlation of Response-Type Road Roughness Measuring Systems. NCHRP, Rept. 228, 1980, 81 pp.
14. B.D. VanDusen. Analytical Techniques for Designing Ride Quality into Automotive Vehicles. SAE, Warrendale, PA, Paper No. 670 021, 1967, 12 pp.
15. J.I. Ribarits, J. Aurell, and E. Andersers. Ride Comfort Aspects of Heavy Truck Design. SAE, Warrendale, PA, Paper No. 781 067, Dec. 1978.
16. M.J. Crosby and E.A. Rush. Cab Isolation and Ride Quality. SAE, Warrendale, PA, Paper No. 740 294, Feb.-March 1974.

*Publication of this paper sponsored by Committee on Pavement Condition Evaluation.*

# State of the Art of Measurement and Analysis of Road Roughness

J. C. WAMBOLD, L. E. DEFRAIN, R. R. HEGMON, K. MCGHEE, J. REICHERT, AND E. B. SPANGLER

This paper is a review of the state of the art of the measurement and analysis techniques used to evaluate road roughness. A summary of some European work is included in this review; however, the emphasis of this paper is on work done in the United States. Road roughness is defined as the deviations of a pavement surface from a true planar surface with characteristic dimensions that affect vehicle dynamics, ride quality, dynamic pavement loads, and pavement drainage. Road roughness is measured by two general types of equipment: profilometers, which measure these characteristic dimensions directly, and response-type equipment, which measure surface roughness as a dynamic response of the measuring equipment to that roughness. This paper discusses (a) the characteristic of road roughness, operating characteristics, and output of each type of roughness measuring equipment and (b) the various methods of analysis and their application to highway safety, ride comfort, dynamic pavement loading, and pavement serviceability. These methods of analysis have been categorized into two general groups: those that provide a single number of index such as root mean square, slope variance, or present serviceability index and those that statistically provide more detail than a single index, such as harmonic analysis or power spectral density. Finally, a summary of present research projects on new equipment and analysis methods is given.

The nation's aging highway system, together with increased traffic and growing competition for the tax dollar, make transportation administration more difficult. As a result, better management systems are needed to enable administrators to make objective assessments. Among the major functions of a highway or transportation department are the planning of maintenance schedules for a system of existing roads and the acceptance or rejection of newly built or resurfaced roads. The decision to resurface a particular section of road, in preference to others, is not a simple one in view of the many factors that should be taken into consideration. However, considerable information is available to support an objective evaluation, and research is under way to permit the development of improved pavement-management systems.

For maintenance management purposes, an evaluation of the condition of a pavement must include at least four factors: (a) safety, (b) pavement performance, (c) pavement distress, and (d) structural capacity. Each of these factors is used in the decision-making process to determine the nature and extent of pavement rehabilitation.

Of these four, pavement performance is most generally related to road roughness in one manner or another. This was initially accomplished with the present serviceability index (PSI), as developed at the American Association of State Highway Officials (AASHO) road test. In its original form, the PSI was developed as a measure of the rider's evaluation, and thus the pavement-performance factor was the only one to reflect the consumer's evaluation of pavement condition.

Passenger's evaluation is used here instead of the usual reference to ride comfort. In much of the work on road roughness, it has been determined that there is a dichotomy between ride quality (a subjective quantity) and pavement serviceability (an objective measure). Ride quality is primarily a measure of acceptance of the roadway as a method of conveyance. Serviceability is a measure of the physical characteristics of the pavement surface. Although some attempts have been made to correlate these quantities, little information exists to define this relation.

The nature of the roughness, for example the

extent of rutting, cracking, and patching, was included in the calculation of PSI. In the interest of expediency, many states have dropped one or more of these terms or simply substituted a constant. The PSI procedure has gone through many such changes, and a variety of other indices have been developed so that now there is no standard practice for quantifying pavement performance.

The measurement of road roughness is of interest to the maintenance manager in determining pavement safety, serviceability, and potential for assessing pavement distress, as well as to the highway or transportation department that wants an acceptance criterion for newly constructed or repaved roads. Some departments already have acceptance criteria for newly constructed or paved roads. In such cases, roughness is not to exceed a specified value as measured by a specified measurement method. Thus, it is recognized that paving equipment and methods are imperfect and some roughness is to be expected in new pavements. In a few cases, the initial roughness is so high as to make the pavement appear to be distressed.

The initial road roughness will normally increase with exposure to traffic and weather. Deformations in the pavement foundation caused by poor drainage, swelling soils, or nonuniform initial compaction will lead to roughness in the surface course. Freeze-thaw cycles cause seasonal changes in roughness and some permanent deformations. Shear forces generated during braking of heavy vehicles may cause shifting of the surface course and initiate a wash-board-type roughness, which is then aggravated by dynamic wheel forces excited by the roughness.

Relatively large faults in the riding surface may develop across pavements to bridge deck joints. Similar faults may develop in the railroad grade crossings. Shifting in the foundations causes the development of roughness (as discussed above) in flexible pavements. In rigid portland cement concrete (PCC) pavements, whole slabs may tilt and result in faults at the joints. Finally, local failures such as potholes may develop and contribute to the overall roughness of the road surface.

Continuing developments in measuring equipment and analysis techniques have greatly expanded the available information. For example, a new commercially available all-digital inertial profilometer system not only provides a more accurately measured road profile but is also able to provide real-time data analysis of the measured road profile, which makes analysis information immediately available as the road profile is measured. Research is in progress to further simplify the inertial profilometer system by the development of an operational noncontacting sensor to replace the road-following wheel in the present inertial profilometers. These developments include acoustic, infrared, and white-light sensors being developed by the Federal Highway Administration (FHWA) and commercially in the United States. Other similar systems are being developed in Europe (1,2). Thus, there will soon be a choice of the noncontact sensors.

## ROAD ROUGHNESS

Before we begin an in-depth discussion of equipment

Figure 1. Typical transfer function for passenger car body relative to axle vibrations at 87 km/h.

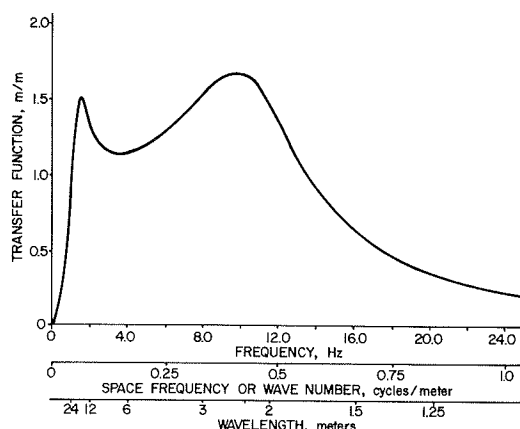


Figure 2. Road that induces automobile body shake.

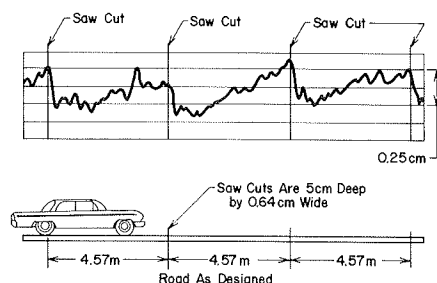
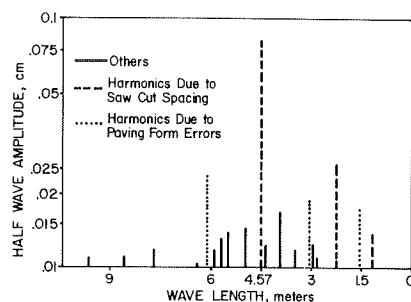


Figure 3. Harmonic analysis of road that causes automobile body shake.



for measuring road roughness, let us define road roughness itself. Road roughness is defined as deviations of a traveled surface from a true planar surface that has characteristic dimensions that affect ride quality, vehicle dynamics, dynamic pavement loads, and pavement drainage. To quantify these characteristic dimensions it is necessary to discuss the dynamic characteristics of the vehicle, vehicle speed, and the wavelength and amplitude content of the road profile over which the vehicle travels.

The dynamic characteristics of a typical vehicle can be represented by a transfer function shown in Figure 1. The plot shows the response of the vehicle in the frequency range from 1 to 24 Hz in terms of the amplitude ratio. For example, a sinusoidal road input to the vehicle at a frequency of 10 Hz would cause the vehicle to oscillate at the same frequency but at an amplitude 1.7 times greater than the input amplitude. As can be seen from the plot,

amplitude ratios greater than 1 extend from below 1 Hz to almost 14 Hz in a typical automotive vehicle.

Vehicle frequency response in the time domain (hertz) is related to spatial frequency in the highway profile by the velocity at which the vehicle travels over the highway profile.

A vehicle that travels at 24 m/s on a road of wavelength of 3 m will experience an 8-Hz excitation; a vehicle that travels at 12 m/s on a 1.5-m wavelength will experience the same 8-Hz excitation. Spatial frequency is defined as the reciprocal wavelength so that it can be converted to a frequency in hertz. Thus, by using a vehicle speed in the proper units, we can convert the spatial frequency to time-domain frequency, as shown by the second scale along the abscissa of Figure 1 (an example case with a vehicle velocity of 24 m/s). With this relationship, we can see that spatial frequencies from 0.04 to 1.0 cycles/m will cause the vehicle body to oscillate at an amplitude greater than the amplitude present in road profile. A third scale in wavelength is also given for the readers' convenience.

With these relationships, we can examine the characteristic dimensions of the road profile content that contribute to road roughness. An example of the short wavelength roughness contribution is the road profile shown in Figure 2, which caused a vehicle to vibrate objectionably at 10 Hz when the vehicle was driven over it at 88 km/h. An analysis of this road profile [Figure 3, (3)] suggests that the objectionable vibration was caused by the short-wavelength, periodic inputs centered about the 2.29-m component, which is half of the slab length.

It also suggests that, in the measurement of short-wavelength road roughness, sufficient resolution will be necessary to measure accurately the amplitudes for the wavelength shown in Figure 3. Currently, it is considered necessary that profiling equipment be capable of measuring amplitudes down to 0.025 cm.

#### MEASUREMENT OF ROAD ROUGHNESS

Road roughness is measured by two types of equipment, that which measures the response to roughness (response-type equipment) and that which measures actual profiles (profilometers). Ideally, the profiling methods give accurate, scaled reproductions of the pavement profile along a straight line. In practice, the range and resolution of any profiling devices are limited, but within these limits the measurement may be called absolute.

The response-type measurement records the dynamic response of mechanical systems as they travel over the rough road at some constant speed. It is, therefore, a relative measurement and depends on the characteristics of the mechanical system and the speed of travel.

#### Response-Type Equipment

As early as 1917, the Bureau of Public Roads (BPR), now FHWA, investigated devices to measure the road roughness of highways. In the early 1920s, the Via-Log was used to some extent by New York highway officials, but it was not generally adopted by other highway departments. Of interest is a 1925 file letter that states that its price (\$750) may have been the principal reason for its limited use.

Various devices to measure road roughness were tried up to May 1925, when the first BPR roughometer (4,5) was introduced. The roughometer is a single-wheel trailer that measures the unidirectional vertical movements of the damped, leaf-sprung wheel (with respect to the frame) by a mechanical inte-

grator. The results are recorded on counters to produce an inches-per-mile count of roughness. Several highway departments (6,7) have added a cumulative tape recorder and an oscillograph. Another modification of the BPR roughometer, developed at Purdue University (8), is designed to provide more information than the original version. It uses several resonance beams that are excited at different frequencies; thus, at a given speed an indication of the wavelength content of the surface is given.

Due to the slow response of the electromechanical counter, measurements with the roughometer are generally made at 32 km/h. Testing at this low speed is a disadvantage in that it is not very safe when other traffic is operating at normal highway speeds. Illinois has reported (9) that this limitation can be corrected by replacing the electromechanical counter by an electronic one for operation at higher speeds. However, the higher speed modifies the operational characteristics of this device.

Another type of response equipment is the group generally called roadmeters (10-13). Two commonly used meters are the Portland Cement Association (PCA) meter (14) and the Mays meter (15). These meters measure the vertical movements of the rear axle of an automobile relative to the vehicle frame. Because of its low-cost and high-speed operation, this method is now in widespread use. The performance and capabilities of the roadmeter were the subject of a workshop held at Purdue University in 1972 (16). This method of measurement is clearly the simplest and least expensive. However, the response-type equipment in use today is known to be time unstable, and the data from these devices will only be usable if suitable calibration procedures are developed to overcome this limitation. Significant progress has been recently made under a National Cooperative Highway Research Program (NCHRP) contract (17) to identify the time-unstable elements in these systems and to develop calibration procedures to account for their changing performance.

All roadmeters measure a dynamic effect of the roughness, but this type of measurement does not define the profile of the roughness. Some wavelengths will be amplified and others will be attenuated; thus, the selection of the mechanical system is critical. Roadmeters are useful for survey work in predicting the users' response regarding the quality of the road. However, to examine further the condition of a road or to determine what characteristics of the road cause the poor condition, profiling equipment (commonly called profilometers) need to be used.

#### Profiling Equipment

The advantages of a profiling system are evident. It contains complete information about the pavement profile (within the limits of the particular device) that can be evaluated according to specific needs. Such systems are expensive, however, either in initial cost or in operation, and require some data processing.

The simplest profilometer is a straight edge (18), and modifications, such as putting it on wheels, have been made. Several straight-edge spans are used, including 10, 12, 15, 16, and 30 ft. This equipment is operated either statically or at very low speed. It is not suitable for profiling because it cannot measure wavelengths longer than its span and can distort wavelengths that are harmonics of its span. Low-speed systems such as the Carey, Huckins, Leathers, and other engineers (CHLOE) are moving reference planes that have little or no dynamic effects because of their slow speed (19,20).

A low-speed profilometer system developed by the Air Force (21) consists of a horizontal laser beam, which is transmitted as a reference, and a tracking vehicle, which moves slowly along the runway and measures the undulations of the pavement. Profiles of wavelengths up to 120 m are measured with precision but at slow speeds of about 5 km/h. The operation of the equipment requires highly trained technicians.

The first modern profiling equipment, the General Motors Research (GMR) Laboratories profilometer (3,22,23), was developed by GMR Laboratories in the 1960s by using an internal reference concept. The GMR profilometer (see Figure 4) uses two spring-loaded, road-following wheels, instrumented with a linear potentiometer to measure relative displacements between the vehicle frame and the road surface. The accelerometers, mounted on the frame over each of the follower wheels, are used to measure the vehicle frame motion by double integration of the signal. The frame motion is then added to the relative displacements motion to yield two voltage signals, which in theory are the road profiles of the wheel paths (see Figure 4). This method of using a road wheel displacement signal plus the double integration of the body accelerations, rather than just the double integrations of wheel accelerations, is used as a means of covering a wider range in the measurement of road roughness. The vehicle suspension acts as a mechanical filter and transmits low-frequency (long wavelengths) vibrations but attenuating high-frequency (short wavelengths) vibrations. Thus, frequencies below 1 Hz are measured primarily by the accelerometers, mounted on the vehicle bodies, whereas the frequencies above 2 Hz are measured primarily by the linear potentiometers, mounted between the body and the follower wheels.

For frequencies between 1 and 2 Hz, the profile is a combination of the two signals. This method has been shown to be extremely useful because it has good resolution of both the short wavelengths, which have low amplitudes, and the long wavelengths, which have much greater amplitudes. The GMR profilometer was originally manufactured with analog processing equipment; however the most recent profilometer has been manufactured with an on-board minidigital computer.

In the digital computer version (see Figure 5), the road profile computation is performed by a digital minicomputer on board the profilometer vehicle, and the computed road profile data points are stored on a digital magnetic tape recorder for later data processing. In this system the sensor signals, acceleration, and displacement are sampled and immediately converted to digital values for use in the profile computation. The sampling and computation of the road profile are performed as a function of distance instead of time, as in the earlier analog system, which makes these independent of vehicle speed and much easier to interpret. The digital system, through the programmability of the minicomputer, reduces considerably the technical expertise previously required to operate and maintain the analog computer system. System calibration, signal scaling, and data formatting for storage of magnetic tape data are functions performed under software program control.

Computation of road profile is scaled so that a wide range of road profile values can be computed and stored on magnetic tape without concern about system overload. Although road profile data points are computed several times per data record point, data points are typically stored on magnetic tape every 6 in of distance traveled for the two-track-wheel paths.

The GMR profilometer system has become known

Figure 4. Diagram of measurement system for GMR profilometer.

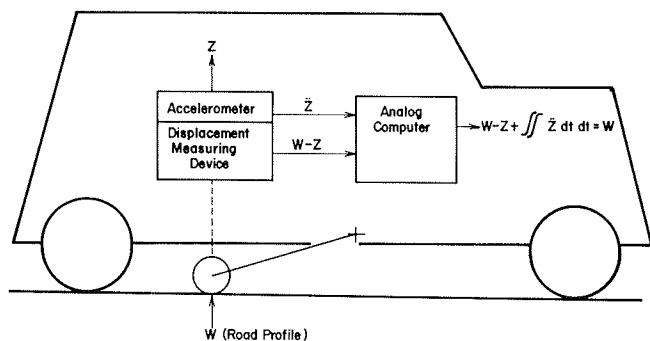
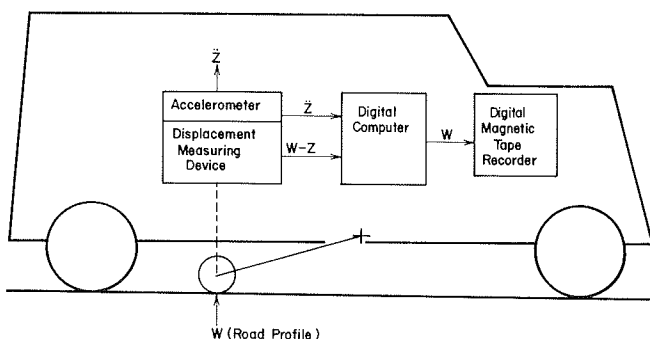


Figure 5. Digital version of GMR profilometer.



under several names: General Motor profilometer, rapid travel profilometer (RTP), and surface dynamics profilometer (SDP). The system is commercially available but is currently being used by only five states: Kentucky, Michigan, Pennsylvania, Texas, and West Virginia. The last system, built for West Virginia, is the new digital system with the application software just described. In addition, Texas is in the process of replacing its early analog system with the new digital design.

There are several reasons that the GMR-type profilometer is not more widely used in the highway community. Certainly its high purchase cost is an important factor, although more than 40 states have skid testers that have almost the same price tag. Another important factor may be the limited use that has been made in the past of the information contained in the roughness profile. Both of these reasons could moderate as more cost-saving application software, like the bituminous fill program, becomes available to the highway community and the output of the profilometer becomes an important input to a well-designed pavement management system. (The bituminous fill program allows one to simulate an overlay and to compute the new profile developed.) Another factor that should improve profilometer performance and assist in user community acceptance will be the replacement of the present road-following wheel with a noncontacting device.

Among various profiling apparatuses developed in Europe, we should mention the French designed dynamic profile analyzer (24) [l'analyseur du profil en long bitrace (APL) du Laboratoire central français des Ponts et Chaussées] (see Figure 6). It provides for the measurement of two tracks of longitudinal profile. Each of the single-wheel trailers (see Figures 6 and 7) that constitutes the measuring device is made up of

1. A profile pick-up wheel that is mechanically conditioned to remain in contact with the road surface (even at relatively high constant speed of up to 144 km/h or 72 km/h for normal tests),
2. An inertial pendulum used as the measurement reference, and
3. A measuring wheel-carrier arm that rotates around the same axis as that of the pendulum.

The center of mass of the inertial pendulum is located at the center of percussion of the trailer relative to the towing point, which allows measurements of the profile to be made by considering the angular displacement of the wheel carrier-arm and the pendulum. This is achieved with a satisfactory mechanical decoupling from the towing vehicle. A transducer transforms the angular displacement into a magnetic tape-recorded electric signal. This information is later available for computation. The transfer function of the APL equipment is flat over the frequency range of 0.4–20 Hz (response between +5 and -5 percent of the mean). The two-track version permits the study of average longitudinal evenness as well as average rolling movements. However, because each trailer has its own reference, there is no assurance that the roll component is correct. A common transverse sensor between the two independent trailers would be required to ensure a correct measurement relative to the same reference.

Another apparatus, the profile analyser from the Technical University of Berlin (24), works on a similar principle; the apparatus involves a reference base of pendulum type and a bogie used as a sensor wheel. The signal corresponds to the gradient between the bogie truck and the reference base. This gradient can be translated by an analog or digital computer into amplitude of differences in level or acceleration. The transfer function is flat between 3 and 25 Hz, but the testing speed is low, about 20 km/h.

Figure 6. Dynamic profile analyzer, French design APL.



Figure 7. Components of APL.

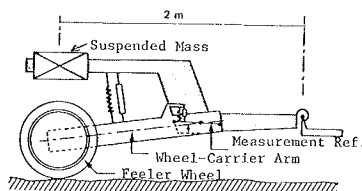




Figure 8. Theoretical differences among GMR profilometer, APL, CHLOE, rolling straightedges, and BPR roughometer.

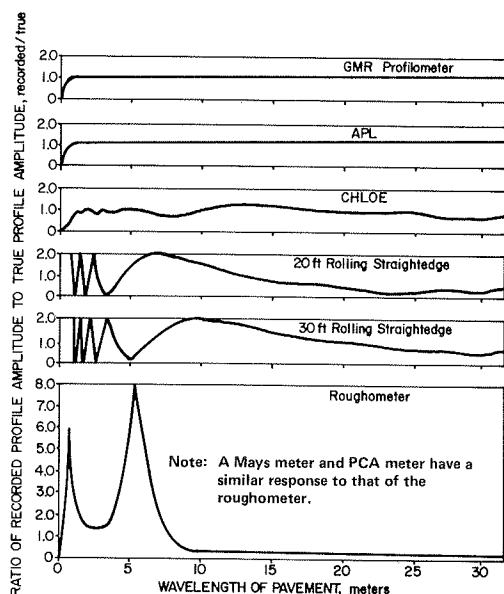
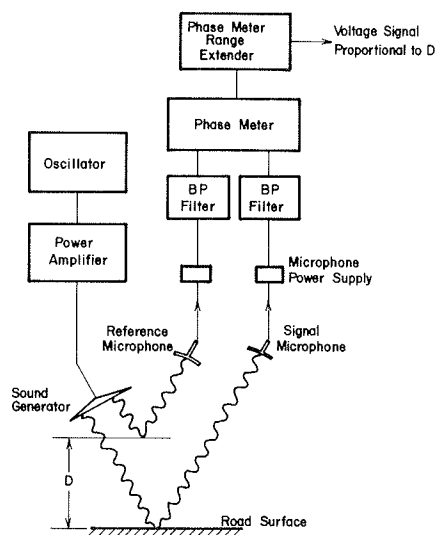


Figure 9. Block diagram of acoustic probe signal conditioning equipment.



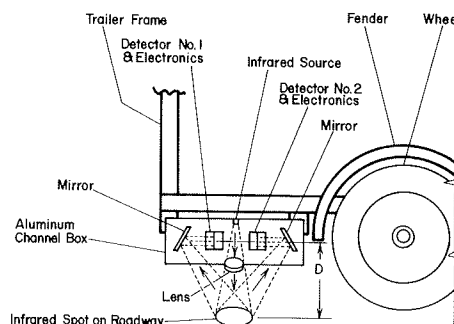
Darlington (25) has analyzed the response of several profiling devices by means of Bode plots. These have been reproduced in Figure 8 (24,25) with the addition of the APL. These plots show that, of the road roughness measurement systems in use today, only the GMR profilometer and the APL can record the true road profile.

#### Research Equipment Under Development

The main limitation of the GMR system has been the road-following wheels (26,27). Because the GMR is a mechanical dynamic system, frequency response, and thus profiling speed, is generally limited to 65 km/h (40 mph). To remedy this weakness in the GMR, several noncontact probes have been developed to replace the road-following wheels.

To date, many types of noncontact probes have been proposed that use various radiation frequencies

Figure 10. Electro-optical height sensor as installed on trailer to measure height D.



(acoustic, infrared, white light, laser, and micro-wave). FHWA is currently investigating two of these, the acoustic and the infrared (see Figures 9 and 10). The acoustic probe is still in a development state (28,29). At present, two projects are under way, one to provide on-board data reduction equipment and the other to provide a rugged version of the probe for everyday road use. The infrared system is now in the evaluation stage. It appears that it will provide a much less expensive probe than the acoustic probe. Further evaluation and development are scheduled. The infrared sensor was developed as a part of a study by the Southwest Research Institute to devise a measuring system for hydroplaning potential. Twelve sensors, mounted transversely on the trailer, measure profile in the longitudinal direction. Each sensor has two differential detectors that produce two voltages proportional to the light intensity received by each half of the detector. The light intensity changes with distance and also with changes in reflectivity within the light spot. The output of one of the detectors is reversed, which has the effect of cancelling the signals for changes in reflectivity but reinforcing them for height changes.

The system also measures acceleration, together with pitch, roll, and yaw rates, to give the motion of the reference frame of the 12 sensors and thus correct the relative measurements in order to produce the 12 road profiles. Processing provides a 1-ft grid from which longitudinal and transverse profile data are available.

A noncontact probe based on white light is being developed by K.J. Law Engineers, Inc., a manufacturer of the GMR-type profilometer. In this approach the noncontact probe (Figure 11) will take the place of the road-following wheel assembly on the profilometer systems now manufactured by that company. The noncontact probe is based on the measurement of the angle at which an incandescent spot, projected vertically down from the vehicle on the pavement, is viewed by the system. A change in the vehicle-to-pavement distance causes a change in the viewing angle that is related to a change in vehicle displacement. A prototype system based on this concept has been built and demonstrated. The displacement measuring resolution of the prototype system has been found to be better than 0.25 mm, which compares favorably with the road-following wheel system it is designed to replace. This noncontact probe has several advantages. The radiated spot or footprint is visible to the human eye, and the shape and size of the footprint can be tailored to the application.

The British Transportation and Road Research Laboratory (1,2,30) is also working on a noncontact sensor (see Figures 12 and 13). This system focuses a laser beam to a 0.282-mm diameter spot and records

Figure 11. GMR profilometer with a noncontact displacement transducer.

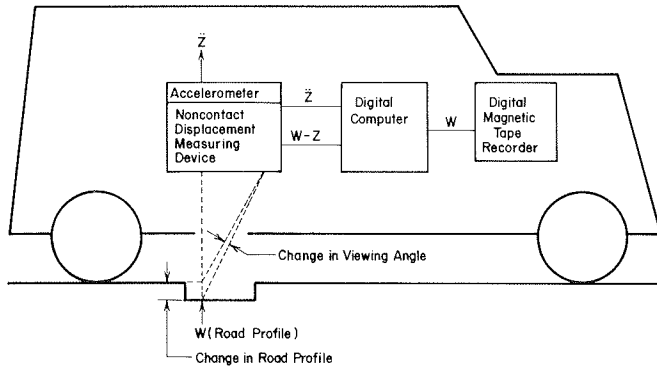
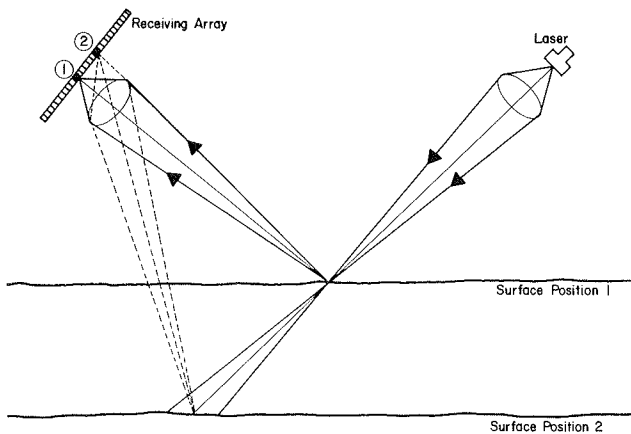


Figure 12. Principle of contactless sensor.



the position of the reflected light spot on a linear array of photocells. The system is claimed to be capable of measuring profile roughness at speeds from 5 to 80 km/h (2). Four noncontact sensors are mounted in line, and the reference is established by computation. Thus, no accelerometer or double integration is required.

#### Calibration of Devices for Measuring Road Roughness

The time instability in devices for measuring road roughness must be accounted for by calibration procedures that convert their present performance to an established standard performance.

Profilometers, for which dynamic effects are negligible, can be calibrated statically. This can be done directly on surfaces for which the absolute profile has been obtained. In the GMR-type profilometer, the complete system can be calibrated by bouncing the profilometer vehicle in a stationary position. In this mode (Figure 5) the output of the system ( $W$ ) should be close to zero because there is no change in the road profile. In the early GMR-type profilometers, the quality of system performance was an operator judgment. In the new digital West Virginia profilometer, a computer program guides the operator through the calibration procedures and makes the judgment about the quality of the system's performance.

Calibration of response-type devices for measuring road roughness is a more difficult task. Calibration of response-type devices was addressed in a recent NCHRP project (17) in which the time instability of the response-type devices was evaluated

Figure 13. Construction of prototype profilometer, without polyurethane foam lagging and cover.

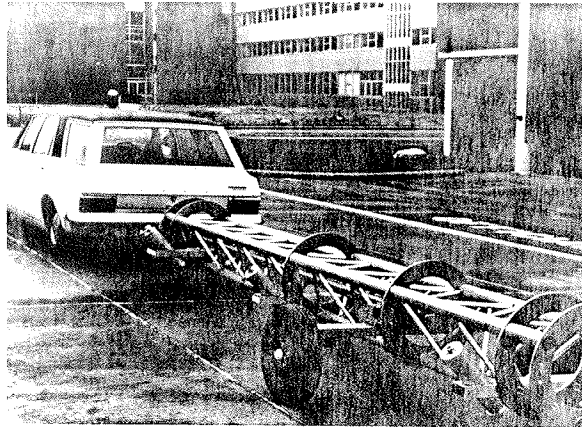
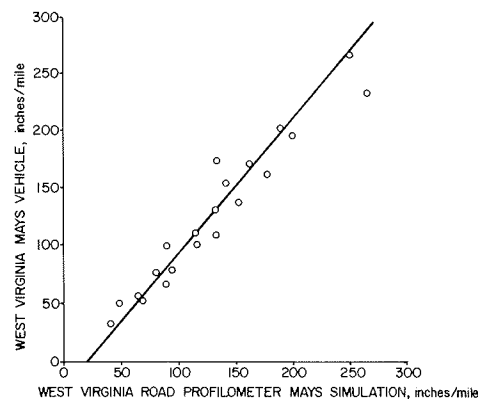


Figure 14. Calibration of West Virginia Mays meter.



and standard calibration procedures were developed. Two procedures were proposed--the primary procedure involves the use of a GMR-type profilometer and the secondary procedure involves the use of a specially designed set of artificial road bumps. In the GMR profilometer approach, the profilometer was used to measure a road profile that was then used as an input to a simulation of a response-type device. The output of the simulation is then the output that would be expected from a response-type device driven on that road profile. Since the output of a response-type device is also a function of road roughness, the same procedure must be done for a range of road roughnesses. A Mays meter calibration capability has been programmed into the West Virginia digital profilometer system, including the simulation of West Virginia's Mays meter vehicle. The resulting calibration for the West Virginia Mays meter vehicle is shown in Figure 14.

The proposed secondary calibration procedure involves driving over a foreshortened set of specially designed artificial bumps at low vehicle speed. The theory is that the system output at the lower speed can be used to calibrate the system output at the normal 80-km/h operating speed. It is also observed that more work needs to be done on this approach.

#### ROAD ROUGHNESS EVALUATION

Measuring the profile of a road is a preliminary

step in evaluating its performance as a riding surface for vehicles and in judging its surface geometry. In recent years the trend in road profilometer design has been toward instruments capable of sensing undulations in the road surface with wavelengths as long as 100 m, and doing this accurately at highway speeds.

Because visual evaluation of the recorded road profile is difficult, the major problem in application is extracting useful roughness data. The methods selected for the reduction of road profile data depend on the ultimate uses for which the roughness measurements are intended and on the inherent limitations of the equipment. Some potential uses of road profile data include the following:

Use	Data
Construction	Specification of surface profile limits in new road construction, evaluation of costs to improve road
Maintenance	Prediction of loss of serviceability in existing roads, establishment of maintenance and replacement criteria
Vehicle behavior	Correlation with vibrational response and fatigue damage in vehicles, development of passenger comfort criteria, evaluation of roughness effects on vehicle steering and braking

Some of these applications require highly sophisticated data processing, which would lead to an entirely mathematical representation of the profile record, for example, of its power spectral density (PSD). Other applications may require only an averaging or summing to establish a single roughness criterion, such as the BPR roughness index. However, departments that have profiling equipment are able, in effect, to bring the road surface into the laboratory and to seek the most useful data-processing method.

Measured records are recognized as random signals of finite duration; as such, they can be viewed and described in terms of three basic domains: space (or time), amplitude, and frequency. The description of the space domain is the unprocessed signal-versus-space (or time). All descriptions of amplitude domain reduce the measured signal to a single number or table of values; this procedure is mathematically equivalent to computing an amplitude probability distribution for the signal. Frequency domain representations of signals are generally considered to contain the most information.

The most commonly used method, the present serviceability index (PSI) (31), is of the amplitude domain type. The equations are determined from subjective evaluations, with one relation for flexible pavement and one for rigid pavement. Both equations are developed to use either the mean slope variance (32) or the roughness index (33) as the required input value to make the PSI calculation. The slope variance is the mean squared deviation of the slope from its mean square, and the roughness value is a reading of inches of displacement per mile of travel.

There are three frequency domain representations used in the analysis of road roughness data: harmonic analysis, PSD, and amplitude-frequency distribution. Harmonic analysis is a representation that assumes that the road roughness data are periodic. This analysis method reduces a complex road roughness wave form to a harmonic series of sinusoidal wave forms that, in effect, are the amplitude contributions of the various harmonics in the road

roughness data being analyzed. The computed amplitudes of the various sinusoidal wave forms can be shown graphically as a function of spatial wave length, Figure 3. Representation of harmonic analysis is useful in isolating periodic spatial wave lengths in a road surface that, when driven over at a certain vehicle speed, can produce time domain frequencies that cause poor ride quality.

The PSD representation assumes that the road roughness data are random. PSD shows the extent that spatial wave lengths within a bandwidth contribute to road roughness. A PSD estimate is obtained by accumulating the squared amplitude within a bandwidth over the length of pavement processed, dividing by the pavement length to obtain mean variance over that pavement length, and then dividing by the bandwidth to obtain an average for that bandwidth. A graph of roughness power spectrum can be plotted with the spectral density in meters squared per cycle per meter as the ordinate and the spatial frequency (inverse of the wavelength) in cycles per meter as the abscissa. The area bounded by the curve, the horizontal axis, and any two selected abscissas represent the total mean square value of roughness for wavelengths that lie between the two ordinates. The total area under a power spectrum curve gives the total mean square roughness of the pavement in meters squared or other comparable units. Several researchers, including Hutchinson (34), Quinn (35), as well as the Michigan Department of Transportation, advocate the use of the PSD. In 1965, Vogel (36) reported on the wavelengths and amplitudes of road surfaces. He stated that, if the PSD of road surfaces are plotted on log-log plots, one obtains straight lines that have a slope at a certain angle. Furthermore, parallel shifting of these lines occurs for different road amplitudes that have similar distributions and change in slope shows different distributions.

Amplitude-frequency distribution (AFD) (37,38) is an effective method for combining the information contained in both the PSD and the amplitude representations. The complete array of numbers of the AFD identifies the random signal as a combined amplitude and frequency distribution (AFD) and includes not only continuous or periodic makeup but also singularities in the input.

From the preceding discussion, we can see that response-type equipment, if properly tuned and calibrated, is useful to highway departments for surveying at low cost. However, the profiling methods provide the more detailed information that is needed for research. In fact, the response data are still available and can be predicted with a quarter-car simulation. With the development of new profiling methods, further analysis can be made available from profiles. Although there is a reluctance to use new technology because of the costs involved (new equipment and trained personnel), new methods are being developed to make available more information contained in the profiles. Although there are many useful analysis methods already developed, many methods, like some of those developed by the University of Texas, have yet to be implemented, and others, like those developed by Michigan, are implemented but relatively unknown.

With the development of the digital GMR-type profilometer, processing of road profile data can be performed as the road profile is being measured, or afterwards, by retrieving data stored on digital magnetic tape. Several computer programs for this purpose have been implemented on the West Virginia digital profilometer by the K.J. Law Company, manufacturer of that system. Two of the programs involve the simulation of low-speed inspection devices (BPR roughometer and moving straight edge) to pro-

duce the output of these devices without the devices being used. In this approach, road profile can be measured at safe normal traffic speed and the output of the slow-speed inspection device computed as required. This approach also allows the retirement of old, difficult-to-maintain inspection equipment without losing continuity with historic inspection procedures. A third computer program involves the simulation of the Mays meter on response-type device calibration. The Mays meter model used in the simulation was developed in the NCHRP project (17) and is the first implementation of the calibration procedure recommended in this project. A fourth program implemented for West Virginia involves a bituminous fill program developed by Michigan. In this program, the measured road profile is input to a simulation of a bituminous paving machine. The outputs of the program are a graphical representation of the repaved surface and the amount of material required to perform the repaving.

On the other hand, the data of response-type measurement systems cannot be reduced to the absolute roughness profile. Nevertheless, these systems, if properly tuned and calibrated, are useful for surveying a highway system at relatively low cost and with a minimum of data processing. The profiling method could obviously replace response-type measurements but, until the cost of procurement and operation of the two becomes competitive, response-type measurements will be used for the bulk of road survey operations.

Two roughness analysis methods used in Europe have been reported by the Permanent Association of Road Congresses (24). One of the methods, which is now traditionally used in Europe, is the determination of the spectral density of the variations in amplitude level. This method, which is very accurate and carried out by means of a specialized analog computer, is effective for research. The minimum length of a section studied with this method is about 3 km.

The other method is the analysis of the average variance of differences in level from the mean classified for various bands of wavelength. By breaking down the whole scale of the results obtained into 10 bands of wavelength of increasing geometry, a scale of values has been set up that allows simple comparison of results of measurements carried out on various roads. This more primitive but more directly accessible method is well adapted to systematic measurements. The lengths of the sections studied need to be at least 200 m.

#### STANDARDIZATION OF ROAD ROUGHNESS MEASUREMENTS

Road roughness measurements have been used for many years in construction control and, with the introduction of the roadmeters, surveys for PSI ratings have become widespread. Standardization of the various measurement methods would be helpful to all current users and particularly to potential users who must select equipment and train operators.

The committee on traveled surface characteristics of the American Society for Testing and Materials (ASTM) has recently organized a third subgroup on roughness. The group is now made up of three subcommittees: (a) on methods for measuring profile and roughness, (b) on measurement and control of roughness in construction and rehabilitation of pavements, and (c) on methodology for analyzing pavement roughness. The groups' principal assignment is to standardize the accepted and widely used measurement methods and to serve as a forum for the exchange of information. Candidate measurement methods for standardization include the high-speed profiling devices and the associated data processing

methods, the roadmeters, PSI calculations, and the various devices used specifically in construction control.

#### FUTURE OF ROAD ROUGHNESS MEASUREMENTS

From the above discussion, it is apparent that both measurement methods, profiling and response-type, are useful in meeting the needs of highway departments. The profiling method provides detailed information on the roughness profile, which may be needed for research or experimental projects. This roughness profile can be processed in various ways and can be used in principle to predict the output of any response-type measurement system if its mechanical properties are known. This capability is used by several states to calibrate response-type measurement systems.

#### REFERENCES

1. P.B. Still and M.A. Wennett. Development of a Contactless Displacement Transducer. Transport and Road Research Laboratory, Crowthorne, Berkshire, England, Rept. LR690, 1975.
2. D.R.C. Cooper. Measurement of Road Surface Texture by a Contactless Sensor. Transport and Road Research Laboratory, Crowthorne, Berkshire, England, Rept. LR639, 1974.
3. E.B. Spangler and W.J. Kelley. GMR Road Profilometer--A Method for Measuring Road Profile. HRB Highway Research Record 121, 1966, pp. 27-54.
4. J.A. Buchanan and A.L. Catudal. Standardizable Equipment for Evaluating Road Surface Roughness. Public Roads, Feb. 1941.
5. R.A. Crawford, D.W. Anderson, and W.E. Chastain, Sr. South Dakota Roughometer Comparison Tests--1962. HRB, Highway Research Record 28, 1963, pp. 63-97.
6. B.R. Petrok and K.L. Johnson. Minnesota Modifications to BPR Roughness Indicator. HRB, Bull. 139, 1956, pp. 29-34.
7. G. Ahlborn and R.A. Moyer. New Developments in BPR Roughness Indicator and Test on California Pavements. HRB, Bull. 139, 1956, pp. 1-28.
8. B.E. Quinn and L.M. Smeyak. Measuring Pavement Roughness Spectra Using the Modified BPR Roughometer with Additional Refinement. FHWA, Rept. FHWA-RD-72-27, Nov. 1972.
9. J.E. LaCroix and E.J. Kubiak. Modification of the BPR-Type Roadmeter. FHWA, Rept. FHWA-RD-76-50427, June 1975.
10. M.F. Clark. Road Meter Output and Its Correlations with Panel Ratings in Saskatchewan. In Pavement Evaluation Using Road Meters, HRB, Special Rept. 133, 1973, pp. 77-90.
11. M.B. Phillips and G. Swift. A Comparison of Four Roughness Measuring Systems. HRB, Highway Research Record 291, 1969.
12. Calibration of Several Road Meters with Panel Serviceability Ratings. Minnesota Department of Highways, St. Paul, 1970.
13. D. Pradubjew and V.J. Marks. Road Meter: Modifications and Improvements. Iowa State Highway Commission, Ames, 1970.
14. M.P. Brokaw. Development of the PCA Road Meter: A Rapid Method for Measuring Slope Variance. HRB, Highway Research Record 189, 1967, pp. 137-149.
15. The Incomparable Mays Ride Meter for Pavement Surveillance. Rainhart Company, Austin, TX, Jan. 1972.
16. Pavement Evaluation Using Road Meters. HRB, Special Rept. 133, 1973, 128 pp.

17. T.D. Gillespie, M.W. Sayers, and L. Segel; Highway Safety Research Institute, University of Michigan. Calibration and Correlation of Response-Type Road Roughness Measuring System. NCHRP, Rept. 228, 1980, 81 pp.
18. F.N. Hveem. Devices for Recording and Evaluating Pavement Roughness. HRB, Bull. 264, 1960, pp. 1-26.
19. CHLOE Profilometer Operating and Servicing Instructions. FHWA, Internal Rept., 1967.
20. Tateishi and others. CHLOE Pavement Serviceability Program. Hawaii Department of Transportation, Honolulu, 1969.
21. N.P. Baum and T.A. Stough. Evaluation of Inertial and Laser Profilometer Systems. Air Force Weapons Laboratory, Dayton, OH, Rept. AFWL-TR-74-289, April 1975.
22. G.G. Balmer. Road Roughness Technology: State of the Art. FHWA, Rept. FHWA-RD-73-54, Dec. 1973.
23. State of the Art of Pavement Condition Evaluation. In Rigid Pavement Design Research on Skid Resistance. In Pavement Condition Evaluation, HRB, Special Rept. 95, 1968, pp. 49-68.
24. Report of Technical Committee on Slipperiness and Evenness. Permanent Assoc. of Road Congresses, 15th Congress in Mexico City, Paris, 1975.
25. J.R. Darlington. Evaluation and Application Study of the General Motors Corporation Rapid Travel Profilometer. Michigan Department of State Highways, Lansing, Rept. R-731, April 1973.
26. J.R. Darlington and P. Milliman. A Progress Report on the Evaluation and Application Study of the General Motors Rapid Travel Profilometer. HRB, Highway Research Record 214, 1968, pp. 50-67.
27. W.R. Hudson. High-Speed Road Profile Equipment Evaluation. University of Texas, Austin, Res. Rept. 73-1, Jan. 1966.
28. R.P. Joyce; IIT Research Institute. Development of a Noncontact Profiling System. FHWA, Rept. FHWA-RD-75-36, Jan. 1975.
29. J.C. Wambold. The Evaluation of a Noncontact Profiling System Using the Acoustic Probe. FHWA, Rept. FHWA-RD-78-43, Jan. 1975.
30. R.S. Dickerson and D.G.W. Mace. A High-Speed Road Profilometer: Preliminary Description. Transport and Road Research Laboratory, Crowthorne, Berkshire, England, TRRL Rept. SR182UC, 1976.
31. The AASHO Road Test, Report 5, Pavement Research. HRB, Special Rept. 61E, 1962, 352 pp.
32. W.N. Carey, Jr., and P.E. Irick. The Pavement Serviceability-Performance Concept. HRB, Bull. 250, 1960, pp. 40-58.
33. V.F. Nakamura and H.L. Michael. Serviceability Ratings of Highway Pavements. HRB, Highway Research Record 40, 1963, pp. 21-36.
34. B.G. Hutchinson. Digital Computation of Pavement Roughness Power Spectra. Paper presented at midyear meeting, Department of Design, HRB, Aug. 1967.
35. B.E. Quinn and J.L. Zable. Evaluating Highway Elevation Power Spectra from Vehicle Performance. HRB, Highway Research Record 121, 1966, pp. 15-26.
36. W. Vogel. Distribution of Wave Lengths and Heights of Various Road Surfaces. Automobil Technische Zeitschrift, No. 67, 1965, pp. 7-11.
37. A.D. Brickman, J.C. Wambold, and J.R. Zimmerman. An Amplitude-Frequency Description of Road Roughness. HRB, Special Rept. 116, 1971, pp. 53-67.
38. J.C. Wambold and W.H. Park. A Data Processing Method Giving a Better Physical Description of Random Signals. Proc. of 20th International Instrumentation Symposium, Instrument Society of America, Pittsburgh, 1974, pp. 371-375.

*Publication of this paper sponsored by Committee on Surface Properties-Vehicle Interaction.*

#### *Abridgment*

## Overview of Road Meter Operation in Measuring Pavement Roughness, with Suggested Improvements

M. SAYERS AND T.D. GILLESPIE

Road meter systems that measure vehicle response to pavement roughness have limited accuracy, but more importantly, cannot be calibrated validly for use on all types of roads without access to a General Motors Research Laboratory-type profilometer. Even with good practice on the part of the users that eliminates the obvious effects of varied tire pressure, cargo weight, faulty components, and the like, limitations inherent to the road meter system remain. These limitations are due to the unique dynamic properties of each vehicle, the nonlinearities inherent to the vehicles and road meter instruments, and nonuniformities of the tire and wheel assemblies. This paper explores various improvements to road meters that will reduce the required calibration effort. The major source of nonlinearities in the vehicle-road meter systems are due to the road meter instruments and can be eliminated by the use of an equivalent electronic meter based on a linear transducer. With linear meters, it becomes possible to measure and correct for vehicle motions caused by tire and wheel nonuniformities. This can be done in the

laboratory on a smooth drum roller or by special processing of on-road measurements keyed to wheel rotation as detected by an inductive pickup. However, even then, reference road-type surfaces are still required for calibration to scale the vehicle dynamic response. Only by the addition of accelerometers is it possible to compensate for vehicle dynamic response by simpler means of calibration. With this level of instrumentation, the road profile can be roughly determined and the road meter system has become a crude profilometer.

Road meter systems have become increasingly popular for quantifying pavement serviceability due to their relatively low cost and simple operation. These systems consist of a conventional automobile or special trailer, together with a road meter [such as

Figure 1. Typical installation of road meter in vehicle.

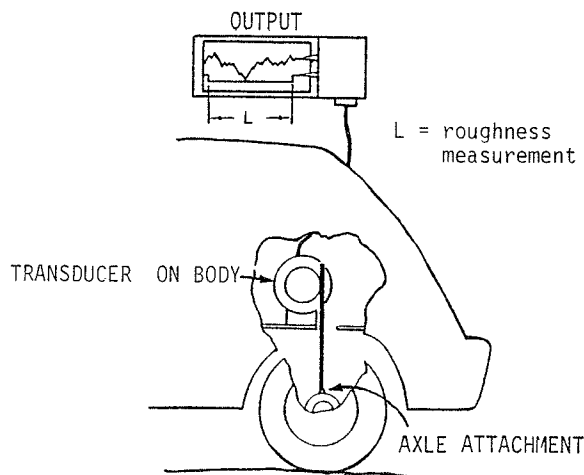
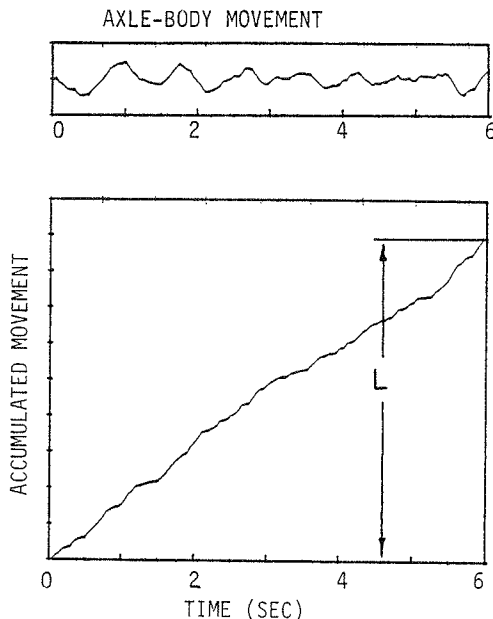


Figure 2. Relation between the road meter measurement and the axle-body movement of vehicle.



a Mays meter or Portland Cement Association (PCA)-Wisconsin meter] that measures motion of a solid axle relative to the vehicle body. Figure 1 shows the essential layout of a typical road meter system. Traversing a road, these motions detected by the road meter constitute the response of the vehicle to road roughness; thus, road meter systems are often called by the more technical name of response-type road-roughness-measuring systems. Ideally, the road meter instrument accumulates the movement of the axle relative to the body, as shown in Figure 2. The total accumulated movement, normalized by the length of the pavement (or more properly, by the time duration of the measurement), is then used as the roughness numeric.

This approach to measurement of road roughness is prone to many sources of variability, such that frequent calibration is needed to maintain acceptable accuracy. Due to shortcomings in the available calibration methods, the National Cooperative Highway Research Program (NCHRP) has sponsored a re-

search project (1) to examine the problems in the calibration and use of road meter systems. The findings of that research indicate that valid calibration methods for existing systems are necessarily and unavoidably time consuming. This paper draws on these findings as a start in addressing the question: Can road-meter-type systems be improved to provide better accuracy and require less calibration effort? The alternate approach for measuring road roughness is with a General Motors Research Laboratory (GMR)-type profilometer, which offers greater precision and flexibility, together with much more modest calibration requirements. But the high initial cost of the profilometer puts it beyond the reach of most highway agencies. In this paper, the GMR profilometer represents a standard of performance that the suggested improvements in road meter design seek to reach.

#### PROBLEMS IN CALIBRATING ROAD METER SYSTEMS

Any calibration method for road meter systems must meet the simple criterion that two systems, properly but separately calibrated, be able to produce nearly identical roughness measurements for any section of road. If this is the case, the calibration is valid.

The first problem in calibrating road meter systems has been the lack of a well-defined roughness numeric that could be used as a reference for the calibrated roughness scale. The present serviceability rating (PSR), developed by the American Association of State Highway Officials (AASHO) (2), requires a panel of judges to subjectively rate the pavement section. PSR is thus an imprecise and inconvenient calibration reference. As a part of NCHRP project 1-18 (1), a reference roughness statistic was developed for the purpose of calibrating road meter systems. By its exact nature, it requires a profilometer to determine its value for existing road sections. But, even with the capability of assigning objective reference roughness values to surfaces, calibration of road meter systems is complicated by four categories of characteristics inherent in passenger cars, trailers, and road meters. These characteristics, outlined below, cannot be eliminated from existing systems by even the most diligent efforts in terms of maintenance and proper use of the equipment and so must be dealt with by the calibration process.

#### Vehicles That Have Unique Dynamic Properties

The overall dynamic properties of a vehicle are determined by the weight, compliance, and damping properties of its individual components. The properties differ from vehicle to vehicle and over the life of a vehicle. The properties of one vehicle can also change with environmental conditions; for example, damping provided by shock absorbers nearly always increases at colder temperatures. Since every vehicle has unique response properties, no two vehicles can be used to measure exactly the same quality of roughness. Tailoring of the dynamic properties of vehicles to match the reference is beyond the scope of available technology. Vehicle sensitivity to unique features in a roughness spectrum can be reduced by installing very stiff shock absorbers, and this practice is recommended as means for improvement (1).

But, overall, one must recognize that differences exist among vehicles and adjust roughness measurements obtained from a particular road meter system with empirical regression equations obtained in a calibration. Because pavements each have a unique roughness spectrum, a road meter system can overrespond to one road section (relative to a reference

Figure 3. Effect of hysteresis in road meter on the measured roughness statistic.

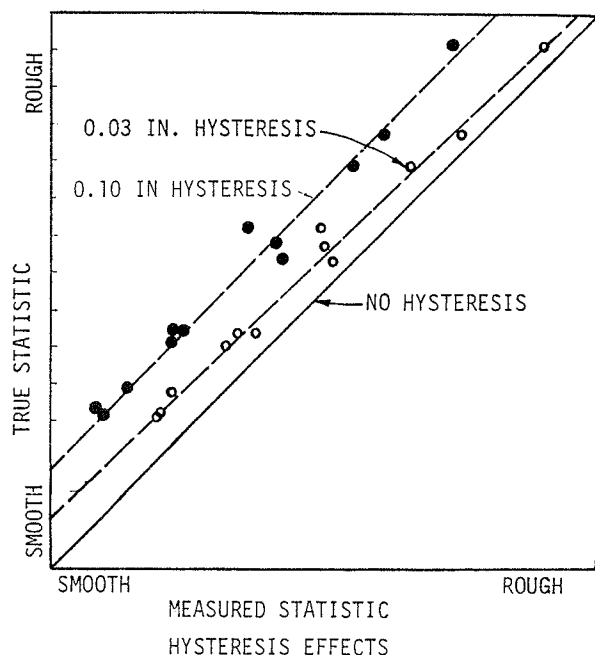
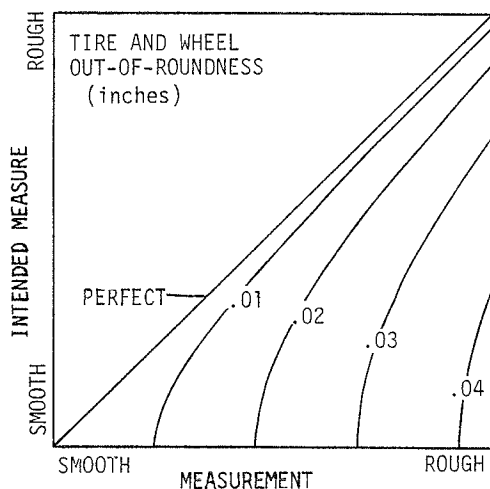


Figure 4. Effects of tire and wheel nonuniformity on the actual road meter measurement.



vehicle) and underrespond to another. This produces a random error and, to prevent bias in the regression equation, a number of pavements must be used to provide the data base for the regression.

#### Vehicles Are Not Linear

Vehicles contain many components that have friction or free play between them and are damped mainly by shock absorbers that are tuned by the manufacturer to provide a good ride over all operating conditions by giving them complicated nonlinear properties. Thus, if the roughness spectra of two surfaces differ by a factor of two, the corresponding vehicle motions will generally change by a different factor. Another characteristic of nonlinear systems is that the response at one frequency is dependent on the excitation at other frequencies. Thus, calibra-

tion must involve broad-spectrum roughness typical of real roads. Also, the best regression equation may not be a straight line that passes through zero, so the calibration must include at least two different levels of road roughness.

#### Road Meters Are Not Linear

Although road meters are intended to transduce and accumulate axle-body motion, as shown in Figure 2, they do so by employing a number of discrete switches that are only capable of detecting position within a certain interval. As a result, they quantize the axle-body position and create random error and compromise meter repeatability when the road is so smooth that the size of the axle-body motion is close to the quantization interval.

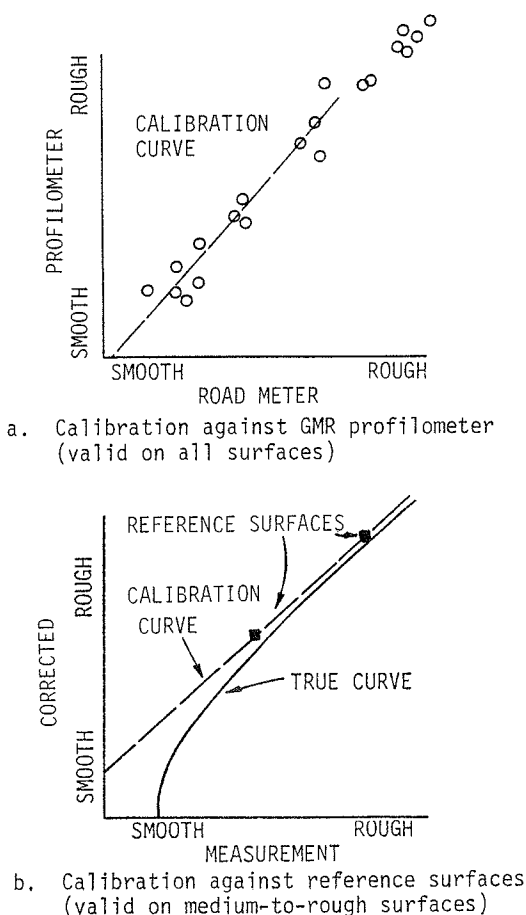
A more serious problem with modern road meters is that there are gaps between the switches, so that when the axle-body position moves from one switch to another, the response is not immediate. If the motion should reverse in this gap, a count is lost. This effect (called hysteresis) results in a roughness measurement that is lower than the true value. Until this time, hysteresis has not been recognized as important to performance and hence is variable among and within models of commercial road meters. Figure 3 demonstrates the effects of hysteresis by comparison of measurements taken simultaneously with two road meters installed in a single passenger car. Note that regression equations between the true roughness values (obtained with a linear transducer) and the measured values do not pass through zero and that the loss due to hysteresis is fairly constant for all roughness levels. In addition to this constant effect, random error also increases with the hysteresis in the road meter. In practice, the hysteresis nonlinearity in many commercial meters is so large that the vehicle nonlinearities are trivial by comparison.

#### Tires and Wheels Are Not Round

A road meter system not only responds to pavement roughness but also to other disturbances, most notably those caused by nonuniformities in the rotating tire and wheel assemblies. Whether the nonuniformity is caused by imbalance, runout (dimensional out-of-roundness), variation in radial stiffness, or all three, it is manifest as a periodic forcing at the rotation frequency of the wheel (approximately 10 Hz at 50 mph). Although the forcing does change with speed, at one particular speed it always has the same amplitude. Hence, its effect on the roughness measurement is more noticeable on smooth roads. Figure 4 shows this effect for different levels of wheel runout amplitude. Tire and wheel nonuniformities can be reduced, but a perfectly uniform assembly is impossible to obtain and roughness measurements on smooth roads will always be biased, as shown in the figure.

In practice, the right-hand and left-hand wheels will always have slightly different circumferences; as a result, the phasing between them will slowly change. When the nonuniformities from each side are in phase, the axle receives maximum excitation. And when they are completely out of phase, they cancel and provoke a minimum response. The distance needed for the phasing to cycle from in-phase to out-of-phase to in-phase again can be more than a mile. Accordingly, measurements on smooth roads may be subject to a slowly changing error that is consistent only over long distances. Measurements for sections shorter than one mile should be obtained by averaging the results of several runs together to reduce the random error from this source.

Figure 5. Examples of road meter calibrations.



#### Calibration of Existing Road Meter Systems

This outline of the quirks and complicated behavior of existing road meter systems should make clear that a valid calibration is no small task. Each of the four categories discussed above must be addressed by the calibration process if on-road measurements from different systems are to be converted to a common roughness scale. Two approaches are possible and are illustrated in Figure 5.

First, regression equations can be calculated by running the road meter system over a number of roads, together with a GMR-type profilometer equipped to provide the reference roughness measures. Vehicle dynamics, nonlinearities, and tire and wheel nonuniformities will all be included and taken into account by the regression relationship that acts as the calibration curve (see Figure 5a). Since tire and wheel nonuniformities provoke a speed-dependent response, different regressions should be made for each measurement speed used in normal practice. And since vehicle properties change with time, temperature, and other variables, calibrations must be conducted frequently. Due to the uniqueness of any one road section, 10 or more sections should be included for each regression to avoid biasing the calibration. This method has been demonstrated to be effective; however, it is time-consuming and requires access to a profilometer, which is both rare and expensive.

A second approach, which eliminates the need for a profilometer, is to perform the calibration with surfaces that have known roughness properties. This can be done with hydraulic shakers, by responding to

tape-recorded reference profile signals, or by fabricating artificial surfaces that have roughness properties typical of real roads. (However, a surface that has a roughness spectrum unusual for real roads cannot provide a calibration that is valid for on-road measurements.) Artificial surfaces were designed as part of the NCHRP project 1-18 to be traversed at 15 mph and to provide excitation typical of rough, bituminous roads that are traversed at 50 mph. The roughness value associated with the surface is defined by its profile; hence, the precision of the calibration is limited by the precision of the surface profile. By reducing the calibration speed, the task of minimizing background roughness from the underlying surface and from fabrication imprecision is reduced. The surfaces were designed to be average to the extent that they had no peculiarities that were significant enough to bias the calibration.

The main problem with a reduced-speed type of surface or a hydraulic shaker is that forcing due to the tire and wheel nonuniformities is not replicated because the wheels are not rotating at the proper rate. As Figure 5b illustrates, the resulting calibration is reasonably accurate for moderate and rough pavements (assuming tire and wheel nonuniformities are small due to good maintenance practice), but not for smooth pavements. If the magnitude of the tire and wheel nonuniformities were known, the calibration curve could be modified analytically, as shown in Figures 4 and 5b; however, it is impossible to establish this magnitude with existing meters.

#### POSSIBLE IMPROVEMENTS IN ROAD METER DESIGN

After a review of the operation and calibration of road meter systems as they now exist, hardware changes that could improve accuracy or ease the task of calibration can now be considered. Table 1 lists, for a number of instrumentation types, the minimum calibration that would be required to correct for each of the four categories of road meter and vehicle performance characteristics that act together to require such a lengthy calibration process.

Note that, for the basic Mays meter or PCA meter-based system, the tire and wheel nonuniformity problem puts the tightest constraints on possible calibration methods, as only a regression with a profilometer is valid. But, if the user of such a system is not interested in rating smooth pavements, the effects of tire and wheel nonuniformities are not as important, and then the major constraints are imposed by the nonlinearities in the system.

#### Linear Transducer

Given that the main nonlinearities in a road meter system are contributed by the meter, the obvious first step in hardware improvement is their elimination. The most simple device that would accomplish this is based on a velocity transducer mounted exactly like a road meter transducer between the axle and body of the vehicle, as shown in Figure 6. The output voltage, after it has been rectified and integrated electronically, is proportional to the accumulated axle-body displacement that existing road meters try to measure. This type of road meter eliminates hysteresis and quantization effects on roughness measurements, requires fewer parts than existing meters, and, if mass produced, could be much less expensive. Building such a meter from scratch today costs about \$200 in parts, including power supply, transducer, electronics, and display.

Perhaps a more significant advantage of a linear transducer over a conventional road meter is that



Table 1. Minimum calibration efforts required to correct for performance variables.

Type of Instrumentation	Performance Variables			
	Individual Vehicle Dynamics	Vehicle Nonlinearities	Meter Nonlinearities	Tire and Wheel Nonuniformities
Mays meter, PCA meter <sup>a</sup>	Artificial surface <sup>b</sup>	Two artificial surfaces <sup>b</sup>	Two artificial surfaces <sup>b</sup>	Regression equations from real roads and profilometer
Linear transducer	Artificial surface <sup>b</sup>	Two artificial surfaces <sup>b</sup>	None	Smooth drum rollers
Linear transducer, inductive rotation pickup	Artificial surface <sup>b</sup>	Two artificial surfaces <sup>b</sup>	None	Single road test, spectrum analyzer or computer
Two accelerometers	One special surface <sup>c</sup>	One special surface <sup>c</sup>	None	Smooth drum rollers
Two accelerometers, inductive rotation pickup	One special surface <sup>c</sup>	One special surface <sup>c</sup>	None	Single road test, spectrum analyzer or computer
Accelerometer, noncontacting probe	None	None	None	None

<sup>a</sup> Existing.<sup>b</sup> Surface must replicate roughness spectrum of average road. It cannot have any peculiarities, typical of individual sections of road, that would bias the calibration.<sup>c</sup> Surface can have any profile, as long as it is known.

Figure 6. Linear road meter system.

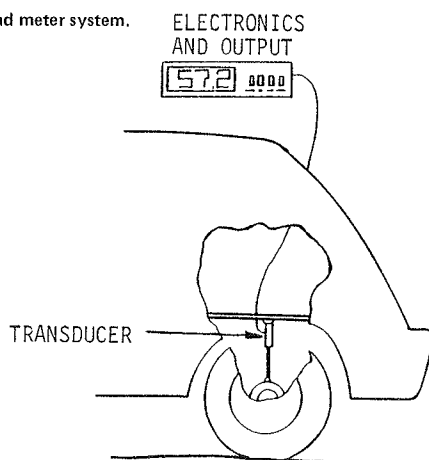


Figure 7. Calibration of linear road meter system.

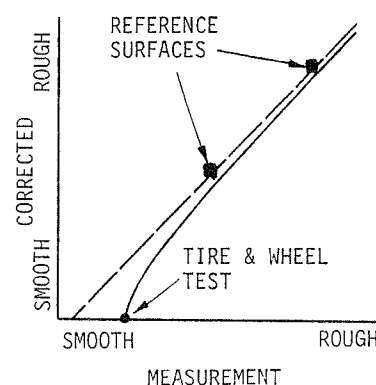
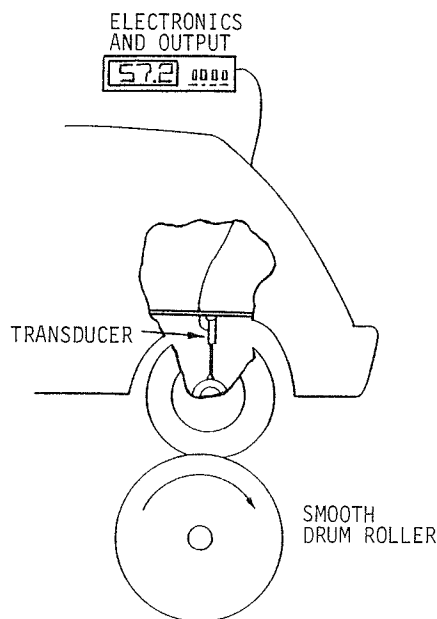


Figure 8. Use of smooth drum roller and linear transducer measured to establish the roughness induced by tire and wheel nonuniformities.

tire and wheel nonuniformities can be quantified and used to adjust a calibration curve found with two reference surfaces. All that is needed is the apparent roughness due only to the wheels on a perfectly smooth road, as indicated in Figure 7. The most direct method is to place the rear wheels of the vehicle on a smooth drum roller, run the vehicle at speed, and observe the measured roughness, as shown in Figure 8. (This approach will not work with existing road meters because they will not respond to small amplitude, high-frequency vibrations unless they are simultaneously subjected to larger amplitude vibrations caused by pavement roughness.)

A second method for determining the role of tire and wheel nonuniformities involves mounting an inductive sensor on a wheel to produce an electric pulse with each revolution. This set-up is illustrated in Figure 9. The record of pulses, together with the linear transducer signal, can be used to quantify the effect of the tire and wheel nonuniformities, even if the vehicle speed and the tire phasing change slowly throughout the test. The two records are used to compute the coherence function between the axle-body motion and the average rotation rate of the wheels. The coherence function tells how much of the output is correlated with the wheel rotation and allows the operator to place a precise number on the apparent roughness provoked by the tire and wheel nonuniformity. Note that the inductive sensor and spectrum analyzer are only required for calibration and not for full-time use. Hence, an agency that has a fleet of road meter systems could obtain a single sensor-spectrum ana-



lyzer package that would be circulated among the different vehicles.

Conceptually, this approach of discerning the apparent roughness induced by tire and wheel nonuniformities is superior to the drum roller approach, due to the nonlinearity of the vehicle suspension. The amount of amplification in the vehicle can be

Figure 9. Use of rotation sensor, linear transducer, and spectrum analyzer to determine the measured roughness induced by tire and wheel nonuniformities while traversing normal pavement.

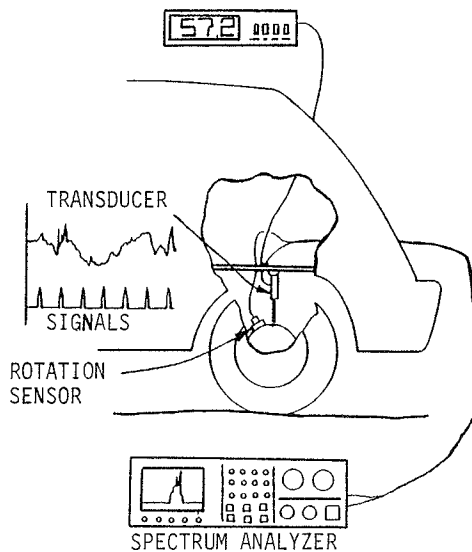
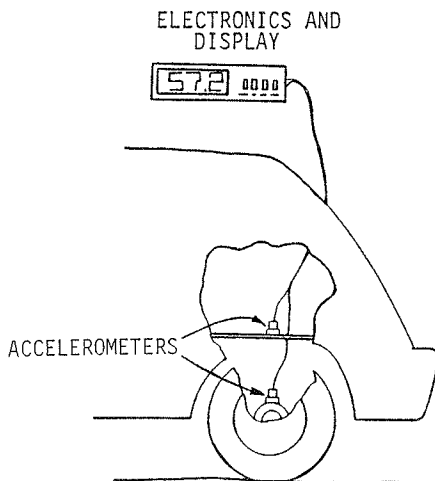


Figure 10. Example of crude profilometer with quarter-car simulation, based on two linear transducers.



different on a drum roller than on the road.

#### Two Accelerometers

Even at this point the unique vehicle dynamic properties are still present to influence the measurement obtained, which mandates calibration on known road-type surfaces. These effects can be eliminated by the addition of an accelerometer with the linear transducer, or alternately, simply two accelerometers, as shown in Figure 10.

The vertical acceleration of the body, immediately above the rear axle, can be written as

$$\ddot{z}_s + (1/M_s) (\text{suspension force}) + (1/M_s) (\text{other forces}) = 0 \quad (1)$$

where  $\ddot{z}_s$  is the acceleration and  $M_s$  is the sprung mass. The suspension force consists of all forces from springs, sway bars, shock absorbers, and friction. Virtually all of the nonlinearities are contained in the suspension force, and in addition,

most of the time-varying components that cannot be maintained (mainly damping characteristics) are also included. The other forces term includes effects due to the front-axle excitation and to wind. The vertical acceleration of the rear axle, neglecting tire and wheel nonuniformities, is

$$\ddot{z}_u - (1/M_u) (\text{suspension force}) + (K_T/M_u) (z_u - z) = 0 \quad (2)$$

where

- $z_u$  = vertical axle position,
- $z$  = average (of the two wheel locations) pavement elevation,
- $\ddot{z}_u$  = axle acceleration,
- $M_u$  = unsprung mass, and
- $K_T$  = tire spring rate (sum of both wheels).

If we neglect the other forces term, Equation 1 can be solved for the suspension force term and combined with Equation 2 to yield

$$z = z_u + (M_u/K_T) (\ddot{z}_u) + (M_s/K_T) (\ddot{z}_s) \quad (3)$$

Since  $z_u$  can be found by doubly integrating  $\ddot{z}_u$ , Equation 3 shows that two accelerometer signals ( $\ddot{z}_s$  and  $\ddot{z}_u$ ) and two coefficients ( $M_u/K_T$  and  $M_s/K_T$ ) can ideally remove all vehicle dynamics and leave the profile. The profile would then be input to the reference quarter-car simulation with well-known response properties (that will not change with time) to obtain the conventional roughness measurement. Note that this scheme also eliminates the nonlinearities in the suspension so that the final measurement is linearly related to roughness.

The basic limitations on the accuracy of the profilometer are imposed by (a) the presence of other forces in Equation 1, (b) the accuracy with which the two coefficients  $M_u/K_T$  and  $M_s/K_T$  can be determined, and (c) the time stability of the two coefficients. Since this type of system has not been built and tested, the importance of these three factors can only be estimated. Tests on a road simulator with four hydraulic shakers, together with computer studies, have indicated that the other forces are indeed small (1).

Determination of the two coefficients is, in fact, the calibration of this system. The two coefficients can be found by running the vehicle over any known profile (which need not have the roughness spectrum of a typical road) at several speeds. Sinusoidal bumps or eccentric drum rollers, run at two speeds, would provide the most straightforward determination of the coefficient values, but there are no theoretical problems with using more convenient shapes, such as a plywood sheet laid on a smooth surface.

Variations in the coefficients with time can be minimized by maintaining a steady load condition ( $M_s$ ), which requires that the level of gasoline be kept within fairly close limits and a constant hot air pressure be maintained in the tires ( $K_T$ ). If necessary, a separate empirical curve could be used to relate the  $M_s/K_T$  coefficient with gasoline level and cargo weight.  $K_T$  might change as the tires wear and age; if so, the coefficients would have to be reestablished periodically.

Since the response properties that vary with temperature, humidity, and so on are eliminated (along with the individual dynamic properties), calibration of this system, of the same kind needed with the others, is not needed. As Figure 11 shows, the relation between the corrected and uncorrected measurements is due solely to tire and wheel nonuniformities. As before, their effect can be compen-

Figure 11. Calibration of crude profilometer.

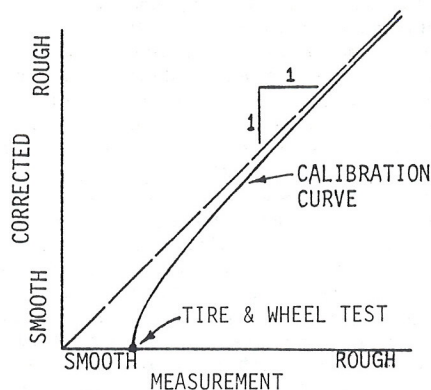
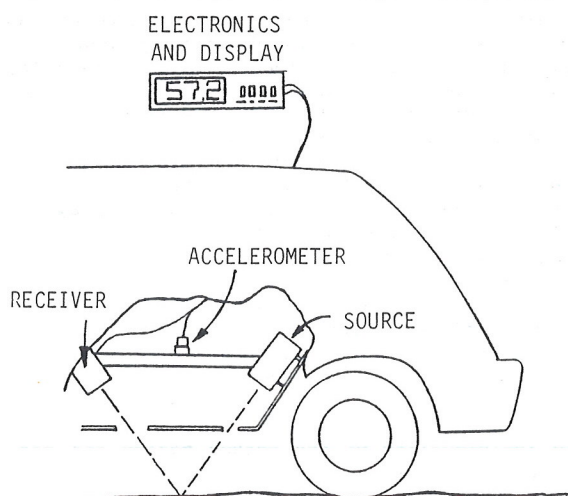


Figure 12. Noncontacting profilometer with quarter-car simulation.



sated by using a drum roller set-up or the inductive pick-up method.

#### Accelerometer and Noncontacting Probe

The final level of sophistication that can be achieved consists of an accelerometer together with

a noncontacting probe that operates as shown in Figure 12. This system should be recognized as a GMR-type profilometer, although the actual instrumentation package would more resemble today's road meters. Note that the trimmings available on most profilometers are lacking. The system simply measures the body-to-ground distance with the probe, along with the body acceleration. After the acceleration is integrated twice, the two signals are added, which yields the profile, which is then input to a quarter-car simulation that provides the well-defined reference roughness statistic. No computers or tape recorders are needed. The calibration task is limited to the following:

1. Calibration of the probe,
2. Calibration of the accelerometer, and
3. Occasional checking of the electronic processor.

As Table 1 shows, all of the problems with existing road meter systems are eliminated.

#### SUMMARY AND CONCLUSIONS

The low cost and simplicity that make road meter systems so popular are offset by limited accuracy and the need for a difficult calibration, as demonstrated in the NCHRP 1-18 project (1). Means for overcoming these limitations by the addition of more complex and sophisticated instrumentation have been explored in this paper. At the level of instrumentation needed to allow calibration on something other than a known, random road surface, the system has actually become a simple profilometer. Thus, the development of improved road meter systems will lead to the development of simplified, low-cost road profilometer systems.

#### REFERENCES

1. T.D. Gillespie, M. Sayers, and L. Segel; Highway Safety Institute, University of Michigan. Calibration and Correlation of Response-Type Road Roughness Measuring Systems. NCHRP, Rept. 228, 1980, 81 pp.
2. W.N. Carey, Jr., and P.E. Irick. The Pavement Serviceability-Performance Concept. HRB, Bull. 250, 1960, pp. 40-58.

*Publication of this paper sponsored by Committee on Pavement Condition Evaluation.*

## Better Method for Measuring Pavement Roughness with Road Meters

M. SAYERS AND T.D. GILLESPIE

Recent research on methods for calibrating road roughness measuring systems has shed new light on improving the use of the currently popular Mays and Portland Cement Association (PCA) roadmeters. The measurement provided by these meters (accrued displacement between the rear axle and vehicle body) is discussed and shown to relate best to pavement serviceability when normalized by the time duration of the test, thus yielding a simple statistic called the average rectified velocity (ARV) of the axle-body motion. Unlike

the inches per mile statistic that is commonly calculated, the ARV is shown to be valid for comparing pavements that are measured (and used) at different speeds. At the same time, the ARV concept provides a logical basis on which to establish calibration for roadmeter systems. In the absence of a universal calibration, the measurements obtained from different systems cannot be compared except in the special case where empirical correlations have been established. Accordingly, an absolute roughness scale is specified based on a refer-

ence ARV (RARV) statistic determined from a quarter-car simulation. RARV constitutes an absolute roughness statistic, rigorously defined at a given test speed, whose validity as a calibration reference has been established from field-test experience with in-use roadmeter systems. An appreciation for the ARV is important to highway engineers because the concept provides the link in understanding between current roughness measurement practice and serviceability of roads as seen by the public at normal traffic speeds.

National Cooperative Highway Research Program (NCHRP) Report 228 (1) has provided an opportunity to take an objective look at the road roughness measurement process with roadmeter systems. In so doing, it has become evident that their ultimate purpose--to assess pavement serviceability--is hampered by the choice of the measured statistic in common use. Specifically, the practice of normalizing inches of roadmeter roughness by the distance traveled (inches per mile statistic) is not appropriate to such systems because it implies that the statistic is a measure of the actual pavement properties, rather than the measure of vehicle response that it is. Further, the inches per mile statistic incorporates a speed dependence that confounds its relation to serviceability on roads that have different prevailing traffic speeds and complicates the calibration of these systems.

Roadmeter systems are subject to many other problems related to day-to-day reliability and calibration procedures, which are more visible to the user than the aforesaid limitations. Thus, it is no surprise that they would remain mostly unknown prior to a research effort that has the scope of the NCHRP project. But, once the performance and operation of roadmeter systems are well understood, we see that these systems are best used to measure the average rectified velocity (ARV) of the axle motion relative to the body.

ARV is obtained simply by normalizing the roadmeter roughness count by the time duration of the test. This statistic, which has units of length per time (e.g., inches per second), has a more direct relation to the dynamic response of vehicles to road roughness. Hence, it has more utility as a roughness measure related to serviceability. Similarly, it provides a more direct basis for calibrating roadmeter systems to a comparable roughness scale.

This paper reviews the concept of pavement serviceability and illustrates the differences between ARV and the inches per mile statistic as a measure of serviceability. A calibration reference for ARV measures is also presented.

#### PAVEMENT SERVICEABILITY

A primary result of the American Association of State Highway Officials (AASHO) road test was the development of the serviceability concept for evaluating the condition of the pavement surface (2). The proper measure of pavement serviceability, defined by AASHO, is an average of subjective opinions provided by a panel of judges by using a present serviceability rating (PSR) scale of 0-5, with a 5.0 being perfectly smooth and 0 being impassable. The PSR numbers were correlated with various objective measurements of pavement features through regression equations so that the objective measurements could be used later to estimate PSR. The estimate of PSR based on a measured pavement statistic is called present serviceability index (PSI). PSI values also vary from 0 to 5 and have the same physical interpretation.

At the time of the AASHO study (1955), the slope variance (SV) produced by the AASHO profilometer [the predecessor to the Carey, Huckins, Leathers, and other engineers (CHLOE) profilometer] was the

objective measurement of roughness obtained on the pavement test sections, although some sections were also run with a Bureau of Public Roads (BPR) roughometer. Each of these devices produces only a single statistic, and thus the AASHO data cannot be used to provide a detailed understanding of exactly which road features influence PSR the most, other than the general conclusion that pavement roughness almost completely determined the PSI (2,3). Another finding from the AASHO study was that different regression equations were needed to relate the objective measures to PSR for different pavement types. This indicates that neither measure is truly related to serviceability; for if this were the case, a single regression equation would be valid for all pavement types. Analyses of the CHLOE and BPR roughometers have shown that they are sensitive to roughness features that are absorbed by the tires on a vehicle and have little effect on ride. At the same time, rigid pavements were found to have more of this type of roughness, and hence the measures are biased against rigid pavements (1).

The exact relation between pavement features and PSR has never been established, but by just considering the interaction among pavement, vehicle, and passenger we can be fairly certain that serviceability is a measure of the ride experienced by the users, as well as perceived wear and tear on the vehicles. A PSR of 5.0 would mean that no vibrations attributable to the road are detected by the panel member, and a PSR of 0.0 would mean damage to the vehicle. In this paper, we will proceed with the understanding that the exact nature of the PSR scale is unknown, but that equal PSR ratings are obtained for different pavements if both excite equivalent vehicle motions, in terms of both passenger vibrations (ride) and suspension and wheel motions (wear and tear). Thus, at a minimum, a single serviceability rating is a function of (a) pavement roughness features, (b) vehicle properties, (c) the individuality of the person making the rating judgment, and (d) speed.

Although the first three points were widely accepted, the speed factor is sometimes ignored, although virtually any section of pavement has a reasonable serviceability if very low speeds are maintained for reasons other than its roughness. For example, a section of pavement in a congested city area could have potholes, cracks, irregular settlement, and still be fair (PSR = 2.5) for the people it services if other conditions (e.g., children, intersections, and many driveways) restrict the speeds to less than 20 mph. Yet, if these other restrictions were removed, the same pavement might be impassable (PSR = 0) for most users at 45 mph, because the vehicle would be damaged by the roughness. Clearly, the serviceability cannot be defined by a physical measure of the pavement roughness alone, but also must take into account the average speed of the traveling public. This fact is not acknowledged in the original AASHO study, no doubt because the concern was in rating highways at high speed. Therefore, the equations provided for PSI do not include speed, and as a result, the validity of comparing PSI values for pavements that are traveled at different speeds is uncertain.

Although the above example might seem extreme, the same argument applies for highways that have close, but dissimilar, speed limits. A section of highway used at 45 mph can be a little rougher (and thus have a lower PSI as determined by the AASHO equations) than a section used at 55 mph, even though they both offer equivalent ride quality and thus equal serviceability.

Figure 1. Illustration of ABD and accumulated ABD on road 1 at 50 mph.

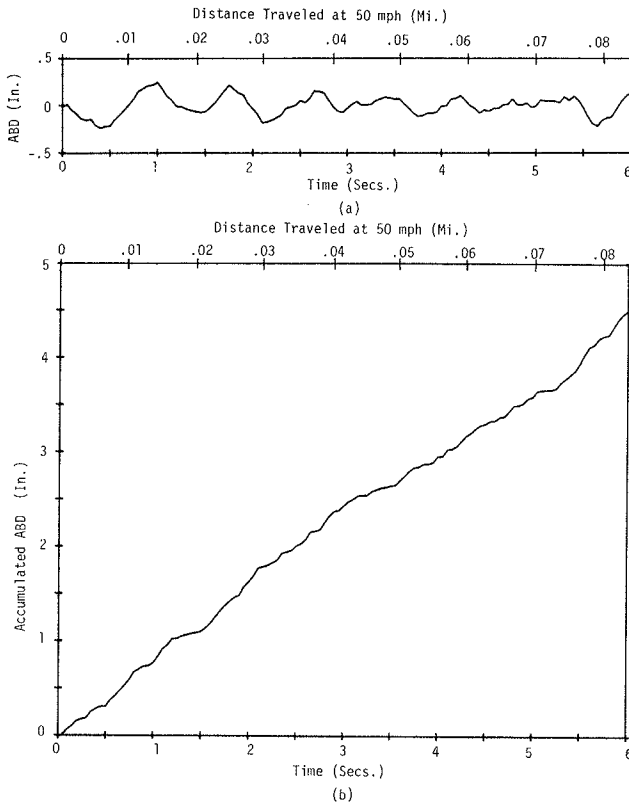
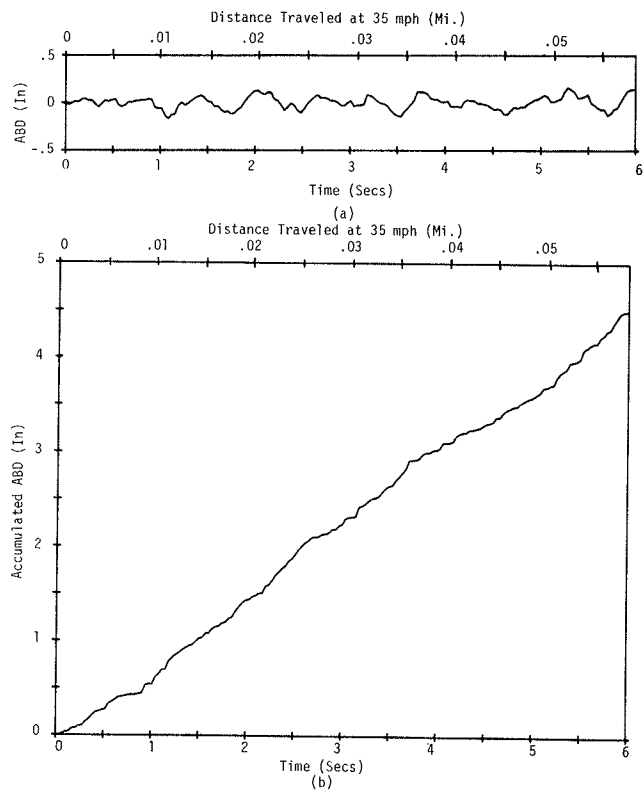


Figure 2. Illustration of ABD and accumulated ABD on road 2 at 35 mph.



#### RATING PAVEMENTS IN INCHES PER MILE

The CHLOE profilometer and the BPR roughometer are seldom used routinely for measuring pavement roughness anymore, mainly because they require low operating speeds that obstruct traffic and slow down the measurement process. Instead, the most popular type of system is that of a conventional passenger car instrumented with a roadmeter. Most roadmeters in use are either Mays meters manufactured by Rainhart Corporation (4) or Portland Cement Association (PCA)-Wisconsin meters (5), also available commercially from several manufacturers but sometimes fabricated by their users. Both types of meters transduce the rear-axle motion relative to the car body. Consider first the measurement process, which assumes that they transduce the motion perfectly and are perfect meters. In fact, they are not, and the resulting effects on the measurement are addressed later.

The axle-body motion is random, as illustrated in Figure 1a for a typical record of axle-body distance (ABD) versus time. Roadmeters are intended to accumulate this motion, as shown in Figure 1b for the same record. When ABD is increasing, which is to say it has a positive velocity, the two plots have identical shapes. But when the ABD is decreasing and has negative velocity, the accumulation on the meter is an inverted duplicate of the ABD plot that has a positive velocity. Therefore, the accumulation on the meter is a version of the ABD record that has the velocity rectified (i.e., unchanged when positive and inverted when negative).

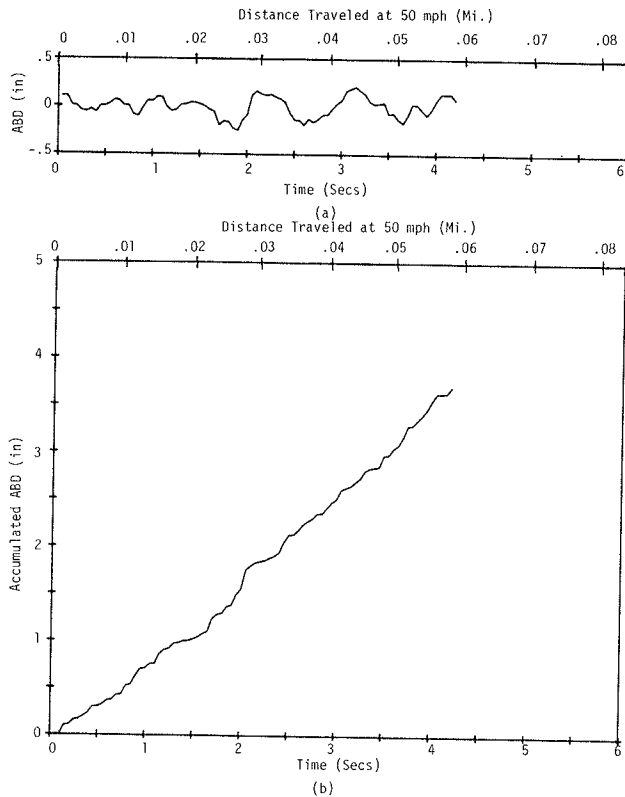
[This figure and the following figures were generated on the computer for the convenience of illustrating certain effects of using a quarter-car simulation together with measured road profiles and a mathematical model of a ridemeter. The models were thoroughly validated with field tests in the

NCHRP project (1) such that the results shown are indeed representative.]

Common practice in the past has been to normalize the total accumulated motion obtained by dividing it by the length of road section under test to obtain an inches per mile statistic. The measure obtained is supposedly an indication of vertical deviation per mile of length—a type of measurement that closely identifies with the engineer's notion of roughness in the roadway as seen by a vehicle. In fact, the value accumulated on the meter at any time is the product of the average rate of vehicle motion and the length of time the meter has been running. The rate of accumulation is directly related to the ride vibration amplitude at any speed. The rate normally increases with the speed, as does the level of ride vibration. However, the travel time over a given length of pavement diminishes with speed, so that the ratio (as reflected in the inches per mile statistic) varies with speed both according to the different level of ride vibration and to the different travel time. This behavior is illustrated here by some examples; a more rigorous treatment is presented elsewhere (1).

In the first example, the vehicle speed is 50 mph during the test illustrated in Figure 1 and thus, in the 6 s shown, 0.083 mile was traveled. The accumulated ABD is 4.5 in, which gives a roughness measurement of 54 in/mile. Figure 2 shows similar time histories, for a different pavement section, with a measurement speed of 35 mph. A comparison of Figures 1 and 2 reveals that both ABD plots are qualitatively similar and that the accumulated ABD in Figure 2b is also 4.5 in after 6 s. From the user's viewpoint, both pavements will cause the same wear and tear to the vehicle and produce the same intensity of vehicle vibration (ride), hence the serviceability of the pavements should be equivalent. But at 35 mph, 6 s is only 0.058 mile, and thus the 4.5

Figure 3. Illustration of ABD and accumulated ABD on road 2 at 50 mph.



in of accumulated ABD result is 77 in/mile. Therefore, judgment of roughness on the basis of the inches per mile statistic leads to the erroneous conclusion that road 2, used at 35 mph, is worse than road 1, used at 50 mph when, in fact, both roads appear equivalent to the user public.

Not only do the inches per mile numerics distort the underlying pavement serviceability, they do not relate to fixed physical features of the road as one might suppose from the implied meaning of the statistic. Regardless of the final units, the statistic is still based on the response of the vehicle to the road at the measurement speed. If the measuring speed on the second road (Figure 2) is increased to 50 mph, the ride is rougher, with more ABD motion, as shown in Figure 3. If the speed limit is raised for this road section, so that 50 mph would be representative of the typical user speed, the road would provide less service because there would be more wear and tear on the vehicle, along with a poorer ride. However, because of the decreased transit time, the accumulated ABD will decrease to 3.7 in, which results in a roughness of 65 in/mile. Thus, this measure would mislead the casual observer into thinking that the road offers better service at 50 mph than at 35 mph.

#### BETTER STATISTIC FOR RATING PAVEMENTS

Clearly, the problem in comparing roadmeter accumulated ABD measurements taken at different speeds results from the conversion of the measurement to the inches per mile statistic. A more useful statistic is obtained by dividing each accumulated ABD measurement by the time duration of the test. By using the same three examples, the data from Figure 1 would yield a measurement of 0.75 in/s. The data in Figure 2 would also give 0.75 in/s, and the data in Figure 3 would give 0.88 in/s. It is clear from

these inch per second statistics that road 1, at 50 mph, provides the same service to its users as road 2 at 35 mph. The change in serviceability when the speed for road 2 is increased from 35 to 50 mph is equally clear from these numbers.

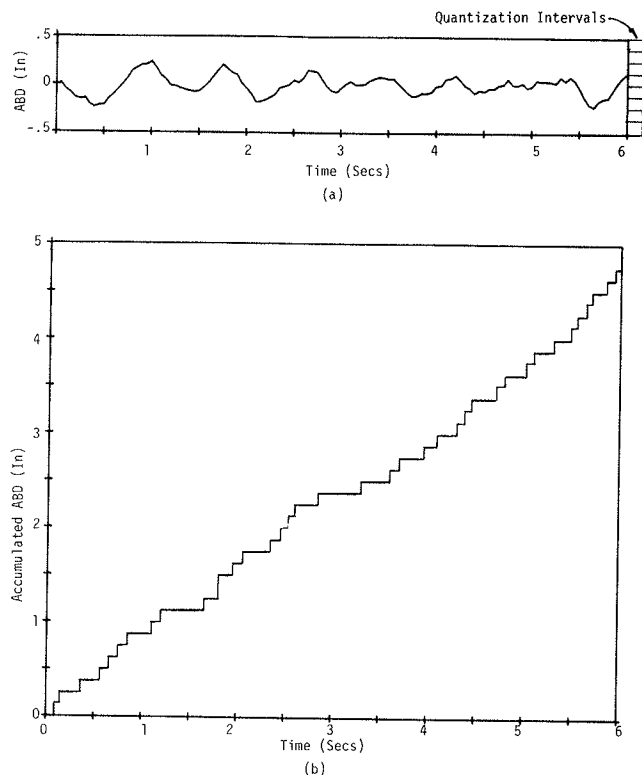
Division of the accumulated axle-body distance by a time interval results in an average velocity. Since the roadmeter rectifies the axle-body motion, the statistic being calculated is the average rectified velocity (ARV) of the axle-body motion. The conversion factor between ARV and inches per mile is the time needed to travel one mile at the test speed. For 50 mph, this factor is 72 s/mile when ARV is given the units inches per second. Thus, data recorded in inches per mile can be easily converted to ARV, after which measurements taken at different speeds can be compared directly. Note that the practice of converting the roughness measurements to an equivalent 50 mph test speed by multiplying the inches per mile figure by the ratio actual speed/50 results in the ARV, which has the units inches per 72 s. This measure is equally valid, but should be recognized for what it is—ARV represented with unconventional units.

Because the basic measure produced by a roadmeter depends on vehicle response, and is therefore speed dependent, measurements must be taken at speeds typical of the users of the pavement. Open highways should be run at 50 mph (or even 55 mph), but other roads should be run at normal prevailing speeds. Measurements made at other speeds (for example, 35 mph on an Interstate highway) are not valid and cannot be converted to an equivalent measure at the correct speed without a tedious correlation exercise. Although all roads have qualitatively similar roughness characteristics, any one section is unique and no universal relation between roughness at different speeds will accurately correct for speed on every road (1).

#### EFFECTS OF ROADMETER TRANSDUCER FEATURES ON MEASURED ROUGHNESS STATISTICS

Up until this point in the discussion, we have assumed that the roadmeters are capable of measuring ABD perfectly and continuously. In fact, current Mays and PCA meters employ transducers that have discrete steps that can only identify the ABD as being within a certain interval. The original PCA meter used switches 1/8-in on-center, and the Mays meter uses an optical pick-up that had 1/10-in steps. Although different versions of the roadmeters detect motion with different hardware setups, they all act to quantize the ABD, as illustrated in Figure 4. For the Mays meter, each step (as in the figure) corresponds to one incremental step in the advance of the strip chart; for the PCA meter, each step corresponds to a count in one of the registers. [Note that the paper length produced by the Mays meter must be multiplied by a scale factor of 6.4 in/in to relate paper displacement to ABD. Similarly, the unweighted sum of PCA meter counts must be multiplied by the quantization interval (typically 1/8 in/count). The practice of weighting the PCA meter counts before summing them is not considered in this paper. Although PCA meters can produce the same measurements as a Mays meter, and thus ARV, the converse is not true and therefore the simple accumulated ABD measure is seen to be of more universal interest.] Note that although the quantized version of the accumulated ABD plot is not a true representation (see Figure 1b), the fractional error in the resulting accumulated ABD is small if the measurement time is long enough. A statistical analysis, which employed random process theory, showed quantization effects to be negligible for

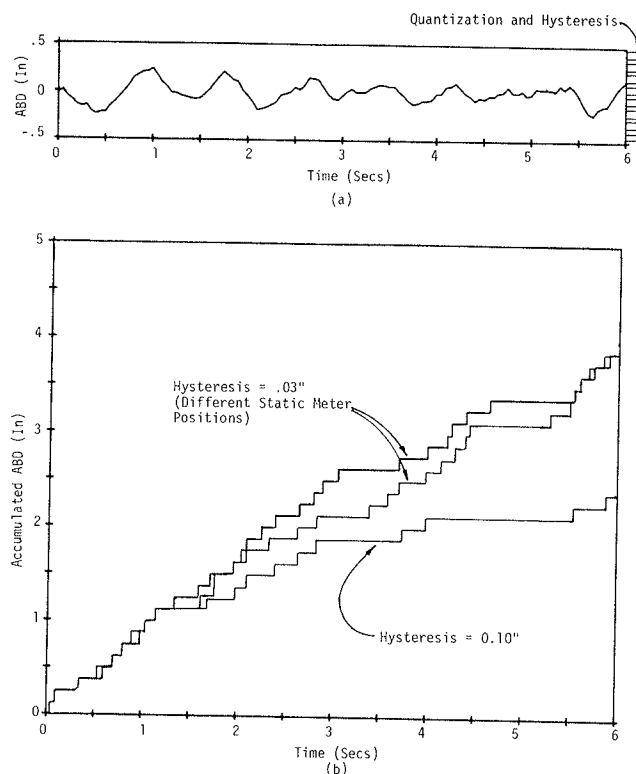
Figure 4. Illustration of accumulated ABD obtained by a meter with quantization.



reasonably long measurement times when the axle-body motion is fairly large compared with the quantization level (1). (The 6-s record length in the figures was selected to clearly illustrate roadmeter operation but is really too short for accurate measures with commercial meters.) In general, if four or more quantization intervals on a Mays or PCA meter are frequently activated in measurement, the quantization should not be a problem. But if the road is so smooth that only a few intervals are activated, a random error will be included in the measurement, depending on the equilibrium position of the axle relative to the switching intervals.

Commercial Mays and PCA meters also have hysteresis in the transducers. This is usually a result of spaces between the switches, as illustrated on the side of Figure 5a. But hysteresis can also be caused by free-play somewhere between the axle attachment and the position sensor, as, for example, with loose mountings or worn bearings. Figure 5b shows the accumulated ABD for two hysteresis levels and also for a second axle-body equilibrium position for one of the levels. The figure illustrates that (a) hysteresis acts to reduce the accumulated ABD from its true value (shown in Figure 1a) and (b) hysteresis, together with the quantization, introduces a random error that depends on the equilibrium ABD within the center switch interval. The practical importance of these two effects is apparent from Figure 6, which compares ARV measurements taken simultaneously from two commercial roadmeters that were installed in the same vehicle. The figure shows that the loss in measured ARV is more or less constant and not proportional to the true ARV. In addition, more scatter occurs with the high-hysteresis meter, which has a standard residual error of 0.140, than for the lower-hysteresis meter, which has a standard residual error of 0.097. The standard residual error used to compare these two

Figure 5. Illustration of accumulated ABD obtained from meters with different hysteresis levels and static positions.



measuring systems is the ratio of the range of scatter to the range of measured values and defines that portion of the standard deviation of one measurement not accounted for in the correlation with the second measurement.

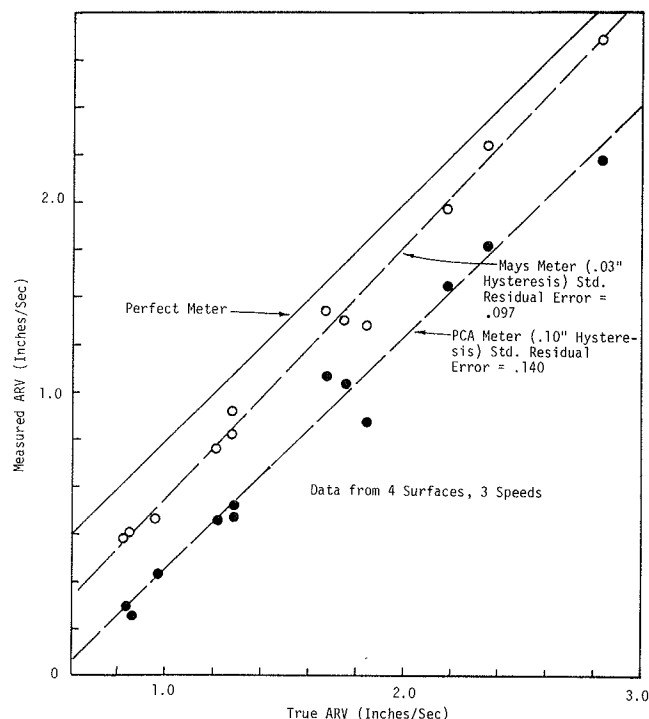
In practice, hysteretic losses can be compensated, on the average, by calibration by using regression equations. However, the increased scatter cannot be reduced by any practice other than by reducing the hysteresis. The calibration, though imprecise, eliminates trends correctly if a large number of roads are included and all measurements are converted to ARV. If the calibration is to be used to relate measurements taken at different speeds, it is vital that all inches per mile measurements be converted to ARV. This is obvious from the figure and preceding discussions because the hysteretic effect is a constant loss of ARV and, therefore, corresponds to a different inches per mile value at each speed. Thus, a calibration obtained from inches per mile statistics measured at different speeds will have even greater scatter. Figure 7 illustrates the scatter effect by showing the same data used in Figure 6 plotted in inches per mile units. The need for presenting calibration curves in terms of ARV instead of the inches per mile statistic is, of course, another argument for its use.

#### REFERENCE ARV MEASUREMENT

The most fundamental problem in calibrating roadmeter systems has been the lack of a well-defined absolute reference measure against which to calibrate. ARV (as well as inches per mile) is a measure of vehicle response at the selected test speed, so no single objective measurement of pavement roughness can be expected to relate to roadmeter statistics at arbitrary test speeds. Further, since



Figure 6. Linear regressions of Mays and PCA meter measurements of ARV against true ARV when mounted in one vehicle.



individual vehicles and roads have unique properties, perfect agreement between any two systems, even after calibration, is impossible. But clearly, the reference measure should agree closely with the measures made with roadmeter systems. In essence, a reference pavement roughness measure should:

1. Provide a measure that correlates highly with PSR for all speed and pavement conditions,
2. Provide a measure that correlates well with existing roadmeter systems for all conditions, and
3. Be clearly defined to the extent that measurements taken anywhere, at any time, have the same scale.

By and large, these objectives are met by use of the ARV concept to describe pavement roughness as measured by roadmeters and by defining a reference against which to calibrate. A reference system is presented in Figure 8 that is defined by the differential equations and parameter values shown in the figure. These equations can be manipulated analytically to provide a linear response function or copied into a digital computer simulation. Alternatively, a physical system can be built that treats the equations as the performance objectives. The most practical physical system is an electronic circuit that, when given a voltage proportional to pavement profile at the correct speed, provides an output voltage proportional to the axle-body motion. Of course, the consequence is the need for an instrument for profiling actual road sections, a natural result of defining a roughness measure so precisely. In fact, the precision of a reference ARV (RARV) measurement is limited only by the precision of the profilometer. With existing General Motors Research Laboratory (GMR)-type profilometers, this results in errors of less than one percent.

The adequacy of the RARV statistic defined in Figure 8 has been established by experimental correlation with a number of roadmeter measurement sys-

Figure 7. Linear regressions for Mays and PCA meter measurements of inches per mile against true inches per mile.

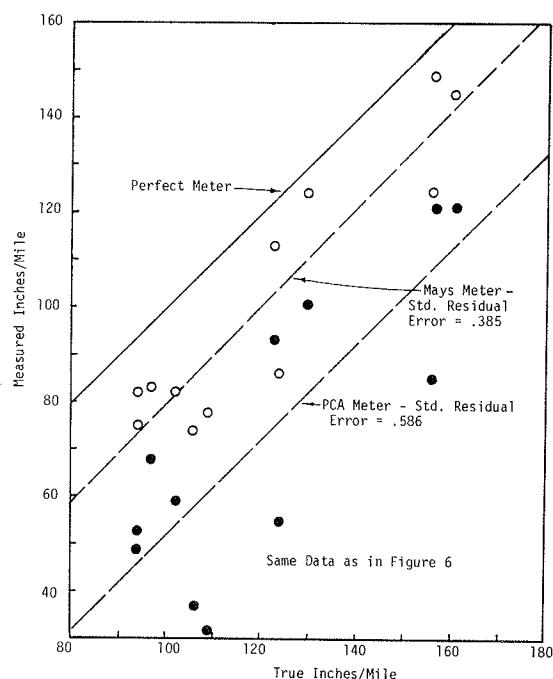
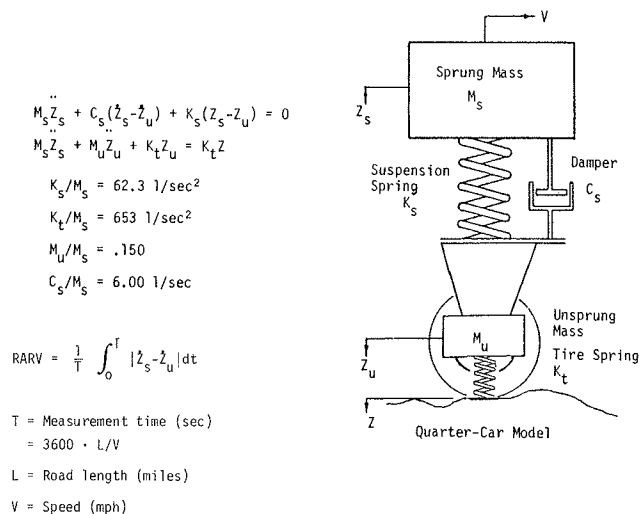


Figure 8. Reference pavement roughness measuring system.



tems (1). A roadmeter measuring system can be calibrated to the RARV roughness scale by using regression equations to relate the true RARV value to the ARV measurement over a selection of roads. The resulting numeric is then designated the calibrated ARV (CARV), which ideally agrees closely with the RARV value. However, a random error is still present, which reflects the uniqueness of each roadmeter system. Although temptation is to report results in the format familiar to most roadmeter users (such as in/72 s = inch/mile at 50 mph), in fact there is no universal inch per mile standard that will yield the same meaning to all users. But on the reference scale, the existing data show that, on a fair road (RARV = 1.0 in/s), the roadmeter systems have a precision of about 10 percent, but on smoother pavements, the relative error is much



greater and can be on the order of 50-100 percent. On the other hand, roadmeter systems demonstrate better accuracy on rougher roads (5 percent and better) (1).

#### REPORTING ARV MEASUREMENTS

In all, three classes of ARV statistics have been presented. The first, ARV as obtained with a roadmeter, will include effects of meter hysteresis and individual vehicle response properties as well as the pavement properties and measurement speeds. Raw ARV measurements from different systems do not quantify roughness on a common scale, and any comparisons between ARV measures from different systems are not valid. The second class is RARV, a well-defined property of pavement profile at a given (simulated) measuring speed. It requires a profilometer, together with the vehicle simulation shown in Figure 8. Its precision is limited only by the precision of the profilometer; errors less than one percent (0.01 in/s) are easy to maintain with current profilometers (1). The third class is the CARV measurement that is obtained by using the regression relation between raw ARV values from a given roadmeter system and the true RARV values. CARV is the best estimate of RARV that can be made with a particular roadmeter system.

CARV measures taken by different systems can be compared directly because they are based on the same RARV scale. Measures taken at different speeds are also comparable if they are taken at typical traffic speeds. Because the ARV measure is dependent on speed, roughness measurement practice with roadmeters will be improved by subscripting measurements with the test speed (e.g.,  $CARV_{35} = 1.6$  in/s).

The validity of the RARV statistic for all types of pavement has not yet been completely established

in the field, although the limited data gathered during a correlation program show no bias for different pavement types (1). Because the RARV statistic is influenced by the same roughness features that cause typical ride and suspension motions, unlike the CHLOE profilometer and BPR roughometer, there is no obvious reason to suppose that the RARV is biased by pavement type. Hence, it is suggested as a single objective measure of pavement serviceability for all conditions until a better measure can be developed through further research to relate subjective ratings to specific road roughness qualities.

#### REFERENCES

1. T.D. Gillespie, M. Sayers, and L. Segel; Highway Safety Research Institute, University of Michigan. Calibration of Response-Type Road Roughness Measuring Systems. NCHRP, Rept. 228, Dec. 1980, 81 pp.
2. W.N. Carey, Jr., and P.E. Irick. The Pavement Serviceability-Performance Concept. HRB, Bull. 250, 1960, pp. 40-58.
3. E.J. Yoder and B.E. Quinn; Purdue University. Comparison of Different Methods of Measuring Pavement Condition--Interim Report. NCHRP, Rept. 7, 1965, 29 pp.
4. Mays Ride Meter Booklet; 3rd ed. Rainhart Company, Austin, TX, 1973, 23 pp.
5. M.P. Brokaw. Development of the PCA Road Meter: A Rapid Method for Measuring Slope Variance. HRB, Highway Research Record 189, 1967, pp. 137-149.

*Publication of this paper sponsored by Committee on Pavement Condition Evaluation.*

## Road Roughness: Its Evaluation and Effect on Riding Comfort and Pavement Life

A.A.A. MOLENAAR AND G.T. SWEERE

This paper describes the evaluation of road roughness and its influence on driving comfort and pavement deterioration. Distinction is made between an inventory and a diagnostic survey. The equipment used for both surveys is described. They are a ridemeter for the inventory survey and a high-speed profilometer for the diagnostic survey. Since the ride index, which is given by the ridemeter, is dependent on the measuring vehicle, relations are established between the ride index and fundamental indicators of road roughness as determined with the high-speed profilometer. Based on measurements with the high-speed profilometer, the impact of road roughness on the structural deterioration of the pavement and on the riding comfort is calculated. Also, the impact of road roughness on the safety of the road user is described. By using the results of these calculations and the relation that exists between ride index and fundamental indicators of road roughness, acceptance levels for the ride index were established. These acceptance levels can be used as a guide in the evaluation of the results of the inventory survey.

In order to know whether pavement is still in a good condition, the highway engineer should frequently perform condition surveys. Those condition surveys should consist of monitoring the strength char-

acteristics (e.g., deflection, cracking, and rutting), skid resistance, and roughness of pavements (1). Since road roughness affects, to a large extent, the dynamic loading of the pavement caused by the tire, it also affects the development of the structural deterioration of the pavement and the safety of the road user. So road roughness should be taken into account in evaluating the strength of the pavement and the safety of the road user (Figure 1). Because evaluation of a whole road network will result in a mass of data, the survey should be done in two phases:

1. An inventory survey and
2. A diagnostic survey.

The inventory survey can be done by means of measurements that are easy and cheap to use and can be executed at high speed. To this group of measurements one can count the Mays meter, the Portland

Figure 1. Relation of pavement roughness evaluation to evaluation of pavement strength and safety.

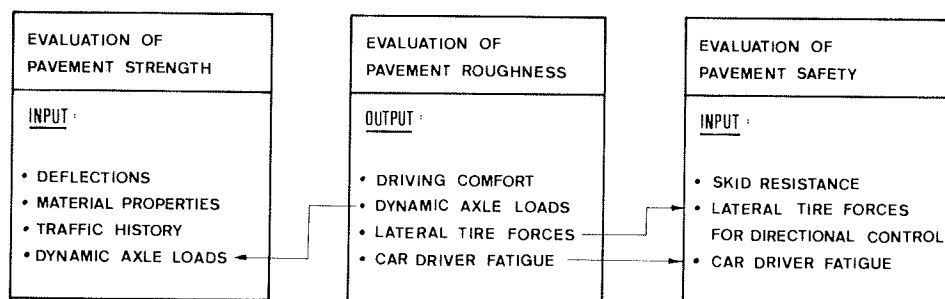
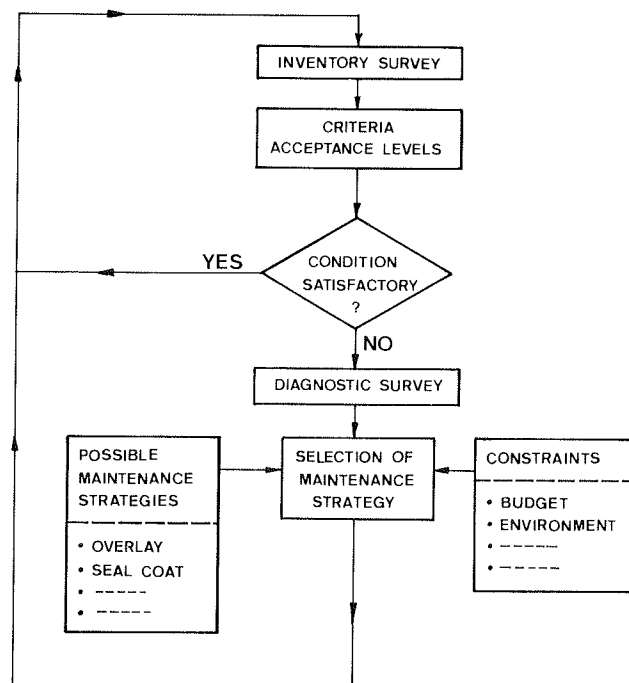


Figure 2. Survey system for pavement management system.



Cement Association (PCA) meter, the Delft University ridemeter (which is used in this study), and even the Bump Integrator [also called the U.S. Bureau of Public Roads (BPR) roughometer]. Each of these is easy to use and rather cheap to operate; besides that, the measurements can be done in a short time. The disadvantage of this type of measurements is that only an indication of road roughness is obtained in terms of vehicle response; so in fact it is not the road profile that is measured by the interaction between the road and the vehicle. The diagnostic survey should be done by means of measurements that will give the exact profile of the road. This road profile can be used as input for all kinds of calculations, such as power spectrum calculations or simulation of vehicle behavior. Based on the results of this type of measurement, we can determine what kind of maintenance activity should be applied in order to reduce pavement roughness to an acceptable level.

For the diagnostic survey, use can be made of the leveling methods for profile determination, which are slow in operation. Sophisticated high-speed profilometers such as the surface dynamics profilometer, originally known as the General Motors profilometer, the APL developed in France, and the Delft University high-speed profilometer, which is used in this study, are much more suited for this

type of survey. By using one of these systems one can get the exact road profile on which one can execute all kinds of calculations, as for instance simulation of the vehicle behavior. Disadvantages of these systems are that they are complex and expensive and require an analog computer to interpret the results.

Measurements with a high-speed profilometer should be seen as diagnostic surveys. Although these measurements can be executed at high speed, specially trained personnel and complex and expensive equipment are needed. Most highway authorities are not in the position to have such equipment.

In order to know from the inventory survey whether or not the pavement is in a satisfactory condition, one should have an insight into the extent to which the results of these inventory measurements will give information about more fundamental properties of road roughness, such as the power spectrum and the slope variance of the road profile, as determined by diagnostic survey methods. In other words, relations between the inventory and diagnostic survey methods are needed.

Furthermore, the results of the diagnostic survey should be translated into values that are meaningful to the road user and highway engineer. The power spectrum of the road profile needs to be translated into, for instance, a present serviceability index and a load safety factor. The latter should represent the damaging effect of a dynamic axle load in comparison with the effect of a static axle load. Once pavement roughness is translated into effects on driving comfort, road user safety, and pavement deterioration, we can set up acceptance levels for the results of the inventory survey. An unacceptable level of road roughness in the inventory survey will result in a diagnostic survey. The results of the diagnostic survey should be taken into account for the selection of the proper maintenance strategy to be applied. This process of the interactions between both survey methods and planning of maintenance works is illustrated in Figure 2. Although the approach illustrated in Figure 2 seems attractive, in general only little work is done to make such a procedure operational. Therefore, a research program was started at the Delft University to work out the approach illustrated in Figure 2. The main goals of this project were as follows:

1. To study the effectiveness of the Delft University ridemeter for inventory road roughness surveys;
2. To determine how the roughness of roads can be translated in such a way that the results can be used directly for the evaluation of the structural pavement deterioration, driving comfort, and road user safety influenced by car-pavement interaction; (Road profiles measured with the Delft University high-speed profilometer were used as input for this study).
3. To determine whether relations exist between

Figure 3. Delft University ridemeter.

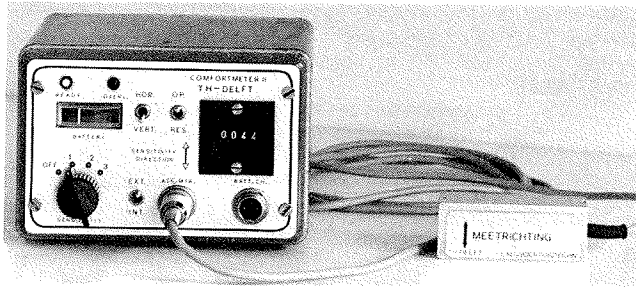


Figure 4. Filter characteristics ridemeter.

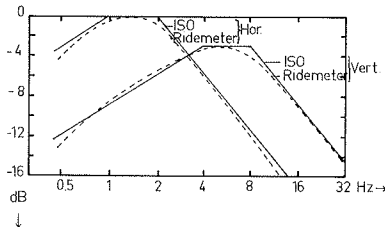


Table 1. Specifications of Delft University ridemeter.

Item	Specification
Criteria	Horizontal and vertical according to International Standardization Organization proposal
Accelerometer	Bruël and Kjaer type 4332
External input	Calibration value, 100 mV/g; input impedance, 1.5 MΩ; acceleration, ±8 g (0.8 V)
Attenuation factors	1 - 2.5 - 6.25 for switch-position 3 - 2 - 1
Ratio horizontal versus vertical	1.4 x
Current consumption	Reset, 40 mA; operate, 40 - 60 mA
Batteries	4 x DEAC -5/500 DK2; voltage-control by means of a meter with zero suppression
Operating time	Fully charged batteries, 8 - 10 h
Recharge time	Discharged batteries, 14 h
Measuring time	15 s
Dimensions and weight	Ridemeter 157 x 107 x 170 mm, 2050 g; external accelerometer including preamplifier, 31 x 31 x 80 mm, 130 g
Purchase cost	About \$3500

the ridemeter values and the factors described in item 2;

4. To set up acceptance levels for the ridemeter values based on road roughness effects on pavement deterioration, driving comfort, and road user safety influenced by road roughness; and

5. To determine relations between the ridemeter values and the results of measurements with equipment that is commonly used in the Netherlands, such as viagraph, straight edge, and bump integrator.

The project described is part of a current project of the Delft University on the development of a pavement management system. The project is sponsored by the Civil Engineering Department. This paper will deal with the first four items.

#### EXPERIMENTAL PROGRAM

In order to fulfill the objectives mentioned above, 18 different road sections were measured with both the Delft University ridemeter and Delft University high-speed profilometer. All measured roads had an asphaltic concrete top layer. The condition of the pavement structures, both in terms of magnitude of

deflection and amount of visible cracking, varied from excellent to marginal. Some sections needed an overlay very much. The quality of the subgrade, expressed in its dynamic modulus of elasticity as determined by means of deflection measurements, varied from 50 MN/m<sup>2</sup> to 250 MN/m<sup>2</sup>. In other words, both weak and strong subgrades were considered.

The ridemeter measurements were performed by two men, one driving and one writing down the ridemeter values. The high-speed profilometer measurements were also performed by two men, one driving and one operating the equipment. Note, however, that, with some small modifications, both measurements can be performed by one person.

#### Delft University Ridemeter

The ridemeter (Figure 3) developed by the Vehicle Research Laboratory of the Delft University is a compact, light-weight instrument for evaluating the riding comfort of vehicles as far as mechanical vibrations are concerned. The vibrations may be measured at various locations within a moving vehicle, such as the floor or the seat. The ridemeter evaluates comfort based on the comfort criteria proposed by the International Organization for Standardization (ISO). Accordingly, the ridemeter is comprised of two weighting networks (filters) based on the ISO proposal: one for horizontal and the other for vertical vibrations (Figure 4).

Accelerations are normally measured by a standard built-in accelerometer. If desired, an external optional transducer can be used. The accelerometer output is weighted by the appropriate network depending on the measuring direction. Subsequently, the average root-mean-square value of the signal is determined over a period of 15 s. This value, which may be termed as ride index, is displayed on the counter of the ridemeter. A relatively high value of the ride index indicates poor comfort and vice versa.

The sensitivity direction is marked by an arrow on the front-panel. Measurements in the desired direction may be carried out simply by turning the ridemeter so that the direction of sensitivity is in line with the desired direction. In case an external accelerometer is used, the sensitivity direction of this device is brought in line with the direction in which measurements are desired. In both cases the appropriate network, depending on the measuring direction, is chosen with the help of the filter selector-switch.

A warning light shows up should an accidental overloading occur, in which case the signal from the accelerometer may be attenuated in two steps. The ridemeter is thereby suited to evaluate comfort over a large variety of operating conditions and for a broad category of vehicles. A second indicator lamp marks the end of the measuring period of 15 s. The counter can be reset to start the next measurement. The power supply of the ridemeter consists of built-in, rechargeable batteries. A recharging device is supplied as a separate unit. Table 1 gives the specification of the ridemeter.

For the ridemeter measurements in this study, use was made of the external accelerometer, which was placed on the floor at the right-hand side of the car beneath the front seat. The car used for the measurements was a normally maintained Opel Kadett passenger car. The tires were inflated to the specified pressure. The measuring speed was 48 km/h, which means that, given the measuring time of 15 s, each 200 m, a ridemeter value was obtained. As mentioned before, the main criteria for equipment to be used in the inventory survey are as follows:

1. Easy to handle,
2. Measurements have to be done at reasonable speed, and
3. Low operating costs.

The ridemeter seems to fulfill these requirements excellently.

#### Delft University High-Speed Profilometer

This profilometer, which is also developed at the Delft University Vehicle Research Laboratory (2), is an acoustical system for measuring road roughness. It consists of the following:

1. A measuring system firmly mounted on a vehicle (Figures 5 and 6),
2. An electronic device to process the measured signals, and
3. A magnetic tape recorder.

The principle of the system (Figure 7) is based on the measurement of acceleration ( $a$ ) and the simultaneous measurement of distance ( $h$ ) between the device and the road surface. The displacement ( $e$ ) of the measuring device is obtained by integration of the acceleration ( $a$ ) twice. The distance ( $h$ ) is measured by means of an acoustical system. Acoustical pulses are sent to the road surface by a transducer (T). The reflected pulses are focused on a microphone (M) by means of an elliptical reflector (R). The distance is calculated from the delay in time between transmitted and received pulses. The pulses have a repetition rate of 860/s and a frequency content of 20-70 kHz. By subtracting  $h$  from  $e$  without phase errors the road profile is obtained, as follows:

$$y = e - h + c = \int_0^t \int_0^t a \, dt \, dt - h + \text{constant} \quad (1)$$

This calculation is performed by an electronic device. The system has been designed for measuring at speeds of 63, 80, or 100 km/h. A suitable nominal speed may be chosen depending on the driving conditions. In order to facilitate measurements, a variation in the test speed of up to 20 percent of the nominal speed is automatically corrected by the electronic device. This is achieved by using the vehicle speed signal as a control input to the electronic system and to the recorder motor drive and modulators.

The measured road profile is obtained in the form of a recorded tape that is IRIG-compatible. To obtain a better signal-to-noise ratio for the shorter wavelength, a prewhitening technique is used before recording. The measurements for this study were performed at a speed of 63 km/h, which means that the road profile was sampled at distances of about 0.02 m. The accuracy of the measuring system is either 2 percent of the measured amplitude or 1 mm depending on which value is the largest.

The great advantage of this system over other high-speed profilometers is believed to be the absence of physical contact between the measuring system and the road surface. Note, however, that the measurements can only be performed on dry roads and during dry weather. Otherwise, moisture in the microphones will cause unusable signals on the tape recorder.

#### Ridemeter Measurements

As mentioned before, ridemeter values were obtained for 200-m long sections of the 18 roads considered (3). On some roads the measurements were also done by using cars other than the standard Opel Kadett.

Figure 5. Acoustical system.



Figure 6. View of the electronics: (a) oscilloscope, (b) electronic device to process measured signals, and (c) magnetic recorder.

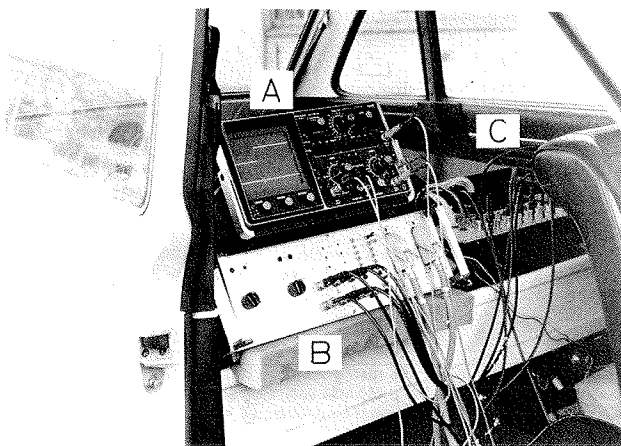
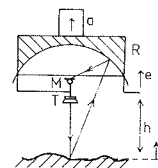


Figure 7. Principle of acoustical high-speed profilometer.



This was done in order to establish relations between ridemeter values measured by using different cars. These relations are shown in Figure 8. For some sections relations were also set up between the ridemeter values as measured with the Opel Kadett and the results of measurements with the bump integrator (4) (see Figure 9). The ridemeter values were related to the present serviceability index (psi) by using the bump integrator versus psi scale given by Auschek (5). This is shown in Figure 10.

It was concluded from this study that

1. The ridemeter is a very simple tool for qualifying road roughness in terms of riding comfort;
2. Although the type of car will influence the results, it is possible to determine which road sections are in a good, marginal, or bad condition in terms of riding comfort; and

Figure 8. Relation between ridemeter values as measured by using an Opel Kadett ( $CI_K$ ) and those measured by using other cars ( $CI$ ).

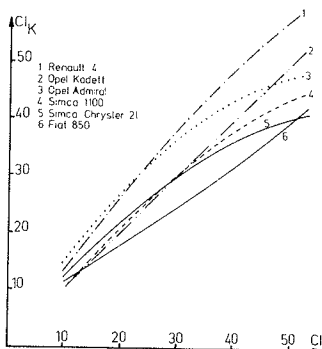


Figure 9. Relation between ridemeter values measured by an Opel Kadett ( $CI_K$ ) and the results of bump integrator measurements.

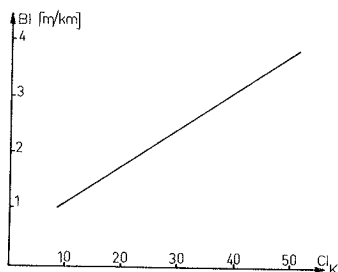
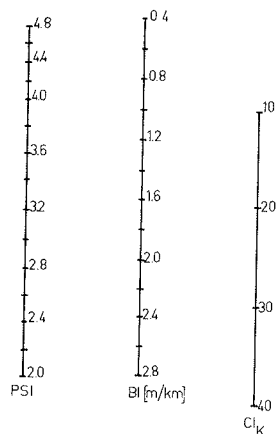


Figure 10. Relation between ridemeter values measured by using an Opel Kadett ( $CI_K$ ) and psi.



3. If the ridemeter value is 30 or higher, a diagnostic survey of the road roughness is recommended.

#### Measurements with High-Speed Profilometer and Calculation of Road Roughness Parameters

The longitudinal profile of the road sections considered was measured by means of the high-speed profilometer (6). From the road-profile signal, which is stored on magnetic tape, energy density spectra were derived by using the fast Fourier transform technique. The energy density [ $A(\lambda)$ ] was determined as a function of the wave length ( $\lambda$ ). An example of a typical plot of energy density is given in Figure 11. According to Stenschke (7), energy density relations can be described with

$$A(\lambda) = A(\lambda_0) (\lambda/\lambda_0)^N \quad (2)$$

where

$A(\lambda)$  = energy density [m] at wavelength  $\lambda$  [m];  
 $A(\lambda_0)$  = energy density at a specific wavelength  
 $\lambda_0$ ,  $\lambda_0 = 5$  m; and  
 $N$  = a constant.

All energy density relations were described in this way.

For all roads but one, the correlation coefficient squared of this relation was higher than 90 percent. For one road the correlation coefficient was much lower. This was because in that specific section the road surface consisted of both bricks and asphalt.

Furthermore, the slope variance of each road profile was calculated with

$$SV = \int_0^\lambda F^2(\lambda) \cdot A(\lambda) d\lambda \quad (3)$$

where

$$F(\lambda) = (2/l) |\sin(\pi l/\lambda) - (1/L) \sin(\pi L/\lambda)| \cdot |l/m| =$$

transfer function of the American Association of State Highway Officials (AASHO) profilometer,  
 $l = 0.24$  m,  
 $L = 7.77$  m, and  
 $|SV| = |\text{radian}|^2 \times 10^{-6}$ .

Next, psi was calculated with

$$\text{psi} = 3.27 - 1.37 (\log SV - 0.78) \quad (4)$$

From these calculations it was determined that psi of the road sections considered varied between 1.98 and 4.1. A relation was determined between the

Figure 11. Example of a power spectral density curve and its representation by a straight line.

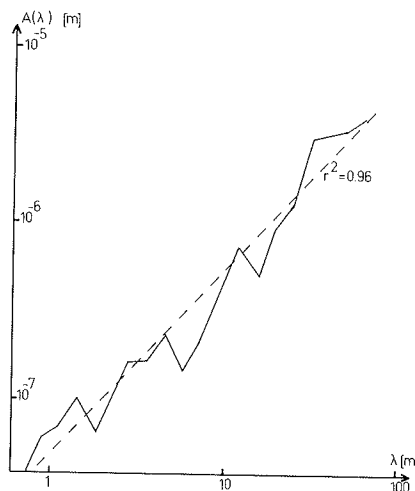


Figure 12. Relation among constants  $A(\lambda_0)$ ,  $N$  from the power spectral density curve, and slope variance (SV).

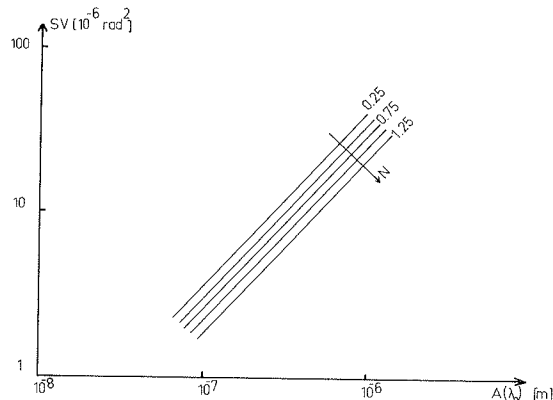


Figure 13. Used mass spring dashpot model in the vehicle simulation.

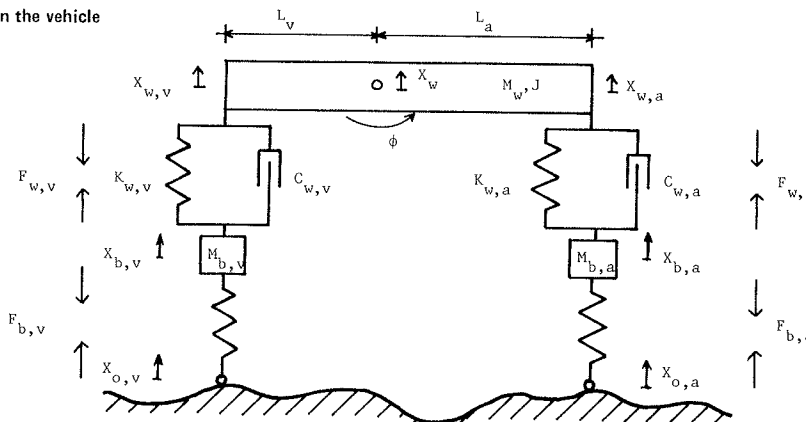
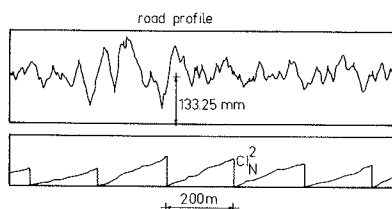


Figure 14. Example of results of passenger car simulation.



factors  $A(\lambda_0)$  and  $N$  from Equation 2 and the slope variance calculated from Equation 3. This relation could be described with

$$\log SV = 7.977 + 1.046 \log A(\lambda_0) - 0.302 N \quad R^2 = 0.99 \quad (5)$$

With  $SV$ ,  $A(\lambda_0)$ , and  $N$  as previously defined, the equation is valid for the following

$$64.2 \times 10^{-9} \leq A(\lambda_0) \leq 982 \times 10^{-9} \text{ and } 0.06 \leq N \leq 1.28$$

A graphical representation of the equation is given in Figure 12. Since the relation between the energy density and the slope variance is excellent, it is stated that representation of road roughness in terms of slope variance is accurate enough to be used in the further analysis.

#### VEHICLE SIMULATIONS

In order to establish the effects of road roughness on vehicle performance, vehicle simulations were carried out on an analog computer with the road profile, measured with the high-speed profilometer and stored on magnetic tape, as input (8).

Two types of vehicle simulations were performed:

1. Simulation of a passenger car and
2. Simulation of a loaded and unloaded truck.

The simulated speed was 63.0 km/h for the passenger car and 63.0 and 31.5 km/h for the truck.

#### Simulation of Passenger Car

Figure 13 gives a schematical representation of the car model that was used in the simulation. The used values for the spring and dashpot characteristics were those of an average passenger car and not those of the Opel Kadett that was used for the rideometer measurements. The output signal ( $X_{w,v}$ ) was differentiated twice with respect to time. With the resulting signal ( $\ddot{X}_{w,v}$ ), an analog model of the

rideometer was fed; this resulted in a simulated rideometer value  $CI_N$ .

Figure 14 gives a graphical representation of the results of the simulation for a rough road. From the growth of the  $CI_N^2$  line (i.e., squared simulated rideometer value), it has been possible to determine those points within a section that caused sudden discomfort (e.g., railroad crossings or pot-holes).

#### Simulation of Truck

This simulation was carried out in order to establish the effects of road roughness on the dynamic tire loading. The simulation was carried out by using the same basic car model as shown in Figure 13 but now with the spring, dashpot, and other characteristics of a two-axle DAF truck (distance between axles is 3.2 m).

Two speeds were used for the simulation of a loaded truck (rear axle load of 100 kN) and an unloaded truck (rear axle load of 30.5 kN). Figure 15 gives a graphical representation of the results of the simulation. For each simulation, the distribution of the axle loads was determined. The standard deviations were calculated from these distributions. It could then be concluded that the effect of road roughness on the dynamic tire loads was the same for the loaded truck driven at a speed of 63 km/h and the loaded and unloaded trucks driven at a speed of 31.5 km/h. Only the unloaded truck driven at a speed of 63 km/h caused very large dynamic forces.

#### RELATIONS BETWEEN RIDEMETER VALUES AND THE INFLUENCES OF ROAD ROUGHNESS ON DRIVING COMFORT AND PAVEMENT DETERIORATION

One of the goals of the research program was to relate rideometer values to parameters that are directly related to driving comfort and pavement deterioration. In the previous sections we described how the rideometer values were obtained, how psi of the road sections considered was calculated from road profile measurements, and how road roughness influences the dynamic axle loads of a given truck. Given these results, now we can relate rideometer values to driving comfort and pavement deterioration. First, a relation was set up between the slope variance, which proved to be a good indicator of road roughness, and the standard deviation of the dynamic axle loads as calculated for the truck, used in the simulation, driven at a speed of 63 km/h (9). These relations are shown in the southwest corner of Figure 16. They are as follows:

$$\sigma_{\text{loaded}} = 0.302 + 0.057SV - 0.00085SV^2 \quad R^2 = 0.85 \quad (6)$$

$$\sigma_{\text{unloaded}} = 0.611 + 0.164SV - 0.0036SV^2 \quad R^2 = 0.70 \quad (7)$$

where  $\sigma_{\text{loaded}}$  is the standard deviation of the dynamic axle load caused by the loaded truck (metric ton) and  $SV$  is the slope variance ( $\text{radian}^2 \times 10^6$ ). Both equations are valid for  $1.51 < SV < 22.65$ .

Next, the relation between the ridemeter value of a given section as determined by the vehicle simulation ( $\overline{CI_N}$ ) and the slope variance was determined. This relation is shown in the northwest corner of Figure 15 and can be described with

$$SV = 2.185 - 6.081\overline{CI_N} + 704.468\overline{CI_N}^2 \quad R^2 = 0.90 \quad (8)$$

The simulated ridemeter value  $\overline{CI_N}$  was used because this value correlated better with  $SV$  than the measured  $CI$  values.

The measured ridemeter values  $CI_k$  as determined by using the Opel Kadett were related to the simulated ridemeter values  $\overline{CI_N}$ , which resulted in

$$CI_N = -0.0511 + 0.0107 CI_k - 0.00013 CI_k^2 \quad R^2 = 0.66$$

and  $7 < CI_k < 42$  (9)

or, by using the mean ridemeter values over a given section,

$$\overline{CI_N} = -0.0807 + 0.0136\overline{CI_k} - 0.00018\overline{CI_k}^2 \quad R^2 = 0.89$$

and  $10 < \overline{CI_k} < 35$  (10)

The first relation is poor mainly because the simulated values were obtained by using a two dimensional vehicle model, which means that roll movements were excluded. The relation between the mean values of  $CI_k$  and  $\overline{CI_N}$  is, of course, much better because the influence of peak values is reduced here. The mean value relation is shown in the northeast corner of Figure 16.

Finally, the relations between the ridemeter values as measured by using different cars (see Figure 7) and those measured with the Opel Kadett, are shown in the southeast corner of Figure 16. From this correlation study we concluded that, if ridemeter values are measured at 40 and higher, the pavement needs to be maintained since the  $\psi$  is lower than 2. This latter value is often used as a minimum acceptance level. Note that this ridemeter value is in close agreement with the value that can be read from Figure 10.

In order to compare the established ridemeter value acceptance level with the comfort and car driver fatigue criterion developed by ISO, reference is made to Figure 17, in which the ridemeter values are related to those criteria. From this figure it can be determined that, after a 20-30 min drive on a road with  $\psi = 2$  (ridemeter value = 40), the car driver will classify the road as not comfortable. After a 3-h drive the car driver will show symptoms of fatigue.

In order to quantify the damaging effect of dynamic axle loads on pavement structures, a damage factor ( $S$ ) was determined by using the calculated dynamic loads caused by the rear axle ( $P_{\text{stat}} = 100$  kN) of the loaded truck traveling at a speed of 63 km/h.

$S$  is calculated in the following way:

1. Determine the standard deviation of the dynamic axle loads from ridemeter measurements by using Figure 16 and

2. Once the axle load distribution is known, calculate the damage factor ( $S$ ) by using the following equation:

$$S = \sum_{i=1}^{170} (p_i/100)^4 \quad (11)$$

where  $S$  is the damage factor and  $p_i$  is the magnitude of the axle loads in group  $i$  (kN).

In other words,  $S$  is calculated by using only the dynamic loads that are larger than the static axle load of 100 kN.

The relation between the measured ridemeter value ( $CI$ ) or simulated ridemeter value ( $\overline{CI_N}$ ) and  $S$  is shown in Figure 18. Figure 18 shows that the influence of road roughness on the number of equivalent 100-kN axle loads is limited. Due to road roughness, the number of 100-kN load applications is at the most 1.3-1.4 times the number of static load applications. Figure 19, which is taken from

Figure 15. Example of results of truck simulation.

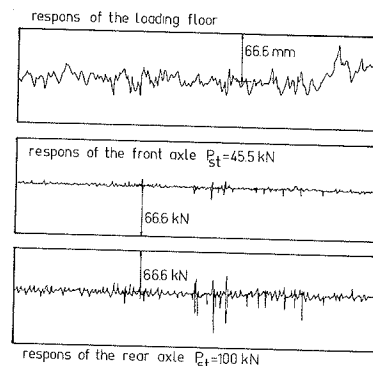


Figure 16. Relation between ridemeter values, slope variance, and standard deviation of the dynamic axle loads of a loaded and unloaded truck.

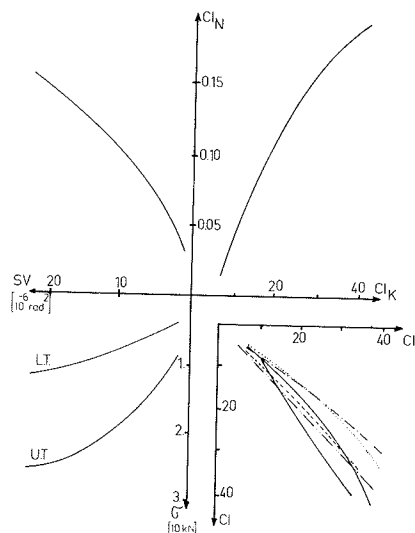


Figure 17. Ridemeter values in relation to ISO levels of comfort and fatigue.

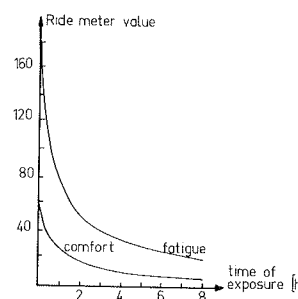


Figure 18. Relation between ridemeter values and damage factor.

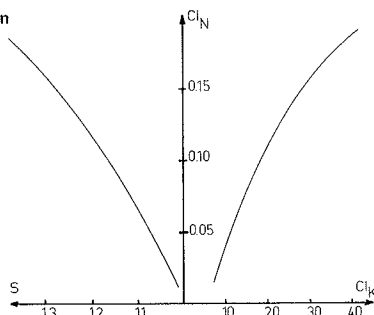
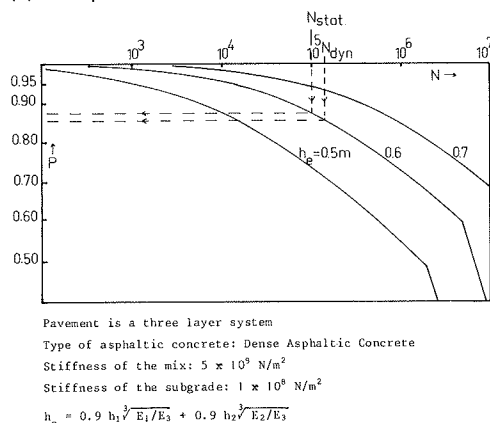


Figure 19. Influence of number of dynamic equivalent 100-kN single-axle loads on the structural deterioration expressed by the probability of survival (P) of the pavement.



another paper (10) shows that the influence of the dynamic axle loads on pavement deterioration is limited.

#### INFLUENCE OF ROAD ROUGHNESS ON ROAD USER SAFETY

For the safety of the road user, the magnitude of the lateral tire forces is an important factor because those forces are necessary for the directional control of the vehicle. The magnitude of the lateral tire force depends on the normal tire force, the tire slip angle, the tire camber angle, and the coefficient of friction between tire and the road surface. By using the information given elsewhere (11-13), lateral tire force distributions were derived for the different pavement sections from the distributions of the normal tire loads. This approach will lead to rather stringent minimum acceptance levels for the road roughness. For instance, if the psi of a road is 2.0, this would be unacceptable for safety reasons; however, this value is only just below the minimum acceptance level established for other reasons.

It is hard to establish criteria for road roughness based on road user safety because the needed lateral tire forces will depend on the need for directional control. In other words, roads that have a relatively large amount of curves or roads that carry both slow traffic (for instance bicycles or agricultural tractors) and fast traffic, which will lead to a relatively large amount of passing movements, need a smoother pavement than roads that do not have such features.

More study is needed to establish roughness criteria based on road user safety. Based on this study, however, we recommend that the psi should not be lower than 2.5 for reasons of safety, which means that the ridemeter values should be lower than 30.

#### CONCLUSIONS

From the study described in this paper the following conclusions have been drawn.

1. In order to establish the roughness of a road network, inventory and diagnostic surveys should be carried out.
2. The inventory survey can be carried out with simple equipment, such as the ridemeter described in this study.
3. Relations exist among the ridemeter values on the one hand and the psi, damaging effect of dynamic tire loads, and standard deviation of dynamic tire loads on the other hand.
4. These relations show that, if the ridemeter values are higher than 40, the road should be maintained for reasons of low serviceability index ( $\text{psi} < 2$ ).
5. Ridemeter values should preferably be lower than 30 for reasons of road user safety.
6. Based on conclusions 4 and 5, we recommend that a diagnostic survey should be carried out if the ridemeter values are between 25 and 30.
7. Energy spectra can be accurately described by two parameters,  $A(\lambda_0)$  and  $N$ .
8. The slope variance and so the psi can be accurately calculated from  $A(\lambda_0)$  and  $N$ .
9. Road roughness has only a limited effect on the structural pavement deterioration.
10. Road roughness seems to have a marked effect on road user safety.
11. More study should be done in order to establish road user safety-based roughness criteria.

#### ACKNOWLEDGMENT

We wish to express our gratitude to the dean of the Department of Civil Engineering for financial support of the study. We also wish to express gratitude to J. Elzenaar who carried out the measurements, to D. Harkema and E. de Vries for their assistance in carrying out the necessary calculations, and to P. Jongeleen for typing the manuscript.

#### REFERENCES

1. A.A.A. Molenaar. Werkwijze voor Rationeel Wegbeheer. Afdeling Civiele Techniek, Technische Hogeschool Delft, Delft, Netherlands, Rept. WB-1, 1976.
2. K. Rop. Ontwikkeling van de THD Wegprofielmeter. Laboratorium voor Voertuigtechniek, Technische Hogeschool Delft, Delft, Netherlands, Rept. 093, 1975.
3. G.T.H. Sweere. Comfortmetingen op Provinciale Wegen in Gelderland en Zuid-Holland. Afdeling Civiele Techniek, Technische Hogeschool Delft, Delft, Netherlands, Rept. WB-16 (7-80-115-9), 1980.
4. A.A.A. Molenaar. Momentopname van de Ontwikkeling van een Rationeel Wegbeheer Systeem. Afdeling Civiele Techniek, Technische Hogeschool Delft, Delft, Netherlands, Rept. WB-12 (7-78-2-115-4), 1978.
5. S. Huschek. Befahrbarkeitsmessungen auf Strassen nach den Winkelmessmethode--Neue Untersuchungen. Mitteilung nr. 28 Institut für Strassen--und Untertagbau Eidg. Technischen Hochschule Zürich, Zürich, Switzerland, 1974.
6. G.T.H. Sweere. Langsprofielmetingen op provinciale wegen in Gelderland en Zuid-Holland. Afdeling Civiele Techniek, Technische Hogeschool Delft, Delft, Netherlands, Rept. WB-17 (7-80-115-10), 1980.
7. R. Stenschke. Abhängigkeit des Subjektiv



- Empfunnenen Fahrcomferts und den Dynamischen Radlasten von Strassenunebenkeiten. Fortschritte der V.D.I. Zeitschriften, Vol. 12, No. 32, 1978.
8. G.T.H. Sweere and J. Elzenaar. Voertuig-simulatie op de Hybride Rekeninstallatie AD4-IBM1800. Afdeling Civiele Techniek, Technische Hogeschool Delft, Delft, Netherlands, Rept. WB-18 (7-80-115-11), 1980.
  9. G.T.H. Sweere and A.A.A. Molenaar. Rijcomfort en Dynamische Aslasten in Relatie tot het Weg-langsprofiel. Afdeling Civiele Techniek, Technische Hogeschool Delft, Delft, Netherlands, Rept. WB-19 (7-80-15-12), 1980.
  10. A.A.A. Molenaar and Ch.A.P.M. van Gurp. Optimization of the Thickness Design of Asphalt Concrete Overlays. Paper presented at the 10th Australian Road Research Board Conference, Sydney, 1980.
  11. J.T. Tielking. Mechanical Properties of Truck Tires. SAE, Publication No. 730183, 1973.
  12. B.E. Quinn and S.R. Kelly. Tentative Road Roughness Criteria Based Upon Vehicle Performance. FHWA, Rept. FHWA-RD-75-3, 1975.
  13. B.E. Quinn and S.E. Hildebrandt. Relating Pavement Roughness to Vehicle Behavior. FHWA, Rept. FHWA-RD-75-1, 1974.

*Publication of this paper sponsored by Committee on Theory of Pavement Systems.*

## Reflex-Percussive Grooves for Runways: Alternative to Saw-Cutting

SATISH K. AGRAWAL AND HECTOR DAIUTOLO

The presence of transverse grooves in runway surfaces helps alleviate aircraft hydroplaning during landing operations. The Federal Aviation Administration has recommended installation of 0.25-in square-grooves spaced at 1.25 in center-to-center on runways where potential of hydroplaning exists. However, many runways remain nongrooved, primarily because the cost of grooving by the conventional saw-cutting method, currently in widespread use, is high. This paper describes the braking effectiveness of an aircraft tire on reflex-percussive grooves produced by a newly developed low-cost groove-installation technique called the reflex-percussive cutting process. This process is based on the principle of controlled removal of concrete. The cutting head causes the material directly under the area of impact to pass through a rapid compression-tension cycle. Because it is weak in tension, the concrete fractures in the localized area of impact without damaging the surrounding concrete. The braking effectiveness of an aircraft tire on these grooves is comparable to conventional saw-cut grooves under similar conditions of wetness, and both types of grooves alleviate hydroplaning. The cost of installation of the reflex-percussive grooves in portland cement concrete, however, can be as low as half the cost of installation of conventional saw-cut grooves at the recommended groove spacing.

The braking performance of an aircraft during landings on water-covered runways depends on the level of friction developed in the contact area between the aircraft tire and the runway surface. The friction level developed in the contact area is affected by aircraft speed, design of the tire tread, runway finish and drainage capacity, characteristics of the braking system, and the amount of water on the runway. Under flooded runway conditions, aircraft may hydroplane whereby very low levels of friction are available and the braking capability is significantly reduced. Loss in braking capability can be considerable even if runways are covered with only a thin film of water.

During hydroplaning, the physical contact between the tire and the runway is lost, and the tires are supported on the intervening layer of water. Hydroplaning occurs as a result of rapid buildup of hydrodynamic and viscous pressures in the tire-runway contact area. Dynamic or viscous hydroplaning are identified according to whether inertial forces or viscous forces, respectively, are predominant. In all cases of hydroplaning, however, both effects are present to some degree. Dynamic hydroplaning can be minimized by a rapid removal of water from the tire-runway contact area; runway grooves accom-

plish this effectively by providing escape channels for water forced out of the contact area during tire passage over the grooves. Viscous hydroplaning can be alleviated by providing adequate microtexture in the runway surface.

The Federal Aviation Administration (FAA) has recommended (1) 0.25-in wide by 0.25-in deep grooves spaced at 1.25 in between centers and has encouraged airport managers, operators, and owners to groove runways where potential of hydroplaning or overrun exists. However, many runways have not been grooved. The major deterrents to the use of runway grooves are the high cost of grooving by the conventional saw-cutting method and the availability of only limited evidence as to the effectiveness of grooved surfaces at the touchdown speeds of jet aircraft.

The objective of the research described in this paper is to evaluate the braking effectiveness of an aircraft tire on grooves produced by a new and less expensive reflex-percussive cutting process and to compare the performance of these grooves with the conventional saw-cut grooves.

### GROOVES PRODUCED BY REFLEX-PERCUSSIVE PROCESS

The reflex-percussive method of controlled removal of concrete was recognized by the Concrete Society of Great Britain in 1972. This method was first developed for providing a very rough finish in the runway surface. When the cutting head strikes the surface of the concrete, it causes the material directly under the area of impact to deflect downward and thus creates a momentary and localized compression. The compressive strain is primarily elastic, and almost immediately the concrete rebounds and passes into tension nearly equal to the initial compression. However, because it is very weak in tension, the concrete fractures and releases the elastic energy as the kinetic energy of the flying fragments. The great advantage of this method of cutting is its ability of not loosening the aggregate particles within the matrix or creat-

ing microfractures in the undamaged surrounding concrete.

Klarcrete Limited, of London, Canada, demonstrated that the reflex-percussive process can be readily adapted for installing grooves in the concrete surfaces. By tilting the cutting heads (three heads were used for this study) at  $13^\circ$ , the reflex-percussive grooving machine (Figure 1) provides nonsymmetrical V-shaped grooves. Figure 2 shows the reflex-percussive grooves in a portland cement concrete (PCC) test surface; Figure 3 shows the dimensions of these grooves and those of conventional saw-cut grooves.

#### BRAKING EFFECTIVENESS OF REFLEX-PERCUSSIVE GROOVES

The experimental program was conducted at the Naval Air Engineering Center, Lakehurst, New Jersey. Test Track 1 at this facility was modified to accomplish the objectives of the research described in this paper.

#### Test Facility and Equipment

The test track is 1 mile long and has guide rails

spaced 52.5 in apart that run parallel to the track. Reinforced concrete strips extend beyond the guide rails to a width of 28 ft. The last 200 ft of the track were used for installing the test bed. The PCC test bed was 30 in wide and 5 in thick. An aircraft arresting system is located beyond the test track to recover the test equipment at the completion of a test run.

The major components of the test equipment are the four-wheeled jet car, the dead-load carriage that supports the dynamometer and wheel assembly, and the measuring system. The jet car is powered with J48-P-8 aircraft engines that produce a total thrust of 24 000 lb·f and is used to propel the dynamometer and wheel assembly and the carriage from the launch end at a preselected speed. The jet car (Figure 4) is disengaged when the test speed is attained, and the dynamometer assembly and the carriage are allowed to coast at this speed into the test bed.

The dynamometer and wheel assembly were jointly developed by the FAA and the U.S. Navy and have the capability of simulating a jet transport tire-wheel assembly under touchdown and rollout conditions. Test speeds of up to 150 knots were attained on the test track. Figure 5 shows the dynamometer and

Figure 1. Machine for installing reflex-percussive grooves.

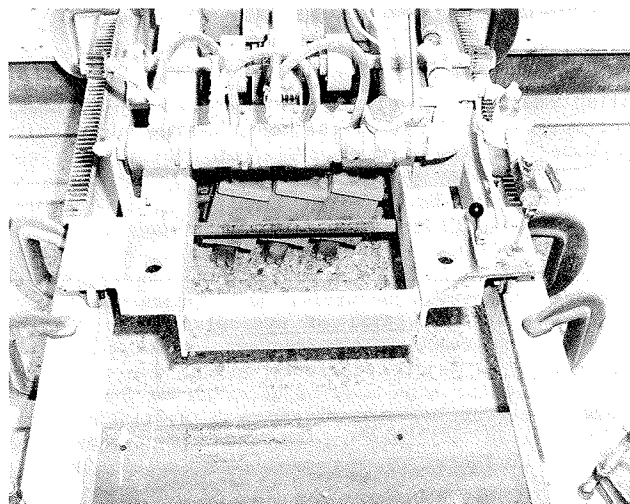


Figure 2. Reflex-percussive grooves in PCC surface.

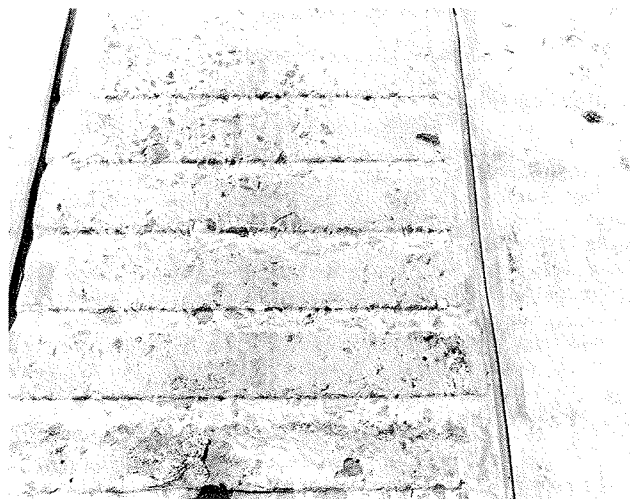


Figure 3. Dimensions of reflex-percussive grooves and conventional saw-cut grooves.

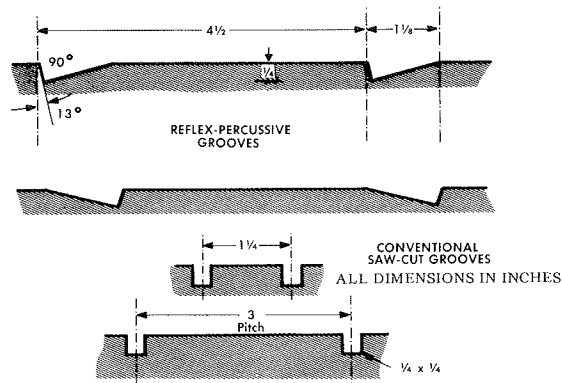


Figure 4. Jet-powered pusher car for providing preselected speeds to test equipment.

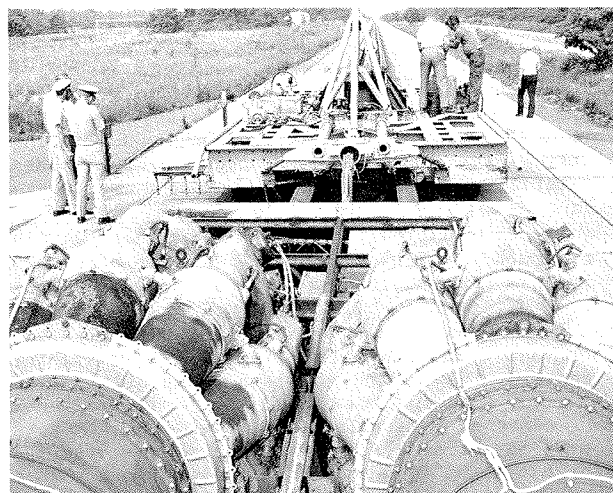


Figure 5. Dynamometer and wheel assembly showing vertical and horizontal load links.

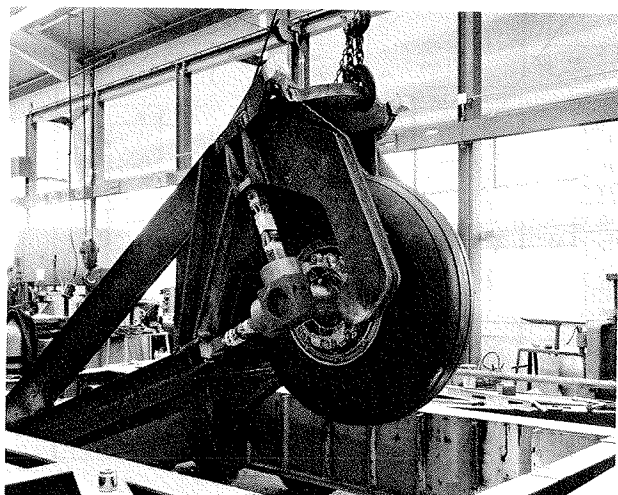
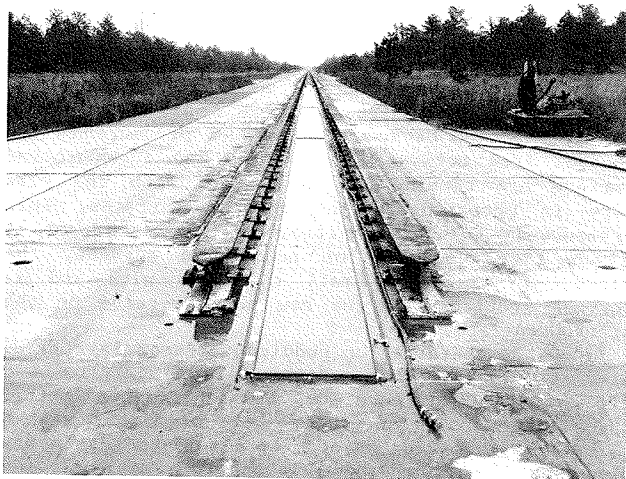


Figure 6. Four sections of 200-ft test bed.



wheel assembly and the details of the instrumentation.

The dynamometer is instrumented to measure the vertical load on the tire, the horizontal force developed at the tire-pavement interface, the angular velocity of the test tire, and the vertical motion of the dynamometer assembly relative to the dead load carriage. The water depth on the test bed was measured by the use of the National Aeronautical and Space Administration (NASA) water level depth gage.

#### Test Sections

The 200-ft test bed (Figure 6) was divided into four 45-ft sections following a 20-ft section; the 20-ft section was intended to ensure proper approach of the test wheel into the test sections. The dimensional tolerance of the test surfaces was held within  $\pm 1/8$  in from horizontal level in each test section. Figure 7 shows the schematic of grooved and nongrooved sections on each test bed. Testing on bed no. 4 is the subject matter of this paper;

Figure 7. Schematic of grooved and nongrooved sections.

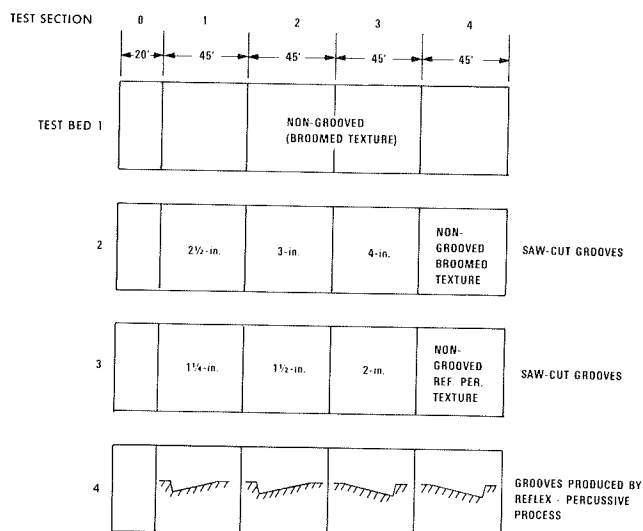


Table 1. Test parameters used in program.

Parameter	Description
Tire	
Vertical load	35 000 lb
Inflation pressure	140 lb/in <sup>2</sup>
Tread design	Worn and fully treaded, six grooves
Size and type	49x17, 26-ply, type 7
Pavement	
Type of surface	PCC
Macrotexture	0.021 in nongrooved, grease smear measure
Type of grooves	Reflex-percussive
Environmental	
Water depth	Under 0.02 in wet, 0.02-0.16 in puddled, 0.17-0.32 in flooded
Operational	
Wheel operation	Rolling to locked
Brake pressure	300-1800 lb/in <sup>2</sup>
Speed	70-150 knots

testing on other beds is described in our other paper in this Record and elsewhere (2).

#### Test Parameters

Four types of parameters were investigated in the test program. These are the tire parameters, the pavement parameters, the environmental parameters, and the operational parameters. The primary criterion was to choose a value for a given parameter such that it represented a value widely used by airlines and aircraft.

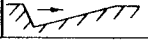
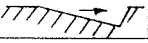
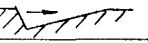
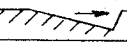
A summary of the test parameters included in the program is given in Table 1.

#### Test Procedure

In order to obtain maximum available friction level for each set of operating conditions, multiple tests were conducted at a constant speed while the brake pressure was gradually increased in successive tests until wheel lock occurred. A wheel slip between 6-18 percent was recorded as the range in which maximum friction level occurred. A maximum of four data points were collected in each test. A complete test consisted of the following steps:

1. Test tire was selected and checked for inflation pressure;

Figure 8. Test on reflex-percussive grooves.

TEST SPEED,  KNOTS		COEFFICIENT OF FRICTION X 100															
		WORN TIRE							NEW TIRE								
		NON-GROOVED SURF.	GROOVE ORIENTATION						NON-GROOVED SURFACE	GROOVE ORIENTATION							
																	
			Average Water Depth, Inches														
A:	A	B	C	A	B	C	A	B	C	A	B	C	A	B	C		
70	18	49 41 40	15 24 19	19	41	32 29 27	- 19 19	33	28 19	20 20	34 34	20 26	26	36	14 15 29	27 23	
90	-	34 35 40	21 15	14	40	26 15	- 13	26 20	10	-	31 25	24 20	11	30	26 27 15		
110	10	31 30	14 12 14	5	33	26 14	- 13 5	23	4 6	-	24 26	-	6	28	19 18	10	
130	9	22 21 25	17 10	10	25	19 14	- 10	26	5	-	27 30	15	6	28	16 19 12 10	6 8	
150	-	-	-	-	-	-	-	18	-	-	-	-	-	-	-	-	

Notes: A = 0.0-0.02 in, wet; B = 0.02-0.16 in, puddled; and C = 0.17-0.32 in, flooded.  
35 000 lb vertical load, 140 lb/in<sup>2</sup> inflation pressure.

2. Desired water depth was obtained on the test sections;

3. Jet engines were started at the launch end and set at the performance level to provide preselected speed in the test sections;

4. Jet car was released to propel the test equipment (dead load and dynamometer); test tire remained in free rolling state during this maneuver;

5. Jet car was braked and separated from the test equipment several hundred feet away from the test bed (This allowed the dead load and dynamometer to enter the first test section at the preselected speed. The test speeds in the remaining sections were within 1 or 2 knots of the speeds in the previous sections as computed from the analog traces.);

6. Before entering the first test section, the hydraulic systems were activated to apply the vertical load and the brake pressure on the tire (the magnitude of each was preselected), thus, the wheel entered the sections at preselected test conditions; and

7. As the wheel left the test bed, unloading and brake release were initiated and the test equipment was recovered by the use of arresting cables.

#### Data Collection and Analysis

Data were collected on oscillographs. Typical data collected in a test included horizontal force at the tire-pavement interface, vertical load on the tire, coefficient of friction developed at the interface, and wheel revolution. Water depth and brake pressure were recorded manually, and the test speed was computed from the distance-time trace on the oscillograph.

Figure 8 shows the test results. The values of the coefficient of friction in this figure represent the maximum available under each set of operating conditions. A least-square fit was obtained between speed and coefficient friction.

#### Discussion of Results

Test results on reflex-percussive grooves and on nongrooved PCC are shown in Figures 9-11. The basic characteristics of the friction-speed relations in these figures indicate a drop in friction with increasing speed—a trend that is well documented in the past (3). These results verify the validity of the experimental procedures of this research and

complement the findings of past research.

The improvement in available friction level as a result of grooving is shown in Figures 9 and 10. Under wet surface conditions (Figure 9), the braking performance of both new and worn tires is improved on the grooved surface compared with the nongrooved surface. The improvement in braking performance in going from a nongrooved to a grooved surface is larger for a worn tire than for a new tire. This may be expected because the viscous pressure in the contact area between a worn tire and a nongrooved surface are considerably high, and when the worn tire is operated on the grooved surfaces, this pressure is reduced significantly. For the case of a new tire operating on nongrooved surface, the viscous pressure is small to start with and is further reduced when the new tire operates on the grooved surface.

When the operation on puddled surfaces is considered (Figure 10), the performance of a new tire on a grooved surface (Figure 10c) is significantly better than on nongrooved surfaces. Note also that a worn tire performs better on a grooved surface than a new tire does on a nongrooved surface. Under flooded surface conditions (Figure 10), the occurrence of frequent wheel lock prevented accumulation of any meaningful data on nongrooved surfaces; the available friction levels were low even on the grooved surfaces.

The reflex-percussive grooves can be installed in two orientations (Figures 9-11) because the cross section of the grooves is nonsymmetrical. Depending on the direction of motion, the tire will encounter different flow conditions as it hits the groove. An attempt to isolate a preferred orientation of the grooves in terms of improved braking performance for one orientation compared with another was not successful; braking performance was comparable for both orientations. However, higher rubber deposits were observed for the orientation shown on the right in Figures 9-11.

#### COMPARISON OF REFLEX-PERCUSSIVE GROOVES WITH CONVENTIONAL SAW-CUT GROOVES

The braking performance of conventional saw-cut grooves was evaluated in another investigation (2) and is reported in our other paper in this Record. Grooves of various pitches between 1.25 and 4 in (Figure 7) were included in the test program. The

general conclusion from the study described in our other paper in this Record is that the conventional saw-cut grooves spaced at 3 in or less will provide an acceptable braking performance to an aircraft tire on water-covered surfaces.

A comparison of the braking performance of the

Figure 9. Coefficient of friction as function of speed on reflex-percussive grooves under wet surface condition.

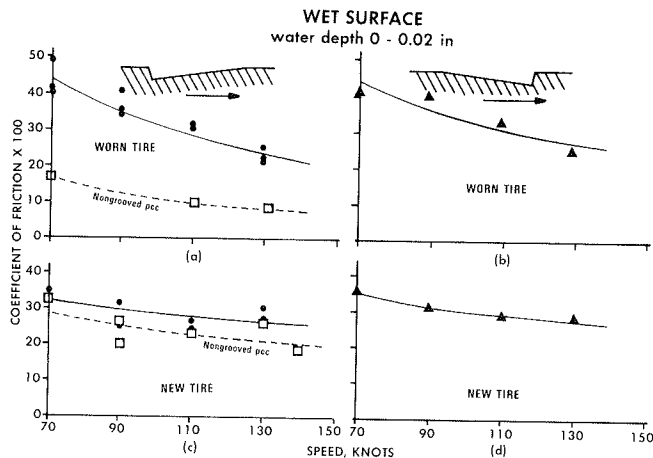


Figure 10. Coefficient of friction as function of speed on reflex-percussive grooves under puddled surface condition.

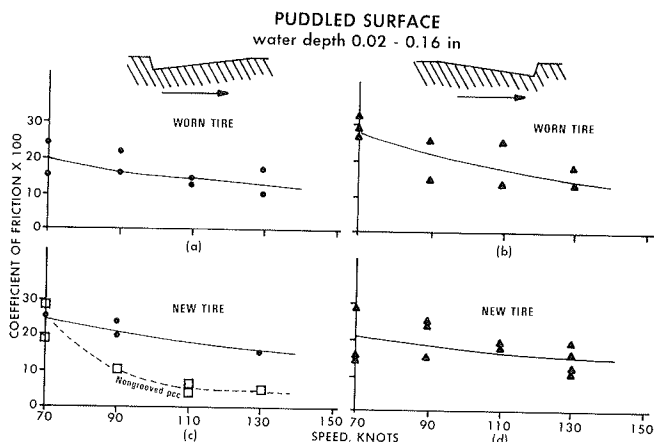
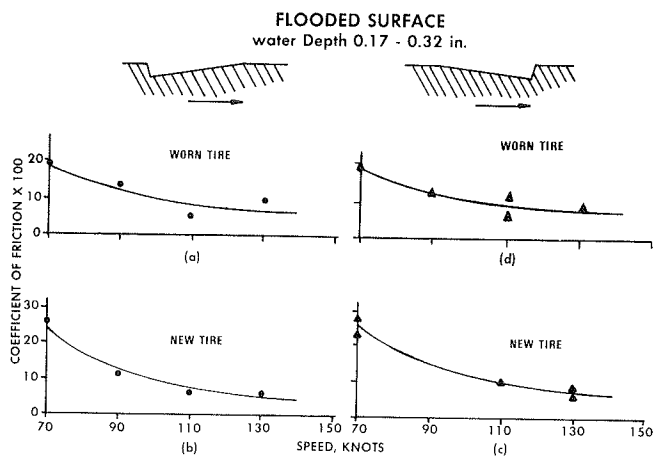


Figure 11. Coefficient of friction as function of speed on reflex-percussive grooves under flooded surface condition.



reflex-percussive grooves with the conventional saw-cut grooves is shown in Figures 12 and 13. The results for the saw-cut grooves are from another report (2); the results for the reflex-percussive grooves are replotted from Figures 9-11 of this paper. Since the orientation of the reflex-percussive grooves did not show definitive trends, the data for these grooves, in Figures 12 and 13, are not separated by orientation. All the curves in Figures 12 and 13 show a least-square fit to the data.

It is evident from Figure 12 that the braking performance of an aircraft tire on the reflex-percussive grooves is comparable to that on the saw-cut grooves under puddled and flooded conditions. Figure 13 shows the performance comparison for wet surface conditions. Here again, the braking performance of the two types of grooves is comparable.

The cost of saw-cut grooves depends on the groove geometry, the groove spacing, and the hardness of the aggregate used in the PCC. An investigation by a construction cost consultant indicated that significant cost savings can result by increasing the groove spacing of the conventional saw-cut grooves. For example, by cutting grooves at 2-in spacing, the cost savings over 1.25-in groove spacing are 15 percent, and at 3- and 4-in spacings, the cost savings are 25 and 28 percent, respectively. Hardness of the aggregate influences the diamond blade life—softer aggregates require less frequent blade changes; harder aggregates require more frequent blade changes. Since the diamond-tipped blades are expensive, the total grooving cost increases for concrete by using harder aggregates.

Figure 12. Comparison of braking performance of reflex-percussive and saw-cut grooves on puddled and flooded surfaces.

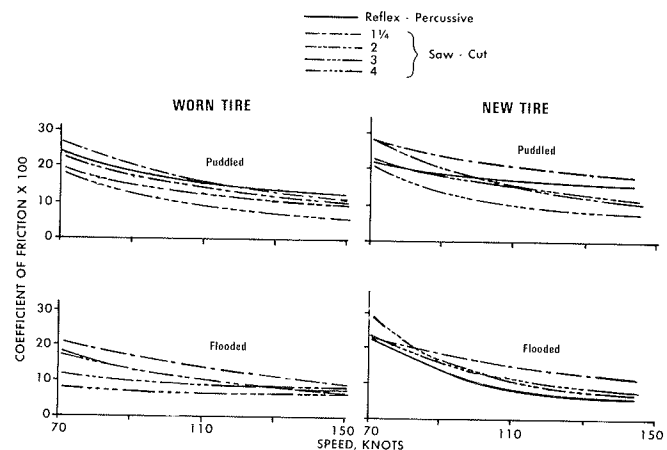


Figure 13. Comparison of braking performance of reflex-percussive and saw-cut grooves on wet surfaces.

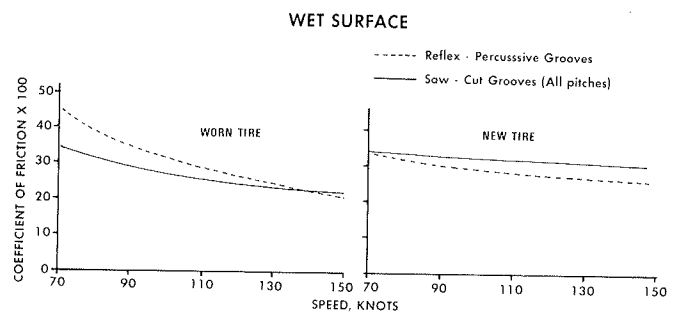
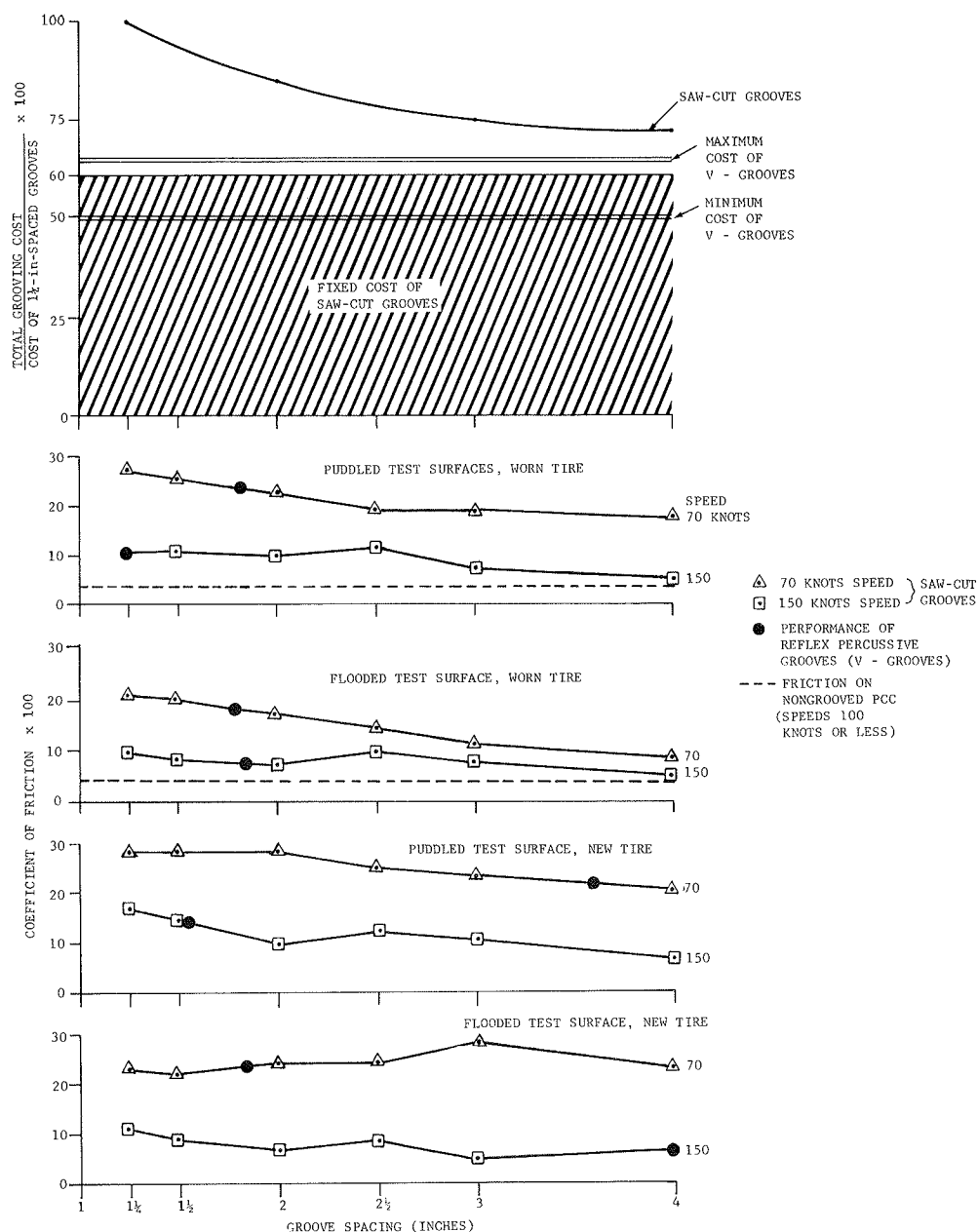


Figure 14. Braking performance and estimated cost as function of groove spacing.



The reflex-percussive grooving process is relatively insensitive to the hardness of the aggregates. This insensitivity coupled with the long life of cutting heads and high operating speed of the machine provide substantial savings to the total grooving cost. The Canadian manufacturer, who holds the patent for the application of this cutting process for grooving, has demonstrated the economics associated with the process during resurfacing of part of an operating runway. However, realistic cost estimates and full savings potential can only be realized after application of these grooves on an operating runway. Figure 14 shows a composite view of performance and estimated grooving costs for both the saw-cut grooves and the reflex-percussive grooves; the latter have the potential of costing only half as much as the 1.25-in spaced conventional saw-cut grooves.

Testing currently being conducted by FAA is directed toward finding a cost-effective groove configuration for the asphaltic concrete surfaces.

As part of its engineering and development program (4), FAA expects to conduct a comprehensive evaluation of the grooves produced by the reflex-percussive process. The evaluation will include the optimization of the groove shape and size and the braking effectiveness of the grooves.

#### CONCLUSIONS

The following conclusions are drawn from the findings of this research and are valid for PCC surfaces:

1. The reflex-percussive cutting process is an alternate groove-installation technique competitive with the conventional saw-cutting method;
2. The braking performance provided by the reflex-percussive grooves on water-covered surfaces is comparable to that provided by the 2-in pitch, conventional saw-cut grooves; and
3. The installation cost of the reflex-percussive grooves can be significantly less than that of the

conventional saw-cut grooves; a potential of costing as low as half as much as conventional saw-cut grooves at 1.25-in spacing exists.

#### ACKNOWLEDGMENT

This research was requested by the Office of Airport Standards, FAA. The Airport Development Division of the Systems Research and Development Service provided the program direction. Herman D'Aulerio provided helpful suggestions and critical reviews throughout the conduct of the research.

#### REFERENCES

1. Method for the Design, Construction, and Maintenance of Skid Resistant Airport Pavement Surfaces. Federal Aviation Administration, U.S. Department of Transportation, Advisory Circular 150/5320-12, June 30, 1975.
2. S.K. Agrawal and H. Daiutolo. The Braking Performance of an Aircraft Tire on Grooved PCC Surfaces. Federal Aviation Administration, U.S. Department of Transportation, Atlantic City, NJ, Interim Rept. FAA-RD-80-78, Jan. 1981.
3. W.B. Horne and G.W. Brooks. Runway Grooving for Increasing Traction--The Current Program and an Assessment of Available Results. Paper presented at the 20th Annual International Air Safety Seminar, Williamsburg, VA, Dec. 4-7, 1967.
4. S.K. Agrawal and H. D'Aulerio. Engineering and Development Program Plan--Airport Runway Surface Traction. Federal Aviation Administration, U.S. Department of Transportation, Rept. FAA-ED-08-7, May 1981.

*Publication of this paper sponsored by Committee on Surface Properties-Vehicle Interaction.*

## Effects of Groove Spacing on Braking Performance of An Aircraft Tire

SATISH K. AGRAWAL AND HECTOR DAIUTOLO

The braking and cornering performance of an aircraft during operations on water-covered runways is improved by the introduction of transverse grooves on the runways. The Federal Aviation Administration has recommended 0.25-in wide x 0.25-in deep saw-cut grooves spaced at 1.25 in, to be installed on runways where the potential of hydroplaning exists. However, a large number of runways have not been grooved. The major reason for this is the high cost of groove installation and the availability of only limited evidence about the effectiveness of the grooved surfaces at the touchdown speeds of modern aircraft. The research reported here indicates that, by increasing the spacings of the conventional saw-cut grooves up to 3 in, the cost of groove installation can be reduced by up to 25 percent compared with the installation cost of grooves spaced at 1.25 in. The results further show that friction levels available on these grooves under wet operating conditions are not significantly below those attained on grooves spaced at 1.25 in. These results are valid for operating speeds up to 150 knots.

The braking performance of an aircraft during landings on water-covered runways depends on the level of friction developed in the contact area between the aircraft tire and the runway surface. The friction level developed in the contact area is affected by aircraft speed, design of the tire tread, runway finish and drainage capacity, characteristics of the braking system, and the amount of water on the runway. Under flooded runway conditions, aircraft may hydroplane because very low friction levels are available and the braking capability is reduced significantly. Loss in braking capability can be considerable even if runways are covered with only a thin film of water.

During hydroplaning, the physical contact between the tire and the runway is lost and the tires are supported on the intervening layer of water. Hydroplaning occurs as a result of rapid buildup of hydrodynamic and viscous pressures in the tire-runway contact area. Dynamic or viscous hydroplaning is identified according to whether inertial or viscous forces, respectively, are predominant. In all cases of hydroplaning, however, both effects are

present to some degree. Dynamic hydroplaning can be minimized by a rapid removal of water from the tire-runway contact area; runway grooves accomplish this very effectively by providing escape channels for water forced out of the contact area during tire passage over the grooves. Viscous hydroplaning can be alleviated by providing adequate microtexture in the runway surface.

The Federal Aviation Administration (FAA) has recommended (1) 0.25-in wide x 0.25-in deep grooves spaced at 1.25 in between centers and has encouraged airport managers, operators, and owners to groove runways where potential of hydroplaning or overruns exists. However, many runways have not been grooved. The major deterrents to the use of runway grooves are the high cost of grooving by the conventional saw-cutting method and the availability of only limited evidence about the effectiveness of grooved surfaces at the touchdown speeds of jet aircraft.

The objective of the research described in this paper is to determine a cost-effective groove configuration for portland cement concrete (PCC) surfaces.

#### SCOPE OF INVESTIGATION

A cost-effective groove configuration was determined by investigating whether an increase in groove spacing beyond the FAA recommended value of 1.25 in can lower the total cost of grooving without adversely affecting the braking performance of an aircraft tire on these grooves under wet and flooded surface conditions.

Low grooving cost and acceptable braking performance are the two key factors used in the determination of a cost-effective configuration for the saw-cut grooves. The term acceptable braking performance is subjective and is defined as follows for

Figure 1. Grooving machine used for cutting 0.25-in x 0.25-in deep grooves at various pitches in test sections.

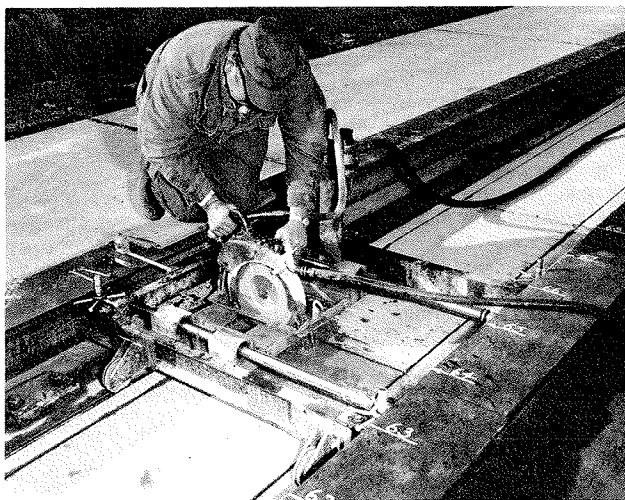


Table 1. Test parameters used in program.

Parameter	Description
Tire	
Vertical load	35 000 lb
Inflation pressure	140 lb/in <sup>2</sup>
Tread design	Worn and fully treaded, six grooves
Size and type	49x17, 26-ply, type 7
Pavement	
Type of surface	PCC
Macrotexture	0.021 in nongrooved, grease smear measure
Type of grooves	Conventional saw-cut grooves, 0.25 x 0.25 in
Groove spacing	1.25, 1.50, 2, 2.50, 3, and 4 in
Environmental	
Water depth	Under 0.02 in wet, 0.02-0.16 in puddled, 0.17-0.32 in flooded
Operational	
Wheel operation	Rolling to locked
Brake pressure	300-1800 lb/in <sup>2</sup>
Speed	70-150 knots

the purposes of this study: The available friction level on water-covered surfaces that have grooves installed at spacings in excess of 1.25 in is significantly higher than on nongrooved surfaces and is not significantly lower than grooves spaced at currently recommended values.

The groove spacing was chosen as the only variable to be included in the test program after an investigation (2) showed that increases in the groove spacing has significantly more potential for cost saving than changes in the groove size. This investigation was conducted by sampling the grooving costs in the northeastern, midwestern, and southwestern United States and included both the PCC and the asphaltic concrete surfaces. This paper describes the results on PCC surfaces only. The saw-cut grooves were installed by a machine (Figure 1) developed by the U.S. Navy.

#### EXPERIMENTAL PROGRAM

The experimental program was conducted at the Naval Air Engineering Center, Lakehurst, New Jersey. Test track 1 at this facility was modified to accomplish the objective of the research. The descriptions of the test facility and equipment, test sections, and the test procedure are given elsewhere (3) and also in our other paper in this Record.

#### Test Parameters

Four types of parameters were investigated in the test program: tire parameters, pavement parameters, environmental parameters, and operational parameters. The primary criterion was to choose a value for a given parameter such that it represented a value widely used by airlines and aircraft.

Table 1 summarizes the test parameters included in the program.

#### Data Collection and Analysis

Data were collected on oscillographs. Typical data collected in a test included horizontal force at the tire-pavement interface, vertical load on the tire, coefficient of friction developed at the interface, and wheel revolutions. Water depth and brake pressure were recorded manually, and the test speed was computed from the distance-time trace on the oscillograph.

Tables 2 and 3 show the test results. The values of the coefficient of friction in these tables represent the maximum available under each set of operating conditions. A least-square fit was obtained between speed and coefficient of friction.

#### DISCUSSION OF RESULTS

Test results on the conventional saw-cut grooves are shown in Figures 2-4. The basic characteristics of the friction-speed relation in these figures indicate a drop in friction coefficient with increasing speed--a well-documented trend (4). These results verify the validity of the experimental procedures of this research and complement the findings of past research.

Wet runway surfaces are normally encountered during or after a light or moderate rain; these surfaces may be saturated with water but would not have measurable water depth. A worn tire operating on a wet, nongrooved surface represents a situation where predominantly viscous hydroplaning may occur. Even when hydroplaning does not occur, the viscous pressures in the contact area are high and remain high at a relatively low speed. The result is low levels of available friction. The broken-line curve in Figure 4a shows the friction levels obtained under these conditions.

When a new tire is operated on wet, nongrooved surfaces, a more complex phenomenon takes place under the tire. The viscous pressure under the tire grooves is smaller than under the ribs. This results in a lower integrated pressure under the tire and provides more contact between the tire and the concrete surface. The friction levels available are increased significantly (over those obtained with a worn tire), as shown by the broken-line curve in Figure 4b.

When the surfaces are grooved, the performance of a worn tire under wet conditions improves significantly, when compared with nongrooved surfaces, as shown in Figure 4a; the performance of a new tire is also improved under similar conditions. However, the introduction of grooves on the surfaces renders the performance of a worn tire comparable to that of a new tire, as shown by the solid-line curves in Figures 4a and b.

The data scatter around the solid-line curves in Figure 4 is not indicative of the effect of groove pitch or shape on the available friction levels. Rather, it shows the sensitivity of the coefficient of friction to changes in the water depth; it is relatively more difficult to control small water depths (0.0-0.02 in) precisely; therefore, it is likely that the water depths are varying from these limits.



The puddled surfaces are representative of conditions that can be expected right after heavy rains of short durations. Puddles can also be formed on poorly drained runways or where large variations in temperature produce undulations in the runway surface. In any event, the water-filled puddles are generally not continuous in either the longitudinal or the lateral direction. The flooded runway conditions can be expected as a result of continuous, heavy rainfall. Braking performances on grooved and nongrooved surfaces when puddled and flooded conditions are encountered are shown in Figure 5.

Comparison of Figures 5a and b shows that, for all groove spacings, the braking performance on

puddled surfaces is improved by the use of a new tire rather than a worn tire. This improvement is available over the entire range of operating speeds. On the other hand, when flooded conditions are present, the new tire provides gradually improving braking performances as operating speeds are reduced. Tire wear is thus an important factor during low-speed operations on grooved, flooded surfaces.

The braking performance on nongrooved surfaces is poor under puddled and flooded conditions, and the probability that hydroplaning may occur is always high. The results on nongrooved surfaces under puddled and flooded conditions with the use of a worn tire are shown in Figures 5a and c. A coeffi-

Table 2. Test results on PCC surfaces with worn tire.

Test Speed (knots)	Coefficient of Friction x 100																							
	Nongrooved Surface, Broomed			Groove Spacings																				
				1.25 in			1.50 in			2 in			2.50 in			3 in			4 in					
	A	B	C	A	B	C	A	B	C	A	B	C	A	B	C	A	B	C	A	B	C	A	B	C
70	26	4	4	38	29	21	36	27	19	36	27	18	31	19	16	31	20	15	33	20	13			
					29	24		28	23		25	22		19	18		19	10		19		8		
90	17	4		37	24	17	34	24	15	37	19	12	29	19	13	29	15	9	29	10	7			
					19	15		18	17		15	14		22	11		20	10		18		6		
100	14	4	4																					
110	9			18	15	14	19	16	8	19	13	9	28	13	13	27	9	11	20	8	6			
					9	15		9	12		7	5		14	6		8	6		10		4		
130	7			18	15	14	19	18	12	20	16	9	30	9	13	30	9	10	26	7	9			
					11	22		13	9	22	12	7		12	10		10	6		8		4		
140				25	15	12	26	15	11	25	14	12			14			11						
						8			8															
150	9												27	16		24	10		24	11				
														12			8							

Notes: Average water depths are as follows: A = 0-0.02 in, wet; B = 0.02-0.16 in, puddled; and C = 0.17-0.32 in, flooded. 35 000 lb vertical load; 140 lb-ft<sup>2</sup> tire inflation pressure.

Table 3. Test results on PCC surfaces with new tire.

Test Speed (knots)	Coefficient of Friction x 100																							
	Nongrooved Surface, Broomed			Grooved Spacings																				
				1.25 in			1.50 in			2 in			2.50 in			3 in			4 in					
	A	B	C	A	B	C	A	B	C	A	B	C	A	B	C	A	B	C	A	B	C	A	B	C
70	30	29		41	30	20	43	29	24	39	32	25	31	22	21	32	24	24	32	23	24			
		19			28	24		29	19		29	21												
		31			24			24			24													
90	26			32	29	24	31	29	24	35	25	20		17	24		23	17	35	24	14			
					25	19		22	21		22	21		24	11		15	20		15	15			
					24			23			19			24				24			16			
110	29	17		23	25	15	24	18	14	26	13	9		16	9		16	6	34	17	10			
					19	11		21	9		17	8		18	17		14	13		11	12			
					20			18			12			19	13		15	11		8	5			
														12			11			12				
130	26			37	22	13	36	13	8	33	16	7	29	17	10	33	16	11	30	13	10			
					21	11		17	8		13	9		14	12		11	5		10	15			
					15			18			14			12			11			10	4			
					15			14			14			11			10							
					13			10			9			12						8				
								15			11													
140	28			37	26	16	39	17	12	34	10	8	33	15		28	17	7	24	11	4			
						10			12															
150	26																							

Notes: Average water depths are as follows: A = 0-0.02 in, wet; B = 0.02-0.16 in, puddled; and C = 0.17-0.32 in, flooded. 35 000 lb vertical load; 140 lb-ft<sup>2</sup> tire inflation pressure.

cient of friction of only 0.05 is available when operating speeds were below 100 knots; above 100-knot operating speeds, the wheel was locked at all of the braking pressures. A friction coefficient of 0.05 is generally accepted as a level that represents hydroplaning. The friction force that corresponds to a coefficient of friction of 0.05 is 5 percent of the vertical load on the tire. The introduction of grooves on the surface has increased the available friction from 0.05 to a maximum of 0.29; the smallest increase occurs for the worn tire in operation on flooded surface; the largest increase occurs for a new tire in operation on puddled surface.

Although the use of newer tires and grooved runways will shift the onset of hydroplaning to a higher speed, they cannot, in all cases, completely eliminate it. As the operating speeds increase, the time available for the fluid particles to escape from the tire-runway contact area decreases. Any increase in number of escape paths, either by pro-

viding patterns in the tire tread or grooves in the runway surface, cannot totally compensate for the reduction in available time brought about by higher operating speeds. Closer spacings between the grooves, however, will provide more discharge outlets to the water entrapped in the contact area. Although the number of discharge outlets will be increased, the reduction in time available for a fluid particle to go from one discharge outlet to another when the groove spacing is reduced from, for example, 3 in down to 1.25 in will be 0.000 87 s at 100-knots operating speed. The question, therefore, arises as to whether the entrapped mass of water, because of its inertia, can respond fast enough to show any significant changes in braking performance on the two spacings used in the above example. Clearly, much larger spacings will have adverse effects on the braking performance; Figure 5 seems to support this argument. It shows a large drop in coefficient of friction for 4-in groove spacing over 1.25-in groove spacing. However, no consistent trend is identifiable regarding the direction in which the friction force is changing when the entire spectrum of groove-spacings is considered.

Figure 2. Coefficient of friction as function of speed under puddled and flooded surface conditions on saw-cut grooves for 1.25- and 1.50-in pitch.

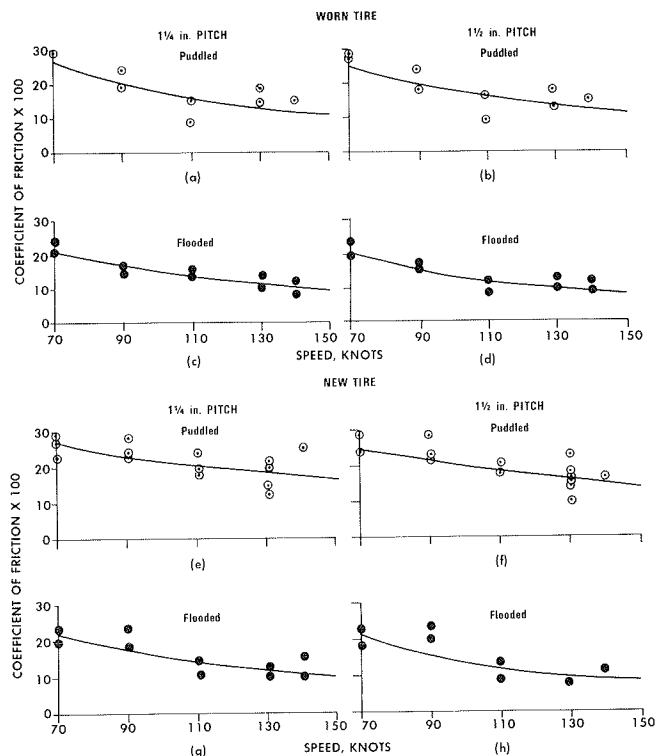


Figure 4. Coefficient of friction as function of speed under wet surface conditions on saw-cut grooves.

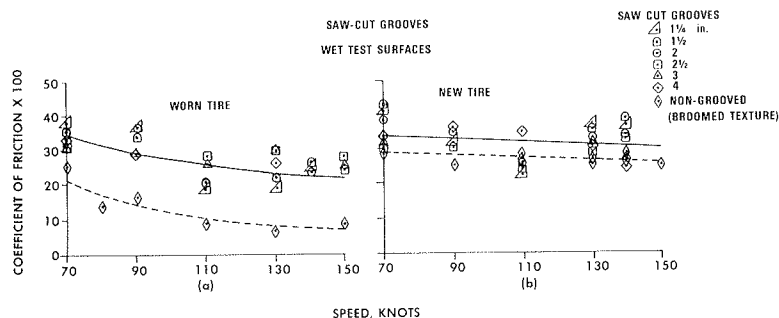


Figure 3. Coefficient of friction as function of speed under puddled and surface conditions on saw-cut grooves for 3- and 4-in pitch.

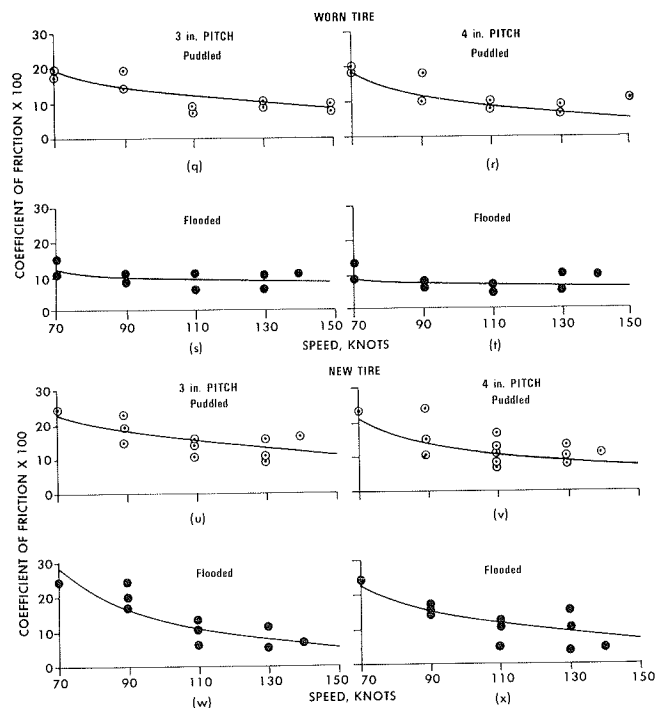


Figure 5. Comparison of relative braking performance of worn and new tires.

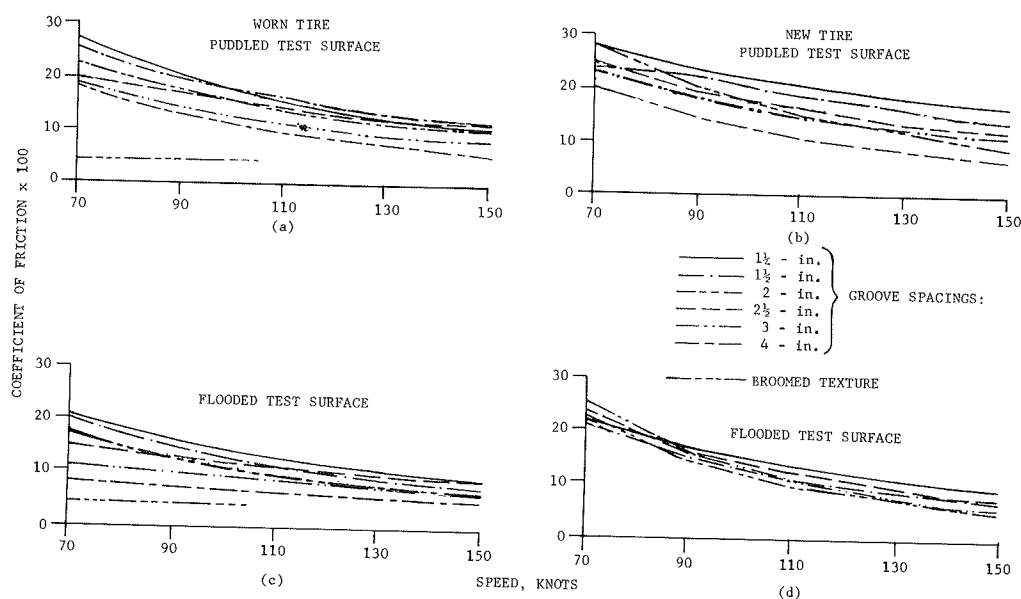
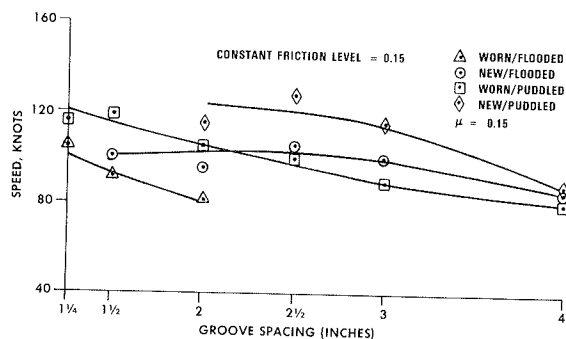
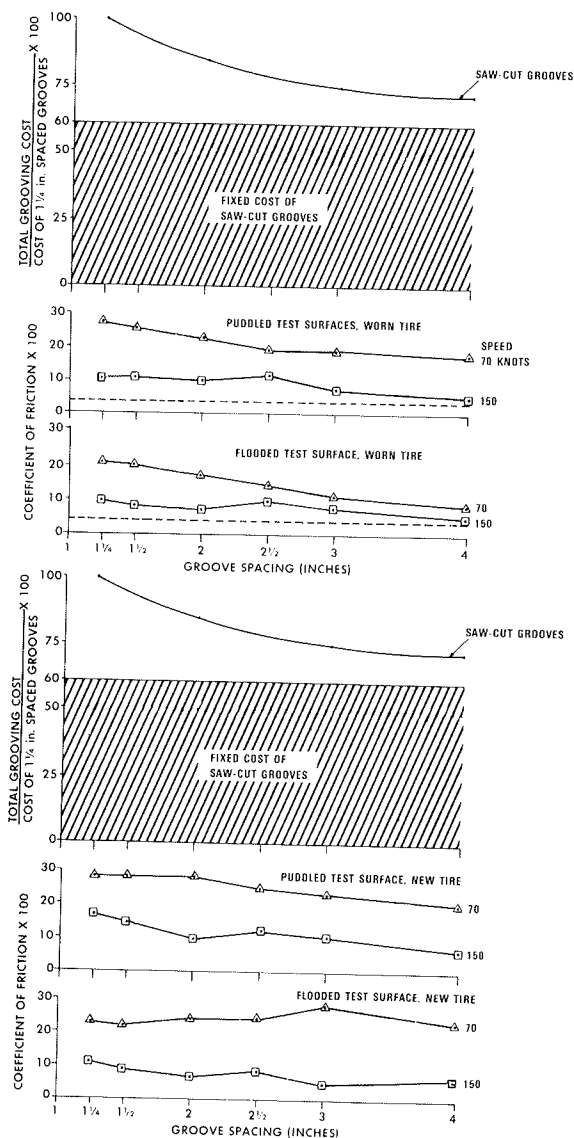


Figure 6. Comparison of attainable speed for constant friction level on saw-cut grooves.



If a coefficient of friction ( $\mu$ ) of 0.15 is arbitrarily chosen as a performance level that is expected from any of the groove configurations included in the test program, it is possible to compare the braking performance on these grooves in terms of attainable speeds under various operating conditions. The data from Figure 5 are replotted in Figure 6 for a constant friction level of 0.15. Certain observations can be made from a review of Figure 6. Under flooded conditions, the grooves spaced beyond 2 in cannot provide a  $\mu$  of 0.15 with worn tires even at low operating speeds. This can be expected because the only channels for water to escape from the contact area are the grooves, and there are not enough of them. In this situation, the smaller the groove spacing, the better the braking performance. However, the consequence that groove spacing beyond 2 in cannot sustain a friction level of 0.15 is of little importance. The completely worn tire and the flooded surface represent two extremes of tire wear and runway contamination, respectively; the likelihood of this combination being present at the runways is very small. If the grooved surfaces were puddled, the same worn tire can now attain a friction level of 0.15 under an operating speed range of 120-80 knots between the groove spacings of 1.25 and 4 in, respectively. In general, as the groove spacing is increased, the operating speed to maintain a constant friction

Figure 7. Braking performance and estimated grooving cost as function of groove spacing.



level of 0.15 decreases. The rate of decrease is smaller with a new tire.

The effect of groove spacing on the braking performance of a worn or a new tire on puddled and flooded surfaces can also be evaluated from Figure 7. This figure shows the data from Figure 5 replotted in an alternate manner; the effect of groove spacing is compared in terms of maximum available coefficient of friction under various other test conditions.

In all cases, the friction coefficient decreases as the speed increases for all the groove spacings. The friction levels attainable on nongrooved surfaces approach the hydroplaning level ( $\mu = 0.05$ ) at operating speeds of 100 knots or less; the introduction of grooves increases both the level of friction available and attainable speeds; the lower the operating speeds, the higher the available level of friction.

When comparing the effects of increased groove spacings under constant operating conditions, note that, although the overall effect is a decrease in friction level with increased spacings, the decrease cannot be classified as significant. If the operation with new tires is considered, by increasing the spacing from 2 to 3 in, the friction force remains unchanged at 150 knots. In fact, the decrease in friction force, when the groove spacing is increased from the current standard value of 1.25 to 2 or 3 in, is a maximum of 0.06 with new tires operated on puddled or flooded surfaces. A slightly higher decrease occurs with a worn tire under similar operating conditions.

#### Cost Analysis

The total cost of grooving is a function of many variables; groove spacing is one of them. The investigation by a Washington, D.C., firm concluded that fixed and variable construction costs for grooving runways are 60 and 40 percent, respectively, of total cost and that the variable cost savings increase nonlinearly with groove spacing. For example, by cutting grooves at 2-in spacing, the cost savings over 1.25-in groove spacing are 15 percent (out of the total available of 40 percent). The cost saving for 3- and 4-in spacings over 1.25-in spacing are 25 and 28 percent, respectively (Figure 7).

#### Cost-Effective Groove Configuration

As pointed out earlier in this paper, the cost-effective groove configuration must meet certain criteria. We showed in Figure 5 that the overall effect of an increase in the groove spacings is a decrease in available friction. However, the decrease is not significant. In addition, the braking performance on all the grooved surfaces tested is significantly higher than on nongrooved surfaces; friction levels that represent hydroplaning condition were observed on both puddled and flooded, nongrooved surfaces (Figures 5a and c). If perfor-

mance alone were a factor for selecting a groove configuration, 1.25-in spaced grooved runways will provide maximum friction levels under all operating conditions included in this study. However, in the majority of cases, both the cost and performance are considered to be important when installing grooves on runways. In these cases the groove spacings of 2 or 3 in will provide sufficient braking to allow a gradual reduction in the speed of an aircraft and thus develop further braking. In addition, savings of up to 25 percent in the cost of groove installation (compared with installation cost of 1.25-in spaced grooves) are available.

#### CONCLUSIONS

The following conclusions are drawn from the findings of this research and are valid for PCC surfaces.

1. The conventional saw-cut grooves spaced at 3 in or less will provide acceptable braking performance to an aircraft on water-covered surfaces. Installation cost of these grooves is up to 25 percent less than that of the grooves spaced at 1.25 in.
2. Conventional saw-cut grooves spaced at 1.25 in provide maximum friction levels under all operating conditions included in this study.

#### ACKNOWLEDGMENT

This research was requested by the Office of Airport Standards, Federal Aviation Administration. The Airport Development Division of the Systems Research and Development Service provided the program direction. Progress of the research was aided by helpful suggestions and critical reviews from Herman D'Aulerio.

#### REFERENCES

1. Method for the Design, Construction and Maintenance of Skid Resistant Airport Pavement Surfaces. Federal Aviation Administration, U.S. Department of Transportation, Advisory Circular 150/5320-12, June 30, 1975.
2. Costs of Runway Grooving, Naval Air Test Facility. Edward Galura Scharf and Sons, Washington, DC, Rept. Job No. 75-119, June 25, 1975.
3. S.K. Agrawal and H. Daiutolo. The Braking Performance of an Aircraft Tire on Grooved PCC Surfaces. Federal Aviation Administration Technical Center, Atlantic City, NJ, Interim Rept. FAA-RD-80-78, Jan. 1981.
4. W.B. Horne and G.W. Brooks. Runway Grooving for Increasing Traction--The Current Program and an Assessment of Available Results. Paper presented at the 20th Annual International Air Safety Seminar, Williamsburg, VA, Dec. 4-7, 1967.

*Publication of this paper sponsored by Committee on Surface Properties--Vehicle Interaction.*

# Effects of Differential Pavement Friction on the Response of Cars in Skidding Maneuvers

GORDON F. HAYHOE AND JOHN J. HENRY

A simulation study of the skidding behavior of cars in plane motion on surfaces with differential friction is described. Vehicle drift angle and forward velocity are taken as indicators of the difficulty a driver will experience in regaining control of the vehicle, and maintaining it within the specified roadway boundaries, should the driver release the brakes at some point during a locked-wheel skidding maneuver. Boundaries of safe vehicle operation are given as functions of roadway coefficients of friction and the length of the roadway where differential friction exists.

Areas of nonuniform tire-pavement friction across a pavement surface can arise from a number of causes, such as patching, resurfacing of worn wheel tracks, and application of marking materials for delineation. A car passing from the normal traveled way to a hard shoulder will also experience different coefficients of friction at the tires on either side of the vehicle, as will a car that has differentially worn tires.

Differential friction can either exacerbate the effects of an emergency maneuver (a locked-wheel skid, for example) or precipitate an emergency during an otherwise normal maneuver (due to the unexpected locking of a wheel, for example). The purpose of this study was to set limits on the tolerable differential friction for the safe operation of cars. Computer simulations were used to study vehicle behavior under a set of prescribed conditions.

Nonskidding maneuvers, or those in which independent locking of one or more of the wheels of the vehicle occurs, usually involve complex interaction between the driver and the vehicle. In these cases, an analytic examination of the vehicle motion is not possible because realistic models of driver behavior have not been formulated. However, a common response of car drivers to an emergency is simply to lock the wheels of the car. As will be shown later, a full, locked-wheel skid on a surface with differential friction is not much more hazardous than one on a surface with uniform friction. But if, on a surface with differential friction, the driver releases the brakes before the vehicle comes to rest, the ensuing maneuver may be extremely hazardous.

Therefore, the following maneuver was chosen to assess the hazard associated with driving a car on a differential-friction surface. The vehicle is skidding on a uniform surface and then passes onto a section of roadway where the coefficients of friction are different for the tires on either side of the vehicle. Steer angle is initially at zero degrees and is held constant during the maneuver. Two parameters describing the yaw motion of the vehicle are monitored throughout the locked-wheel skidding maneuver and, if either exceeds a certain level, it is assumed that the driver will not be able to regain control should he or she release the brakes. The primary objective of the study was then to establish boundaries of safe operation in terms of the two coefficients of friction: the length along the pavement for which the differential friction exists and the initial vehicle speed. Figure 1 shows the assumed roadway conditions for the maneuver.

In this paper, the parameter that describes the ability of a surface to provide frictional forces is referred to as "coefficient of friction" rather than "skid number". This nomenclature emphasizes the

fact that the results are given in terms of vehicle-tire/pavement properties and not in terms of pavement properties as described by a locked-wheel skid number ( $SN_{40}$ ) measured according to American Society for Testing and Materials (ASTM) test method E274 (1). Skid numbers are used for ranking assumed uniform sections of pavement in terms of their "skid resistance" and are not intended to describe the true coefficient of friction experienced by a typical highway vehicle. In contrast, the present work aims at assessing the relative hazard associated with different levels of suddenly changing friction on a pavement surface. Estimates of the true coefficients of the pavement surfaces are therefore required.

## VEHICLE RESPONSE DURING A SKIDDING MANEUVER

In a pure skidding maneuver, the presence of differential friction on the pavement causes vehicle yaw and an increase in stopping distance that depends on the change in effective total friction. If the vehicle is maintained in a skid (i.e., the wheels are kept locked), the trajectory of the center of gravity is very close to a straight line; the only difference in vehicle response on pavement surfaces with and without differential friction is the increased stopping distance and vehicle yaw. In this case, the procedures currently used to determine acceptable skid resistance can be applied by estimating the "effective" coefficient of friction and by allowing for the increased hazard of an increase in effective vehicle width as the vehicle rotates. The effective friction and additional hazard would have to be determined for each individual site, which would make a general criterion for acceptability difficult to formulate. However, the full skidding maneuver is a special case of the general maneuver in which a driver locks the wheels, the vehicle skids some distance, and the driver then releases the brakes. If the coefficient of friction is uniform over the pavement surface, the vehicle will not rotate during the maneuver and the driver can reapply the brakes while maintaining steering control. If the friction is nonuniform, the vehicle will rotate during the skid and, on release of the brakes, will travel in a direction different from the original. If the yaw angle is great enough, the driver may not have steering control.

Figure 1. Pavement surface with differential friction as idealized in simulation study.

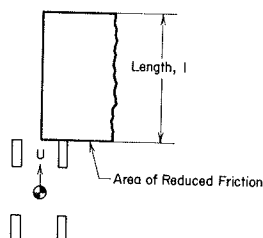


Figure 2. Vehicle axis system and vehicle parameters.

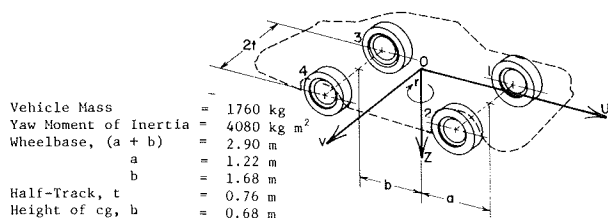


Figure 3. Simulation tire model results for free rolling and locked-wheel sliding.

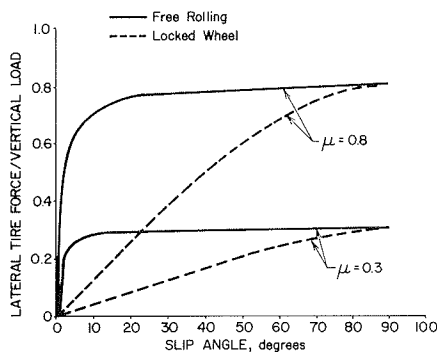
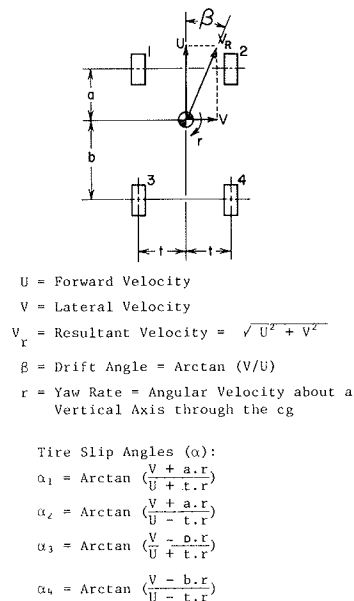


Figure 4. Variables defining kinematics of four-wheeled vehicle motion.



## SIMULATION MODEL

The effect of differential friction on safe car operation was studied by means of a digital computer simulation in which the vehicle was given an initial velocity, direction, and position relative to the nonuniform portion of the pavement. By an extension of the argument given in the previous section, the particular pavement configuration was considered to be unsafe if (a) at some point during the skid the heading of the vehicle changed by more than 20° from its original direction or (b) at some point during the skid the product of drift angle (body sideslip angle) and forward velocity exceeded a value of 3.66

m/s (where drift angle is defined as the angle between the longitudinal axis of the vehicle and the resultant velocity vector at the center of gravity, as shown later in Figure 4).

The first condition expresses the fact that the driver has no steering control over the vehicle at large yaw angles and that the vehicle will not continue to travel in the original direction when the brakes are released. The second condition expresses the fact that, after the brakes are released, the vehicle is likely to travel off the highway before the driver has an opportunity to take control and change the vehicle heading.

The simulation model has three degrees of freedom: forward velocity (U), lateral velocity (V), and yaw velocity (r). Figure 2 shows the variables and the general layout of the model. The vehicle model has four wheels; the tire forces at each wheel are found by using a tire model (2) that calculates the forces under all conditions of lateral and longitudinal slip. Vehicle suspension effects, such as roll steer and compliance steer, are neglected, although load transfer is included through a quasi-static analysis.

## DETERMINATION OF CRITERIA FOR SAFE OPERATION

Vehicle control is, in general, a process in which the driver turns the steering wheel to modify the lateral forces generated at the front tires of the vehicle. Whether the front tire forces can be changed by small steering motions is therefore of fundamental importance to efficient control and, by extension, so is the shape of the lateral tire force characteristic. Figure 3 shows plots of lateral tire force versus slip angle for free rolling and locked-wheel sliding at coefficients of friction of 0.8 and 0.3. [Slip angle is the angle between the diametral plane of the wheel and the resultant velocity vector (in the horizontal plane) of the wheel axle.] The plots were taken from tire model results with the coefficient of friction constant with speed. But, since coefficient of friction generally decreases with increasing speed, experimental free-rolling lateral tire force characteristic curves typically show a peak in lateral force at a slip angle between 10° and 20°. This somewhat unrealistic aspect of the plots does not affect the following discussion; the important characteristic is that, for a free-rolling tire, the slope of the curves at large slip angles (greater than about 5°) is small compared with the slope at small slip angles.

Consider a vehicle sliding with locked wheels on a surface that has a uniform coefficient of friction at a given drift angle ( $\beta$ ), yaw rate (r), and sliding velocity ( $V_r$ ), as shown in Figure 4. [In Figures 4-7, a = locked-wheel sliding on a split-coefficient surface, b = locked-wheel sliding on a uniform-coefficient surface ( $y = 0.6$ ), and c = free-rolling wheels on a uniform-coefficient surface ( $y = 0.6$ ) and brake release is at 1.5 s.] Under these conditions, the vehicle will rotate about its center of gravity and travel in the direction of the  $V_r$  vector at decreasing rates until it stops. However, if the brakes are released during the maneuver, the lateral tire forces will rapidly attain the values given by the free-rolling tire force characteristic curve, disturbing the vehicle from its straight-line motion.

With free-rolling wheels, the net yaw moment about the center of gravity of the vehicle is given by the expression

$$M_z = a \cdot Y_f - b \cdot Y_r \quad (1)$$

where  $Y_f$  and  $Y_r$  are front and rear lateral tire

forces, respectively, as determined from the characteristic curves (Figure 3). Therefore,

$$M_z = a \cdot [f(\alpha_1) + f(\alpha_2)] - b \cdot [F(\alpha_3) + F(\alpha_4)] \approx a \cdot f[(V + a \cdot r)/U] - b \cdot F[(V - a \cdot r)/U] \quad (2)$$

For the vehicle-pavement configuration shown in Figure 1, yaw rate ( $r$ ) will be negative and lateral velocity ( $V$ ) will, in general, be positive during the maneuver. Negative slip angles give positive

Figure 5. Yaw rate, heading angle, and drift angle response of four-wheeled vehicle when brakes are released during skidding maneuver across 3-m-long split-coefficient surface.

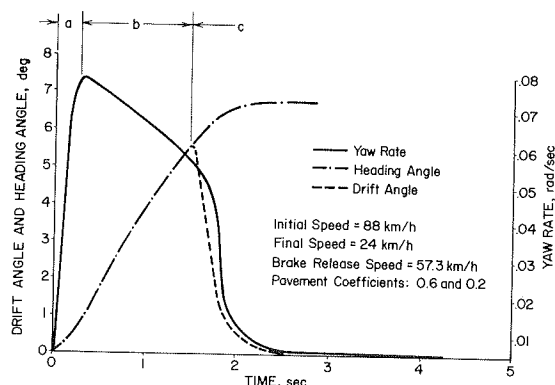


Figure 6. Yaw rate, heading angle, and drift angle response of four-wheeled vehicle when brakes are released during skidding maneuver across 12-m-long section of split-coefficient surface.

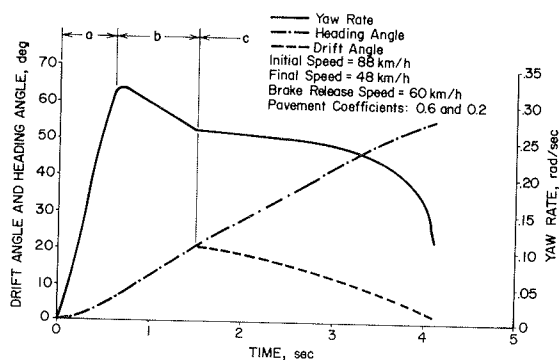
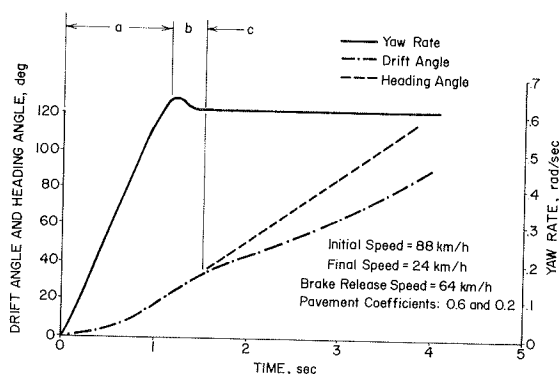


Figure 7. Yaw rate, heading angle, and drift angle response of four-wheeled vehicle when brakes are released during skidding maneuver across 24-m-long section of split-coefficient surface.



side forces, and the net yaw moment will therefore be positive for both locked and free-rolling wheels.

If, during the skidding maneuver, drift angle is small, the lateral velocity will be of the same order of magnitude as the  $a \cdot r$  and  $b \cdot r$  terms in the slip-angle expressions. The locked-wheel side forces will also be small. When the brakes are released, the lateral tire forces will increase and generate a large positive yaw moment that will decrease yaw rate and stabilize the vehicle motion at some final heading angle (to the original direction of  $V_r$ ). When the front tire force is on the part of the tire curve that has high slope (small  $\alpha_f$ ), it is clear that vehicle yaw rate will always go to zero when there is no control action by the driver and that the front tire force can easily be changed by the driver if he or she turns the steering wheel.

At large drift angles, lateral velocity ( $V$ ) will be the dominant term in the slip-angle expressions except when yaw rate is unreasonably large. When the brakes are released, the magnitude of the lateral tire forces at the front and rear will be determined almost wholly by the drift angle and will therefore give approximately equal and opposite yaw moments about the center of gravity while both front and rear tires are operating at large slip angles. Modification of the slip angles by the yaw-rate terms will have little effect because of the small slope at large slip angles. The result is that the vehicle will maintain an approximately constant yaw rate while moving laterally under the influence of the large lateral tire forces.

Figures 5, 6, and 7 show yaw-rate, drift-angle, and heading-angle responses for lengths of differential friction of 3, 12, and 24 m, where the brakes are released 1.5 s after the start of the maneuver (drift angle is positive for negative yaw rate and heading angle). The pavement coefficients of friction are 0.6 and 0.2. [Heading angle is defined as the angle through which the vehicle rotates from the start of the maneuver ( $t = 0$ ) to time  $t$  (as shown later in Figure 9). The different scales on the vertical axes of the three plots should be noted.]

In Figure 5, yaw velocity, drift angle, and heading angle increase while the vehicle is sliding on the split-coefficient surface. Yaw rate then decreases when the vehicle is sliding on the uniform-coefficient surface, while drift and heading angle continue to increase. When the brakes are released and the wheels are allowed to turn freely, drift angle is 5.5°; this small value causes the yaw rate and the drift angle to decrease rapidly to zero through the mechanism described previously. The heading angle goes to a constant value, and the final vehicle trajectory is a straight line at the steady-state heading angle. Full steering control is available to the driver as soon as the brakes are released.

In Figure 6, the vehicle motion follows the same pattern as in Figure 5 until brake release, except that the three variables reach larger values because of the increased length of time on the split-coefficient surface. When the brakes are released, the drift angle has a value of 20° and the yaw rate decreases much more slowly than in Figure 5. The yaw rate does not begin to decrease at a significant rate until the drift angle has become less than 10°, 2 s after brake release. To gain sufficient steering control to stabilize the vehicle, the driver must reduce the front-wheel slip angle to less than 5°. For a drift angle of 20°, the driver must therefore turn the steering wheel through at least 300° (assuming a steering gear ratio of 20:1). The maximum steering-wheel rotation rate for a typical driver is approximately 400°/s (3). Thus, if driver

Figure 8. Lateral deviation during skidding maneuvers when brakes are released 1.5 s after initiation of skid.

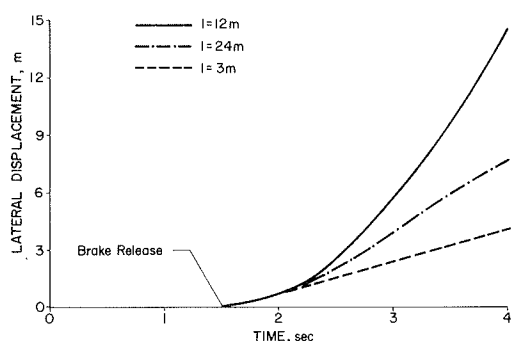
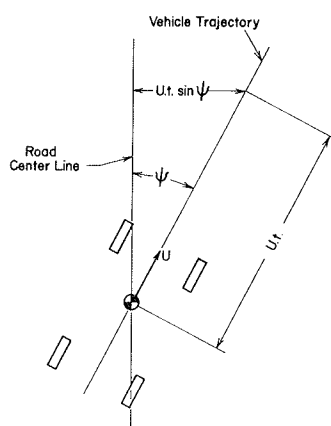


Figure 9. Lateral displacement of vehicle traveling obliquely across a road at steady forward speed.



response time is ignored, about 1 s will pass after brake release before the driver can begin to significantly influence the behavior of the vehicle. This analysis also assumes that the driver makes the correct response.

In Figure 7, drift angle is  $33^\circ$  when the brakes are released, and the vehicle continues to spin at a constant yaw rate through the remainder of the maneuver. The drift angle also continues to increase in this case because the increase in lateral velocity due to vehicle rotation exceeds the decrease due to lateral acceleration. It is clear that the vehicle motion is completely unstable and that the driver cannot influence vehicle behavior during either the locked-wheel or the free-rolling wheel phases by turning the steering wheel.

Figure 8 shows the lateral deviation of the vehicle perpendicular to the initial heading. Lateral deviation in the last two cases ( $l = 12$  m and  $l = 24$  m) is in excess of 3 m 1.75 s after brake release. However, driver control action may be expected to reduce this for  $l = 12$  m.

From these results, and from the general description already given of vehicle response in skidding maneuvers, it is clear that releasing the brakes is the most hazardous response that a driver can make in a skidding maneuver where all four wheels are locked and the vehicle is sideslipping at a large drift angle. Once the brakes are released, the ability of the driver to regain control before colliding with another vehicle or with a roadside obstacle depends in the first case on the drift angle of the vehicle. Consequently, an unsafe condition would exist if, at any point during either of the

simulated locked-wheel skidding maneuvers, the vehicle drift angle exceeded a value of  $20^\circ$ . This value was chosen partly because it represented the transition between a decrease or an increase in the drift angle after brake release in the maneuvers used to produce the results shown in Figures 5-7. A further reason was that  $20^\circ$  is an upper limit on the angle through which a driver can reasonably be expected to turn the wheels of a car in 1 s. A longer delay will probably result in the vehicle passing into a potential collision zone before the driver can regain full control.

The  $20^\circ$  drift-angle limit is independent of speed, but experience suggests that vehicle control becomes more difficult as speed increases. A full explanation of this effect cannot be given, although important to the present work is the fact that a vehicle traveling at a nonzero heading angle will travel sideways, relative to the center of the road, at a rate in direct proportion to forward speed times the sine of the heading angle ( $U \cdot \sin \psi$ ), as demonstrated in Figure 9. The parameter  $U \cdot \sin \psi$  is given in terms of steady-state forward speed and heading angle with free-rolling wheels, but the desired parameter should be expressed in terms of vehicle variable values measured during a locked-wheel skid. The substitution of drift angle ( $\beta$ ) for heading angle is later shown to be a reasonable transformation. In addition, if  $U \cdot \sin \beta$  is taken as a limiting factor in vehicle response, it will be the deciding factor only when drift angle is less than  $20^\circ$ . The expression may therefore be simplified to  $U \cdot \beta$  with little change in the numerical values.

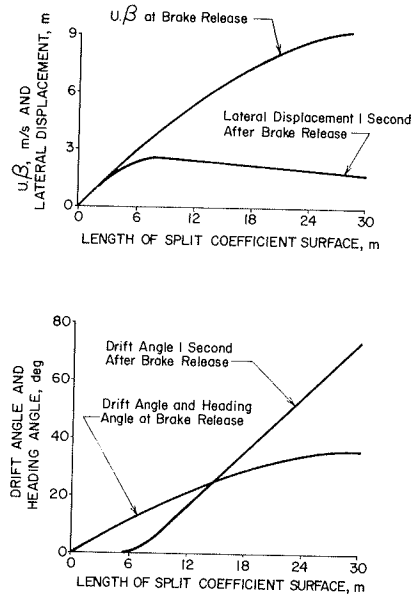
An upper limit of 3.66 m/s was placed on  $U \cdot \beta$ ; if this value was exceeded during a simulated maneuver, a hazard was considered to exist ( $U$  is in meters per second and  $\beta$  is in radians). The choice of  $U \cdot \beta = 3.66$  m assumes that (a) the vehicle must travel 3.66 m laterally to enter a potential collision zone, (b) the yaw rate reduces instantaneously to zero and the vehicle travels in the direction of its heading at brake release, and (c) the driver is allowed 1 s to regain control and steer the vehicle to a safe path. The third assumption is the most difficult to justify, since both driver response time and time to regain control must be taken into account. For example, if the driver makes no steering correction at all, he or she will exceed the 3.66-m allowed lateral displacement in 1 s. But if the driver begins steering action at, say, 0.5 s after brake release, the heading angle will decrease during the remaining time, thus effectively allowing more time to steer the vehicle to a safe path within the 3.66-m lateral displacement limit.

The allowance of just 1 s for the driver to respond and control the vehicle would probably be too short if the yaw rate did indeed reduce to zero instantaneously. But Figures 5-7 show that this assumption becomes less true as the drift angle at brake release increases. Figure 8 shows the effect on lateral displacement. For example, when  $l = 3$  m,  $U \cdot \beta = 1.55$  m at brake release and lateral displacement 1 s later is 1.43 m. Lateral displacement 1 s after brake release is therefore slightly overpredicted by  $U \cdot \beta$ . In contrast,  $U \cdot \beta$  overpredicts lateral displacement by more than a factor of two when  $l = 12.2$  m. Drift angle, heading angle, and  $U \cdot \beta$  at brake release, and drift angle and lateral displacement 1 s after brake release, are shown in Figure 10.

The maximum allowable lateral deviation of 3.66 m was chosen to conform with work by Burns (4), where a vehicle is considered to have entered a potential collision zone when it moves from the center of a



Figure 10. Vehicle response at brake release and 1 s after brake release.



lane 3.66 m in width to the center of an adjacent lane also 3.66 m in width. The maximum allowable lateral deviation may be increased or decreased according to the width of the roadway.

Burns (4) also gives an experimental justification for some of the conclusions drawn from the simulation. He describes a series of experiments in which a professional driver locked the wheels of a car on a split-coefficient surface and then released the brakes after the car had rotated through a specified angle. Specific findings were that (a) a rotation in excess of  $30^\circ$  caused the vehicle to be completely uncontrollable; (b) the permissible angle of rotation at brake release, without loss of control, decreased as vehicle speed increased; and (c) the vehicle entered a potential collision zone after release of the brakes at a rotation of  $10^\circ$  and a vehicle speed of 80 km/h. These results are important because they are based on the only full-scale experimental data on vehicle loss of control on split-coefficient surfaces. However, the number of tests conducted was small, and the experienced driver's performance may not be typical of that of the general driving population confronted with an unexpected maneuver. Direct correlation of the simulation results with the experimental results therefore was not possible. [Zuk (5) gives a plot of a typical trajectory for a scale-model car sliding with locked wheels on a split-coefficient surface, but the effect of releasing the brakes is not considered.]

A study of vehicle-driver behavior after brake release by including a steering controller in the simulation was not attempted because none of the available models (6,7) accurately reproduced the behavior of a human driver, particularly in emergency maneuvers.

#### BOUNDARIES OF SAFE OPERATION

The simulation runs were made at an initial vehicle speed of 88 km/h. In most cases, either the  $U \cdot \beta$  limit was exceeded before the drift-angle limit or neither of the two limits was exceeded. However, in some runs  $U \cdot \beta$  reached a maximum value that was less than 3.66 while drift angle exceeded its limit at a relatively low speed. When this occurred, the

maneuver was considered to be hazardous if drift angle exceeded  $20^\circ$  at a vehicle speed of 32 km/h or more. It should be noted that changing the vehicle parameters or the initial speed may reverse the order in which the parameters are exceeded, as will changing the specified safe limit for  $U \cdot \beta$  or  $\beta$ .

Figures 11 and 12 show the maximum values of  $U \cdot \beta$  attained during the simulation runs, plotted as a function of split-coefficient length at various combinations of coefficients of friction. The lengths where the curves cross the  $U \cdot \beta = 3.66$  line are shown in Figure 13. Also shown in Figure

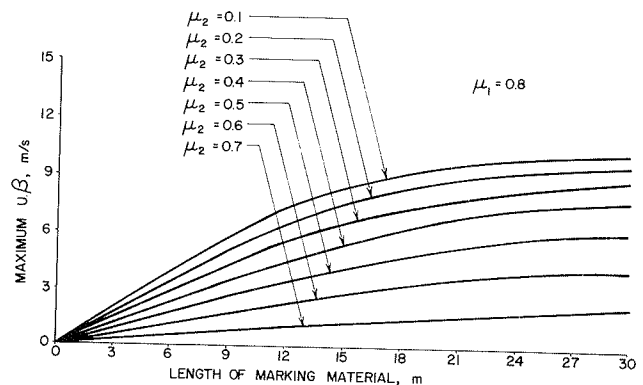
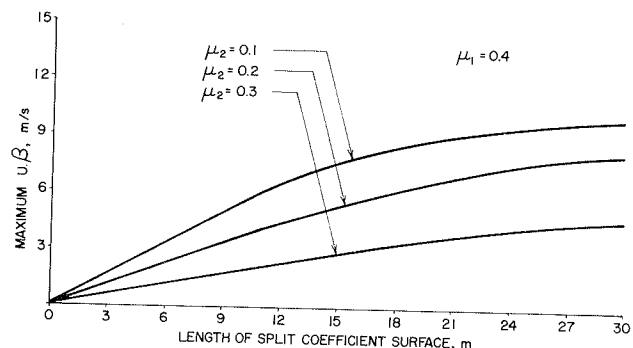
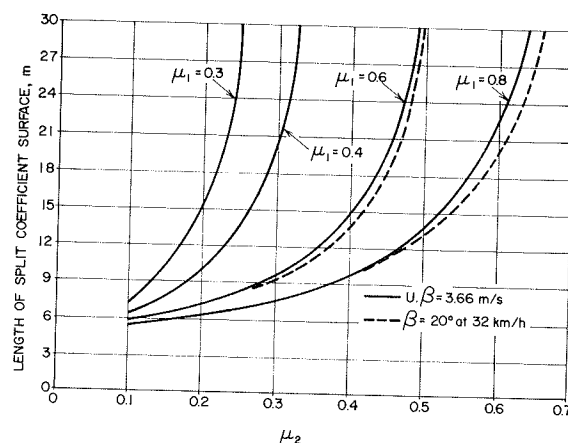
Figure 11. Maximum  $U \cdot \beta$  attained during locked-wheel skid on split-coefficient surface (initial vehicle speed = 88 km/h).Figure 12. Maximum  $U \cdot \beta$  attained (initial vehicle speed = 88 km/h).

Figure 13. Recommended maximum lengths of differential friction for safe operation of cars in skidding maneuvers (vehicle speed at inception of skid = 88 km/h).



13 are curves indicating when drift angle exceeded  $20^\circ$  at a vehicle speed of 32 km/h. Figure 13 shows boundaries of safe operation: If a given combination of the two coefficients of friction and the length of differential-friction surface falls to the left of the appropriate curve, unsafe operation is indicated; if the combination falls to the right of the appropriate curve, safe operation is indicated.

In using Figure 13, a first estimate of the coefficients of friction may be obtained by taking values of  $SN_{40}$  measured by ASTM E274 (1) for the respective surfaces, dividing by 100, and entering directly. If it is required to account for the fact that an  $SN_{40}$  measurement [made with an ASTM E501 (1) tire] overestimates the skid resistance of a low-macrotexture surface as experienced by a worn tire, the coefficient of friction may be estimated from values of skid resistance measured with an ASTM E524 (1) blank tread tire or from macrotexture and microtexture measurements. However, skid-resistance measurements made by the ASTM E274 method (1) should be used with care. The transformation and interpretation of such measurements should be made at the discretion of the user.

### CONCLUSIONS

The results presented in Figure 13 are applicable only to skidding maneuvers in which the skid was initiated by some factor other than the presence of differential friction. Maintaining the vehicle in the skid is then considered to be the safest course of action for the driver if the differential friction causes the vehicle to exceed a given value of angular deviation from the original path. The previously defined parameters of angular deviation are measures of how difficult it will be for the driver to regain control and subsequently steer the vehicle on a path within the roadway boundaries should he or she release the brakes at some point during the skid. Only tangent sections with 3.66 m of allowable lateral maneuvering space were considered, although smaller lateral distances and curved sections could also be included by changing the allowable limit of the parameter  $U \cdot \beta$ .

However, the extremely complex and variable nature of human behavior and a lack of experimental data make it very difficult to set numerical values for the parameter limits. This constitutes the most serious source of error (or uncertainty) in the boundaries of safe operation shown in Figure 13. Further studies of driver behavior and an analysis of accidents occurring on split-coefficient roadway surfaces are required to validate (a) the choice of parameters to indicate potential loss of control and (b) the numerical parameter values that give the boundaries of safe operation.

The chart shown in Figure 13 is therefore a first approximation of the boundaries of safe operation and should be used only as a guide. It should also be noted that a boundary of safe operation implies an acceptable level of risk rather than a definite boundary below which no accidents will occur.

Differential friction may also initiate an emergency when a vehicle is being braked, since the wheels on the low-coefficient surface may lock if the surface cannot generate sufficient tire friction force. The locking of three or fewer of the wheels will yaw the vehicle in much the same manner as will a four-wheel skid on a split-coefficient surface, except that the driver retains a measure of lateral control through the wheels that are not locked. Skidding maneuvers initiated by pavement markings may therefore not be as serious as maneuvers that result from releasing the brakes of a vehicle during a four-wheel skid. But this consideration should be

weighed against the fact that the emergency has been caused by the differential friction.

Other factors that contribute to differences between the simulated trajectories from which Figure 13 was generated and the trajectory of a car on the highway involve modeling simplifications and estimation of coefficients of friction. In view of the difficulty of predicting human behavior during emergencies, improving the accuracy of modeling would probably not give a significant improvement in the degree of uncertainty associated with the use of Figure 13. Estimation of the effective coefficients of friction is a practical matter that depends on the procedure used to measure skid resistance and on the vehicle tire configuration (worn, mixed, winter tread, etc.) that is to be considered as typical or representative.

The most important factors likely to contribute to discrepancies in the simulation results are the following:

1. The vehicle parameters used in the simulation were for a full-sized sedan. Other vehicle configurations or off-design values will give different results.
2. The coefficient of friction was modeled as being independent of tire sliding speed. Low-speed skid resistance and the relation between skid resistance and speed for different tire-pavement pairs are to a large extent independent. Allowing the coefficient of friction to vary with speed would therefore have greatly increased the number of simulation runs because of the increased number of possible combinations of pavement friction coefficients.
3. The roadway was considered to be flat and horizontal. A vehicle sliding on a superelevated roadway will tend to slide laterally, and changes in grade will change the distance required for the vehicle to stop.
4. The vehicle model did not have a roll degree of freedom. Probably the most serious aspect of this restriction is that there is some evidence of coupling between vehicle roll and driver steering input, during severe maneuvers, which may lead to instability. At this time, such complications cannot be modeled.

### ACKNOWLEDGMENT

The research described in this paper was developed from work conducted as part of a Federal Highway Administration research project. Edward Harrigan served as technical monitor of this project, and his assistance is greatly appreciated.

### REFERENCES

1. Annual Book of ASTM Standards. ASTM, Philadelphia, Part 15, 1980.
2. H. Dugoff, P.S. Fancher, and L. Segel. An Analysis of Tire Traction Properties and Their Influence on Vehicle Dynamic Performance. Trans., SAE, Vol. 79, Paper 700 377, 1970.
3. W. Lincke, B. Richter, and R. Schmidt. Simulations and Measurement of Driver Vehicle Handling Response. SAE, Warrendale, PA, Paper 730 489, 1973.
4. J.C. Burns. Differential Friction: A Potential Skid Hazard. TRB, Transportation Research Record 602, 1977, pp. 46-53.
5. W. Zuk. The Dynamics of Vehicle Skid Deviation as Caused by Road Condition. Virginia Council of Highway Investigation and Research, Charlottesville, June 1958.
6. G.F. Hayhoe. A Driver Model Based on the Cerebellar Model Articulation Controller. Vehicle

- System Dynamics, Vol. 8, 1979, pp. 49-72.
7. D.T. McRuer and R.H. Klein. Automobile Controllability: Driver/Vehicle Response for Steering Control: Volume 1--Summary Report. U.S. Department of Transportation, Rept. TR-

1040-1-I, 1975, 269 pp. NTIS: PB 240 208.

*Publication of this paper sponsored by Committee on Surface Properties-Vehicle Interaction.*

# Groove-Depth Requirements for Tine-Textured Pavements

JOHN E. GRADY AND WILLIAM P. CHAMBERLIN

This paper discusses the depth required for grooves on new tine-textured concrete pavements in order to ensure an adequate skid resistance over their entire design life. It is based on measures of texture depth and skid resistance, with both ribbed and smooth tires, made on new to 5-year-old pavements in New York. Initial groove-depth needs of 3/16-in minimum were calculated from two values estimated from the study data: (a) minimum groove depth (0.050 in) to ensure adequate skid resistance with a minimum legal tire tread and (b) mean groove wear rate (0.013 in/million vehicle passes). Groove depth measurements on new concrete pavements and bridge decks indicated 21 and 14 percent compliance, respectively, with the proposed new standard of 3/16-in minimum, and 60 and 44 percent compliance with the current standard of 2/16-in minimum. Prospects for improving the compliance rate were judged to be most promising in two areas--increasing the awareness and motivation of construction personnel and improving the design of tining rakes over those now in use. Although the findings of this study are specific to standards and conditions in New York, the methodology should be of general interest.

Many highway agencies require a tined finish on new portland cement concrete pavements (1). The method was introduced because textures obtained by previous methods were found to wear too quickly, and pavements provided only marginal skid resistance after passage of a relatively few vehicles (2). Although assumptions of improved durability and skid resistance over other methods have been generally confirmed (3), the relative newness of tine texturing has precluded evaluation of its long-term durability and skid resistance under actual traffic. Ensurance of adequate skid resistance over a pavement's entire design life requires knowledge of minimum texture needs and the rate at which texture and skid resistance decay, so that the depth of groove required at construction can be judged. This paper describes the collection and analysis of data to address these questions. Although the findings reflect specific needs and conditions in New York State, the methodology is generally applicable.

## PURPOSE AND SCOPE

The primary purpose of the study was to determine the rate at which tined textures, and the skid resistance they provide, decay under traffic, and thus to determine what initial groove depth is required to sustain adequate skid resistance over a pavement's entire design life. A related consideration was that an evaluation of the effectiveness of current design practices, including skid-resistance-decay rates, had been recommended by the Federal Highway Administration (FHWA) (4), though this policy is under review (5).

A secondary purpose was to evaluate newly constructed pavements and bridge decks for compliance with specified texture depth. New York requires a groove depth of  $3/16 \pm 1/16$  in (6), but past ex-

perience has shown that texture depths vary significantly from job to job, and even within the same job (7). It was believed that data collected on new construction would show whether depths actually obtained are sufficient to permit adequate skid resistance over the entire design life, given the decay rate measured.

The study was based on measures of skid resistance and texture parameters collected in 1978 and 1979 on 11 in-service pavements, 9 unopened pavements, and 25 unopened bridge decks. These sites represented all of those that, by the summer of 1978, had been finished with a tined texture under new specifications implemented in 1974. In all cases, pavements were built with a New York State class C concrete mix (nominal water-cement ratio = 0.44, cement factor = 6.4), and bridge decks were built with a class E mix (nominal water-cement ratio = 0.44, cement factor = 7.0).

## PROCEDURES AND RESULTS

Texture wear rates were estimated from texture depth measurements and ribbed-tire skid resistance tests on 11 pavements in service (series 1). To extend the range of corresponding traffic volumes, measurements were made in both the driving and passing lanes and for two years (1978 and 1979). Five sites were tested in each lane of each pavement, for a total of 110 sites.

The minimum mean groove depth (MGD) required to provide adequate drainage beneath a minimum legal tire tread (2/32 in deep in New York) was estimated from texture and skid resistance measurements with both ribbed and smooth tires at 30 additional sites, selected from these same 11 pavements (series 2). These additional sites were chosen to represent as wide a range in groove depth among sites as possible and also because each was relatively uniform within the distance required for a valid skid test--about 60 ft.

To judge compliance with the current specification as well as with initial texture depth needs determined from this study, depths were also measured on 9 unopened pavements and 25 unopened bridge decks (series 3). The entire testing program is outlined in the table below.

Variable	Series 1	Series 2	Series 3
Objective	Wear	Groove	Compliance
	rates	depth	
Test pavements	11	4	9, including 25 bridge decks

Table 1. Performance data for fine-textured pavements, series 1.

Sites	Lane	1978					1979					
		CVP <sup>a</sup> (000 000s)	SN <sub>40</sub>	SN <sub>55</sub>	MTD (in)	MGD (in)	BPN	CVP <sup>a</sup> (000 000s)	SN <sub>40</sub>	SN <sub>55</sub>	MTD (in)	MGD (in)
1-10	Driving	2.911	38.6	32.5	0.025	0.092	53.5	3.472	41.2	36.1	0.022	0.079
	Passing	NA	59.2	52.8	0.033	0.113	68.9	NA	56.4	49.0	0.035	0.099
11-20	Driving	2.494	39.3	30.4	0.023	0.088	66.7	3.003	39.9	33.4	0.022	0.078
	Passing	0.212	50.8	52.8	0.032	0.111	78.5	0.255	56.5	50.2	0.030	0.103
21-30	Driving	NA	41.6	36.8	0.035	0.153	72.9	NA	40.9	35.7	0.035	0.141
	Passing	0.098	61.1	54.3	0.032	0.127	74.4	0.198	59.2	52.5	0.033	0.125
31-40	Driving	0.720	39.9	36.2	0.035	0.136	70.7	1.362	34.4	30.2	0.035	0.126
	Passing	0.079	59.0	52.4	0.045	0.147	79.9	0.149	53.1	46.7	0.043	0.138
41-50	Driving	0.785	46.5	40.8	0.048	0.163	71.7	1.480	38.9	34.6	0.046	0.144
	Passing	0.070	62.0	55.2	0.067	0.191	82.7	0.131	55.1	50.3	0.059	0.174
51-60	Driving	1.920	39.5	33.3	0.030	0.128	61.5	2.758	36.2	31.8	0.028	0.121
	Passing	0.143	58.9	52.9	0.039	0.128	76.4	0.206	54.4	47.6	0.031	0.121
61-70	Driving	1.920	40.6	34.7	0.018	0.091	56.3	2.758	35.5	30.6	0.017	0.093
	Passing	0.143	58.3	53.7	0.019	0.074	70.6	0.206	54.7	47.2	0.018	0.090
71-80	Driving	1.880	43.1	35.9	0.027	0.115	60.5	2.700	35.7	30.6	0.027	0.113
	Passing	0.183	60.0	55.5	0.026	0.117	73.7	0.263	54.3	48.1	0.033	0.125
81-90	Driving	1.559	35.7	30.0	0.032	0.131	54.7	2.149	34.5	30.9	0.036	0.129
	Passing	0.123	56.5	50.1	0.036	0.124	69.1	0.169	54.9	49.2	0.035	0.126
91-96	Driving	2.946	35.4	31.1	0.014	0.051	57.4	3.982	39.3	32.0	0.011	0.036
	Passing	1.036	44.0	39.4	0.018	0.063	70.1	1.400	45.5	39.7	0.028	0.063
97-100	Driving	5.451	34.8	30.6	0.016	0.072	48.0	7.366	38.9	31.9	0.015	0.062
	Passing	1.387	44.4	40.8	0.033	0.110	65.2	1.875	47.4	41.8	0.035	0.100
101-110	Driving	2.919	37.3	34.3	0.017	0.066	59.1	3.945	41.7	35.4	0.018	0.057
	Passing	0.468	47.7	44.6	0.025	0.082	72.4	0.633	48.2	43.0	0.028	0.078

Note: Each value is the mean of five individual test results, each from a different test site.  
aCVP = cumulative vehicle passes.

Variable	Series 1	Series 2	Series 3
Measurement sites	110	30	115
Texture measurements			
Sand patch	1978- 1979		
Gage depth	1978- 1979	1979	1978-1979
Skid measurements			
Ribbed tire	1978- 1979	1979	
Smooth tire		1979	

All skid tests were made at 40 and 55 mph, according to ASTM E 274-77, at fixed distances from the pavement edge in the left wheelpath of both driving and passing lanes. The tests employed a ribbed tire that meets the requirements of ASTM E 501-76, and a smooth tire that meets those of ASTM E 524-76. Results of the series 1 and 2 skid tests are given in Tables 1 and 2.

Pavement macrotexture was measured by using both the sand-patch method (7,8) and a dial depth gage. The latter had been used previously in New York to measure flailed grooves (9) and is similar to gages used in Louisiana (10). In series 1, 10 individual sand-patch tests were made in both 1978 and 1979 at randomly selected locations at each 60-ft measurement site (7), and mean texture depths (MTDs) were calculated. Also, during both years, dial-gage measurements were made at close intervals along the entire length of each 60-ft site, and MGDs were calculated. Because these two measures were found to correlate well, only the dial gage was used for series 2 and 3 tests. Mean values for series 1 and 2 texture measurements are given in Tables 1 and 2, and series 3 values are plotted as histograms in Figure 1.

Traffic volumes, without regard to vehicle classification, were estimated at the time of skid testing, from available annual average daily traffic (AADT) (11) plus individual traffic counts to determine distributions between driving and passing lanes. They are expressed in Table 1 in millions of vehicle passes.

Table 2. Skid resistance with ribbed and smooth tires, series 2.

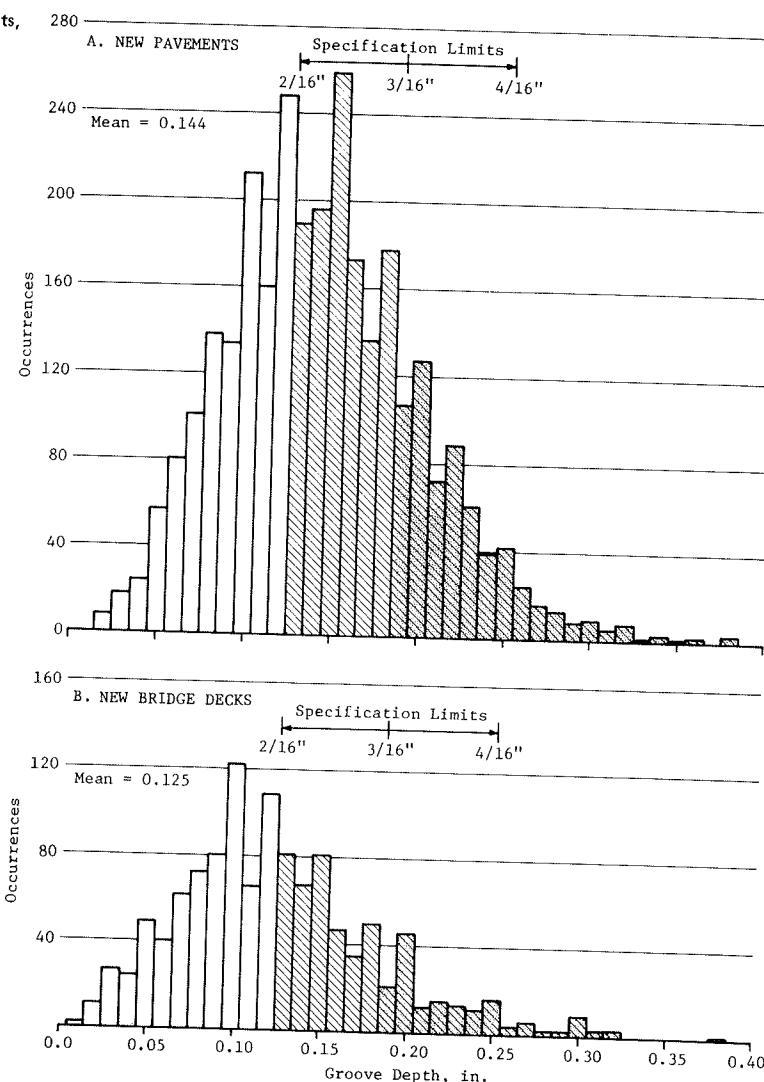
Route	Site	MGD (in)	SN <sub>40</sub>		SN <sub>55</sub>	
			Ribbed	Smooth	Ribbed	Smooth
I-88 Oneonta to Otego	111	0.0788	45.4	37.9	38.9	31.6
	112	0.0815	42.7	36.3	37.0	28.7
	113	0.0385	43.3	27.3	36.8	21.5
	114	0.1056	49.4	44.5	42.3	36.7
I-88 Franklin to Unadilla	115	0.0608	37.9	30.0	31.7	25.8
	116	0.0856	37.9	31.4	31.7	28.5
	117	0.0489	34.8	26.7	30.1	23.0
	118	0.1174	41.7	38.6	35.7	34.0
	119	0.1223	43.2	40.3	37.0	34.1
	120	0.1225	41.2	38.3	34.9	32.6
	121	0.1261	40.9	37.1	34.8	33.9
	122	0.1342	38.5	35.5	33.0	32.5
	123	0.0191	41.6	19.8	33.2	19.2
	124	0.0181	35.7	14.7	30.2	12.6
	125	0.0847	31.9	30.2	29.6	27.2
	126	0.1184	32.6	32.4	30.5	30.0
I-88 Sidney to Bainbridge	127	0.1486	37.0	35.6	32.6	31.5
	128	0.1376	39.1	36.6	33.5	31.7
	129	0.0766	37.4	35.4	31.4	27.6
	130	0.1357	40.2	38.7	34.1	29.9
	131	0.1151	38.1	34.5	32.5	28.1
	132	0.0886	40.8	37.6	34.7	28.5
	133	0.0924	37.6	35.9	33.5	29.2
	134	0.0239	37.6	22.5	29.4	16.1
I-88 Oneonta bypass <sup>a</sup>	135	0.0123	36.0	17.8	28.5	11.9
	136	0.0229	41.2	21.3	32.2	16.0
	137	0.0509	44.1	30.5	37.7	27.6
	138	0.0190	45.4	23.9	39.9	16.5
	139	0.0115	54.9	29.3	41.7	21.4
	140	0.0150	53.4	27.0	43.1	18.3

<sup>a</sup>Broom-textured section used to simulate totally worn fine texture.

#### Decay of Skid Resistance (Series 1)

Values of mean skid resistance at both 40 mph (SN<sub>40</sub>) and 55 mph (SN<sub>55</sub>) are plotted in Figure 2 against values of cumulative vehicle passes (CVPs). Separate plots and their regression lines are given on both linear (Figures 2a and b) and logarithmic (Figures 2c and d) rectangular coordinate grids. Previous skid-resistance-decay studies in New York,

Figure 1. Distribution of groove-depth compliance measurements, series 3.



primarily those that involve asphalt pavements (2,12-14), used semi-log regressions of skid-number (SN) versus CVP. However, these data were found to be better represented by log-log regressions. The least-squares lines and their regression equations are based on all of the skid data; however, for simplicity, the figures show only the mean values given in Table 1. (Also, the variance within these groups of five was small and corresponded to a standard deviation of 2.64.)

In Figures 2c and d, the rate of skid resistance decay appears to stabilize at about 2 million vehicle passes. This pattern is interpreted to mean that the tined grooves, though wearing, are providing adequate drainage, that the observed decay in skid resistance primarily reflects the polishing of microtexture (i.e., that small-scale roughness on the horizontal surfaces between grooves), and that a level of polishing equilibrium has been reached. Skid resistance from this point on can be expected to remain stable until the grooves become too shallow to provide adequate drainage, at which point skid resistance will again begin to decay as hydroplaning effects appear.

From a design point of view, it is important to consider what measures can be taken to increase the skid-resistance level at which equilibrium occurs and to ensure that grooves are deep enough in the first instance to give adequate drainage for the design life. The former concern is usually addressed

by such practices as selecting hard, angular fine aggregate (15) or by the application of sprinkle treatments (16). Use of burlap-drag or broom texturing between tined grooves, now recommended by FHWA (17), may enhance initial skid resistance but is not likely to affect the level at which equilibrium occurs. The latter concern (adequate groove depth) will be considered later.

A useful concept in judging the adequacy of design and construction practices, from the standpoint of skid resistance durability, has been the 90th percentile critical traffic volume (90 percent CTV), defined as the cumulative traffic volume beyond which less than 90 percent of measured SNs are expected to equal or exceed 32 (2,12). The value of 32 corresponds to the American Association of State Highway and Transportation Officials (AASHTO) minimum stopping sight distance at 40 mph (18) and is used in New York as a design guide for minimum acceptable SN. The 90 percent CTV for tine-textured pavements in New York, calculated from the standard error of estimate for the regression in Figure 2a, was found to be 7.83 million vehicle passes at 40 mph. Any increase that may occur in the equilibrium skid resistance while groove depth is still adequate would be reflected in an increase in this value.

#### Decay of Texture Depth (Series 1)

To assess from experience what minimum nominal

groove depth may be required during construction to ensure an acceptable level of skid resistance at the end of design life, three pieces of information are needed:

1. Minimum groove depth capable of sustaining adequate skid resistance,
2. Groove wear rate, and
3. Design life.

Average groove wear rate is estimated in this section.

Figure 3 shows the decay of texture with traffic as measured by the sand-patch method and dial-depth gage. Results by the two methods were found to be highly correlated ( $r = 0.92$ ), as shown in Figure 4. Because dial-gage measurements related more directly to provisions of New York's specifications, they were used alone in estimating texture wear rate, and

Figure 2. Decay of skid resistance with traffic, series 1.

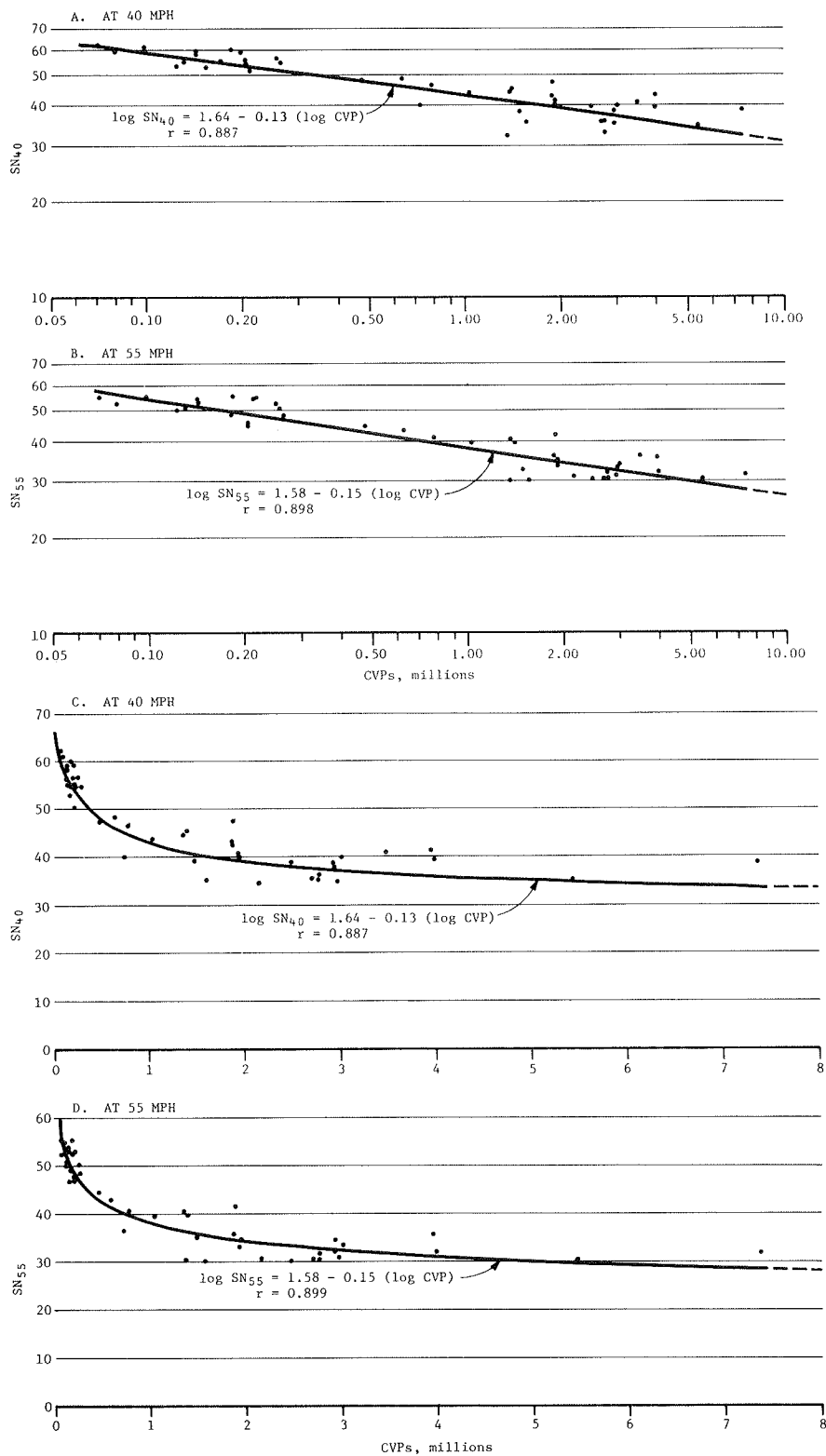


Figure 3. Decay of surface texture with traffic, series 1.

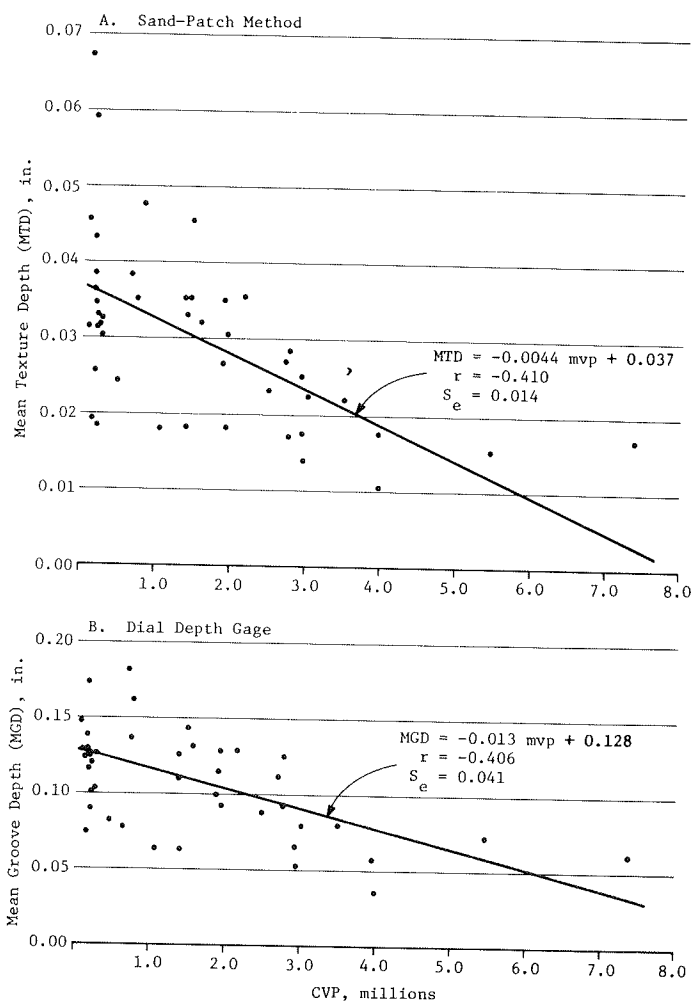
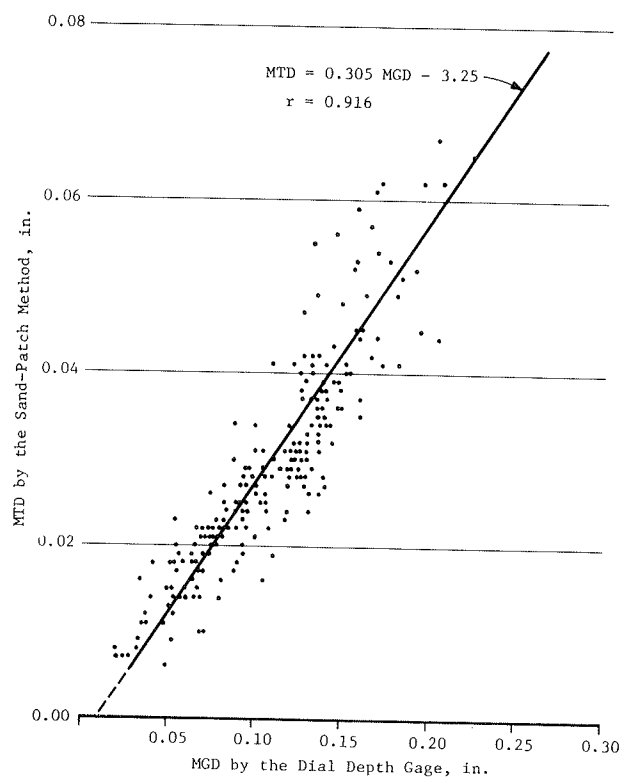


Figure 4. Correlation of sand-patch and dial-gage measurements, series 1.



for the series 2 and series 3 tests as well. The wear rate estimated from the slope of the regression in Figure 3b is equivalent to an average loss of 0.013 in in MGD for each 1 million vehicle passes.

Tire texturing was originally chosen by New York because of its presumed longer life. The greatest threat in recent years to the durability of any textured surface on portland cement concrete pavement has been the use of tungsten-carbide-studded snowtires. Thus, one consideration in extrapolating texture-wear studies is the anticipated change in studded-tire use from the time or location of the study. Their use has declined in New York from a statewide average of 28 percent of vehicles in 1969-1970 to 19 percent in 1974-1975, and to less than 10 percent in 1978-1979 (2,19). Considering dates of pavement opening and the relative density of studded tire use in particular parts of the state (19), studded-tire use on the 11 tested pavements was estimated to be in the 6-14 percent range during the study period.

#### Minimum Required Groove Depth (Series 2)

In an attempt to determine the minimum groove depth required for tined textures to sustain adequate skid resistance, skid resistance was measured with both ribbed and smooth tires. Although a ribbed tire can drain much of the water beneath it through its grooves even on nearly smooth surfaces, a smooth tire relies on the pavement's macrotexture for nearly all drainage and thus is more sensitive to differences in macrotexture (20).

Thirty sections of pavement were tested that had relatively uniform within-section groove depth, but varied in MGD among sections from very deep to nearly smooth. Data from these tests are given in Table 2 and plotted in Figures 5 and 6. The curves that represent the ribbed tire show a slight decline in SN with increasing groove depth. This is probably due to a slight increase in tire-pavement contact as the new surface begins to wear, in a situation where the water drainage qualities of the surface are more than adequate. Curves that represent the smooth tire, on the other hand, show SN increasing markedly with increasing groove depth, as pavement contact increases with improved drainage. The MGD at which curves for ribbed and smooth tires converge is taken to represent the minimum value that will permit full drainage beneath a smooth tire--that is, about 0.015 in at 40 mph.

Also of interest in these figures are the curves that represent the difference in SNs between the two tires for the same groove depth. Much of the scatter in the individual sets of data is thereby removed. Common variables are eliminated by subtraction, and good correlations for both 40- and 55-mph tests remain. Note that, although skid resistance with either the ribbed or smooth tire is significantly lower at 55 than at 40 mph at all texture depths, the difference in skid resistance between the two tires is virtually the same at both speeds.

These graphs were used to estimate the minimum MGD that would provide sufficient drainage beneath a minimally legal treaded tire (2/32 in in New York State) to maintain adequate skid resistance, defined for design purposes in New York as SN=32. The approach taken was to construct an SN-MGD curve on Figure 5 to represent test tire grooves of 2/32 in and to identify the MGD at which the ordinate of that curve equalled an SN of 32. The 2/32-in curve was constructed by linear interpolation between the existing curves for ribbed and smooth tires (broken line in Figure 5). Since the ribbed tire was new (0.385 in or about 13/32 in) and all of the 30 ex-

perimental sites were tested within about two days, an average tread depth of 12/32 in during this period was assumed. By using this approach, a minimum acceptable groove depth of 0.050 in for a 2/32-in tire was determined. As an aside, the difference in skid resistance between that estimated for a 2/32-in treaded tire and that found by testing with a smooth tire was in the range of 1.5 to 2 SNs at relatively low levels of texture (MGD = 0.040 to 0.070 in). This value compares favorably with research in Virginia (21), in which it was estimated that a loss of 2/32 in in tire tread depth corresponded to a loss of about 1.25 SNs.

By using an estimate for minimum acceptable groove depth of 0.050 in and by applying the mean groove-wear rate established earlier (0.013 in/million vehicle passes), initial groove depths required at construction to ensure a terminal groove depth  $\geq$  0.050 at the end of design life were calculated for pavements that have different AADTs. These calculations were based on a distribution of single-lane, one-way AADTs for concrete pavements in service in 1977 and are given in Table 3.

Table 3 shows that, had those concrete pavements in service in 1977 been built in compliance with the current New York groove-depth requirement of 3/16  $\pm$  1/16 in (minimum 0.125 in), a minimum of only 43 percent of them would have had textures adequate to provide acceptable skid resistance for their design life. Similarly, if the mean groove depth then specified (3/16 in or 0.1875 in) had been attained, a minimum of 71 percent would have had a sufficient groove depth. An extension of this logic results in Table 4, which shows the diminishing return of each incremental increase in MGD. For instance, an increase from 2/16 to 3/16 in is associated with a 66.0 percent increase in benefit, from 3/16 to 4/16 in with 19.0 percent, and from 4/16 to 5/16 in with 10.8 percent. Although the data probably argue for increasing the minimum in New York from 2/16 in, it is difficult to argue for more than 4/16 in on the basis of Table 4. Even 4/16 in may be impractical because of the difficulty of its attainment in practice and undesirable because of the level of noise that it may generate.

#### Specifications Compliance (Series 3)

As noted, New York specifications require a minimum texture groove depth of 2/16 in (0.125 in) on both new pavements and bridge decks. The preceding analysis suggests that a minimum depth of 3/16 in (0.1875 in) or greater would be more consistent with expectations for acceptable design-life skid resistance. To determine what levels of texture depth are actually being obtained, 9 new pavements and 25 new bridge decks were evaluated by dial depth gage. These results are given for individual paving contracts and bridge decks in Table 5 and represented graphically without regard to source in Figure 1.

The mean of all groove-depth measurements was found to be 0.144 in for pavements and 0.125 in for bridges. Forty percent of all measurements on pavements and 56 percent on bridge decks were less than 2/16 in, the specified minimum value. If 3/16 in were to become the required minimum, then 79 percent of pavement measurements and 86 percent of bridge deck measurements would be deficient. Obviously, greater groove-depth requirements would result in an even higher proportion of deficiencies. It is clear then that, though deeper groove standards are needed, it would be impractical to impose them without also acting to improve construction compliance. Experience in this study suggests that the best hopes in this regard are (a) increasing awareness of construction personnel as to the importance of the



Figure 5. Relation between skid number and mean groove depth at 40 mph, series 2.

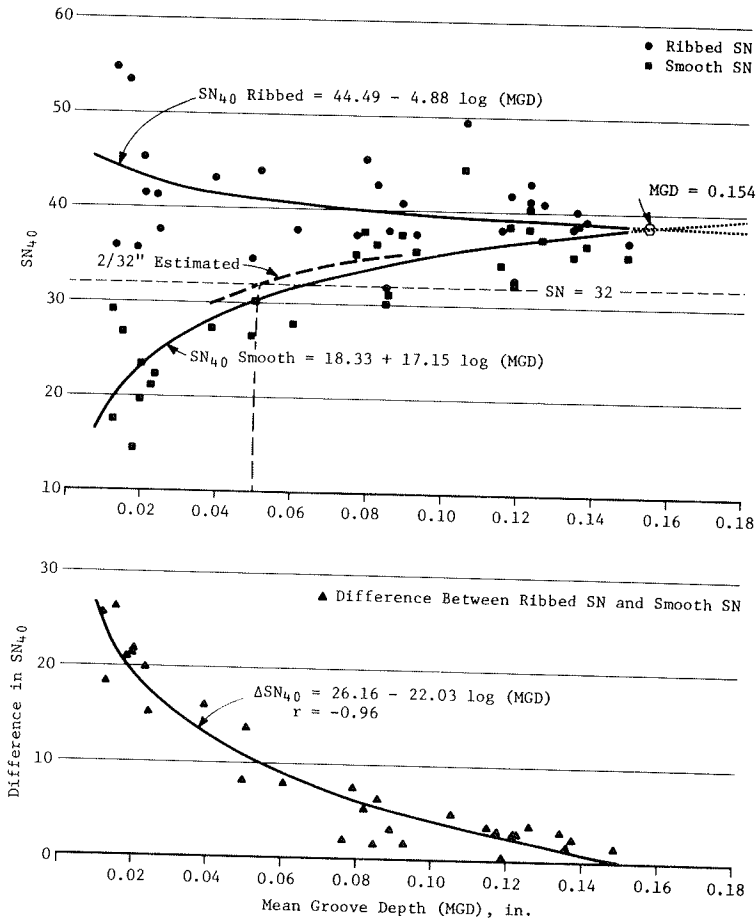


Figure 6. Relation between skid number and mean groove depth at 55 mph, series 2.

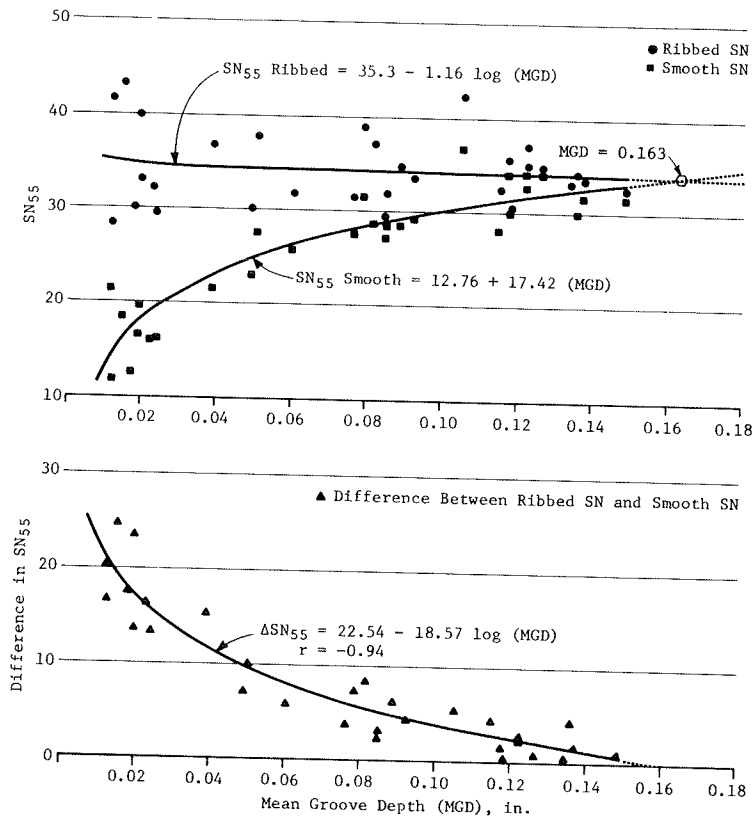


Table 3. Analysis of groove depth needs for New York pavements.

Traffic	Cumulative Passes After 15 Years (000 000s) <sup>a</sup>	Groove Depth		Distribution of Lane Miles	
		Cumulative Loss After 15 Years (in) <sup>b</sup>	Initial Required (in) <sup>c</sup>	Percent <sup>d</sup>	Cumulative Percent
One-Lane, One-Way AADT					
0-500	1.369	0.018	0.068	12.2	12.2
500-1000	4.106	0.053	0.103	20.4	32.6
1053 <sup>e</sup>	5.769 <sup>e</sup>	0.075 <sup>e</sup>	0.125 <sup>e,f</sup>	- <sup>e</sup>	43.0 <sup>e</sup>
1000-1500	6.844	0.089	0.139	17.1	49.7
1500-2000	9.581	0.124	0.174	17.8	67.5
1932 <sup>e</sup>	10.577 <sup>e</sup>	0.1375 <sup>e</sup>	0.1875 <sup>e,g</sup>	- <sup>e</sup>	71.4 <sup>e</sup>
2000-2500	12.319	0.160	0.210	10.8	78.3
2500-3000	15.056	0.196	0.246	6.3	84.6
3000-3500	17.794	0.231	0.281	3.4	88.0
3500-4000	20.531	0.267	0.317	3.7	91.7
4000-4500	23.269	0.302	0.352	1.8	93.5
4500-5000	26.006	0.338	0.388	2.5	96.0
5000-5500	28.744	0.374	0.424	0.8	96.8
5500-6000	31.481	0.409	0.459	0.4	97.2
6000-6500	34.219	0.445	0.495	0.1	97.3
6500-7000	36.956	0.480	0.530	0.2	97.5
7000-7500	39.694	0.515	0.565	0.2	97.7
7500-8000	42.431	0.552	0.602	0.0	97.7
8000-8500	45.169	0.587	0.637	0.3	98.0
8500-9000	47.906	0.623	0.673	0.2	98.2
9000-9500	50.644	0.658	0.708	0.3	98.5
>9500	53.381	0.694	0.744	1.5	100.0

<sup>a</sup>Based on assumed 15-year design life and calculated from AADT class mean.

<sup>b</sup>Calculated from mean annual rate of 0.013 in./million vehicle passes.

<sup>c</sup>Calculated from minimum acceptable of 0.050 in.

<sup>d</sup>From New York State data.

<sup>e</sup>Value that corresponds to initial minimum and mean specified groove depth.

<sup>f</sup>Minimum specified in New York State.

<sup>g</sup>Mean specified in New York State.

texture depth requirement and then motivating and supporting them to strive for it and (b) improving the actual texturing equipment.

The most critical aspect of attaining deeper grooves may be to place the same priority on meeting groove-depth specifications as is placed on meeting other requirements, regardless of the type of rake used. Experience shows that the depth currently specified in New York (2/16-in minimum) is attainable if appropriate attention is given by construction personnel to timing, technique, and equipment used in the texturing process.

#### Improvements in Texturing Equipment

Most tine rakes now in use (at least in New York) have been shop-fabricated from available materials and designed so that the tines contact the concrete surface at a relatively steep angle (i.e.,  $\pm 45^\circ$ ). Such devices tend to scratch the surface, which often results in nonuniform depth and frequent aggregate displacement. A typical example is a comb made from the tines of a common leaf rake mounted between blocks of wood. Compliance with texture depth requirements by using these devices has generally been unsatisfactory. The example cited is not unique.

One commercial rake, the Flexi-Glide tine manufactured by the A.R.M. Corporation of Anderson, Indiana, has recently come on the market and appears to offer some improvement. This rake (Figure 7) employs an uncommonly low angle of attack that seems to impress the texture into the concrete rather than scratching it in. Based on limited trial use in New York, results are encouraging. Versions mountable on pavement finishing machines are also available.

Another approach has incorporated two sets of tines of different lengths (and therefore different stiffnesses) mounted on opposite sides of the same unit. This allows the rake to be reversed when stiffer concrete is encountered, which brings the

Table 4. Satisfaction of pavement groove depth needs.

Minimum Groove Depth (in)		Pavement Percentage of Lane Miles	Percentage Increase Between Increments
Fraction	Decimal		
2/16	0.125	43.0	
3/16	0.1875	71.4	66.0
4/16	0.250	85.0	19.0
5/16	0.3125	94.2	10.8
6/16	0.375	96.8	2.76
7/16	0.4375	97.3	0.05
8/16	0.500	97.6	0.03
9/16	0.5625	97.8	0.02
10/16	0.625	98.2	0.04
11/16	0.6875	98.9	0.07
12/16	0.750	100.0	1.01

Note: Based on an assumed design life of 15 years, 1977 traffic volume distribution, and groove wear rate of 0.013 in./million vehicle passes.

Table 5. Groove depth measurements on new pavements and bridge decks, series 3.

Surface	Pavement Contract	Deck	Groove Depth		Compliance (percentage >2/16 in)
			n	x (in)	
Pavement	C		254	0.182	81
	E		232	0.168	75
	A		436	0.165	72
	I		450	0.157	71
	B		250	0.138	57
	H		442	0.137	57
	F		246	0.129	50
	D		343	0.126	36
	G		288	0.113	36
	E	7	19	0.230	95
Bridge deck	I	19	96	0.195	91
	B	16	50	0.162	76
	D	6	117	0.141	60
	F	10	126	0.141	60
	F	13	39	0.137	51
	A	18	43	0.123	49
	A	17	59	0.123	42
	B	3	20	0.128	40
	A	2	25	0.113	36
	F	15	48	0.121	35
	F	8	24	0.108	33
	A	1	39	0.116	31
	F	11	114	0.102	30
	D	5	54	0.106	26
	F	14	46	0.117	24
	F	12	41	0.094	24
	D	4	60	0.100	22
	F	9	42	0.089	21
	I	20	128	0.089	20

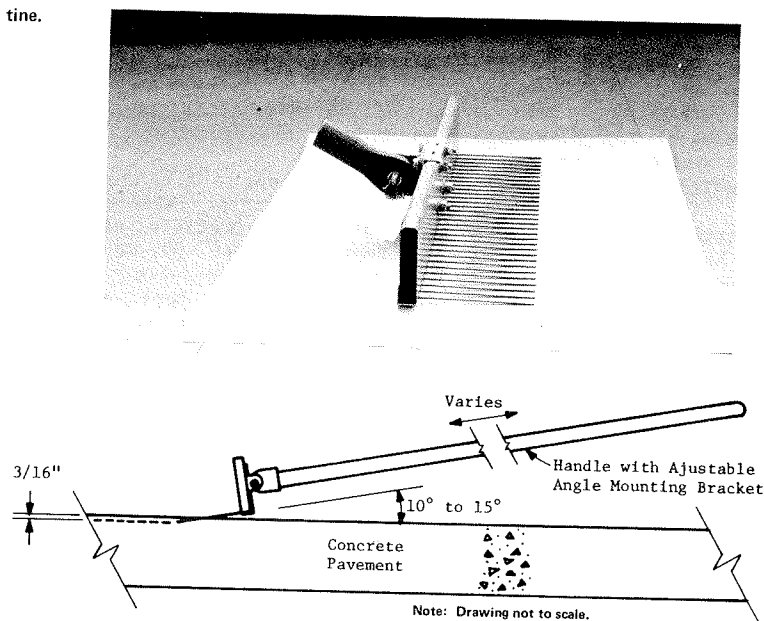
shorter and more rigid tines into use.

Consideration has also been given to using narrower tines. However, reducing tine width without also reducing tine spacing would theoretically provide less drainage area. Use of 1/8-in tines on 1/2-in centers, rather than 3/4-in centers, has been considered (in New York) and would provide both the same drainage and land area (riding surface) as before but with a narrower tine that might penetrate more easily.

#### CONCLUSIONS

The following conclusions have been drawn from the results of this study of the performance of tine-textured pavements in New York State. They are influenced by the concrete materials, finishing practices, pavement design assumptions, and traffic conditions found on the specific pavements studied, but they are probably applicable in much of New York. We believe, however, that the methodology employed in the analysis is generally applicable

Figure 7. Flexi-Glide tine.



beyond New York, and in that sense the paper may be looked on as a case study.

1. Skid resistance of concrete pavements textured to produce 3/16-in wide grooves on 3/4-in centers begins to decay from an initial value when opened to traffic but appears to stabilize after passage of about 2 million vehicles. This stability is believed to correspond to equilibrium polishing of the microtexture at a time when the grooves are still sufficiently deep to provide complete drainage. Thus, attempts to improve skid resistance should be directed toward practices that will enhance the equilibrium microtexture or ensure that grooves are sufficiently deep to provide complete drainage for the pavement's entire design life, thereby fully mobilizing the equilibrium microtexture.

2. Decay of skid resistance on tine-textured pavements appears to be best represented on  $\log_{10}$ - $\log_{10}$  plots.

3. The 90th percentile critical traffic volume for tine-textured pavements in New York, defined as the CTV beyond which less than 90 percent of measured SNs at 40 mph are expected to equal or exceed 32, is estimated to be 7.83 million vehicle passes.

4. Pavement grooves 3/16 in wide on 3/4-in centers were found to wear at a mean rate of 0.013 in/million vehicle passes, as measured by dial-depth gage.

5. Measurements of MGD with a dial-depth gage correlated significantly with measurements of mean texture depth by the sand-patch method ( $r = 0.92$ ).

6. A MGD of 0.050 in was found necessary to ensure an acceptable level of pavement skid resistance of at least SN = 32 for legally treaded tires. It is estimated that a minimum depth of 3/16 in would ensure that at least 71 percent of the concrete pavement placed in New York retains grooves for 15 years that are at least 0.050 in deep (based on 1977 data). The corresponding value for 4/16 in is 85 percent.

7. Present tine-texturing practice with conventional concrete in New York is resulting in 60 percent compliance on pavements and 44 percent on bridge decks with the current 2/16-in minimum groove depth standard. If the current standard had been 3/16-in minimum, compliance would be 21 and 14 percent, respectively.

8. Experience indicates that MGDs of 2/16 and 3/16 in are attainable with proper attention to equipment, technique, and particularly timing of the texturing process. Redesign of the texturing rake to result in tines of greater stiffness that intersect the pavement surface at a lower angle appears to offer possibilities for better penetration without otherwise tearing the surface.

#### ACKNOWLEDGMENT

This paper was prepared in cooperation with FHWA under administrative supervision of William C. Burnett, Director of Engineering Research and Development, New York State Department of Transportation. We gratefully acknowledge the work of William G. Leslie, senior civil engineer, who began the study and supervised the first year of testing and data analysis. We wish to thank the technicians involved in collection of field data, particularly Roger J. Hordines, Edward J. Rice, and Robert V. Viti. In addition, we thank Robert W. Rider, Wayne R. Shrome, and Gerald K. Smith for the collection of skid resistance data.

#### REFERENCES

1. P.J. Nussbaum and E.C. Lokken. Design and Construction of Concrete Pavements. Proc., International Conference on Concrete Pavement Design, Purdue Univ., Lafayette, IN, Feb. 15-17, 1977, pp. 19-71.
2. W.P. Chamberlin and W.G. Leslie. Concrete Pavement Texturing Methods: A Review of New York's Experience. Engineering Research and Development Bureau, New York State Department of Transportation, Albany, Res. Rept. 70, April 1979.
3. G.K. Ray and L.T. Norling. More Macrotexture in Concrete Pavement for Greater, Longer Lasting Skid Resistance. Portland Cement Assoc., Skokie, IL, TA034.01P, 1974.
4. Skid Accident Reduction Program. FHWA, Instructional Memorandum 21-2-73, July 19, 1973.
5. Federal Register, Vol. 45, No. 71, April 10, 1980.
6. New Texturing Method for Portland Cement Concrete Pavement. New York State Department of

- Transportation, Albany, Engineering Instruction 74-22, Feb. 21, 1974.
7. D.E. Amsler and W.P. Chamberlin. Measuring Surface Texture of Concrete Pavements by the Sand-Patch Method. Engineering Research and Development Bureau, New York State Department of Transportation, Albany, Res. Rept. 62, July 1978.
  8. Guideline for Texturing of Portland Cement Concrete Highway Pavements. American Concrete Pavement Assoc., Arlington Heights, IL, Tech. Bull. 19, March 1975.
  9. E.D. McNaught. Demonstration of a Flail-Type Pavement Grooving Machine. Engineering Research and Development Bureau, New York State Department of Transportation, Albany, Special Rept. 53, Feb. 1977.
  10. J.E. Ross and S.M. Law. Texturing of Concrete Pavements. Research and Development Section, Louisiana Department of Transportation and Development, Baton Rouge, Rept. FHWA-LA-Interim 3, Aug. 1977.
  11. 1979 Traffic Volume Report. Planning Division, New York State Department of Transportation, Albany, 1980.
  12. R.W. Miller and W.P. Chamberlin. Skid Resistance of Bituminous Pavements Built with Carbonate Aggregates. Engineering Research and Development Bureau, New York State Department of Transportation, Albany, Res. Rept. 77, April 1980.
  13. E.J. Kearney, G.W. McAlpin, and W.C. Burnett. Development of Specifications for Skid-Resistant Asphalt Concrete. HRB, Highway Research Record 396, 1972, pp. 12-20.
  14. W.P. Chamberlin. Identifying and Specifying Durable High-Friction Aggregates for Surface Courses. Paper presented at the Annual Meeting of the Association of Highway Officials of the North Atlantic States, Washington, DC, March 1974.
  15. B.E. Colley, A.P. Christensen, and W.J. Nowlen. Factors Affecting Skid Resistance and Safety of Concrete Pavements. HRB, Special Rept. 101, 1969, pp. 80-99.
  16. D. Brown. Sprinkle Mix Construction in Georgia. FHWA, Rept. on Demonstration Project DOT-FH-15-315, Region 15, Jan. 1980.
  17. Texturing and Skid Resistance of Concrete Pavements and Bridge Decks. FHWA, Tech. Advisory T 5140.10, Sept. 18, 1979.
  18. A Policy on Geometric Design of Rural Highways: 1965. 5th ed., AASHO, 1966, p. 136.
  19. J.P. Bozik. Studded Snowtire Use in New York State. Engineering Research and Development Bureau, New York State Department of Transportation, Albany, Special Rept. 40, Jan. 1976.
  20. J.J. Henry. Use of Blank and Ribbed Test Tires for Evaluating Wet Pavement Friction. TRB, Transportation Research Record 788, 1980, pp. 1-6.
  21. D.C. Mahone. An Evaluation of the Effects of Tread Depth, Pavement Texture, and Water Film Thickness on Skid Number-Speed Gradients. Virginia Highway and Transportation Research Council, Charlottesville, Rept. VHTRC 75-R40, March 1975.

*Publication of this paper sponsored by Committee on Surface Properties-Vehicle Interaction.*

## Short-Term, Weather-Related Skid Resistance Variations

BARRY J. HILL AND JOHN J. HENRY

A three-year research program was initiated in 1978 at the Pennsylvania Transportation Institute by the U.S. Department of Transportation to investigate possible causes for seasonal and short-term skid resistance variations. The primary objective is to determine the parameters that can be used to predict the influence of seasonal and short-term effects. Results concerning short-term, weather-related skid resistance variations are presented and discussed. Twenty-one test surfaces in State College, Pennsylvania, were selected for testing. The testing program includes daily skid measurements according to ASTM test method E274 and the collection of daily weather data. After the data are adjusted for long-term variations, the short-term residuals are regressed against rainfall and temperature parameters. The number of days since the last significant rainfall and the test pavement temperature are both found to be significant causes of short-term skid resistance variations. Further unexplained variations are attributable to measurement errors, particularly the lateral placement of the skid test trailer. The Pennsylvania results are supported by data collected in a similar study of 10 sites located in North Carolina and Tennessee (Federal Highway Administration Region 15).

Skid resistance measurements made according to ASTM test method E274 (1) exhibit both long-term seasonal and short-term variations on public highways in Pennsylvania and other states (2,3). These variations make the establishment of a maintenance program in which skid resistance is one of the important factors a difficult task. Variations from day to day, seemingly due to rainfall pattern and local

weather conditions, are superimposed on an annual cycle. At least in the northern states, this annual cycle tends to be higher in winter through spring than summer through fall. Frequent tests during the summer period indicate that pavement skid resistance may vary by as much as 25 percent during a single week. In analyzing these large changes, which occur rather systematically, Hegmon (4) concluded that they are real skid resistance changes related to changing conditions.

During the past two decades, several state highway departments and other agencies in the United States have conducted extensive skid resistance surveys, but until the past few years little attention was paid to seasonal and short-term variations. Until recently, the most comprehensive documented studies involving seasonal and short-term skid resistance variations were the ones undertaken by the Pennsylvania Department of Transportation (2,5). In the course of evaluating skid resistance measurements, some cyclic patterns were observed. Measurements showed that, once a pavement surface had stabilized after being exposed to traffic and weather for one to two years, the surface had cyclic skid resistance variations. The skid number gen-

Figure 1. Skid-number history for limestone surface completed on June 8, 1969.

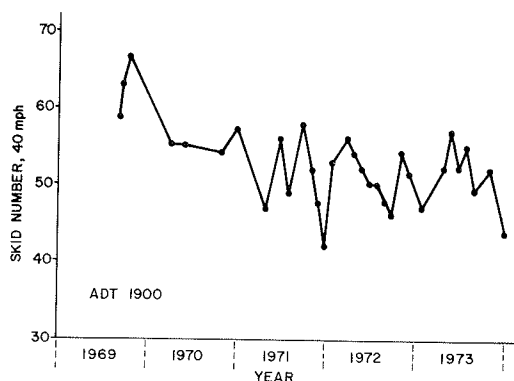
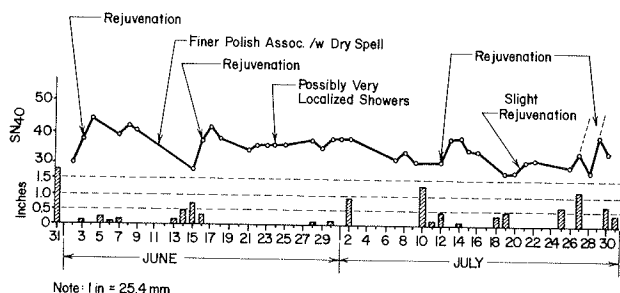


Figure 2. Influence of precipitation on skid resistance.



erally decreased to a minimum over the summer months and was rejuvenated to about its original level over the winter season (see Figure 1) (2,5). Superimposed on this seasonal cycle were short-term variations that resulted in low skid numbers after a dry period and in high (rejuvenated) skid numbers after a rainy period (see Figure 2) (5).

Several other states have reported to the Federal Highway Administration (FHWA) their observations relative to seasonal skid resistance variations. The observations were summarized in 1977 by Rice (3). Although these and other observations from various agencies are helpful in providing qualitative information relative to trends and magnitudes of seasonal and short-term variations in skid resistance, the measurements are spaced too far apart in time to offer sufficient information to develop a model for predicting the low skid number expected to occur during the year on a given pavement.

To establish further means of interpreting skid resistance data subject to seasonal and short-term variations, the U.S. Department of Transportation initiated in 1978 a three-year research program at the Pennsylvania Transportation Institute. This paper describes the findings regarding short-term skid resistance variations on 21 pavements in Pennsylvania and compares them with short-term variations experienced on 10 pavements in Tennessee and North Carolina (FHWA Region 15). The results of studies on long-term seasonal variations are reported elsewhere (6).

#### TEST SITES

The selection criteria for the test pavements include the requirements that they should be at least three years old, so that their surface characteristics would have stabilized, that they should contain

a variety of aggregates and mix designs and include portland cement concrete (PCC) pavements, and that they should have as wide a range of average daily traffic (ADT) as possible. A full description of the test-site construction materials and locations is given elsewhere (7).

The number of test pavements of each type at the Pennsylvania and FHWA Region 15 sites is as follows:

Area	Pavement	
	Type	Number
Pennsylvania	Dense-graded asphalt	10
	Open-graded asphalt	5
	PCC	6
Total		21
FHWA Region 15	Dense-graded asphalt	4
	Open-graded asphalt	2
	Bituminous surface treatment	2
	PCC	2
Total		10

#### DATA COLLECTION

##### Skid Resistance Tests

##### Pennsylvania

In 1979, skid testing was performed between 31 March and 28 November. A total of between 64 and 72 tests were made on each test section. All tests were made in the transient slip mode (8), which, while providing  $SN_{64}$  skid number data at a speed of 64 km/h (40 mph) according to ASTM E274, also provides brake slip numbers at 16, 32, and 48 km/h (10, 20, and 30 mph), which can be used to approximate  $SN_{16}$ ,  $SN_{32}$ ,  $SN_{48}$  (8).

##### FHWA Region 15

During the 12-month period starting on July 6, 1979, skid tests were performed at approximately weekly intervals according to ASTM E274. These tests were done at 64 km/h (40 mph) and also at 48 and 80 km/h (30 and 50 mph) to permit the relation between skid resistance and speed to be developed in terms of the percentage normalized gradient (8) and the zero-speed skid number intercept ( $SN_0$ ) by using the relation in Equation 1. The temperature of the test tire and the test pavement and the ambient temperature were recorded in each case.

##### Weather Data

Weather data for the Pennsylvania sites were obtained from records provided by the Pennsylvania State University Weather Station at University Park and for FHWA Region 15 sites from weather stations located at Asheville, North Carolina, and Knoxville, Tennessee.

##### MECHANISTIC MODEL

The Penn State Model relates skid resistance to speed and texture (8) according to the exponential relation

$$SN_V = SN_0 \exp[(-PNG/100)V] \quad (1)$$

where

$SN_V$  = skid number at velocity  $V$ ,  
 $SN_0$  = zero-speed skid number intercept (a function of pavement microtexture), and  
 PNG = percentage normalized gradient (a function

of pavement macrotexture) =  $-(100/SN_0)/[d(SN)/dV]$  (h/km).

The  $SN_0$  deduced from data collected throughout the year typically exhibits long-term variations (6), as shown in Figures 3, 4, and 5. Figures 3 and 4 show the results for a dense-graded and open-

Figure 3.  $SN_0$  versus time for dense-graded Pennsylvania site 17.

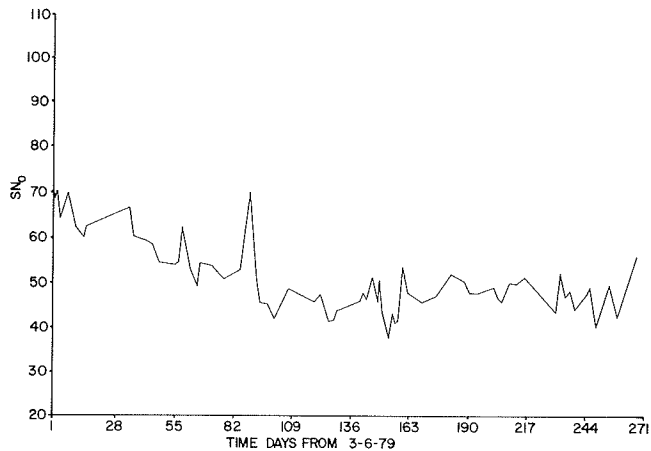


Figure 4.  $SN_0$  versus time for open-graded Pennsylvania site 22.

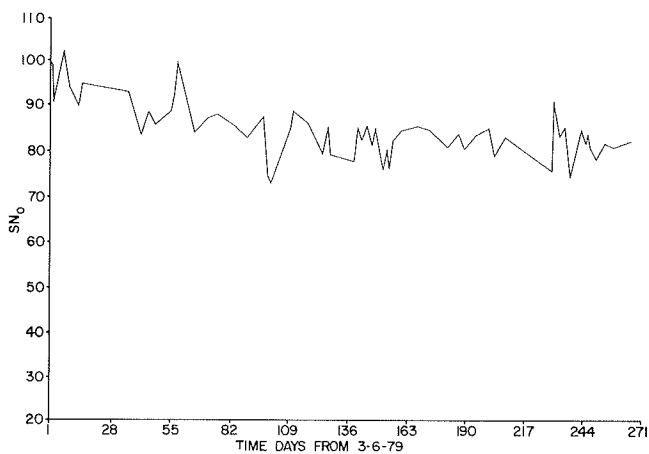
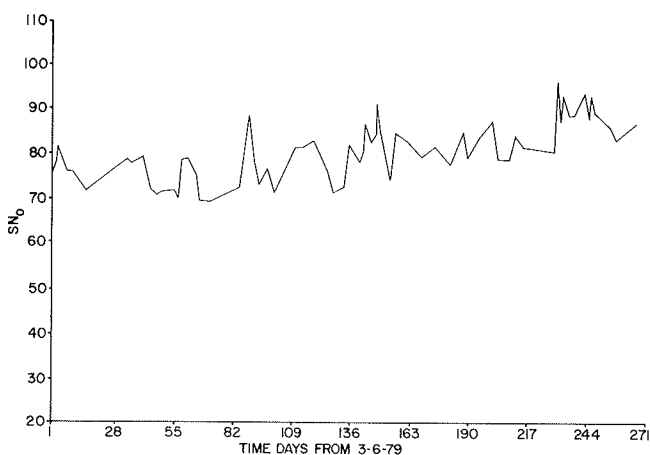


Figure 5.  $SN_0$  versus time for PCC Pennsylvania site 10.



graded asphalt surface, and Figure 5 shows the results for a PCC surface. It has been found that long-term variations in skid resistance for asphalt surfaces can be considered to be an exponential relation whereas the PCC surfaces exhibit a linear increase in skid resistance with time. Hence, the value of  $SN_0$  at any time  $t$  can be expressed as

$$SN_0 = SN_{0R} + SN_{0L} + SN_{0F} \quad (2)$$

where  $SN_{0R}$  is the short-term residual and  $SN_{0F}$  is a measure of  $SN_0$ , which is independent of short- and long-term variations.

For asphalt surfaces,

$$SN_{0L} = \Delta SN_0 \exp(-t/\tau) \quad (3)$$

whereas, for PCC surfaces,

$$SN_{0L} = (\Delta SN_0 / \Delta t) t \quad (4)$$

where

$\Delta SN_0$  = change in  $SN_0$  over testing season, a function of aggregate polish susceptibility;

$\tau$  = rate at which polishing takes place, a function of ADT; and

$\Delta t$  = length of the testing season (days).

The determination of the parameters for long-term seasonal variation is described in detail elsewhere (6), and the results are given in Table 1.

Initially,  $SN_0$  and PNG values were obtained from the skid test data for each day, and variations in PNG with time similar to those found for six Pennsylvania sites in 1977 and 1978 (5) were noticed for all of the sites considered here. The variations in PNG appear to be random measurement errors and are of sufficiently small magnitude to allow an average value to be used for each site without altering significantly the  $SN_0$  values subsequently obtained. Figure 6 shows a plot of PNG versus time for site 22, and Figure 7 shows the originally calculated  $SN_0$  values compared with  $SN_{0P}$ , the values calculated by using the average PNG. Similar relations were found for all the sites. Equation 2 can now be written

$$SN_{0P} = SN_{0R} + SN_{0L} + SN_{0F} \quad (5)$$

The skid number at 64 km/h (40 mph) will contain

Table 1. Parameters for seasonal variations at Pennsylvania sites.

Site	$SN_{0F}$	$\Delta SN_0$	$\Delta SN_0 / \Delta t$	$\tau$ (days)
1	50.5	8.28		55
2	49.4		0.036	
3	72.4		0.040	
4	55.4	9.60		45
7	69.8		0.058	
8	43.0	22.57		75
9	57.7	21.90		75
10	77.6		0.053	
11	44.6	12.87		50
12	59.8	6.89		27
13	89.9	2.61		58
14	63.6		0.034	
15	92.1	4.98		25
16	39.1	13.56		45
17	44.3	29.28		53
18	73.7		0.008	
19	49.2	12.56		30
21	45.2	17.35		65
22	80.5	14.04		65
24	44.4	3.57		27
25	80.5	3.36		63

Figure 6. Variation of PNG with time for Pennsylvania site 22.

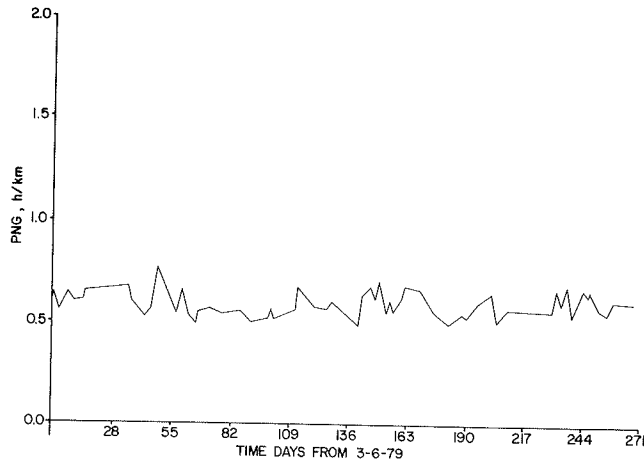
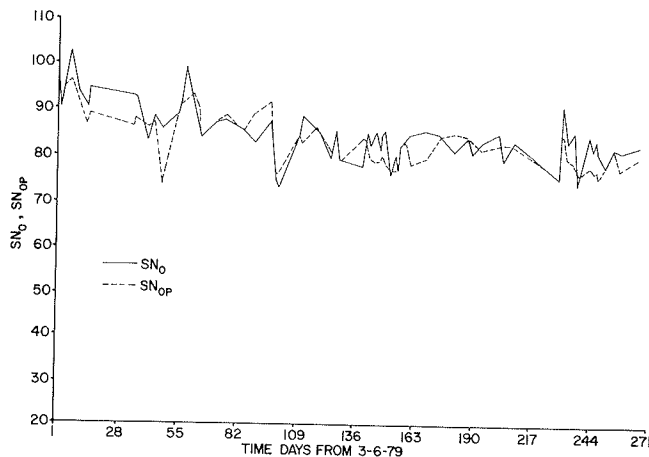
Figure 7.  $SN_0$  and  $SN_{OP}$  versus time for Pennsylvania site 22.

Table 2. Skid numbers versus WRF for selected sites.

Site	Year	Equation	r
16	1976	$SN_{64} = 32.8 + 0.089 \text{ WRF}$	0.133
1	1979	$SN_{OR} = -1.49 + 1.47 \text{ WRF}$	0.113
21	1979	$SN_{OR} = 0.12 + 0.112 \text{ WRF}$	0.077

similar long- and short-term effects according to Equation 1, and the value of  $SN_{64}$  after removal of these effects can be expressed as

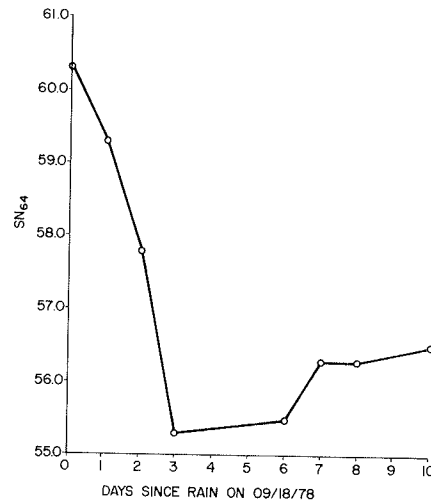
$$SN_{64F} = SN_{OF} \exp(-0.64 \text{ PNG}) \quad (6)$$

Combining Equations 1, 5, and 6 yields

$$SN_{64F} = SN_{64} - (SN_{OR} + SN_{OL}) \exp(-0.64 \text{ PNG}) \quad (7)$$

#### PREDICTION OF SHORT-TERM RESIDUALS

The long-term variations in skid resistance are assumed to be a function of pavement aggregate properties and traffic density, whereas the short-term residuals are a result of (a) rainfall effects, (b) temperature effects, and (c) errors in skid number measurements, the largest source of which is variation in the lateral placement of the test tire.

Figure 8.  $SN_{64}$  versus length of dry spell for Pennsylvania site 22.

#### Rainfall Effects

A number of studies (5,9,10) have recognized the influence of precipitation on skid resistance. In this study, as in others (5), it has been found that the skid resistance of a pavement decreases during dry periods and increases after heavy rain. A weighted rain function (WRF) has been suggested by Dahir, Henry, and Meyer (5) as a measure of the effect of rain on skid resistance, where

$$\text{WRF} = \sum_{i=1}^5 (R_i/i) \quad (8)$$

where  $R_i$  is the rainfall on the  $i$ th day prior to the test.

By using data given by Dahir, Henry, and Meyer (5) and by Dry (10), the correlation between skid number and WRF was determined for a number of cases at Pennsylvania sites. The results are given in Table 2. The correlation coefficients ( $r$ ) were found to be consistently low, and it is obvious that, if a correlation exists between precipitation and skid resistance, a parameter other than WRF must be used. Figure 8 shows  $SN_{64}$  measurements for a typical Pennsylvania site taken during a dry period and illustrates well the decrease in skid resistance with time when no rain has fallen. Relations similar to that shown in the figure were found for a number of cases. The decrease in skid number reaches a maximum after about seven days, and  $SN_{64}$  remains at a low level until the next significant rain. The following dry-spell factor (DSF) is proposed:

$$\text{DSF} = \ln(t_R + 1) \quad (9)$$

where  $t_R$  is the number of days since the last rainfall of 2.5 mm (0.1 in) or more (the upper limit is 7 days). Hence,  $0 \leq t_R \leq 7$ .

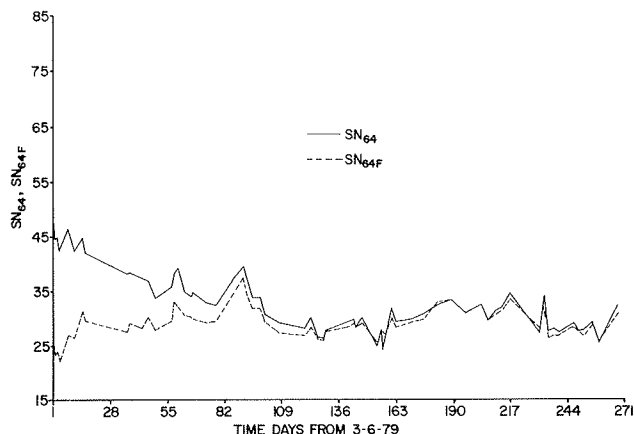
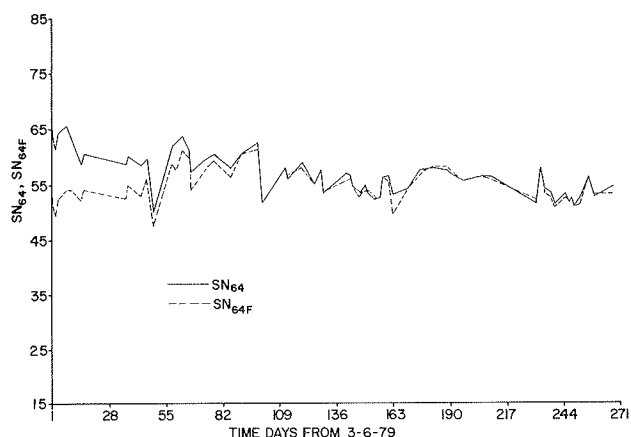
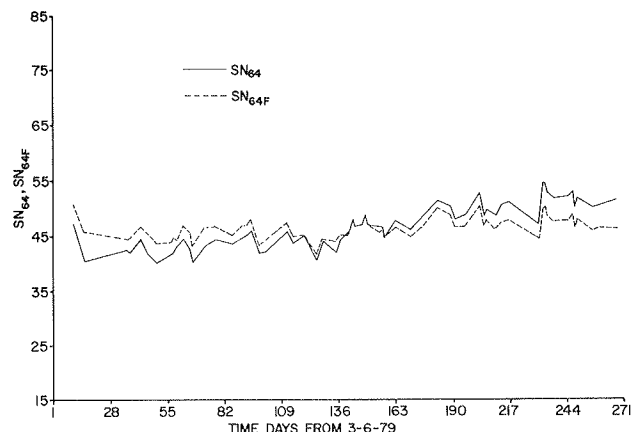
The correlations for the cases in Table 2 were repeated by using DSF as the rainfall parameter with a significant improvement in correlation coefficient  $r$ , as given in Table 3. As a final comparison,  $SN_{OR}$  values for all 21 Pennsylvania sites were regressed against both WRF and DSF with the following results:

$$SN_{OR} = 1.00 + 2.74 \text{ WRF} \quad r = 0.20 \quad (10)$$

$$SN_{OR} = 1.14 - 1.17 \text{ DSF} \quad r = 0.35 \quad (11)$$

Table 3. Skid numbers versus DSF for selected sites.

Site	Year	Equation	r
16	1976	$SN_{64} = 34.77 - 1.45 \text{ DSF}$	0.463
1	1979	$SN_{0R} = 0.53 - 0.94 \text{ DSF}$	0.161
21	1979	$SN_{0R} = 2.05 - 1.58 \text{ DSF}$	0.318
18	1978	$SN_{64} = 52.17 - 1.89 \text{ DSF}$	0.398
16	1978	$SN_{0R} = 2.23 - 2.05 \text{ DSF}$	0.561

Figure 9. Comparison of  $SN_{64}$  and  $SN_{64F}$  for Pennsylvania site 17.Figure 10. Comparison of  $SN_{64}$  and  $SN_{64F}$  for Pennsylvania site 22.Figure 11. Comparison of  $SN_{64}$  and  $SN_{64F}$  for Pennsylvania site 10.

The conclusion is that, although  $r$  is still small, the length of time since the last significant rainfall is a better measure of the effect of rainfall on the skid resistance of pavements.

#### Temperature Effects

Some researchers (9,11) have found that an increase in temperature results in a corresponding decrease in skid resistance, whereas others (5) have not noticed this effect to be significant. A linear regression for Pennsylvania site 1 (1979) produces the following relation:

$$SN_{0R} = 5.09 - 0.232 T_p \quad r = 0.50 \quad (12)$$

where  $T_p$  is the pavement temperature ( $^{\circ}\text{C}$ ). This result, at least, indicates that pavement temperature is significant in its effect on skid resistance measurements and should not be eliminated as a parameter in further investigations.

Pavement temperature was chosen as the temperature parameter because (a) it is a more accurately defined measurement than ambient temperature and more easily measured than tire temperature and (b) good correlation exists among the three measures of temperature.

For the Pennsylvania data, the regression equations found to relate the three measures of temperature are as follows:

$$T_t = 8.54 + 0.810 T_A \quad r = 0.91 \quad (13)$$

$$T_t = 6.78 + 0.558 T_p \quad r = 0.87 \quad (14)$$

$$T_A = 0.87 + 0.573 T_p \quad r = 0.79 \quad (15)$$

where

$T_t$  = tire temperature ( $^{\circ}\text{C}$ ),  
 $T_p$  = pavement temperature ( $^{\circ}\text{C}$ ), and  
 $T_A$  = ambient temperature ( $^{\circ}\text{C}$ ).

The magnitude of the effects of rainfall and temperature on the short-term variations in skid resistance can be determined by performing a multiple regression of  $SN_{0R}$  versus  $T_p$  and DSF for the data available. For the Pennsylvania sites, the regression equation is

$$SN_{0R} = 3.79 - 1.17 \text{ DSF} - 0.104 T_p \quad (16)$$

with  $r = 0.35$ . For the FHWA Region 15 sites, the regression equation is

$$SN_{0R} = 1.88 - 0.77 \text{ DSF} - 0.15 T_p \quad (17)$$

with  $r = 0.57$ .

Equations 16 and 17 can be used with Equation 7 to determine the value of  $SN_{64}$  after adjustment for seasonal and short-term effects. Figures 9, 10, and 11 show the adjusted  $SN_{64F}$  values compared with the original data for three Pennsylvania sites. All of the other sites show similar results. Ideally,  $SN_{64F}$  should be constant with time after all seasonal and short-term weather effects are accounted for. The low correlation coefficients obviously limit the ability of regression Equations 16 and 17 to "smooth" the data for short-term variations. The standard deviation of the "smoothed"  $SN_{64F}$  values is, however, between 2.04 and 2.54 skid numbers for the Pennsylvania sites and between 2.21 and 3.06 skid numbers for the FHWA Region 15 sites. These values must be compared with the possible variations in  $SN_{64}$  measurements due to measurement errors and other sources of error.



## SIGNIFICANCE OF THE RESULTS

Meyer, Hegmon, and Gillespie (12) list a number of factors responsible for errors in locked-wheel pavement skid resistance tests and the average error band associated with each type of error. These include

Factor	Avg Error Band (SN)
Speed holding	$\pm 1.5$
Pavement variability	
Lateral	$\pm 4$
Longitudinal	$\pm 2$
Dynamic wheel-load change	$\pm 1$
Data evaluation by operator	$\pm 3$

The magnitude of these average error bands can be reduced by taking adequate precautions, and it is unlikely that speed holding, longitudinal pavement variability, or evaluation of the data by the operator would, in the case of the data used in this study, be a significant contributor to the variations in  $SN_{64}$ . It is believed that variations due to small errors in lateral placement of the skid test tire are a major contributing factor. All skid test measurements are made in the wheel tracks on the pavement where contamination by foreign particles and polishing of the aggregate causes the measured skid resistance to be minimal (12). A deviation of only 125 mm (5 in) in lateral placement of the test tire relative to the wheel track can lead to variations in the measured  $SN_{64}$  of as much as  $\pm 2$  SN. It would be unusual for an operator to place the skid test trailer consistently with such accuracy. The fluctuations in  $SN_{64F}$ , after the long- and short-term effects are eliminated, are less than the expected variations due to measurement errors, and further improvement in the correlation between the short-term residuals  $SN_{OR}$  and weather-related parameters would seem unlikely.

The data used to obtain Equations 16 and 17 were subjected to a Student's t-test of the hypothesis that the coefficients for DSF and  $T_p$  are zero. In each case, the t-values obtained had a probability of occurrence of 0.0001 if the hypothesis was true, which leads to a rejection of the hypothesis. Equations 16 and 17 are considered to be statistically significant.

## CONCLUSIONS

The following conclusions can be made based on the results of this study:

1. Large variations in skid resistance measurements occur systematically over a short-term period (day to day or week to week).
2. The mechanisms that cause skid resistance variations appear to be complex. Rainfall and temperature appear to be the most significant causes of short-term variations. A seven-day period without rain can result in a decrease in skid resistance at 64 km/h of 1.7 SN. An increase in temperature of 10°C can result in a decrease in  $SN_{64}$  of about 1.2 SN.
3. A major cause of apparent skid resistance variations is measurement error, particularly lateral placement of the test tire, which can account for as much as  $\pm 4$  SN at a speed of 64 km/h.
4. The standard deviation of skid resistance variations not explained by rainfall and temperature effects is about  $\pm 2.5$  SN at a speed of 64 km/h.
5. The validity of the results is supported by the good agreement between the regression equation coefficients for the Pennsylvania sites and those for the FHWA Region 15 sites.

6. The weather conditions to which the Pennsylvania sites are subjected are different from those experienced by the FHWA Region 15 sites. However, the influence of weather on short-term skid resistance variations is similar for both data sets.

The results obtained are preliminary, and additional research in this area is continuing.

## ACKNOWLEDGMENT

This paper is based on research sponsored by the U.S. Department of Transportation in cooperation with FHWA. The research has been conducted at the Pennsylvania Transportation Institute, Pennsylvania State University. Personnel from FHWA and Pennsylvania State University have assisted in the research. Valuable assistance was contributed by FHWA engineers R.R. Hegmon, H.C. Huckins, J.M. Rice, and M. Symons.

## REFERENCES

1. Annual Book of ASTM Standards. ASTM, Philadelphia, Part 15, 1980.
2. W.L. Gramling and J.G. Hopkins. Skid Resistance Studies: Aggregate Skid Resistance Relationships as Applied to Pennsylvania Aggregates. Pennsylvania Department of Transportation, Harrisburg, Final Rept., 1974.
3. J.M. Rice. Seasonal Variations in Pavement Skid Resistance. Public Roads, Vol. 40, No. 49, March 1977.
4. R.R. Hegmon. Seasonal Variations in Pavement Skid Resistance: Are These Real? Public Roads, Vol. 42, No. 2, Sept. 1978, pp. 55-62.
5. S.H. Dahir, J.J. Henry, and W.E. Meyer. Seasonal Skid Resistance Variations. Pennsylvania Department of Transportation, Harrisburg, Final Rept., 1979.
6. B.J. Hill and J.J. Henry. Surface Materials and Properties Related to Seasonal Variations in Skid Resistance. Presented at ASTM Symposium on Traveled Surface Characteristics, Orlando, FL, Dec. 1980.
7. J.J. Henry and S.H. Dahir. Predictor Models for Seasonal Variations in Skid Resistance. FHWA, Interim Rept. 1, 1979.
8. V.R. Shah and J.J. Henry. The Determination of Skid Resistance: Speed Behavior and Side Force Coefficients of Pavements. TRB, Transportation Research Record 666, 1978, pp. 13-18.
9. M.A. Furbush and K.E. Styers. The Relationship of Skid Resistance to Petrography of Aggregates. Pennsylvania Department of Transportation, Harrisburg, Final Rept. 3, July 1972.
10. D.R. Dry. Short-Cycle Seasonal Variations in Skid Resistance. Pennsylvania State Univ., University Park, Automotive Research Program Rept. S81, 1978.
11. S.H. Dahir and H.J. Lestz. Laboratory Evaluation of Pavement Surface Texture Characteristics in Relation to Skid Resistance. Office of Research and Development, FHWA, Final Rept. FHWA-RD-75-60, 1972.
12. W.E. Meyer, R.R. Hegmon, and T.D. Gillespie. Locked-Wheel Pavement Skid Tester Correlation and Calibration Techniques. NCHRP, Rept. 151, 1974.

# Economic Factors Related to Raising Levels of Skid Resistance and Texture

DON L. IVEY AND W. FRANK McFARLAND

An evaluation of the requirements for skid resistance and pavement texture is presented. Economic factors other than accident costs are considered for the first time. The primary economic factors recognized at this time, in addition to accident costs, are fuel cost and tire wear. The study indicates that significantly increasing levels of skid resistance and texture will result in decreases in fuel economy and tire life. These losses will have a major economic impact. The extent of this impact is estimated. A method of calculating the comparative cost of using polish-resistance aggregates and polish-susceptible aggregates for surface treatments is presented. A method to determine the increase in cost that is economically justified to acquire polish-resistant aggregates is developed.

The relation between the level of available friction on highway surfaces and accident rates has been well established. Perhaps the cleanest relation was established by the Dutch (1) in 1977. These relations, illustrated by Figure 1 (1), show a clear interdependence of traffic volume and accident sensitivity as influenced by different levels of skid resistance.

Recent work on this subject was done at Texas A&M University (2). Equations 1 and 2 give the new relations that were developed. The degree of accuracy of these equations is illustrated by Figure 2.

For low speed (urban), speed limit > 50 mph,

$$WAR_{LS} = -21.7 + 0.0009ADT + 2.34ACC - 0.40SN + 286TW + 1.32LN \quad (1)$$

For high speed (rural), speed limit = 55 mph,

$$WAR_{HS} = -0.75 + 0.0001ADT - 0.053VM + 0.54\Delta V + 0.69ACC - 0.025SN \quad (2)$$

where

ADT = average daily traffic,  
ACC = access,  
SN = skid number at 40 mph,  
TW = proportion of time wet,  
VM = mean traffic speed,  
 $\Delta V$  = variation in traffic speed, and  
LN = lanes of traffic.

Figure 1. Accident sensitivity to volume of traffic as influenced by friction.

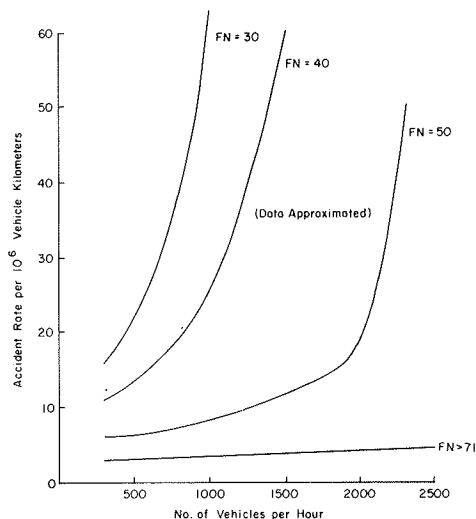


Figure 3 illustrates the relative insensitivity of accident rate to skid number on rural highways and the high sensitivity on urban highways. The obvious conclusion is that major accident, and thus economic savings, can be realized predominantly in urban areas (i.e., areas where speeds are posted at less than 55 mph).

There is much more to the problem of maintaining adequate levels of skid resistance than simply building surfaces with a high value of SN. Davis and Epps (3) have treated the problem of aggregate polishing, attrition of surface aggregate, and fat spots on the surface caused by overasphalting.

## OVERVIEW OF ECONOMIC ASPECTS

Increases in tire-pavement friction have a variety of economic influences. The most sought-after influence is accident reduction, but several other in-

Figure 2. Observed versus predicted wet-accident rate.

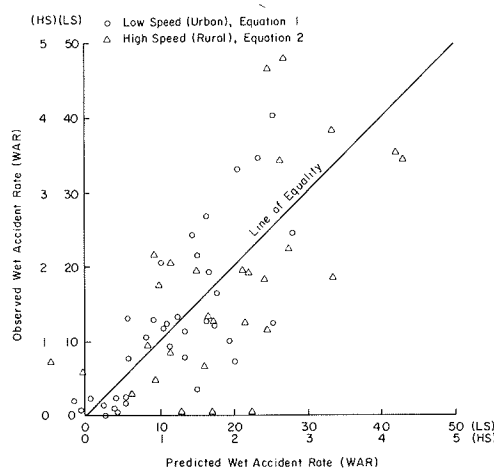
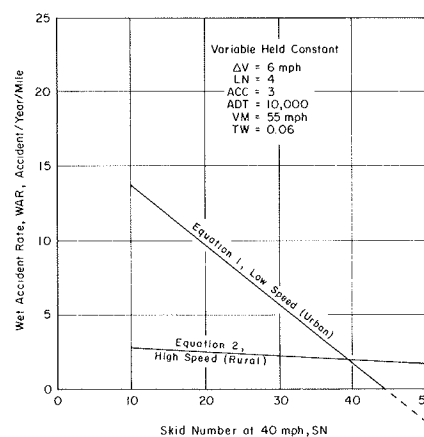


Figure 3. Sensitivity of Equations 1 and 2 to SN.



fluences are not positive. These influences are summarized below.

#### Consequence of

#### Increased

#### Tire-Pavement

#### Friction

#### Positive

#### Economic Influence

Reduction in accidents in wet weather, resurfacing required less frequently

#### Negative

Increased fuel consumption, increased tire wear, increased costs for surfacing

#### Other

Increased noise and vibration levels imposed on vehicle occupants

Of the two positive influences, the second is actually somewhat dependent on the first and reflects the requirement of maintaining generally adequate levels of pavement skid resistance. The first two negative influences (increased fuel consumption and increased tire wear rates) may prove of some significance, at least in imposing some upper limit on the amount of macrotexture that will be tolerated by the public. Increased traffic noise, although not necessarily of economic importance, may also impose a practical upper limit on macrotexture.

Arbitrarily increasing the pavement macrotexture to produce increases in friction and reduce hydroplaning tendencies must be subject to some compromise to prevent the negative influences from growing intolerable.

#### Methods Available to Increase Friction

Many methods are available to increase tire pavement friction. They have been discussed in detail by Davis and Epps (3). Seventeen methods are described by Davis and Epps, including acid etching, scabbing, grooving, portland cement concrete (PCC) overlays, chip seals, open-graded friction courses, epoxy seals, heater-planer treatment, and milling. Discussions of the practicality of each method are given as well as costs and estimates of surface life. A relatively new innovation is the pavement-milling method.

#### Pavement Milling

One of the most innovative methods of achieving high values of pavement texture, and thus tire-pavement friction, is cold milling. Several companies now perform this service and others are building equipment for cold milling. The resulting surface is an extremely highly textured, longitudinally striated surface that should provide excellent skid resistance. In apparent conflict with this expectation is that early determinations of SN do not show high values. It may be that a texture has been achieved that has a directional geometry so pronounced that the reduction of contact area in the tire contact zone generates lower values of locked wheel-braking friction force. If this is true, the value of SN may even increase as the most extreme textured projections are abraded and worn, although this must be considered unlikely. It seems obvious that the pattern will greatly improve directional stability as does pavement grooving. Also apparent is the high-speed insensitivity to friction reduction of a texture so pronounced. Although this is a hypothesis, if verified, it will prove an excellent characteristic.

There seem to be only two drawbacks to the cold-milling process. First, these newly completed sections have drawn criticism from motorcyclists and

drivers of small cars. They complain that the surface may produce stability problems. Another way of interpreting this is that the surface provides too much directional stability. A human factors study conducted by Martinez (4) showed that early surfaces milled in Texas posed some problem to the riders of some motorcycles, but as the technology has matured, the problem has receded.

The second drawback is a negative economic influence. Elevated pavement textures add to rolling resistance and thus to decreased fuel economy. Although this seems to have been appreciated only intuitively until now, recent tests indicate that the difference in the rolling resistance for a full-sized vehicle between a pavement that has low textural value (approximately 10-20/1000 in) and one that exhibits a very high cold-milled texture (approximately 70-80/1000 in) is approximately 85 lbs. (Pavement texture is normally expressed as the average depth of the depressions between aggregate particles. Another way to view it is the average height of the pavement surface asperities.) Based on limited data, the curves shown in Figure 4 are hypothesized.

As an example, consider the possibility that the Federal Highway Administration (FHWA) is successful over a period of the next four years in increasing the average macrotexture of the federal and state highway systems from the currently assumed average of about 30/1000 to a level of 50/1000.

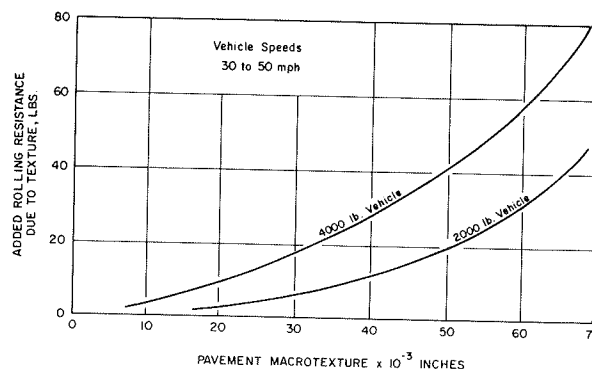
According to Winfrey (5, p. 292), total rolling resistance for a 4000-lb automobile is about 65-70 lb at speeds of 55-60 mph. If the added rolling resistance from increasing macrotexture from 30/1000 to 50/1000 increased total rolling resistance, by 20 lb (from 60 to 80 lb), this is an increase in rolling resistance of 33 percent. Since about 36 percent of total horsepower used is for rolling resistance at speeds of 55-60 mph (5, p. 292), the 20 lb of added rolling resistance would increase horsepower required by about 10 percent.

Thus, for a full-size automobile that achieves 20 mile/gal with a macrotexture of 30/1000, fuel efficiency would drop to about 18 miles/gal with a macrotexture of 50/1000. Assuming that 1.8 trillion miles are driven per year in 1984 and fuel costs are \$1.30/gal (assumed 1981 cost), this translates to a difference in cost of about \$13 billion/year for this increase in macrotexture. If fuel increases in price by 7 percent/year between 1981 and 1984, this would amount to an increase of about \$16 billion/year.

#### Effect on Rates of Tire Wear

A corollary to the increased rolling resistance is the increase in tire wear. It has been estimated

Figure 4. Influence of macrotexture on rolling resistance.



that tire life is inversely related to pavement texture.

Although there is no direct verification of the influence of pavement texture on tire wear rates, the contour map of tread wear in the United States by Snyder (6) provides strong indirect evidence [Figure 5 (6)]. In the highest wear areas of Utah and North Carolina, angular polish-resistant, igneous aggregates, such as crushed granite, are predominantly used. In the lowest wear area of Texas, relatively soft rocks, such as crushed limestone and well-rounded gravels, have been widely used. Note, however, that no quantitative relations have been derived from this information. An obvious factor--the influence of microtexture--is involved in the Snyder contour map and is neglected in current considerations of the effect of macrotexture. Further complicating this relation is the research that shows that most tire wear occurs when pavements are wet (7). This seems somewhat in conflict with the Snyder contour map, where states such as Washington and Louisiana have relatively low wear rates (i.e., high values of mileage to wear out a tire).

In spite of this lack of quantitative evidence, in consultation with Bob M. Gallaway, we have intuitively derived the graph shown in Figure 6. Certain end points of this curve have been roughly quantified by tread life values occurring at the main automotive proving ground (APG) tire wear track and the El Camino track. Even so, the graph is somewhat speculative.

As Figure 6 illustrates, the construction of surface textures much greater than 0.50 in on highways

could result in precipitous wear rates. By using the previous example of increases from 30 to 50/1000 in of macrotexture, it might be possible to decrease the average life of a tire by 10-20 percent. If we assume that 250 million tires are consumed per year with average macrotexture at 30/1000 (this includes retreads), the decreased tire life of 10-20 percent with macrotexture at 50/1000 would increase tire consumption by 25-50 million tires/year. If we assume that tires cost \$50 each in 1984, this would amount to an increase in tire cost of \$1.25-5 billion/year.

Overall, the increase in fuel and tire costs, from increasing macrotexture from 30 to 50/1000, would approach \$20 billion/year in 1984.

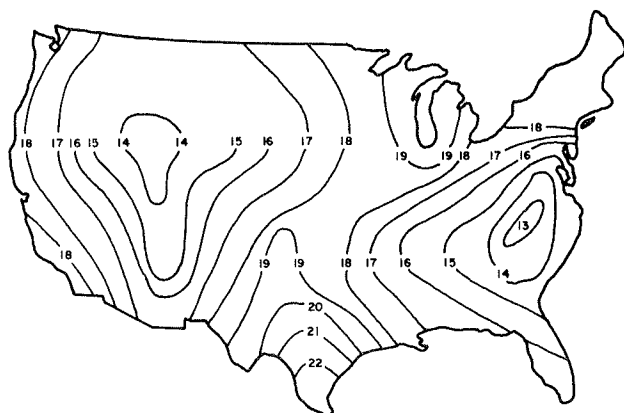
#### Accident Savings

The major economic gain due to increasing pavement texture-friction is that of accident reduction. Table 1 illustrates the savings achievable by increasing average tire pavement friction from 35 to 45, an increase that might be considered achievable [see the following table (8-10) and Table 2 (2) for assumptions.]

Accident Type	Estimated Cost to Society of Accidents (\$)	Estimated Distribution of Accidents (%)
Fatality	500 000	0.26
Disability injury	18 000	7.67
Property damage only and non-disability injury	1 000	92.07

The total estimated societal savings computed amounts to slightly more than \$2 billion/year by 1984. It may seem inappropriate to estimate the cost of these accidents in terms of dollars. The prevention of more than 0.5 million accidents is a worthy societal goal unless the costs incurred by

Figure 5. Contour map of tread wear for United States, showing equal tire mileage lines.



Note: Contours designate the average number of miles in thousands driven by vehicles where one tire rib has been worn to the 2/32 s-in wear line.

Figure 6. Influence of pavement macrotexture on tire life.

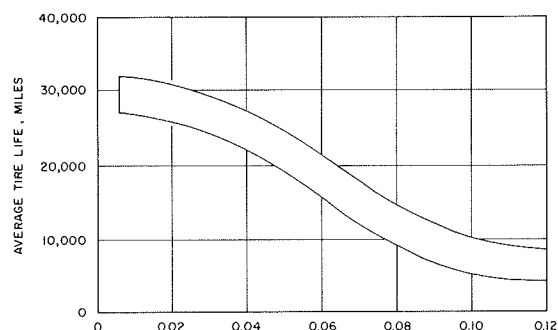


Table 1. Estimate of accident cost savings in 1984 if average SN is raised from 35 to 45.

Road Type	1984 Total Mileage <sup>a</sup>	1984 Vehicle Miles <sup>a</sup> (000 000 000s)	Estimated No. of Accidents Prevented	Estimated Accident Cost Savings (\$000 000s)
Interstate				
Urban	10 000	185	2 500	9
Rural	35 000	173	8 750	32
Other highways				
Urban	115 000	513	460 000	1657
Rural	450 000	470	112 500	405
Total			583 750	2103

<sup>a</sup>From FHWA (7).

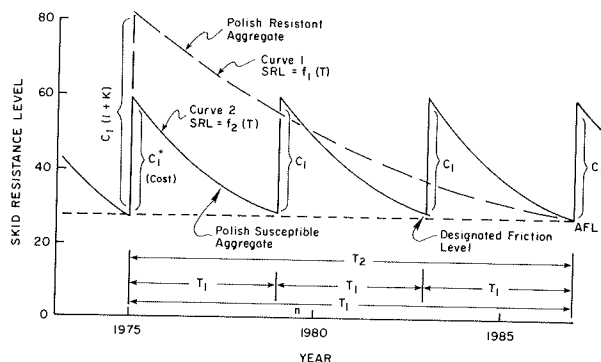
Table 2. Values assumed for accident reduction computations.

Item	Interstate		Other Highway	
	Urban <sup>a</sup>	Rural <sup>a</sup>	Urban <sup>b</sup>	Rural <sup>a</sup>
ADT	50 000	13 500	12 200	2860
ACC	2	1	4	2
TW	0.05	0.05	0.05	
LN	6	4	4	
VM				60
ΔV				6
SN	35, 45	35, 45	35, 45	35, 45

<sup>a</sup>Use Equation 2.

<sup>b</sup>Use Equation 1.

Figure 7. Comparison of renewal frequency for polish-resistant and polish-susceptible aggregates.



\* $C_1$  is the cost required to achieve the change in skid resistance shown.

such prevention detract from more productive preventative methods.

#### Direct Economic Effects on State Transportation Departments

Considering those factors of direct economic influence on state transportation departments, the problem translates into a comparison of the costs of specific treatments with the cost of maintenance and the frequency of resurfacing.

A simplified approach to this economic problem is illustrated by Figure 7. This figure compares the difference in several resurfacing operations over a period of years with a polish-susceptible aggregate to the cost of a single surfacing operation that has a more costly polish-resistant aggregate.

The total cost over a period of  $T_2$  years is  $nC_1$  (for the polishing aggregate) and  $C_1(1+K)$  (for the polish-resistant aggregate)

where

- $T_1$  = the time the polish-susceptible aggregate surface treatment will last,
- $T_2$  = the time the polish-resistant aggregate surface treatment will last,
- $n = T_2/T_1$ ,
- $C_1$  = the cost of a surface treatment using the cheaper polish-susceptible aggregate, and
- $K$  = the decimal increase in cost of the polish-resistant aggregate surface treatment relative to the cost of the polish-susceptible aggregate surface treatment.

If the total costs over the period  $T_2$  are equated, then a value of  $K$  derived from the equation

$$nC_1 = C_1(1+K) \quad (3a)$$

can be justified

$$K = n - 1 \quad (3b)$$

This is an obviously oversimplified economic treatment, but one that may be roughly justified on the basis of comparing the value of money originally invested in the surface at time zero to the escalation of all material costs over the period  $T_2$ .

This simple equation shows that the amount of cost differential justified is linearly related to  $n$ , the ratio of the respective treatment lives, if a discount rate of zero is used.

There is a distinct advantage, however, to this apparent equalization of costs. The average level

of friction provided to the public over the period  $T_2$  is significantly greater for the polish-resistant than for polishing aggregates, even though they both approach the same low value during the period. In the example of Figure 7, the polishing aggregate surface approaches the minimum level three times during the period  $T_2$ , but the polish-resistant surface approaches the minimum level only once.

In the hypothetical example shown by Figure 7, the value selected arbitrarily is approximately 30. The average level of friction provided by the polishing aggregate is the integration of curve 2,

$$SRL_{avg} = \int_0^{T_1} f_2(T) dT / T_1 \quad (4)$$

In the hypothetical example this value is approximately 40.

The average level of friction provided by the polish-resistant aggregate is the integration of curve 1,

$$SRL_{avg} = \int_0^{T_2} f_1(T) dT / T_2 \quad (5)$$

This value is approximately 52. This demonstrates that the average value provided over the period  $T_2$  by the polish-resistant aggregate is roughly 30 percent greater than that provided by the polishing aggregate.

This difference in the average skid resistance provided has a modest influence on accident costs. For example, if  $T_2$  is 9 years and the highway parameters are described as follows, for 5 miles of highway,

$$\begin{aligned} ADT &= 10,000, \\ ACC &= 4, \text{ and} \\ \text{Speed limit} &= 45. \end{aligned}$$

The application of Equation 1 for the average friction levels of 52 and 40 will yield a predicted reduction in wet-weather accidents of 180 over the 9-year period, if the cost of the average accident is \$3600 (a weighted average of property-damage only, injury, and fatal accidents) (7). This is a direct savings of \$648,000, not to mention the humanitarian contribution.

In the previous economic comparison, no discount rate has been used for the polishing aggregate to discount future costs to present terms. Use of a positive discount rate ( $r$ ) results in the following analogous cost comparison. If we assume that  $T_2$  is some multiple ( $n$ ) of  $T_1$ , as before,

$$C_1 + [C_1/(1+r)^{T_1}] + [C_1/(1+r)^{2T_1}] + \dots + [C_1/(1+r)^{(n-1)T_1}] = C_1(1+k) \quad (6a)$$

or

$$C_1 \sum_{j=0}^{n-1} 1/(1+r)^{jT_1} = C_1(1+k) \quad (6b)$$

or the premium  $k$  that can be justifiably paid for the nonpolishing aggregate based on cost alone is

$$k = \sum_{j=0}^{n-1} [1/(1+r)^{jT_1}] - 1 = \sum_{j=1}^{n-1} 1/(1+r)^{jT_1} \quad (7)$$

which equals  $n-1$  with  $r$  equals 0. With  $n$  equal to 3,  $T_1$  equal to five years, and  $r$  equal to 0.05 (i.e., with a discount rate of 5 percent/year), we get the following results:

$$k = [1/(1+0.05)^5] + [1/(1+0.05)^{10}] = (1/1.276) + (1/1.629) = 0.784 + 0.614 = 1.398 \quad (8)$$

The premium that can be paid for the skid-resistant aggregate, in decimal terms, thus is 1.398 or, in percentage terms, would be 139.8 percent. In this example, 139.8 percent is the amount extra that can be paid for the skid-resistant aggregate and still have the same cost per year, assuming the factors of fuel efficiency and tire wear are roughly equivalent under the two situations. In the case where  $T_2$  is not an even multiple of  $T_1$ , probably the preferable way to compare alternatives is to determine the equivalent uniform annual cost (EUAC) for each alternative and compare these. For example, if  $T_1$  is 5 years and  $T_2$  is 14 years, EUAC associated with the polishing aggregate would be obtained by multiplying the uniform series capital recovery factor for an interest rate of 0.05 and a life of 5 years, denoted by  $\text{crf}(r=0.05, t=5)$ , by  $C_1$ . Similarly, for the nonpolishing aggregate, EUAC would be obtained by multiplying  $\text{crf}(r=0.05, t=14)$  by  $C_1(1+k)$ , and  $k$  can be obtained by solving:

$$C_1 \times \text{crf}(0.05, 5) = C_1(1+k) \times \text{crf}(0.05, 14)$$

$$\text{crf}(0.05, 5) = \text{crf}(0.05, 14) + k \times \text{crf}(0.05, 14)$$

$$k = [\text{crf}(0.05, 4) / \text{crf}(0.05, 14)] - 1 \quad (9)$$

where  $\text{crf}(r, t) = [r(1+r)^t / (1+r)^t - 1]$  and,  $\text{crf}(0.05, 5) = 0.23097$  and,  $\text{crf}(0.05, 14) = 0.10102$  and thus,  $k = (0.23097 / 0.10102) - 1 = 2.286 - 1 = 1.286$

This same approach can be used, of course, even if  $T_2$  is an even multiple of  $T_1$ ; for example, in the case previously considered where  $T_1 = 5$  years and  $T_2 = 15$  years:  $k = [\text{crf}(0.05, 5) / \text{crf}(0.05, 15)] - 1 = (0.23097 / 0.09634) - 1 = 2.397 - 1 = 1.397$

which is the same answer as obtained previously (except for the small rounding error).

#### SUMMARY

There are direct economic benefits to state transportation departments and to the public from increasing friction on road surfaces. Judgment must be exercised to prevent unacceptably high levels of macrotexture from alienating the public through the negative influences of noise, vibration, reduced fuel economy, and high levels of tire wear. Many

proven methods of accomplishing this goal are available and new methods are becoming available. Careful economic analyses of alternative aggregate sources must be prepared relative to specific natural resources in different parts of the country to accurately determine the benefits that can be realized, but they are significant and should be pursued.

#### REFERENCES

1. L.H.M. Schlosser. Traffic Accidents and Road Surface Skidding Resistance. TRB, Transportation Research Record 623, 1976, pp. 11-20.
2. D.L. Ivey, L.I. Griffin III, T.M. Newton, K.C. Hankins, C.W. Blumentritt, and R.L. Lytton. Development of a Wet Weather Safety Index. Texas Transportation Institute, Texas A&M Univ., College Station, Res. Rept. 221-1F, Nov. 1977.
3. M.M. Davis and J.A. Epps. Skid Resistant Surfaces. Texas Transportation Institute, Texas A&M Univ., College Station, Res. Rept. 214-7, Dec. 1975.
4. J.E. Martinez and others. Effects of Milled Pavement Surfaces on Motorcycle Rideability. Texas Transportation Institute, Texas A&M Univ., College Station, Res. Rept. 237-1F, 1968 (unpublished).
5. R. Winfrey. Economic Analysis for Highways. International Textbook Co., Scranton, PA, 1969.
6. R.H. Snyder. Environmental Effects on Tire Treadwear. Tire Science and Technology, Vol. 1, No. 2, May 1973.
7. Roadway Report. In 1975 Highway Statistics, Section 4, FHWA, FHWA-HP-HS-75-04, 1975.
8. W.F. McFarland and J.B. Rollins. Discussion of Concepts, Principles, and Objectives of Economic Analysis Applicable to Traffic Accidents. TRB, Transportation Research Record 680, 1978, pp. 50-52.
9. R. Winfrey. Concepts, Principles, and Objectives of Economic Analysis Applicable to Traffic Accidents. TRB, Transportation Research Record 680, 1978, pp. 40-50.
10. Accident Facts. National Safety Council, Chicago, 1975.

*Publication of this paper sponsored by Committee on Surface Properties-Vehicle Interaction.*